



CONSULTING ENGINEERS
& SCIENTISTS

Tel: 519.823.1311
Fax: 519.823.1316

Rowan Williams Davies & Irwin Inc.
650 Woodlawn Road West
Guelph, Ontario, Canada
N1K 1B8

LAKE BRIDGES

Kentucky Lake Bridge and Lake Barkley Bridge

Final Report (Draft)

Wind Engineering Studies

RWDI # 1301291
September 18, 2013

SUBMITTED TO:

Gregory D. Stiles, PE
Bridge Technical Manager
Michael Baker Jr., Inc.
797 Haywood Road, Suite 201
Asheville, NC 28806
GStiles@mbakercorp.com

SUBMITTED BY:

Mark A. Hunter, C.E.T.
Principal/Senior Project Manager
Rowan Williams Davies & Irwin Inc.
650 Woodlawn Road West
Guelph, Ontario, Canada N1K 1B8
Mark.Hunter@rwdi.com

Stoyan Stoyanoff, Ph.D., P.Eng., ing.
Principal/Project Director
Rowan Williams Davies & Irwin Inc.
109 Boul. Bromont
Bromont, Québec, Canada J2L 2K7
Stoyan.Stoyanoff@rwdi.com

Pierre-Olivier Dallaire, M.A.Sc., ing.
Project Engineer
Rowan Williams Davies & Irwin Inc.
109 Boul. Bromont
Bromont, Québec, Canada J2L 2K7
Pierre-Olivier.Dallaire@rwdi.com

This document is intended for the sole use of the party to whom it is addressed and may contain information that is privileged and/or confidential. If you have received this in error, please notify us immediately.

© RWDI name and logo are registered trademarks in Canada and the United States of America



TABLE OF CONTENTS

EXECUTIVE SUMMARY

1. INTRODUCTION.....	1
1.1 Study Scope.....	1
2. WIND CLIMATE ANALYSIS	2
2.1 Introduction.....	2
2.2 Wind Climate and Site Analysis	2
2.2.1 Source of Data.....	2
2.2.2 Local Terrain.....	2
2.2.3 Analysis	2
2.2.4 Joint Probability of Wind Speeds and Directions	3
2.2.5 Upcrossing Method to Determine Design Winds	4
2.3 RESULTS.....	5
2.3.1 Wind Directionality Effects.....	5
2.3.2 Terrain at the Bridge Sites.....	5
2.3.3 Wind Speeds at Deck Height	6
2.3.3.1 Structural Design Wind Speed	6
2.3.3.2 Design Wind Speed for Aerodynamic Stability.....	6
2.3.4 Turbulence Properties at the Bridge Sites	6
2.4 Wind Climate Analysis: Summary.....	7
3. SECTIONAL MODEL TEST	8
3.1 Objectives and Criteria.....	8
3.2 Description of the Sectional Models.....	9
3.3 Description of the Wind Tunnel Test Procedures	10
3.3.1 Stability Tests	10
3.3.2 Static Force and Moment Coefficient Tests	10
3.4 Wind Tunnel Test Results: Aerodynamic Stability	11
3.5 Wind Tunnel Test Results: Static Force and Moment Coefficients.....	11
4. BUFFETING RESPONSE ANALYSIS AND WIND LOADS	13
4.1 Response Simulations	13
4.2 Mean and Background Fluctuating Wind.....	14
4.3 Inertial Loads Due to Wind-Induced Bridge Motions	14
4.4 Simplified Wind Load Distributions for Structural Design	15
5. HANGER VIBRATION ASSESSMENT	18



TABLE OF CONTENTS - CONTINUED

5.1	Background	18
5.2	Cable Assessment	19
5.2.1	Introduction	19
5.2.2	Vortex Shedding Oscillations	20
5.2.3	Rain-Wind Induced Vibrations (RWIV)	20
5.2.4	Assessment of Dry Cable Galloping	20
5.2.5	Assessment of Motion-Induced and Parametric Excitations	21
5.2.6	Iced Galloping	21
5.3	Conclusions and Recommendations	22

Tables

Table 2-1:	Recommended Wind Speeds at the Site at Deck Elevation (80 ft)
Table 2-2:	Turbulence Properties at Deck Level
Table 3-1:	Sectional Properties (Completed Bridge)
Table 3-2a:	Static Force and Moment Coefficients vs. Angle of Wind Attack (Completed Bridge)
Table 3-2b:	Weighted Force and Moment Coefficients (Completed Bridge)
Table 4-1a:	Static Force and Moment Coefficients used for the Wind Load Derivation (Preliminary)
Table 4-1a:	Static Force and Moment Coefficients used for the Wind Load Derivation (Final)
Table 4-2a:	Completed Bridge, Preliminary Wind Gust Factors, 100-Year Return Period
Table 4-2b:	Completed Bridge, Final Wind Gust Factors, 100-Year Return Period
Table 4-3a:	Completed Bridge, Peak Modal Deflections, 100-Year Return Period (Preliminary Loads)
Table 4-3b:	Completed Bridge, Peak Modal Deflections, 100-Year Return Period (Final Loads)
Table 4-4a:	Completed Bridge, Design Wind Loads, 100-Year Return Period (Preliminary Loads)
Table 4-4b:	Completed Bridge, Design Wind Loads, 100-Year Return Period (Final Loads)
Table 4-5:	Completed Bridge, Descriptions of Design Load Cases, 100-Year Return Period (Preliminary and Final)
Table 5-1a:	North Arch Hanger Properties
Table 5-1b:	South Arch Hanger Properties
Table 5-2a:	Vibration Control for North Arch Hangers
Table 5-2a:	Vibration Control for South Arch Hangers

Figures

Figure 1-1:	Elevation & Plan Views of the Kentucky Lake Bridge
Figure 1-2:	Kentucky Lake Bridge, Details of the Arch
Figure 1-3:	Kentucky Lake Bridge, Cross-sections
Figure 2-1:	Plan of Bridges Sites over Kentucky and Barkley Lakes
Figure 2-2:	3-second Gust Speed at 33 ft



TABLE OF CONTENTS - CONTINUED

- Figure 2-3: Mean Wind Speeds at Deck Level (80 ft)
- Figure 2-4: Wind Directionality at the Bridge Sites
- Figure 3-1: Sectional Model Test - Photographs of the Model in the Wind Tunnel
- Figure 3-2: Peak Vertical and Torsional Deflections – Completed Bridge
- Figure 3-3: Static Force and Moment Coefficients – Completed Bridge
- Figure 5-1: Hanger Identification System

Appendices

- Appendix A: Bridge Dynamic Properties
- Appendix B: Preliminary Design Wind Load Distributions
- Appendix C: Final Design Wind Load Distributions
- Appendix D: Background Information on Buffeting Analysis and Wind Loads



VERSION HISTORY

Lake Bridges RWDI Project No. 1301291		
Report	Releases	Dated
1. Final Report	2 nd Draft – Wind Engineering Studies	September 18, 2013
2. Companion Studies	1 st draft – Wind Engineering Studies Preliminary Design Wind Loads Wind Climatology Report	July 25, 2013 May 5, 2013 March 12, 2009
3. Project Team	Pierre-Olivier Dallaire, M.A.Sc., ing. Shayne Love, Ph.D. Mark Hunter, C.E.T. Stoyan Stoyanoff, Ph.D., P.Eng., ing.	Project Engineer Project Engineer Project Manager Project Director
4. Project Director Signature/Date	 Stoyan Stoyanoff, Ph.D., P.Eng., ing.	September 18, 2013



CONSULTING ENGINEERS
& SCIENTISTS

Lake Bridges - Kentucky Lake Bridge and Lake Barkley Bridge
Preliminary Wind-Induced Buffeting Analysis
RWDI#1301291
September 18, 2013

EXECUTIVE SUMMARY

Rowan Williams Davies & Irwin Inc. (RWDI) was retained by Michael Baker Jr., Inc., to conduct a wind engineering study for the proposed Lake Bridges over Kentucky Lake and Lake Barkley, KY. This study had the following objectives:

- to determine the wind design criteria required for aerodynamic stability and wind loading;
- to derive preliminary equivalent static wind loads, prior to the wind tunnel tests;
- to evaluate the basic aerodynamic characteristics of the completed deck via sectional model tests;
- to conduct wind buffeting analysis to design wind loads on the completed bridge design; and
- to assess the hangers for wind vibration stability.

Detailed Wind Climate Analysis was carried out in 2009 and included below. Table 2-1 summarizes the wind design criteria. For the completed bridge, a minimal flutter speed of 82.7 mph is recommended, being a 10-minute mean speed with a return period 10,000 years. For structural design, the mean hourly speed 69.6 mph is proposed. All speeds refer to the deck elevation 80 ft. Note that those speeds are specified in the Bridge Structure Design Criteria document and are applicable for both bridges. With almost identical configurations (except for the foundations) and with the results of each individual wind climate analysis being similar, the design criteria were combined to use the same wind speeds for both sites. Table 2-2 contains estimates of the local turbulence properties required for derivation of wind loads.

A sectional model test of the completed bridge deck was carried out in scale 1:60 examining its stability against vortex-shedding, galloping or flutter. The section was found to meet or exceed project criteria both for winds blowing to the walkway upwind and downwind. Static force and moment coefficients were also measured as required for derivation of design loads.

A wind buffeting analysis was conducted for the completed bridge (based on the Kentucky Lake dynamic information) where 28 different equivalent static load cases were derived for design. These loads include the effects of wind gusts and the dynamic response of the bridge. Design drawings, mass information and dynamic properties supplied by Michael Baker Jr., Inc. were applied (Appendix A). Theoretical buffeting response analysis was carried out and a set of equivalent static loads developed. Preliminary design loads were supplied early in the project design and included here in Appendix B. These were based on our experience with similar projects and a review of relevant literature. Aerodynamic properties of the arch ribs and bracings, piers and cables were assigned. Following completion of the sectional model tests, final design loads were derived and also included in this report, Appendix C. **All wind loads provided in this study do not contain any safety or load factors and are to be applied in the same manner as would wind loads calculated by code analytical methods.**

Cable vibration assessment on the hangers was also carried out. Conclusions and recommendations for control of hanger vibrations are presented.



CONSULTING ENGINEERS
& SCIENTISTS

1. INTRODUCTION

Rowan Williams Davies & Irwin Inc. (RWDI) was retained by Michael Baker Jr., Inc. to conduct a wind engineering study for the proposed Lake Bridges over Kentucky Lake and Lake Barkley, KY. The Kentucky Lake Bridge located on the north side of the existing Eggners Ferry Bridge, and the Lake Barkley Bridge located on the north side of the existing Lawrence Memorial Bridge. Both new bridges will be basket-handle, tied arch design and will have a main span length of 550' and a composite deck 100' wide including a 10' sidewalk and bike path. The arch South and North ribs are braced with Vierendell members. The design of both bridges is identical with the exception of the foundation properties. Figures 1-1 through 1-3 present drawings of the current design of the bridges.

1.1 Study Scope

The wind engineering services presented in this report included the following studies:

- **Local Wind Climatology Analysis:** This study included a wind climate and site analysis to determine the design wind speeds for aerodynamic stability and structural design of each bridge. Analysis of the turbulence properties at the site was also completed.
- **Sectional Model Study:** This study involved design, construction, and testing of a sectional model of the completed deck. The purpose of this test was to provide the design team with initial feedback on the aerodynamic stability of the deck configuration. The testing also provided static aerodynamic force and moment coefficients needed for wind loading calculations.
- **Buffeting Analysis and Equivalent Static Wind Loads:** A wind-induced buffeting analysis based on information assumed early in the project and also measured from sectional model tests was carried out. Preliminary and final wind loads were derived.
- **Cable Vibration Assessment:** An assessment of the potential for wind and wind/rain induced vibration of the hangers was carried out.

The following sections present the main findings of these studies. Based on previous experience¹ the expected effect of the existing truss Eggners Ferry and Lawrence Memorial Bridges will be to shadow and break the correlation in the incoming winds thus reducing wind loads and eliminating wake induced aerodynamic instabilities. Therefore in this study it was conservatively ignored. Appendix A contains the dynamic properties of the Kentucky Lake Bridge used in this study as prepared by Michael Baker Jr., Inc., of the completed bridge. Preliminary design wind loads were derived for the 100-year wind speed (Appendix B). Appendix C presents the final wind loads based on the static force and moment coefficients measured in the tunnel. Appendix D provides background information on buffeting response analyses and derivation of wind loads.

¹ Stoyanoff, S., Kelley, D., Irwin, P. Abrahams, M. and Bryson J. Aerodynamic Analysis and Wind Design for the Cooper River Bridges Replacement, in Proc. IBC Pittsburgh, Pennsylvania, IBC 03-52, June 9-11, 2003.



CONSULTING ENGINEERS
& SCIENTISTS

2. WIND CLIMATE ANALYSIS

2.1 Introduction

This section of the report presents the analysis of the wind climate and wind turbulence properties undertaken at the two bridge sites. The results presented in this section are used in subsequent analyses to assess the aerodynamic stability of the bridges and to determine their wind loads for structural design.

2.2 Wind Climate and Site Analysis

2.2.1 Source of Data

The wind statistics used to determine the design wind speeds at the bridge site were based on the surface wind measurements taken between 1951 and 2007 at Fort Campbell Army Air Field. This section recommends design wind criteria required for stability analysis and derivation of wind loads for the bridge. References to ASCE 7-05 Standard are also given.

2.2.2 Local Terrain

The terrains surrounding the airport anemometer and the two bridge sites were reviewed based on topographic maps produced by The United States Geological Survey (USGS), (Figure 2-1), satellite images and site photographs. Adjustments were made, where necessary, for the terrain roughness upwind of the anemometer and for the anemometer height above the ground.

2.2.3 Analysis

The design wind speeds for the bridge site were determined using the following steps:

- (i) The joint probability of wind speed and direction for the site was determined based on the available meteorological data. The analyzed wind data were then expressed in the form a mathematical model.
- (ii) The mathematical model developed for the selected station was used to evaluate wind speed as a function of return period and also to evaluate the component of the wind velocity normal to the bridge span as a function of return period. A procedure called an "Upcrossing Analysis" was used in this second step.

According to the speed map of ASCE 07-05 Standard, the 3-sec gust speed for this region is 90 mph. Figure 2-2 shows the 3-second gust speed in open terrain at elevation 33 ft derived for the bridge site from the Fort Campbell Army Air Field as well as the ASCE-7 recommendations. For the purposes of this study, the Fort Campbell data has been scaled to match the ASCE-7 Standard at the 50-year return period as shown in Figure 2-2. This scaled data set is the basis for the recommended wind speeds for the bridge sites.



CONSULTING ENGINEERS
& SCIENTISTS

Results contained in this report are discussed as mean-hourly (i.e., 1-hour mean) speeds, which are directly applicable for design, or as a 10-minute mean speeds. In this study, these 10-minute speeds are given since this is the typical time for an aerodynamic instability to develop on a large structure as bridge. To relate the mean-hourly wind speed to the 10-minute mean, the relationship shown in Figure C6-1 of the ASCE 7-05² was assumed. According to this curve, a 10-minute mean wind speed can be converted from the 1-hour mean speed multiplying it by a factor of 1.067. According to the same relationship curve, a 3-second gust speed is higher by a factor of 1.52 than a 1-hour mean speed. Further conversions to account for the local terrain conditions at bridge site were made using the ESDU³ methodology.

2.2.4 Joint Probability of Wind Speeds and Directions

A mathematical model of the joint probability of wind speed and direction was fitted to the meteorological wind data assuming Weibull type distribution. This distribution expresses the probability of the wind speed at a given elevation exceeding a value U as

$$P_{\theta}(U) = A_{\theta} \exp \left[- \left(\frac{U}{C_{\theta}} \right)^{K_{\theta}} \right], \quad (2-1)$$

where P_{θ} is the probability of exceeding the wind speed U in the angle sector θ ,
 θ is the central angle of an angle sector, measured clockwise from true North; and
 $A_{\theta}, C_{\theta}, K_{\theta}$ are coefficients selected to give best fit to the data.

Note that A_{θ} is the fraction of time the wind blows from within the angle sector θ . The size of angle sectors used in this analysis was 10 degrees. To provide additional flexibility in curve fitting for normal winds, two Weibull curves were fitted, one to lower velocities and one to higher velocities, with a blending expressions being used to provide a smooth transition. This “double” fitting technique was used in modeling the normal winds data recorded at the Fort Campbell Army Air Field.

From the probability distributions given by Equation (2-1), the overall probability of wind speed was obtained by summing over all wind directions.

$$P(U) = P_N(U) = \sum_{\theta} [P_{\theta N}(U)] \quad (2-1)$$

where the subscript N refers to normal winds.

At the gradient height the wind speeds are well above the earth’s surface roughness effects. The height used for determining gradient speed was 2000 ft (600 m) for the local meteorological stations. Since the

² American Society of Civil Engineers 7-05 Minimum Design Loads for Buildings and Other Structures, *Revision of ANSI/ASCE 7-02*.

³ ESDU International, *Wind Engineering Subseries Volumes 1a and 1b*, 1993 Edition, London, England.



CONSULTING ENGINEERS
& SCIENTISTS

anemometer is near ground level at the bottom of the planetary boundary layer, it is affected by ground roughness. These ground roughness effects were assessed using the methods given in ESDU⁴ combined with information on the local terrain roughness gathered from the topographic maps and other site information. Factors were developed to convert the anemometer records to wind speeds at gradient height and then to the bridge site.

2.2.5 Upcrossing Method to Determine Design Winds

By adapting random noise theory to meteorological data (Rice⁵), it can be shown that the return period, R , in years of a given gradient wind speed, U_G , is related to $P(U_G)$ by

$$R = - \left[\frac{|\dot{U}_N|}{2} \frac{dP_N(U_G)}{dU_N} (T_A) \right]^{-1}, \quad (2-3)$$

where $|\dot{U}|_N$ are the averages of the absolute rates of changes of the hourly values of U for normal winds with time, T_A , is the total number of hours in a year, i.e., $T_A \approx 8766$.

Equation (2-3) was used to determine the return periods for a series of selected wind speeds. The wind speed corresponding to a required return period (e.g., 100, 1000 years etc.) could then be determined by interpolation. This method is called the Upcrossing Method.

Since there is evidence⁶ that for flutter instability the important component of wind velocity is that normal to the span, it is of interest to evaluate this normal component as a function of its return period. It can be shown^{7,8} that if U_B denotes the wind velocity on the boundary of instability (in this case, the flutter velocity as defined for wind normal to the span, divided by the cosine of the actual angle between the wind direction and the normal to the span), then the return period R is given by

$$R = - \left[\sum_{\theta} \left(\frac{|\dot{U}_{NB}|}{2} \frac{dP_{\theta N}}{dU_{NB}} \sqrt{1 + \left(\frac{|\dot{\theta}_{NB}|}{|\dot{U}_{NB}|} \frac{dU_{NB}}{d\theta_N} \right)^2} (T_A) \right) \right]^{-1}, \quad (2-4)$$

where $|\dot{\theta}|_N$ are the averages of the absolute rates of changes of wind direction for normal winds.

⁴ Engineering Sciences Data Unit, Characteristics of the Atmospheric Turbulence Data Near the Ground: Part III, Variations in Space and Time for Strong Winds, ESDU 86010, London, UK, 1986.

⁵ Rice, S.O., Mathematical Analysis of Random Noise, *The Bell System Technical Journal*, Vol. 23, 1944.

⁶ Irwin, P.A. and Schuyler, G.D., Experiments on a Full Aeroelastic Model of Lions' Gate Bridge in Smooth and Turbulent Flow. National Research Council of Canada, *NAE Report LTR-LA-206*, 1977.

⁷ Lepage, M.F., and Irwin, P.A., A Technique for Combining Historic Wind Data with Wind Loads, *Proc. 5th U.S. National Conference on Wind Engineering*, Lubbock, Texas, 1985.

⁸ Irwin, P.A., Prediction and Control of the Wind Response of Long Span Bridges with Plate Girder Decks, *Proc. Structures Congress '87/ST Div/ASCE*, Orlando, Florida, August 17-20, 1987.



CONSULTING ENGINEERS
& SCIENTISTS

2.3 RESULTS

Figure 2-3 shows various mean-hourly wind speeds at deck level of 80 ft as a function of return period. This figure presents the following information:

- Mean hourly speeds at deck level for both the Kentucky Lake Bridge and the Lake Barkley Bridge for return periods from 1 to 10,000 years derived from the available meteorological data from Fort Campbell Army Airfield scaled to match the ASCE-7 Standard at the 50-year return period.
- The 10-min mean speed of 1,000 and 10,000-year return period including the effect of wind directionality on flutter stability.

Mean hourly speeds are to be used for derivation of design loads whereas 10-minute speeds are to be applied for stability verifications.

2.3.1 Wind Directionality Effects

For the Kentucky Lake Bridge, the main span axis is oriented at about 80° angle taken clockwise from North (see Figure 2-1). Therefore, winds normal to the span would blow from approximately 170° (~South) and 350° (~North). For the Lake Barkley Bridge, its axis is at about 110° (see Figure 2-1). Therefore, normal to its span winds would blow from the directions of approximately 200° (South-Southwest) and 20° (North-Northeast).

Figure 2-4 shows 10, 100 and 1,000-year probability of exceeding various mean-hourly wind speeds at deck height (taken as 80 ft) as a function of wind direction. The directionality of the wind shown in this figure was determined by using the probabilities of exceeding various mean wind speeds from within each of thirty-six sectors. Figure 2-4 shows that the most probable directions for strong winds (e.g., once in 100 years) are from the west-southwest (250°). Since the loading of individual structural components varies differently with wind direction, it is difficult to develop a generally applicable directionality reduction factor for all structural components. This, combined with the above-mentioned alignment of strong winds, indicates that no directionality reduction should be applied to the wind loads for design winds. However, there is evidence (Irwin and Schuyler⁵) that flutter instability is essentially a function of the wind velocity component normal to the span. Therefore, using the method described by Irwin and Lepage⁷, directionality reductions of 0.92 and 0.91, corresponding to the Kentucky Lake Bridge and the Lake Barkley Bridge, respectively, have been computed to arrive at wind speed normal to the spans as a function of return period for speeds in the range of interest for flutter.

2.3.2 Terrain at the Bridge Sites

The terrain surrounding the existing bridge is a combination of open water, farmland with many trees and hedges, light suburban areas and hills. As an approximate approach to assess the terrain effects, the ESDU⁹ method was used. The farmland, hills and suburban terrain were taken as having roughness

⁹ ESDU International, Computer program for wind speeds and turbulence properties: flat or hilly sites in terrain with roughness changes, ESDU 01008, 2001.



CONSULTING ENGINEERS
& SCIENTISTS

lengths in the range of $z_0 = 0.6$ ft to 1.0 ft. The roughness lengths of the water fetches were determined by ESDU and were in the range of 0.01 ft to 0.016 ft. Note that the wind speed profiles around the bridge site, determined using this method, resulted in α (power law exponent) values ranging from 0.12 to 0.17.

2.3.3 Wind Speeds at Deck Height

The ratio of the mean velocity at the deck height 80 ft to the mean velocity in standard open terrain at 33 ft (from Section 2.2.3) was found to be 1.1. The 100-year mean-hourly velocities at the deck level were predicted as 69.0 mph and 69.6 mph, corresponding to the Kentucky Lake Bridge and the Lake Barkley Bridge, respectively. Figure 2-3 also shows the mean wind speeds at deck height as a function of return period relevant for this study.

2.3.3.1 Structural Design Wind Speed

For structural design of bridges, a return period of 100 years is typically used. As described in the previous section, the 100-year mean-hourly speeds were estimated to be 69.0 mph and 69.6 mph at deck level (Table 2-1). For the construction phase, a 10-year return period is typically recommended for which the estimated mean-hourly speeds are 60.0 mph and 60.5 mph, respectively.

2.3.3.2 Design Wind Speed for Aerodynamic Stability

For flutter instability of the completed bridges, a very long return period needs to be considered because, if flutter occurs, there is a very high probability of structural failure. The recommended return period is 10,000 years. Figure 2-3 indicates that the ratio of the 10,000-year wind velocity to 100-year wind velocity is 1.22. Therefore, if directionality is not included, the mean-hourly velocities for the 10,000-year return period are predicted to be 84.1 mph and 84.9 mph, corresponding to the Kentucky Lake Bridge and the Lake Barkley Bridge, respectively. If directionality is included, the 10,000-year mean-hourly speeds normal to the spans are predicted to be 77.4 mph and 77.3 mph, respectively. As previously discussed, flutter oscillations can build up over shorter periods than 1 hour; therefore, the recommended 10,000-year speed is a 10-minute mean value. The design flutter velocities are calculated to be 89.8 mph and 90.6 mph without directionality and 82.5 mph and 82.7 mph with directionality. For construction, a shorter return period is justifiable due to the shorter length of the construction period, and 1,000 years is recommended. The 1,000-year 10-minute mean recommended flutter speeds, arrived at by a similar approach, are 75.5 mph and 75.6 mph, respectively, with directionality included.

2.3.4 Turbulence Properties at the Bridge Sites

The same ESDU⁹ methodology used in determining the wind speeds at the deck level was also applied in estimating the turbulence intensities and length scales at the site. The turbulence intensities (I_u , I_w , I_v and length scales (xL_u , xL_w , yL_u , yL_w , and zL_u), which are most important for the buffeting response of long-span bridges to strong winds, are given in Table 2-2. The effect of the existing truss bridges was ignored based on previous experience¹ expecting it to be reducing wind loads and mitigating (if any) aerodynamic instabilities.



CONSULTING ENGINEERS
& SCIENTISTS

2.4 Wind Climate Analysis: Summary

The design wind speeds resulting from the wind climate and site analysis for the Kentucky Bridges are summarized in Table 2-1. The resulting turbulence properties are shown in Table 2-2. The mean-hourly speeds are recommended for bridge design, and the 10-minute mean speeds are recommended for stability evaluations both during construction and for the completed bridge. The long-term wind records from Fort Campbell Army Airfield were used, as well as reference made to the design wind information in the ASCE Standard. Open water and the open/suburban terrain around Kentucky Lake and Lake Barkley affect the exposure of the bridge sites. Their influence has approximately been accounted for in arriving at the recommended speed values given in Table 2-1.

Note that the final speeds to be used for load derivation and stability verification are indicated in the Bridge Structure Design Criteria document and are applicable for both bridges. With both bridge designs being almost identical (except for the foundations) and with the results of each individual wind climate analysis being very similar, the design criteria were combined to use the same wind speeds for both sites (upper bound values). Therefore, the recommended 100-year mean hourly and 10,000-year speed 10-minute mean values are 69.6 mph and 82.7 mph, respectively. Those speeds refer to the elevation of 80 ft.



CONSULTING ENGINEERS
& SCIENTISTS

3. SECTIONAL MODEL TEST

3.1 Objectives and Criteria

The objectives of the sectional model tests were to:

- i. Examine the aerodynamic stability of the deck in its completed state with the walkway upwind and downwind.
- ii. Extract the static force and moment coefficients for winds normal to the deck.

For the Lake Bridges, only the section of the main span was of concern considering vortex shedding. Given the relatively high torsional frequencies, flutter was less of a concern for these bridges.

To meet the project schedule, RWDI rented the wind tunnel test facility of the University of Sherbrooke in Sherbrooke, Quebec. Through comparative sectional model tests, all equipment including the test rig and instrumentation has been tested and verified by RWDI. Figure 3-1 shows a view of the model in this tunnel with a working section of 6 ft x 6 ft. During this test, model builder support and engineering staff was supplied by RWDI.

The following aerodynamic instabilities were investigated during the testing:

- i. **Flutter:** is a self-excited aerodynamic instability that could grow to very large amplitudes in torsional motion only, or into coupled torsional and vertical motions. Flutter instability should be avoided at all costs since it can lead to bridge failure.
- ii. **Vortex-Induced Oscillations:** are self-limiting vibrations caused by the alternate and regular shedding of vortices from both sides of a bluff body, such as the bridge deck. These types of vibrations can be tolerated provided their amplitudes, and associated accelerations, do not exceed recommended thresholds. The main concerns associated with excessive vortex shedding responses are serviceability and fatigue. Serviceability relates to the comfort of bridge users, since excessive motions could cause user discomfort. Fatigue relates to cyclic loading of key structural elements, which could compromise the integrity of the structure.
- iii. **Galloping:** is a quasi-static type of instability that is sometimes found on narrow bridge decks (ratio width/depth < 5). Due to a negative rate of change in lift, the section may start to move vertically across-the-flow to very large amplitudes. The 2DOF (two-degree-of-freedom) sectional test procedure for flutter allowing for vertical and torsional motions, can also identify whether this type of instability exists.

As discussed in Section 2, a minimum mean wind speed of 82.7 mph is required for flutter stability verifications of both completed bridges with a return period of 10,000 years. Given speeds are 10-minute mean referring to deck height. For the testing conducted during the current study, the onset of flutter instability has been defined as when the peak torsional amplitude exceeds 1.5 degrees. This level of



CONSULTING ENGINEERS
& SCIENTISTS

motion could approximately be excited at high wind speeds by turbulence, even on a stable section, and it was therefore assumed as a reasonable amplitude threshold for instability. Considering the open terrains at the bridge site and expected high flutter speeds, only zero degree angle of wind attack was examined.

A construction stage deck configuration of this bridge was not examined expecting measures be taken by the erection engineers and the contractor depending on the selected erection scheme. We recommend these erection conditions be verified by a Wind Engineering Consultant.

Criteria for vortex excitation of bridges are typically expressed in terms of maximum allowable accelerations. For this bridge, the peak vertical acceleration should be kept below 5% of gravity for mean winds up to 30 mph and below 10% of gravity above 30 mph up to 45 mph. Based on the dynamic properties of the bridge adopted for sectional model testing, these accelerations were converted to deflections. For rotational accelerations, the critical torsional radius was established at a distance from the center of rotation to the middle of the walkway 32 ft. For winds above about 45 mph, this criterion with respect to vortex excitation becomes less important since people and vehicles on the bridge are more likely to be severely affected by the wind and therefore there would be very few vehicles and pedestrians on the bridge.

3.2 Description of the Sectional Models

A sectional model of the Lake Bridges was constructed at a scale of 1:60 representing a 360 ft long section at full scale. The sectional model of the main span was used for extracting all basic information required for stability and force coefficients. Figure 3-1 shows images of the modeled cross section. The proximity effects of the river were taken into account by a ground plate installed at the expected normal pool level beneath the deck model.

The sectional model was constructed of wood, plastic and metal. The design of sectional model was based on the geometry, the average mass per unit length, and the dynamic properties of the bridge (e.g., natural frequencies and mode shapes), provided by Michael Baker Jr. Table 3-1 lists the design parameters at model scale and full scale main span of for the completed bridge.

The sectional model of the main span was mounted on a spring suspension system. The suspension system was built directly into the sidewalls of the wind tunnel with the springs located outside of the tunnel walls. This suspension system allowed 2DOF vertical and torsional motions to be simulated. Laser displacement transducers were used during the tests for measurement of these vertical and torsional motions. The loading on the section was measured using strain-gauged flexures attached to the model's centre of rotation and the end spring supports. Figure 3-1 presents a photograph taken at the wind tunnel showing the actual setup.

Selection of an appropriate stiffness and spacing of the springs permitted tuning of the model of the main span to the desired vertical and torsional frequencies for testing. The first symmetric vertical modal frequency (Mode 6 with a frequency of 1.035 Hz) and first symmetric lateral/torsional modal frequency (Mode 9 with a frequency of 1.226 Hz) of the Completed Bridge were selected as target values for the



CONSULTING ENGINEERS
& SCIENTISTS

wind tunnel tests. These modes were selected because of their potential coupling during wind-induced response, which could result in coupled vertical-torsional flutter. It is worth noting that although the sectional model was designed primarily for a given pair of modes, the test results can also be extended to other modes by adjusting the velocity scale.

Damping was added to the system by energy absorption devices located outside of the tunnel. These devices allowed the structural damping for vertical and torsional motions to be adjusted as desired. The assumed vertical and torsional modal damping ratios were taken to be approximately 0.5% of critical. The target damping levels for testing and the obtained levels are listed in Table 3-1. Corrections with the appropriate mode shape factors were also applied.

In this report, unless otherwise stated, all results (e.g., speeds and deflections) are presented at full scale. The full-scale wind speeds in smooth flow are interpreted as 10-minute mean wind speed at deck height.

3.3 Description of the Wind Tunnel Test Procedures

3.3.1 Stability Tests

The stability tests were conducted on the main span section for angles of wind attack 0 and ± 2.5 degrees. Given that there are no important topographical features to deflect the flow permanently off the horizontal this was considered sufficient. The angle of attack is the inclination of the wind to the horizontal plane of the deck being positive when the windward leading edge moves upwards. For each test, the wind speed was gradually increased in small steps and the motions in both the vertical and torsional directions were recorded. The wind speed is increased until the model attains flutter instability or beyond the 10,000-year return period flutter speed for the Completed Bridge (if tested in would be the 1,000-year return period flutter speed for the Construction Stage). Due to the asymmetry of the deck section, tests were completed with the pedestrian walkway upwind and downwind for the Completed Bridge. Although not tested, the typical removal of the barriers for the Construction Stage configuration is expected to improve aerodynamic stability and reduce the lateral wind loads.

Stability tests were conducted on the main span sectional model in smooth for all angles of attack. The purpose of the smooth flow tests was to allow instabilities such as vortex shedding or flutter to be readily identified. Results that are based on smooth flow tests can be considered conservative. Turbulent flow tests, on the other hand, give a more realistic indication of the bridge's response in strong winds, since the natural wind tends to be turbulent.

3.3.2 Static Force and Moment Coefficient Tests

The same suspension rig with rigid connections instead of springs (to minimize motions of the model) was used to measure the static force and moment coefficients on the main span. These coefficients were measured within the angles of attack ranging ± 10 degrees in 2-degree increments in smooth flow. The following deck configurations were examined:

- Completed Bridge with the walkway upwind; and
- Completed Bridge with walkway downwind



CONSULTING ENGINEERS
& SCIENTISTS

3.4 Wind Tunnel Test Results: Aerodynamic Stability

The vertical and torsional responses from the sectional model tests of the main span section for aerodynamic stability are provided in Figure 3-2. These tests were performed at with a 0.5% damping ratio.

Figure 3-2 shows the peak vertical and torsional responses as a function of wind speed for various angles of attack and wind directions. The governing criteria for vortex shedding and flutter instabilities are also provided. Recall that for winds above about 45 mph, comfort criteria with respect to vortex excitation becomes less important since bridge users and vehicles are more likely to be affected by wind buffeting.

No vortex shedding, flutter and/or galloping were observed through wind speeds greater than 110 mph for all tested configurations. The gradual response increase at higher wind speeds is due to self-induced buffeting which normal and not considered being instability. Therefore the main span section is considered to be aerodynamically stable for the Completed Bridge.

3.5 Wind Tunnel Test Results: Static Force and Moment Coefficients

Static force and moment coefficients were calculated by normalizing forces and moments measured on the deck section as follows:

$$C_x = \frac{F_x}{\frac{1}{2}\rho U^2 D}, \quad C_z = \frac{F_z}{\frac{1}{2}\rho U^2 B}, \quad C_m = \frac{M}{\frac{1}{2}\rho U^2 B^2}, \quad (3-1)$$

where, F_x , F_z and M are lateral force (drag), vertical force (lift) and moment per unit length;

ρ is the air density (0.07647425 lb/ft³);

U is the mean wind speed at deck height;

D , the representative depth of the deck;

B is the representative width of the deck.

The measured force coefficients are illustrated in Figure 3-3. Force and moment coefficients were measured in 2-degree increments for angles of attack ± 10 degrees. As the force and moment coefficients are a function of angle of attack, and the effective angle of attack varies as a result of vertical turbulence and the bridge motion, the weighted averages of these coefficients are required for the buffeting analysis. These weighted averages were calculated from the following formulae:

$$\bar{C} = \int_{-\infty}^{\infty} C(\alpha) p(\alpha) d\alpha, \quad \frac{d\bar{C}}{d\alpha} = \int_{-\infty}^{\infty} \frac{dC(\alpha)}{d\alpha} p(\alpha) d\alpha, \quad (3-2)$$



CONSULTING ENGINEERS
& SCIENTISTS

where $p(\alpha)$ is the probability density of the angle of attack. A reasonable assumption is that this probability density could be expressed as a Gaussian distribution (since the fluctuations of the wind velocities in a turbulent flow are in general Gaussian). Also, the angle of attack is mainly due to the vertical component of turbulence velocity. Thus, the probability density of the angle of attack can be rewritten as

$$p(\alpha) = \frac{1}{\sqrt{2\pi}I_w} \exp\left(-\frac{1}{2}\left(\frac{\alpha}{I_w}\right)^2\right), \quad (3-3)$$

where I_w is the vertical turbulence intensity (see Table 2-2).

Tables 3-2 present the values of the coefficient measured at the tested angles of wind attack and as well, the turbulence weighed coefficients and their slopes for the two test configurations (i.e. walkway downwind and walkway upwind).



CONSULTING ENGINEERS
& SCIENTISTS

4. BUFFETING RESPONSE ANALYSIS AND WIND LOADS

4.1 Response Simulations

For derivation of the wind loads acting on the bridge, theoretical buffeting response analysis was carried out¹⁰ at the design wind speed of 69.6 mph. Dynamic information used for this analysis is given in Appendix A for the Completed Bridge (Kentucky Lake Bridge). Appendices B and C contains plots of all load distributions derived in this study. The background methodology^{11,12} of all the analysis is available upon request. The theoretical buffeting analysis estimates the bridge's responses in each of its modes of vibration to the random excitation of wind turbulence. Input parameters include static aerodynamic force coefficients, mass and polar moment of inertia, bridge dimensions, modal frequencies and shapes, structural damping, and wind turbulence properties. Typical forms of power spectra and co-spectra of turbulence, and representative aerodynamic admittance functions are then used for estimation of the resonant and background dynamic responses. The methodology can be traced back to Davenport¹³ (1961) and Irwin¹⁴.

Wind loads for the Kentucky Lake Bridge were derived using the design speed of 69.6 mph, which is the 100-year return period mean hourly value at 80-ft elevation from Table 2-1. Table 2-2 contains the turbulence properties used for derivation of these loads. The analyses are based on the dynamic properties of the bridge obtained from Michael Baker Jr., Inc. on April 18, 2013 (see Appendix A). For the preliminary design loads, representative static force and moment coefficients (C_x , C_y , C_z , C_{mx}) and their slopes (dC_x/da , dC_y/da , dC_z/da , dC_{mx}/da) were estimated based on previous wind tunnel measurements carried out on a similar deck section, literature, experience of previous projects with similar features. For the final design wind loads, static force and moment coefficients were obtained from the sectional model tests. Tables 4-1a and 4-1b summarize the retained static force and moment coefficients used for each analysis, which are consistent with the convention described in the notes below the tables. A structural damping ratio of 0.5% was applied through the calculations. In order to carry out predictions of the bridge response, a discrete model made of a collection of "strips" representing the deck, the arches and the hangers was established based on the bridge geometry and dynamic information. For each discrete strip, corresponding mass, mass moment of inertia, mode shapes, representative dimensions and aerodynamic properties were assigned. Turbulence was simulated numerically based on the site properties in terms of mean profile, intensity of turbulence, length scales, correlations and wind power spectra. The simulation included time series of $u(t)$, $v(t)$, and $w(t)$ wind components at all 342 strips of the wind numerical model (206 strips to represent the deck assembly, arch ribs & bracings, piers elements and 136 additional strips

¹⁰ Stoyanoff, S. A unified approach for 3D stability and time domain response analysis with application of quasi-steady theory, *Journal of Wind Engineering and Industrial Aerodynamics*, v. 89, pp. 1591-1606, 2001.

¹¹ RWDI BR01-2007, Numerical Simulation of Wind Turbulence, March 7, 2007.
RWDI BR02-2007, Wind Response Analysis and Design Loads, March 30, 2007.

¹² Stoyanoff, S. and Dallaire, P-O., A Direct Method for Calculation of Wind Loads on Long-Span Bridges, in Proc., of The 12th Americas Conference on Wind Engineering (12ACWE), Seattle, Washington, USA, June 16-20, 2013.

¹³ Davenport, A.G., The response of Slender Line-Like Structures to a Gusty Wind, *Institute Civil Eng.* 23, 389-408, 1962.

¹⁴ Irwin, P.A., Wind Tunnel and Analytical Investigations of the Response of Lions' Gate Bridge to a Turbulent Wind, National Research Council of Canada, *NAE Report LTR-LA-210*, June 1977.



for the hangers). A total of 21 wind simulations, each of 54.6 minutes in duration were carried out in a time step of 0.05 sec. 3D Buffeting Response Analysis¹¹ was then carried out and the required statistics were extracted from the results.

4.2 Mean and Background Fluctuating Wind

The total wind loads considered for the structural design should be the peak loads, which include the mean wind loads, the background fluctuating wind loads, and the inertial loads due to the structural motions. The mean loads for winds acting on a bridge are calculated as

$$F_x = \frac{1}{2} \rho U^2 C_x D, \quad F_y = \frac{1}{2} \rho U^2 C_y D, \quad F_z = \frac{1}{2} \rho U^2 C_z B, \quad M_x = \frac{1}{2} \rho U^2 C_{mx} B^2, \quad (4-1)$$

where U is the mean wind speed at deck height. In this example (Eq. 4-1), D and B are the depth and width of the deck elements (note: these reference lengths can differ on other members), and C_x , C_y , C_z and C_{mx} are the static force coefficients. Wind turbulence or gustiness causes fluctuations in wind loading about the mean. These loads are complex since wind gusts are not well correlated along the span and even over the width of the deck. However, via integration of the instantaneous wind loads over the entire bridge structure in a time domain simulation, appropriate gust factors g_{gust} were derived (Tables 4-2). These gust factors when applied on the mean wind pressure, adequately account for the direct gust loading on the bridge. As a reasonable simplification, the background forces and moments were derived by multiplying the corresponding mean loads by factors of

$$g_{l,back} = (g_{l,gust} - 1), \text{ to obtain} \quad (4-2)$$

$$F_{l,back} = g_{l,back} F_l, \quad \text{where } l = x, y, z, mx.$$

As previously mentioned, the static force and moment coefficients on the deck section used for derivation of the wind loads for winds normal to the bridge span (considering an allowance for skewed angles) are presented in Tables 4-1a and 4-1b.

4.3 Inertial Loads Due to Wind-Induced Bridge Motions

An important effect of fluctuating wind loads is to induce structural motions, which in turn creates inertial loads. The magnitude of the inertial loads depends on the structural dynamic properties. Generally, the peak inertial loads due to the j^{th} mode of vibration are given by:

$$F_j(s) = (2\pi f_j)^2 \delta_j m(s) \Phi_j(s), \quad \text{for } j = 1, 2, \dots, n, \quad (4-3)$$

where

- $m(s)$ is the mass (for inertial force) or mass moment of inertia (the inertial torsional moment) of each section;
- f_j is the modal frequency;



CONSULTING ENGINEERS
& SCIENTISTS

- δ_j is the peak modal value of the j^{th} modal resonant deflection;
- $\Phi_j(s)$ is the mode shape; with s as a coordinate along deck, arch; and
- n the number of modes considered for response analysis.

On April 18, 2013, modes of vibration were compiled and provided to RWDI by Michael Baker Jr., Inc., to carry out a preliminary 3D Buffeting Analysis. These modes are presented in Appendix A. After reviewing this information, RWDI selected the first 16 modes with regards to wind load effects. The predicted peak modal deflections used to derive the wind loads are summarized in Table 4-3a. The estimated resonant deflections together with the expected mean and background pressures were used to derive the simplified wind loads. This process was repeated using the static force and moment coefficients from the sectional model tests (see Table 4-3b).

4.4 Simplified Wind Load Distributions for Structural Design

To estimate the overall load effects on the structure (such as stress or strain on each structural member), a general approach is to calculate the load effects for each load component and then use an appropriate statistical approach (such as the root-sum-of-squares method) to combine the peak dynamic effects due to the fluctuating loads and the inertial loads. However, this approach does not always fit the normal procedures of design offices. In view of this, sets of more approximate simplified wind load cases are provided based on linear combinations of the dynamic loads in the various modes of vibration. These simplified load distributions are provided electronically in Tables 4-4a and 4-4b and are plotted in Appendixes B and C. Pressures and formulae to calculate the loads on the hangers are also provided in Tables 4-4a and 4-4b. For convenience, the loading tables are designated as Electronic Tables 4-4a and 4-4b (Excel format) containing loads for the bridge. The wind coordinate system (see Sketch 1 provided in Electronic Table 4-4) used for derivation of these wind loads is consistent with the structural coordinate system from Michael Baker Jr., Inc. Descriptions of the loads cases are provided in Table 4-5 and are applicable for both the preliminary and final loads.

Loads on the bridge deck assembly per unit length at node location are then defined as:

Along-the-bridge Loads,	$F_x = \rho_x D,$
Lateral Loads,	$F_y = \rho_y D,$
Vertical Loads,	$F_z = \rho_z B,$
Torsional Loads,	$M_x = \rho_{mx} B^2,$

where,

The respective pressures given in (psf) are $\rho_{x, y, z, mx},$	
Deck depth,	$D = 9.38 \text{ ft},$
Deck width,	$B = 100 \text{ ft}.$

The loads provided should be applied at the centre of gravity of each deck assembly element. Linear interpolation between consecutive nodes is recommended. These loads can be distributed over the exposed deck areas to produce the same overall loads about the center of gravity.



CONSULTING ENGINEERS
& SCIENTISTS

Loads per unit length of arch rib, arch bracing, pier cap and footing:

Along-the-bridge Loads,	$F_x = \rho_x D,$
Lateral Loads,	$F_y = \rho_y D,$
Vertical Loads,	$F_z = \rho_z B,$

where,

The respective pressures given in (psf) are $\rho_{x,y,z}$

Depth, varies, see Electronic Table 4-4,

Width, varies, see Electronic Table 4-4.

The loads provided should be applied at the centre of gravity of each element. Linear interpolation between consecutive nodes is recommended. These loads can be distributed over the exposed member areas to produce the same overall loads about the center of gravity.

Loads per unit length of column:

Along-the-bridge Loads,	$F_x = \rho_x B,$
Lateral Loads,	$F_y = \rho_y D,$
Vertical Loads,	$F_z = \rho_z B,$

where,

The respective pressures given in (psf) are $\rho_{x,y,z}$

Column depth, $B = 12$ ft,

Column width, $D = 12$ ft.

The loads provided should be applied at the centre of gravity of each column element. Linear interpolation between consecutive nodes is recommended. These loads can be distributed over the exposed column areas to produce the same overall loads about the center of gravity.

Formulae were given in order to calculate wind loads on the hangers:

Along-the-deck loads per unit length of hanger (lb/ft),	$F_x = 5 D \text{ sign}A,$
Lateral loads per unit length of hanger (lb/ft),	$F_y = 19 D$
Total along-the-deck force per hanger (lb),	$T_x = F_x L,$
Total lateral force per hanger (lb),	$T_y = F_y L,$

where,

$\text{sign}A$ is defined for each load case (see in Electronic Table 4-4),

D is the outer diameter of each hanger (ft), and,

L is the total length of hanger *anchor-to-anchor* (ft).

Provided wind loads should be applied along each hanger.



CONSULTING ENGINEERS
& SCIENTISTS

In each of the load combinations, the load patterns on the bridge are given as distributed vertical, lateral, along-the-deck, and torsional moment loads, which have to be applied simultaneously to the deck members, the arch members, the piers and the hangers. Each of these load cases presents an individual worst case in terms of the vertical or lateral loading on the deck, lateral loading on the arch, with various combinations of the bridge modes of vibration. For every load case, pressures are given at selected nodes of the numerical model of the Kentucky Lake Bridge.

It is recommended that all of the given load cases are to be used and that each main structural member should be designed based on the corresponding load case that gives the worst load effects (i.e., stress and strain). These presented wind load distributions correspond to south winds. For consideration of north winds, the loads may be considered to be reversible. For all wind load cases, the transverse wind loads (p_y) given for each case could also be considered for the opposite sign to that provided in the table. To apply the transverse loads in this fashion, the simultaneous moments (p_m) should also have their sign reversed and all simultaneous loading on the arch and pier members would need to be mirrored about the x-axis.

Note that the design wind loads provided in this report do not contain any safety or load factors and are to be applied to the structural system in the same manner as would wind loads calculated by code analytical methods.



CONSULTING ENGINEERS
& SCIENTISTS

5. HANGER VIBRATION ASSESSMENT

5.1 Background

Bridge hangers may vibrate due to the following causes:

1. Vortex shedding
2. Rain/wind induced vibrations (RWIV)
3. Galloping of a hanger due to its inclination to the wind
4. Wake galloping
5. Galloping due to ice accretion
6. Excitation from vibrations in other parts of the bridge being transmitted through the anchorages
7. Buffeting from wind turbulence

Wind-induced vibrations of hangers occur primarily due to their low inherent damping. In the absence of any supplementary damping devices the damping ratio is typically in the range of 0.1% to 0.3% and values as low as 0.03% have been measured on very long cables.

Vortex shedding is the alternate shedding of vortices from the two sides of a hanger, which causes cross-wind forces at well-defined frequencies. This results in limited amplitude oscillations in various vibration modes. Typically, the amplitudes are less than half the hanger diameter, and do not cause problems.

Rain/wind induced vibration (RWIV) can reach much larger amplitudes and are due to the aerodynamic effects of rivulets of water running down the hanger. In the past, RWIV has caused problems on a number of bridges, and have necessitated the development of solutions. Since the hangers are expected to be spiralled, which will disrupt the water rivulets, we anticipate that the potential for RWIV will be reduced. However, if the damping is low enough, RWIV may still occur.

Galloping of inclined hangers appears to be limited to cables with very low values of damping and may be due to small amounts of asymmetry (ovalling) in the cable cross section. If sufficient damping is present to quell RWIV, then typically inclined cable galloping will not occur. Wake galloping can occur when cables run parallel to each other and are in close proximity. The wake from an upstream cable can produce velocity gradients that cause downstream cables to gallop. Although the Kentucky Lake crossing has parallel hangers, the center-to-center hanger spacing is almost ten cable diameters, making it unlikely that wake galloping will occur. Ice accretion on cables can also cause galloping by changing the cross-sectional cable shape to one that is aerodynamically unstable. This type of instability is also known as Den Hartog galloping and is a recognized problem for power transmission cables.



CONSULTING ENGINEERS
& SCIENTISTS

Hanger vibrations originating from motions of the anchors can occur when the deck or bridge superstructure is excited by wind or traffic loading. If the excited deck/arch natural frequency matches a hanger natural frequency, small deck or arch motions may produce much larger hanger motions. This phenomenon is referred to as parametric excitation.

The last common cause of hanger vibration is buffeting. The spectrum of wind turbulence covers a broad range of frequencies. As a result, turbulence can excite a large number of bridge vibration modes. Typically, the amplitudes of motion are small at common wind speeds; however, at design level speeds the motions can be significant. There is little that can be done to avoid hanger motions due to buffeting, as buffeting affects the entire bridge structure, not just the hangers. They are described here for completeness but generally do not cause any cable specific problems during common wind events.

A universal and often implemented method for cable vibration control is the application of supplementary damping devices, which increase the damping of the cables. A criterion for how much damping is needed can be expressed in terms of the Scruton number¹⁵

$$Sc \equiv \frac{m\zeta}{\rho D^2} \quad (5-1)$$

where m = mass of cable per unit length, ζ = damping ratio, ρ = air density, and D = cable diameter. The excitation mechanisms described above will not produce substantial hanger motions if a minimum Sc value is achieved. In the following section, a minimum Sc value is therefore specified for each excitation mechanism, which is subsequently related to a minimum required damping ratio for each hanger. The governing cable damping ratio is then determined after considering all possible cable excitation mechanisms.

5.2 Cable Assessment

5.2.1 Introduction

Table 5-1 provides the hanger properties of the bridge for the north (Table 5-1(A)) and south (Table 5-1(B)) arches. Figure 5-1 shows the cable identification system used. In Table 5-1, the cable lengths, outer diameter, and tensions are based on the information provided by Michael Baker Jr., Inc on July 1, 2013. The hanger mass per unit length were provided via email on July 19, 2013. The hanger inclination angles were calculated using the hanger work point coordinates provided on April 18, 2013.

The estimated fundamental frequencies and mass-damping properties of the hangers are given in Table 5-2 for the north (Table 5-2(A)) and south (Table 5-2(B)) arches. Pipe outside diameters, masses per length and various damping levels were used for calculations of the Sc demands.

¹⁵ PTI Guide Specification. Recommendations for stay cable design, testing and installation. Post-Tensioning Institute Committee on Cable Stayed Bridges, 6th edition, April, 2012.



CONSULTING ENGINEERS
& SCIENTISTS

5.2.2 Vortex Shedding Oscillations

Vortex shedding may occur in the wind speed range of 1 to 7 mph for the fundamental modes of the hangers. Higher modes could be excited at higher wind speeds. Oscillations generated by vortex shedding will be suppressed if a Scruton number of at least $Sc = 2.5$ is maintained through the addition of supplementary damping. Table 5-2 shows the cable damping ratio required to achieve $Sc > 2.5$.

5.2.3 Rain-Wind Induced Vibrations (RWIV)

Our assessment for control of RWIV is based on a review of existing experimental data, discussions with researchers, and previous experience with existing bridges. An appropriate design for mitigation of these vibrations should include the following:

- Disrupting the flow of the water rivulet. For these hangers, the spiral of the wire rope is expected to disrupt the rivulet.
- Mass-damping characteristics that provide a minimum Scruton number $Sc > 5$ on those modes susceptible to RWIV (i.e., those modes with frequencies less than 3 Hz, and inclined between 20 and 60 degrees). This minimum value for Sc assumes that the water rivulet is disrupted by the spiraled wire rope. If the hangers were smooth, then the Scruton number would need to be at least $Sc = 10$.

Table 5-2 shows the damping ratios required to obtain the minimum Scruton numbers for the hangers with spiralling ($Sc \geq 5$) and smooth hangers ($Sc \geq 10$), as well as the hanger modes susceptible to RWIV. The recommended damping values provided in the last column of Table 5-2 have been determined assuming the hangers are spiralled, which disrupts the water rivulets.

5.2.4 Assessment of Dry Cable Galloping

The PTI Guide Specification¹⁵ stipulates that if cables have sufficient damping to prevent RWIV, dry cable galloping is also likely to be suppressed. Since this phenomenon has not been observed on any existing bridges having helical fillets on the cables, and since this phenomenon only occurs in a very narrow wind speed range, the probability of having dry cable galloping is considered to be very small. It should be noted that the PTI recommendation is based on $Sc = 10$, which is consistent with the damping requirements for suppression of RWIV on smooth cables. This suggests the theoretical possibility that dry galloping may still occur should the lower Scruton number be used for the suppression of RWIV. However, many cables on the existing bridges have Scruton numbers less than 10, and there are no documented cases of cables with fillets galloping. Therefore, we believe that the damping ratios required to control RWIV will also control dry cable galloping.



5.2.5 Assessment of Motion-Induced and Parametric Excitations

When a deck/arch natural frequency is close to a hanger natural frequency, it is possible that the hanger will experience large motions due to small motions of the deck/arch. We have compared the first 30 modal frequencies of the deck/arch to the fundamental frequencies of the hangers. Several hangers are found to have frequencies very close to those of bridge modes 17 to 30. To avoid parametric excitation, we recommend that the Scruton number of these hangers is at least $Sc = 5$. This requirement is typically not onerous, since RWIV requirements must achieve the same Scruton number.

5.2.6 Iced Galloping

Cable galloping due to ice and snow accretion is the classical Den Hartog¹⁶ case. The critical galloping speed can be estimated from

$$V_{cr} = U_R f D, \quad U_R = \frac{8\pi S_c}{-\left(\frac{dC_L}{d\alpha} + C_D\right)}, \quad (5-2)$$

where f is the fundamental cable frequency, $\frac{dC_L}{d\alpha}$ is the slope of lift coefficient (rate of lift coefficient change with angle of wind attack); and C_D is the drag coefficient (typically within range of 0.7 to 1.5, taken as 1.0).

The drag and slope of the lift coefficient vary depending on the shape of ice accretion. On a cable, ice would typically adhere to the windward side, producing an egg-shaped cross-section^{17,18}. On such a shape, the slope coefficient may take a value as low as -2.0. With these typical coefficient values, one can derive the Eurocode recommended formula^{19,20}

$$V_{cr} = K_{cr} S_c f D, \quad K_{cr} = 8\pi \approx 25, \quad (5-3)$$

which has also been suggested in earlier work done by the National Research Council of Canada²¹. The above formulae were applied to assess the iced galloping instability of cables on the proposed bridge.

Before estimating the required hanger damping for iced galloping, it is necessary to set the critical wind speed, V_{cr} , that is considered. The 100-year return period, 1-hour mean wind speed at deck elevation is estimated to be 69.6 mph. However, since hangers can become excited faster than the remainder of the

¹⁶ Den Hartog, J.P. Mechanical Vibrations, Dover Publications, New York, ISBN 0-486-64785-4, 1984.

¹⁷ K.F. Jones, Coupled vertical and horizontal galloping, ASCE, J. Eng. Mech. 118, pp. 92-107, 1992.

¹⁸ Institut Montefiore, University of Liege.

¹⁹ B. Svensson, L. Emanuelsson, & E. Svensson, Øresund bridge cable system-vibration incidents and alleviating measures, 4th Int. Cable Supported Bridge Operators' Conf., Copenhagen, 16-19 June 2004, 99-108.

²⁰ Eurocode EN 1993-1-11, feb. 2003.

²¹ Cooper, K.R. A Note on the Wind Induced Vibrations of Bundled Bridge Stay Cables, National Research Council of Canada, Note provided to RWDI circa 1985.



CONSULTING ENGINEERS
& SCIENTISTS

bridge, a 1-minute mean is suggested as a reasonable averaging time for galloping instability to become noticeable. The ASCE 7 recommends using a factor of 1.25 to convert 1-hour mean speeds to 1-minute mean speeds. The 1-minute mean wind speed is therefore 87 mph. In this case, the damping demand is generally within the range of 0.1%-0.3%. Iced galloping is found to govern the damping requirements for many of the hangers.

5.3 Conclusions and Recommendations

This study addresses wind-induced vibration of the hangers for the Kentucky Lake Bridges.

Possible causes for wind induced hanger vibrations are assessed individually. Table 5-2 provides the minimum recommended damping ratio for each hanger, which are within the range of 0.1% to 0.3%. Table 5-2 indicates that, generally, the amount of required damping increases as the cable length increases. These recommended damping ratios have been determined assuming the hanger surface is not smooth (due to the spiraling of the wire rope), which reduces their susceptibility to RWIV.

While it is possible that these relatively short hangers may have inherent damping that is within the range of 0.1% to 0.3% which would be sufficient to suppress noticeable motions, this cannot be guaranteed. For this reason, we recommend that the hangers are monitored after installation to determine if they experience excessive vibrations. A hanger monitoring program of 6 months to 1 year duration is expected to be sufficient to determine whether wind-induced hanger vibrations will be problematic for this bridge.

Since the hanger damping levels are currently unknown, the design team should include provisions for supplemental damping in case the measurements indicate hanger vibrations are problematic. If supplemental damping is required, the hanger spacers, which are located at the intersection points of the hangers, are a potentially favorable location for adding supplemental damping to the hangers as a reasonably simple corrective measure.

The cable spacers are currently shown to consist of three ½" plates to which the hangers are fastened using U-bolts. The plates are separated using 7/8" diameter rods. The damping at the spacers can be increased by incorporating a resilient material or system component that exhibits considerable hysteretic behavior. One option we recommend would be to add wire rope isolators at the spacers to increase the hanger damping. As shown in Figures 5-2, wire rope isolators consist of wire rope that is coiled between the two retaining bars. The stiffness and hysteretic damping of such a connection will depend upon the diameter of the wire rope, the diameter of the coil, and the number of coils. A significant advantage of the wire rope isolators over other resilient materials (such as neoprene), is that these are relatively insensitive to temperature changes. The isolators may replace a segment of the 7/8" spacer rods (Option 1), or the hangers may be connected to a wire rope isolator via a spacer plate (Option 2) as shown in Figure 5-3. For Option 2, it may be necessary to twist the wire rope isolators to align with the non-parallel hangers. While the wire rope isolators are pliable; a detailed design would confirm whether the necessary angle of twist would be attainable, or whether the interface plates will need to be enlarged to accommodate the non-parallel hanger orientation.



CONSULTING ENGINEERS
& SCIENTISTS

In conclusions, after the hangers are installed, to ensure vibration-free hangers, a vibration monitoring program should be employed to confirm that the hanger vibration levels are acceptable. If the vibrations are found to be excessive however, a supplemental damping system should be employed to increase hanger damping and reduce the observed vibration levels. Two supplementary damping system options are suggested in which wire rope isolators at the hanger spacers are used to quell vibrations.

TABLES

TABLE 2-1: RECOMMENDED WIND SPEEDS AT THE SITE AT DECK ELEVATION (80 FT)

Kentucky Lake Bridge

Wind Speed Applicable for	Return Period (years)	Mean Wind Speed (mph) at Deck Level	Description
Design during renovation	10	60.0	Mean hourly
Design of completed bridge	100	69.0	Mean hourly
Stability during renovation	1,000	75.5	10-min mean
Stability of completed bridge	10,000	82.5	10-min mean

Lake Barkley Bridge

Wind Speed Applicable for	Return Period (years)	Mean Wind Speed (mph) at Deck Level	Description
Design during renovation	10	60.5	Mean hourly
Design of completed bridge	100	69.6	Mean hourly
Stability during renovation	1,000	75.6	10-min mean
Stability of completed bridge	10,000	82.7	10-min mean

TABLE 2-2: TURBULENCE PROPERTIES AT DECK LEVEL

Kentucky Lake Bridge

α	I_u (%)	I_v (%)	I_w (%)	xL_u (ft)	xL_w (ft)	yL_u (ft)	yL_w (ft)	zL_u (ft)
0.13	15.0	11.7	8.3	1612	383	437	417	264

Lake Barkley Bridge

α	I_u (%)	I_v (%)	I_w (%)	xL_u (ft)	xL_w (ft)	yL_u (ft)	yL_w (ft)	zL_u (ft)
0.14	16.6	13.0	9.1	1806	429	490	468	296

Notes:

1. α - power law constant of mean wind profile
2. $I_{u,v,w}$ - longitudinal, horizontal-across-wind, and vertical turbulence intensities
3. $^{x,y,z}L_{u,v,w}$ - turbulence length scales



TABLE 3-1: SECTION PROPERTIES (COMPLETED BRIDGE)

Item	Full scale	Model scale	
		Target	Actual
Mass (slug/ft)	443.44	14.0	13.95
Mass moment of inertia (slug.ft ² /ft)	324756	0.275	0.272
Vertical frequency (Hz)	1.035	5.5-6.0	5.76
Torsional frequency (Hz)	1.226	7.0-8.0	7.67
Frequency ratio	1.18	1.18	1.33
Vertical damping ratio (%)	0.5	0.5	0.5
Torsional damping ratio (%)	0.5	0.5	0.5

TABLE 3-2A: FORCE AND MOMENT COEFFICIENTS VS. ANGLE OF WIND ATTACK (COMPLETED BRIDGE)

Angle of attack (degree)	Walkway					
	Downwind			Upwind		
	Cy	Cz	Cm	Cy	Cz	Cm
-10.0	1.6419	-0.3421	-0.0783	1.5189	-0.5406	-0.0717
-8.05	1.6370	-0.2958	-0.0707	1.5173	-0.4912	-0.0675
-6.05	1.6049	-0.2368	-0.0590	1.5283	-0.4123	-0.0584
-4.0	1.5258	-0.1907	-0.0489	1.5040	-0.3084	-0.0477
-2.0	1.5062	-0.1152	-0.0398	1.4606	-0.2048	-0.0454
0.0	1.4549	-0.0135	-0.0328	1.4625	-0.0574	-0.0359
2.0	1.3292	0.1366	-0.0068	1.3217	0.0998	-0.0089
4.0	1.3305	0.3148	0.0250	1.3425	0.2898	0.0270
6.0	1.3722	0.4209	0.0351	1.4124	0.4294	0.0409
8.05	1.4921	0.4718	0.0330	1.5411	0.4763	0.0366
9.95	1.6008	0.5108	0.0338	1.6592	0.4971	0.0354

Notes:

1. Coefficient Cy is normalized with deck depth $D = 9.4$ ft
2. Coefficients Cz and Cm are normalized with deck width $B = 100$ ft

TABLE 3-2B: WEIGHTED FORCE AND MOMENT COEFFICIENTS (COMPLETED BRIDGE)

Configuration	Cy	dCy/d α	Cz	dCz/d α	Cm	dCm/d α
Walkway downwind	1.4613	-0.6625	0.0421	2.8429	-0.0199	0.3903
Walkway upwind	1.4454	-0.1533	-0.0281	3.4945	-0.0201	0.3912

Note: 1. All coefficients and slopes were weighted with a vertical turbulence intensity $I_w = 9\%$.

TABLE 4-1A: STATIC FORCE AND MOMENT COEFFICIENTS USED FOR THE WIND LOAD DERIVATION – PRELIMINARY

Bridge Element	C_x	$dC_x/d\alpha$	C_y	$dC_y/d\alpha$	C_z	$dC_z/d\alpha$	C_{M_x}	$dC_{M_x}/d\alpha$
Deck assembly	±0.425	-	1.7	-2.0	±0.1	5.0	±0.05	-0.5
North rib	±0.425	-	1.7	-	1.0	-	-	-
South rib	±0.425	-	1.7	-	-1.0	-	-	-
Vierendeel bracing	±0.4	-	0.15	-	-	-	-	-
Column	±0.175	-	0.7	-	-	-	-	-
Pier cap	±0.35	-	0.1	-	-	-	-	-
Hanger	±0.175	±0.7	0.7	-	-	-	-	-

Notes:

1. Force coefficients given are based on the structural coordinate system where X is the along longitudinal axis of the bridge (parallel to the bridge span), Y is the along transverse axis of the bridge and Z is the vertical axis (positive when up).
2. C_{M_x} follows the right-hand rule.

TABLE 4-1B: STATIC FORCE AND MOMENT COEFFICIENTS USED FOR THE WIND LOAD DERIVATION – FINAL

Bridge Element	C_x	$dC_x/d\alpha$	C_y	$dC_y/d\alpha$	C_z	$dC_z/d\alpha$	C_{Mx}	$dC_{Mx}/d\alpha$
Deck assembly	± 0.425	-	1.45 / -1.46	-0.66 / -0.15	-0.03 / 0.04	3.49 / 2.84	± 0.02	± 0.4
North rib	± 0.425	-	1.7 / -1.7	-	1.0	-	-	-
South rib	± 0.425	-	1.7 / -1.7	-	-1.0	-	-	-
Vierendeel bracing	± 0.4	-	0.15 / -0.15	-	-	-	-	-
Column	± 0.175	-	0.7 / 0.7	-	-	-	-	-
Pier cap	± 0.35	-	0.1 / 0.1	-	-	-	-	-
Hanger	± 0.175	± 0.7	0.7 / -0.7	-	-	-	-	-

Notes:

- Force and moment coefficients given are based on the structural coordinate system where X is the along longitudinal axis of the bridge (parallel to the bridge span), Y is the along transverse axis of the bridge and Z is the vertical axis (positive when up).
- C_{Mx} follows the right-hand rule.

TABLE 4-2A: COMPLETED BRIDGE – PRELIMINARY WIND GUST FACTORS - 100-YEAR RETURN PERIOD

Description	Gust factors on loads	Gust factors on speeds
Along the bridge (X)	1.8	1.34
Drag (Y)	1.8	1.34
Lift (Z)	8.0	2.83
Deck torsion (XX)	2.6	1.61

TABLE 4-2B: COMPLETED BRIDGE – FINAL WIND GUST FACTORS - 100-YEAR RETURN PERIOD

Description	Gust factors on loads Walkway South Winds/North Winds	Gust factors on speeds Walkway South Winds/North Winds
Along the bridge (X)	1.8 / 1.8	1.34 / 1.34
Drag (Y)	1.8 / 1.8	1.34 / 1.34
Lift (Z)	18.2 / 10.4	4.27 / 3.22
Deck torsion (XX)	3.9 / 3.9	1.97 / 1.97

TABLE 4-3A: COMPLETED BRIDGE - PEAK MODAL DEFLECTIONS - 100-YEAR RETURN PERIOD (PRELIMINARY LOADS)

Mode	Modal frequency (Hz)	Mode description		Peak modal	
		DOF of max modal component	Corresponding FE & Wind Model node	Deflection (ft)	Acceleration (%g)
1	0.257	X	477	0.054	0.4
2	0.351	Y	3317	0.097	1.5
3	0.415	Y	550	0.034	0.7
4	0.882	Y	441	0.065	6.2
5	0.897	X	6121	0.020	2.0
6	1.035	Z	2205	0.047	6.2
7	1.085	Z	2213	0.062	8.9
8	1.147	Y	3312	0.004	0.6
9	1.226	X	5121	0.002	0.3
10	1.336	Z	2221	0.021	4.6
11	1.350	X	477	0.007	1.6
12	1.395	Y	1213	0.001	0.3
13	1.484	Y	3307	0.009	2.3
14	1.652	Z	477	0.010	3.3
15	1.851	Z	1215	0.008	3.4
16	1.915	Z	1205	0.005	2.3

TABLE 4-3B: COMPLETED BRIDGE - PEAK MODAL DEFLECTIONS - 100-YEAR RETURN PERIOD (FINAL LOADS)

Mode	Modal frequency (Hz)	Mode description		South/North Winds Peak modal	
		DOF of max modal component	Corresponding FE & Wind Model node	Deflections (ft)	Accelerations (%g)
1	0.257	X	477	0.051/0.051	0.41/0.41
2	0.351	Y	3317	0.086/0.087	1.30/1.31
3	0.415	Y	550	0.030/0.030	0.64/0.64
4	0.882	Y	441	0.062/0.064	5.89/6.13
5	0.897	X	6121	0.014/0.012	1.41/1.16
6	1.035	Z	2205	0.036/0.031	4.72/4.02
7	1.085	Z	2213	0.047/0.040	6.78/5.76
8	1.147	Y	3312	0.003/0.003	0.46/0.48
9	1.226	X	5121	0.001/0.001	0.24/0.22
10	1.336	Z	2221	0.016/0.013	3.46/2.93
11	1.350	X	477	0.005/0.004	1.14/0.94
12	1.395	Y	1213	0.002/0.002	0.45/0.40
13	1.484	Y	3307	0.007/0.007	1.98/1.98
14	1.652	Z	477	0.007/0.006	2.51/2.13
15	1.851	Z	1215	0.007/0.007	2.95/2.77
16	1.915	Z	1205	0.004/0.004	1.78/1.71

TABLE 4-4A: COMPLETED BRIDGE – PRELIMINARY DESIGN WIND LOADS - 100-YEAR RETURN PERIOD

Note: Due to the size of this table, it is available in an electronic format as an Excel spreadsheet:
[RWDI PreliminaryLoads April25.2013.xlsm](#)

TABLE 4-4B: COMPLETED BRIDGE – FINAL DESIGN WIND LOADS - 100-YEAR RETURN PERIOD

Note: Due to the size of this table, it is available in an electronic format as an Excel spreadsheet:
[RWDI Loads July1.2013.xlsm](#)

TABLE 4-5: COMPLETED BRIDGE - DESCRIPTIONS OF DESIGN LOAD CASES - 100-YEAR RETURN PERIOD (PRELIMINARY AND FINAL)

Load Case #	Description
1	Max lateral on deck, middle of the span
2	Peak lateral with reversed dynamic component on deck, middle of the span
3	Max uplift on deck, middle of the span
4	Max down force on deck, middle of the span
5	Max positive moment on deck, middle of the span
6	Max negative moment on deck, middle of the span
7	Max lateral, middle of the span, differential between deck and arch
8	Max lateral, middle of the span, differential between deck and arch
9	Max lateral on deck, differential between 1/4 and 3/4 span
10	Max lateral on deck, differential between 1/4 and 3/4 span
11	Max uplift on deck, differential between 1/4 and 3/4 span
12	Max uplift on deck, differential between 1/4 and 3/4 span
13	Max uplift on deck, differential between 1/4 and 3/4 span
14	Max uplift on deck, differential between 1/4 and 3/4 span
15	Max moment on deck, differential between 1/4 and 3/4 span
16	Max moment on deck, differential between 1/4 and 3/4 span
17	Max moment on deck, differential between 1/4 and 3/4 span
18	Max moment on deck, differential between 1/4 and 3/4 span
19	Max uplift on deck, differential between middle and 1/4 & 3/4 span
20	Max uplift on deck, differential between middle and 1/4 & 3/4 span
21	Max lateral on arch ribs, differential between 1/4 and 3/4 span
22	Max lateral on arch ribs, differential between 1/4 and 3/4 span
23	Max uplift on arch ribs, differential between 1/4 and 3/4 span
24	Max uplift on arch ribs, differential between 1/4 and 3/4 span
25	Max positive longitudinal
26	Max negative longitudinal
27	Max positive longitudinal, differential between piers and deck
28	Max positive longitudinal, differential between piers and deck

TABLE 5-1(A): NORTH ARCH HANGER PROPERTIES

Cable ID	Angle (deg)	Length (ft)	Pipe Dia. (in)	Weight (lb/ft)	Tension (Kips)
C1a	55.1	29.4	2.50	13.1	130.0
C1b	55.1	29.4	2.50	13.1	130.3
C2	66.3	58.5	3.25	22.2	86.6
C3a	56.1	55.5	2.50	13.1	130.0
C3b	56.1	55.6	2.50	13.1	143.3
C4	65.3	88.9	3.25	22.2	151.7
C5a	57.1	77.7	2.50	13.1	126.9
C5b	57.1	77.8	2.50	13.1	138.7
C6	64.2	116.9	3.25	22.2	162.5
C7a	59.1	95.6	2.50	13.1	112.6
C7b	59.1	95.6	2.50	13.1	123.6
C8	63.2	124.3	3.25	22.2	179.3
C9a	60.2	109.8	2.50	13.1	113.2
C9b	60.2	109.8	2.50	13.1	124.0
C10	62.2	124.8	3.25	22.2	184.5
C11a	61.2	119.7	2.50	13.1	101.4
C11b	61.2	119.7	2.50	13.1	112.1
C12a	61.2	119.7	2.50	13.1	101.4
C12b	61.2	119.7	2.50	13.1	112.1
C13	62.2	124.8	3.25	22.2	184.5
C14a	60.2	109.8	2.50	13.1	113.2
C14b	60.2	109.8	2.50	13.1	124.0
C15	63.2	124.3	3.25	22.2	179.3
C16a	59.1	95.6	2.50	13.1	112.6
C16b	59.1	95.6	2.50	13.1	123.6
C17	64.2	116.9	3.25	22.2	162.6
C18a	57.1	77.7	2.50	13.1	126.9
C18b	57.1	77.8	2.50	13.1	138.8
C19	65.3	88.9	3.25	22.2	151.7
C20a	56.1	55.5	2.50	13.1	130.0
C20b	56.1	55.6	2.50	13.1	143.3

Cable ID	Angle (deg)	Length (ft)	Pipe Dia. (in)	Weight (lb/ft)	Tension (Kips)
C21	66.3	58.5	3.25	22.2	86.6
C22a	55.1	29.4	2.50	13.1	128.6
C22b	55.1	29.4	2.50	13.1	128.8

TABLE 5-1(B): SOUTH ARCH HANGER PROPERTIES

Cable ID	Angle (deg)	Length (ft)	Pipe Dia. (in)	Weight (lb/ft)	Tension (Kips)
C1a	55.1	29.4	2.50	13.1	130.3
C1b	55.1	29.4	2.50	13.1	129.8
C2	66.3	58.5	3.25	22.2	86.5
C3a	56.1	55.5	2.50	13.1	143.3
C3b	56.1	55.6	2.50	13.1	129.7
C4	65.3	88.9	3.25	22.2	151.5
C5a	57.1	77.7	2.50	13.1	138.8
C5b	57.1	77.8	2.50	13.1	126.6
C6	64.2	116.9	3.25	22.2	162.3
C7a	59.1	95.6	2.50	13.1	123.6
C7b	59.1	95.6	2.50	13.1	112.4
C8	63.2	124.3	3.25	22.2	179.1
C9a	60.2	109.8	2.50	13.1	124.1
C9b	60.2	109.8	2.50	13.1	113.0
C10	62.2	124.8	3.25	22.2	184.4
C11a	61.2	119.7	2.50	13.1	112.2
C11b	61.2	119.7	2.50	13.1	101.2
C12a	61.2	119.7	2.50	13.1	112.2
C12b	61.2	119.7	2.50	13.1	101.3
C13	62.2	124.8	3.25	22.2	184.3
C14a	60.2	109.8	2.50	13.1	124.1
C14b	60.2	109.8	2.50	13.1	113.0
C15	63.2	124.3	3.25	22.2	179.1
C16a	59.1	95.6	2.50	13.1	123.6
C16b	59.1	95.6	2.50	13.1	112.4
C17	64.2	116.9	3.25	22.2	162.4
C18a	57.1	77.7	2.50	13.1	138.9
C18b	57.1	77.8	2.50	13.1	126.6
C19	65.3	88.9	3.25	22.2	151.6
C20a	56.1	55.5	2.50	13.1	143.4
C20b	56.1	55.6	2.50	13.1	129.8



Cable ID	Angle (deg)	Length (ft)	Pipe Dia. (in)	Weight (lb/ft)	Tension (Kips)
C21	66.3	58.5	3.25	22.2	86.5
C22a	55.1	29.4	2.50	13.1	128.8
C22b	55.1	29.4	2.50	13.1	128.3

TABLE 5-2(A): VIBRATION CONTROL OF NORTH ARCH HANGERS

Cable ID	Estimated frequencies ¹ (Hz)						Expected Sc	Required ζ (%) to reach				Recommended minimum ζ (%)
	f ₁	f ₂	f ₃	f ₄	f ₅	f ₆	$\zeta=0.03\%$	Sc=2.5	Sc=5	Sc=10	V _{ice} =86 mph	
C1a	9.60	9.60	19.19	19.19	28.79	28.79	1.19	0.06%	0.13%	0.25%	0.06%	0.1%
C1b	9.60	9.60	19.21	19.21	28.81	28.81	1.19	0.06%	0.13%	0.25%	0.06%	0.1%
C2	3.03	3.04	6.06	6.06	9.08	9.09	1.19	0.06%	0.13%	0.25%	0.16%	0.2%
C3a	5.08	5.08	10.16	10.16	15.24	15.24	1.19	0.06%	0.13%	0.25%	0.12%	0.2%
C3b	5.33	5.33	10.66	10.66	16.00	16.00	1.19	0.06%	0.13%	0.25%	0.11%	0.2%
C4	<u>2.64</u>	<u>2.64</u>	5.28	5.28	7.92	7.92	1.19	0.06%	0.13%	0.25%	0.18%	0.2%
C5a	3.59	3.59	7.17	7.17	10.76	10.76	1.19	0.06%	0.13%	0.25%	0.17%	0.2%
C5b	3.75	3.75	7.50	7.50	11.25	11.25	1.19	0.06%	0.13%	0.25%	0.16%	0.2%
C6	<u>2.08</u>	<u>2.08</u>	4.16	4.16	6.23	6.24	1.19	0.06%	0.13%	0.25%	0.23%	0.3%
C7a	<u>2.75</u>	<u>2.75</u>	5.49	5.49	8.24	8.24	1.19	0.06%	0.13%	0.25%	0.22%	0.3%
C7b	<u>2.88</u>	<u>2.88</u>	5.75	5.75	8.63	8.63	1.19	0.06%	0.13%	0.25%	0.21%	0.3%
C8	<u>2.05</u>	<u>2.05</u>	4.10	4.10	6.16	6.16	1.19	0.06%	0.13%	0.25%	0.23%	0.3%
C9a	<u>2.40</u>	<u>2.40</u>	4.80	4.80	7.19	7.20	1.19	0.06%	0.13%	0.25%	0.25%	0.3%
C9b	<u>2.51</u>	<u>2.51</u>	5.02	5.02	7.53	7.53	1.19	0.06%	0.13%	0.25%	0.24%	0.3%
C10	<u>2.07</u>	<u>2.08</u>	4.15	4.15	6.22	6.22	1.19	0.06%	0.13%	0.25%	0.23%	0.3%
C11a	<u>2.08</u>	<u>2.09</u>	4.17	4.17	6.25	6.25	1.19	0.06%	0.13%	0.25%	0.29%	0.3%
C11b	<u>2.19</u>	<u>2.19</u>	4.38	4.38	6.57	6.57	1.19	0.06%	0.13%	0.25%	0.28%	0.3%

¹ Bolded/underlined frequencies are susceptible to rain/wind induced vibration

Cable ID	Estimated frequencies ¹ (Hz)						Expected Sc $\zeta=0.03\%$	Required ζ (%) to reach				Recommended minimum ζ (%)
	f ₁	f ₂	f ₃	f ₄	f ₅	f ₆		Sc=2.5	Sc=5	Sc=10	V _{ice} =86 mph	
C12a	<u>2.08</u>	<u>2.09</u>	4.17	4.17	6.25	6.25	1.19	0.06%	0.13%	0.25%	0.29%	0.3%
C12b	<u>2.19</u>	<u>2.19</u>	4.38	4.38	6.57	6.57	1.19	0.06%	0.13%	0.25%	0.28%	0.3%
C13	<u>2.07</u>	<u>2.08</u>	4.15	4.15	6.22	6.22	1.19	0.06%	0.13%	0.25%	0.23%	0.3%
C14a	<u>2.40</u>	<u>2.40</u>	4.80	4.80	7.19	7.20	1.19	0.06%	0.13%	0.25%	0.25%	0.3%
C14b	<u>2.51</u>	<u>2.51</u>	5.02	5.02	7.53	7.53	1.19	0.06%	0.13%	0.25%	0.24%	0.3%
C15	<u>2.05</u>	<u>2.06</u>	4.10	4.10	6.16	6.16	1.19	0.06%	0.13%	0.25%	0.23%	0.3%
C16a	<u>2.75</u>	<u>2.75</u>	5.49	5.49	8.24	8.24	1.19	0.06%	0.13%	0.25%	0.22%	0.3%
C16b	<u>2.88</u>	<u>2.88</u>	5.75	5.75	8.63	8.63	1.19	0.06%	0.13%	0.25%	0.21%	0.3%
C17	<u>2.08</u>	<u>2.08</u>	4.16	4.16	6.23	6.24	1.19	0.06%	0.13%	0.25%	0.23%	0.3%
C18a	3.59	3.59	7.17	7.17	10.76	10.76	1.19	0.06%	0.13%	0.25%	0.17%	0.2%
C18b	3.75	3.75	7.50	7.50	11.25	11.25	1.19	0.06%	0.13%	0.25%	0.16%	0.2%
C19	<u>2.64</u>	<u>2.64</u>	5.28	5.28	7.92	7.92	1.19	0.06%	0.13%	0.25%	0.18%	0.2%
C20a	5.08	5.08	10.16	10.16	15.24	15.25	1.19	0.06%	0.13%	0.25%	0.12%	0.2%
C20b	5.33	5.33	10.67	10.67	16.00	16.00	1.19	0.06%	0.13%	0.25%	0.11%	0.2%
C21	3.03	3.04	6.06	6.06	9.08	9.09	1.19	0.06%	0.13%	0.25%	0.16%	0.2%
C22a	9.54	9.54	19.09	19.09	28.63	28.63	1.19	0.06%	0.13%	0.25%	0.06%	0.1%
C22b	9.55	9.55	19.09	19.09	28.64	28.64	1.19	0.06%	0.13%	0.25%	0.06%	0.1%

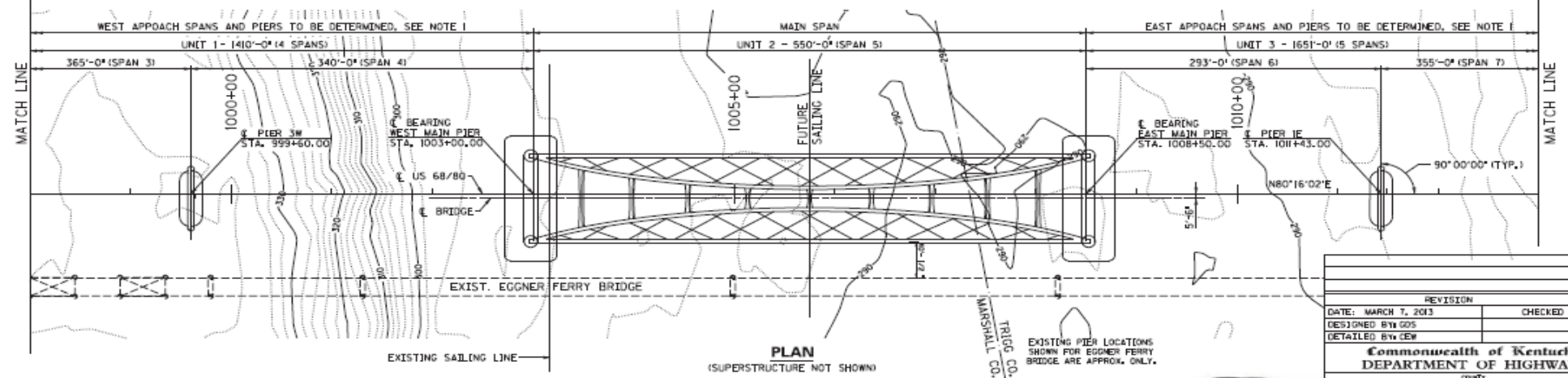
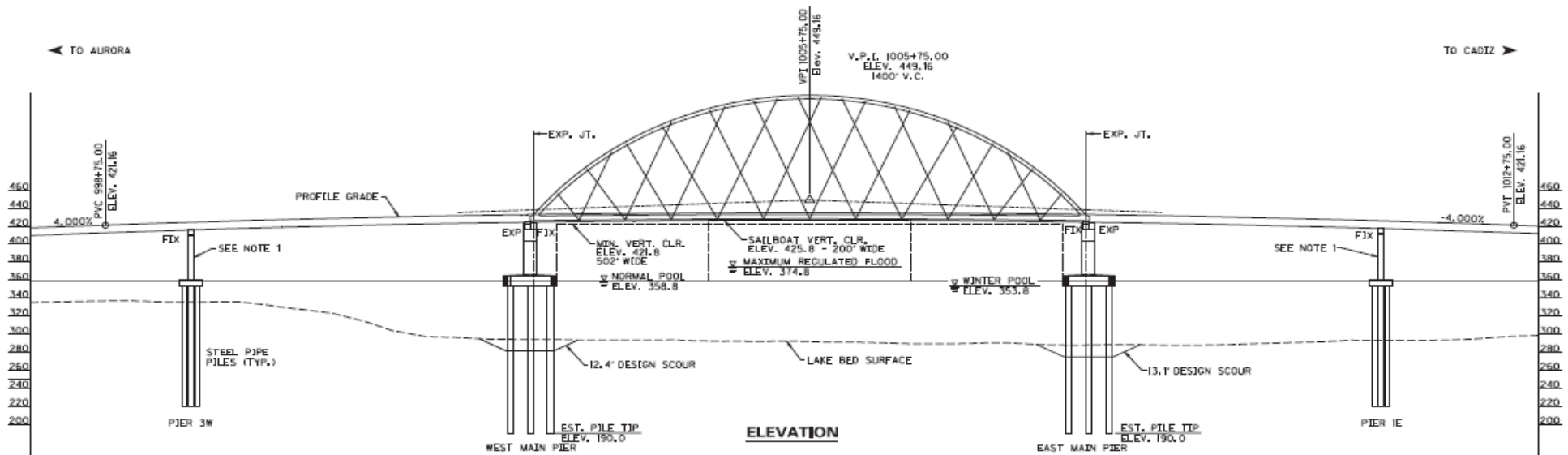
TABLE 5-2(B): VIBRATION CONTROL OF SOUTH ARCH HANGERS

Cable ID	Estimated frequencies ² (Hz)						Expected Sc	Required ζ (%) to reach				Recommended minimum ζ (%)
	f ₁	f ₂	f ₃	f ₄	f ₅	f ₆	$\zeta=0.03\%$	Sc=2.5	Sc=5	Sc=10	V _{ice} =86 mph	
C1a	9.61	9.61	19.22	19.22	28.83	28.83	1.19	0.06%	0.13%	0.25%	0.06%	0.1%
C1b	9.58	9.58	19.17	19.17	28.75	28.75	1.19	0.06%	0.13%	0.25%	0.06%	0.1%
C2	3.03	3.03	6.05	6.05	9.08	9.09	1.19	0.06%	0.13%	0.25%	0.16%	0.2%
C3a	5.33	5.34	10.67	10.67	16.00	16.00	1.19	0.06%	0.13%	0.25%	0.11%	0.2%
C3b	5.07	5.07	10.15	10.15	15.22	15.22	1.19	0.06%	0.13%	0.25%	0.12%	0.2%
C4	<u>2.64</u>	<u>2.64</u>	5.28	5.28	7.91	7.92	1.19	0.06%	0.13%	0.25%	0.18%	0.2%
C5a	3.75	3.75	7.50	7.50	11.25	11.26	1.19	0.06%	0.13%	0.25%	0.16%	0.2%
C5b	3.58	3.58	7.16	7.16	10.75	10.75	1.19	0.06%	0.13%	0.25%	0.17%	0.2%
C6	<u>2.08</u>	<u>2.08</u>	4.15	4.15	6.23	6.23	1.19	0.06%	0.13%	0.25%	0.23%	0.3%
C7a	<u>2.88</u>	<u>2.88</u>	5.76	5.76	8.63	8.64	1.19	0.06%	0.13%	0.25%	0.21%	0.3%
C7b	<u>2.74</u>	<u>2.75</u>	5.49	5.49	8.23	8.23	1.19	0.06%	0.13%	0.25%	0.22%	0.3%
C8	<u>2.05</u>	<u>2.05</u>	4.10	4.10	6.15	6.16	1.19	0.06%	0.13%	0.25%	0.23%	0.3%
C9a	<u>2.51</u>	<u>2.51</u>	5.02	5.02	7.53	7.54	1.19	0.06%	0.13%	0.25%	0.24%	0.3%
C9b	<u>2.40</u>	<u>2.40</u>	4.79	4.79	7.19	7.19	1.19	0.06%	0.13%	0.25%	0.25%	0.3%
C10	<u>2.07</u>	<u>2.08</u>	4.14	4.14	6.22	6.22	1.19	0.06%	0.13%	0.25%	0.23%	0.3%
C11a	<u>2.19</u>	<u>2.19</u>	4.38	4.38	6.57	6.57	1.19	0.06%	0.13%	0.25%	0.28%	0.3%
C11b	<u>2.08</u>	<u>2.08</u>	4.16	4.16	6.24	6.25	1.19	0.06%	0.13%	0.25%	0.29%	0.3%

² Bolded/underlined frequencies are susceptible to rain/wind induced vibration

Cable ID	Estimated frequencies ² (Hz)						Expected Sc $\zeta=0.03\%$	Required ζ (%) to reach				Recommended minimum ζ (%)
	f ₁	f ₂	f ₃	f ₄	f ₅	f ₆		Sc=2.5	Sc=5	Sc=10	V _{ice} =86 mph	
C12a	<u>2.19</u>	<u>2.19</u>	4.38	4.38	6.57	6.57	1.19	0.06%	0.13%	0.25%	0.28%	0.3%
C12b	<u>2.08</u>	<u>2.08</u>	4.16	4.16	6.24	6.25	1.19	0.06%	0.13%	0.25%	0.29%	0.3%
C13	<u>2.07</u>	<u>2.08</u>	4.14	4.14	6.22	6.22	1.19	0.06%	0.13%	0.25%	0.23%	0.3%
C14a	<u>2.51</u>	<u>2.51</u>	5.02	5.02	7.53	7.54	1.19	0.06%	0.13%	0.25%	0.24%	0.3%
C14b	<u>2.40</u>	<u>2.40</u>	4.79	4.79	7.19	7.19	1.19	0.06%	0.13%	0.25%	0.25%	0.3%
C15	<u>2.05</u>	<u>2.05</u>	4.10	4.10	6.15	6.16	1.19	0.06%	0.13%	0.25%	0.23%	0.3%
C16a	<u>2.88</u>	<u>2.88</u>	5.76	5.76	8.63	8.64	1.19	0.06%	0.13%	0.25%	0.21%	0.3%
C16b	<u>2.74</u>	<u>2.75</u>	5.49	5.49	8.23	8.23	1.19	0.06%	0.13%	0.25%	0.22%	0.3%
C17	<u>2.08</u>	<u>2.08</u>	4.15	4.15	6.23	6.23	1.19	0.06%	0.13%	0.25%	0.23%	0.3%
C18a	3.75	3.75	7.50	7.50	11.26	11.26	1.19	0.06%	0.13%	0.25%	0.16%	0.2%
C18b	3.58	3.58	7.16	7.16	10.75	10.75	1.19	0.06%	0.13%	0.25%	0.17%	0.2%
C19	<u>2.64</u>	<u>2.64</u>	5.28	5.28	7.92	7.92	1.19	0.06%	0.13%	0.25%	0.18%	0.2%
C20a	5.34	5.34	10.67	10.67	16.01	16.01	1.19	0.06%	0.13%	0.25%	0.11%	0.2%
C20b	5.07	5.08	10.15	10.15	15.22	15.23	1.19	0.06%	0.13%	0.25%	0.12%	0.2%
C21	3.03	3.03	6.05	6.05	9.08	9.09	1.19	0.06%	0.13%	0.25%	0.16%	0.2%
C22a	9.55	9.55	19.11	19.11	28.66	28.66	1.19	0.06%	0.13%	0.25%	0.06%	0.1%
C22b	9.53	9.53	19.06	19.06	28.59	28.59	1.19	0.06%	0.13%	0.25%	0.06%	0.1%

FIGURES



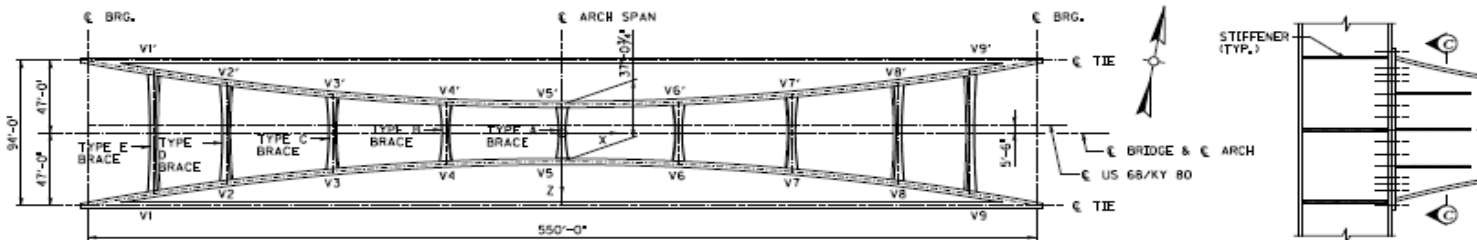
- NOTES**
1. WELDED STEEL PLATE GIRDER ALTERNATE SHOWN FOR APPROACH SPAN ALTERNATES, SEE SHEET NO. 538-556.
 2. WATER SURFACE ELEVATIONS ARE GIVEN IN PROJECT DATUM NAVD88.
 3. SCOUR DEPTHS ON APPROACH PIERS NOT SHOWN.



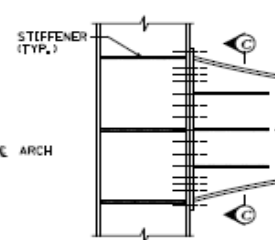
REVISION		DATE
DATE: MARCH 7, 2013	DESIGNED BY: GOS	CHECKED BY:
DETAILED BY: CEW		
Commonwealth of Kentucky DEPARTMENT OF HIGHWAYS		
COUNTY MARSHALL / TRIGG		
CROSSING KENTUCKY LAKE		
LAYOUT SHEET		
ITEM NUMBER	DRAWING NO.	
01-180.70	24686	
PREPARED BY MICHAEL BARBER, JR., INC. 4700 DANFORTH STATION ROAD, SUITE 300 LOUISVILLE, KY 40202		DATE MAY 6, 2013

Elevation & Plan Views of the Kentucky Lake Bridge
Wind Engineering Study





ARCH RIB BRACING PLAN



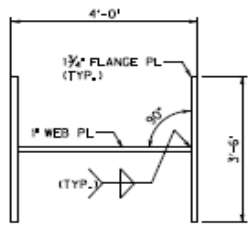
DETAIL 1

NOTES

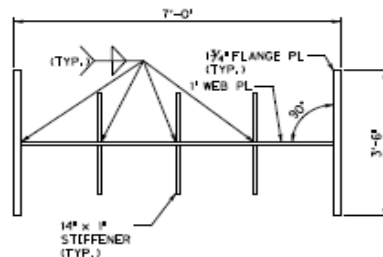
- RIB BRACING AND CONNECTIONS SHALL CONFORM TO ASTM A709 GRADE 50W.
- SEE SHEET NO. S11 FOR MAIN SPAN ARCH DETAILS.

LEGEND

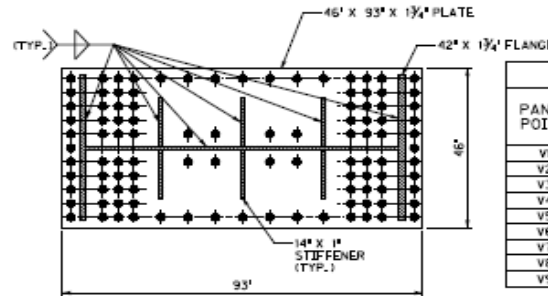
W(n) INDICATES RIB BRACING WORKING POINT



SECTION A-A

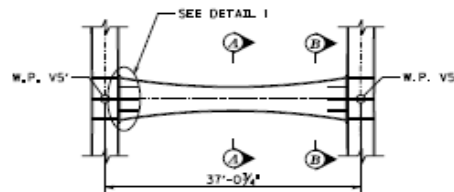


SECTION B-B



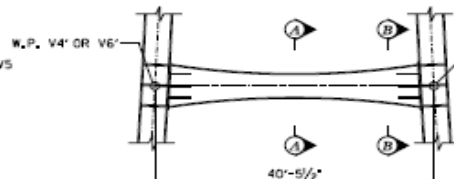
SECTION C-C

RIB BRACING PANEL POINT COORDINATES								
PANEL POINT	X (FT.)	Y (FT.)	Z (FT.)	PANEL POINT	X (FT.)	Y (FT.)	Z (FT.)	
V1	-236.729	31.030	38.685	V1'	-236.729	31.030	-38.685	
V2	-194.741	57.195	31.675	V2'	-194.741	57.195	-31.675	
V3	-133.036	84.183	24.443	V3'	-133.036	84.183	-24.443	
V4	-67.492	100.694	20.019	V4'	-67.492	100.694	-20.019	
V5	0.000	106.252	18.530	V5'	0.000	106.252	-18.530	
V6	67.492	100.694	20.019	V6'	67.492	100.694	-20.019	
V7	133.036	84.183	24.443	V7'	133.036	84.183	-24.443	
V8	194.741	57.195	31.675	V8'	194.741	57.195	-31.675	
V9	236.729	31.030	38.685	V9'	236.729	31.030	-38.685	



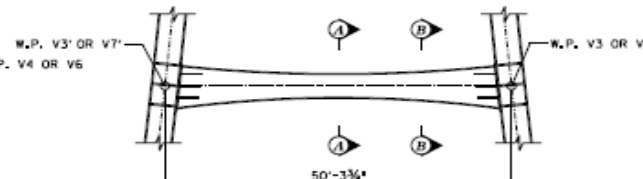
TYPE A BRACE

(VIEW PERPENDICULAR TO WEB OF BRACE)



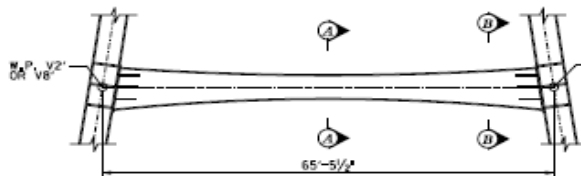
TYPE B BRACE

(VIEW PERPENDICULAR TO WEB OF BRACE)



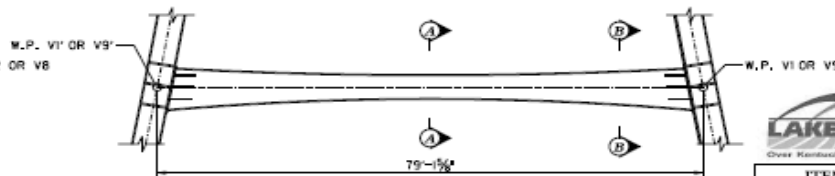
TYPE C BRACE

(VIEW PERPENDICULAR TO WEB OF BRACE)



TYPE D BRACE

(VIEW PERPENDICULAR TO WEB OF BRACE)



TYPE E BRACE

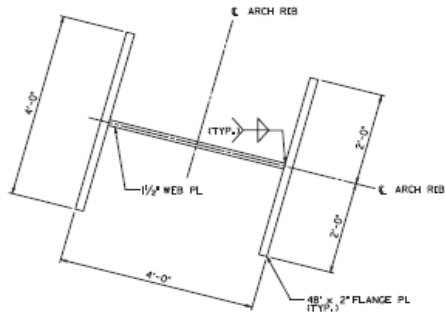
(VIEW PERPENDICULAR TO WEB OF BRACE)



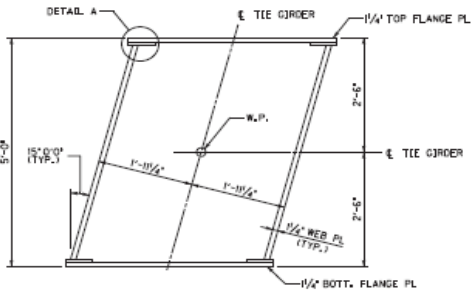
ITEM NUMBER	01-180.70
-------------	-----------

REVISION	DATE
DATE: MARCH 7, 2013	CHECKED BY:
DESIGNED BY: CY	
DETAILED BY: MJD	
Commonwealth of Kentucky DEPARTMENT OF HIGHWAYS	
DRAFT MARSHALL / TRIGG	
ROUTE US68	CROSSING KENTUCKY LAKE
RIB BRACING	
PREPARED BY Baker	DESIGNED BY MICHAEL BAKER JR., INC. 790 GARDNER STATION ROAD, SUITE 200 LOUISVILLE, KY 40202
	DRAWING NO. 24686

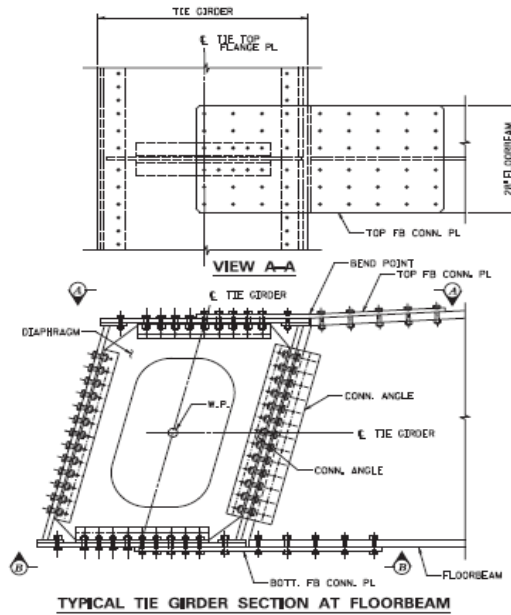




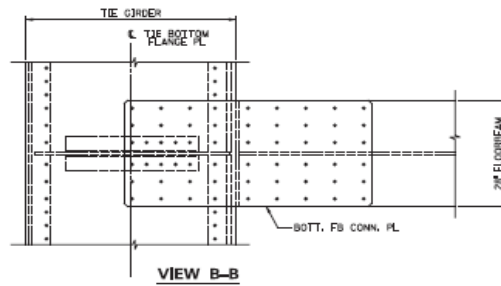
TYPICAL ARCH RIB SECTION



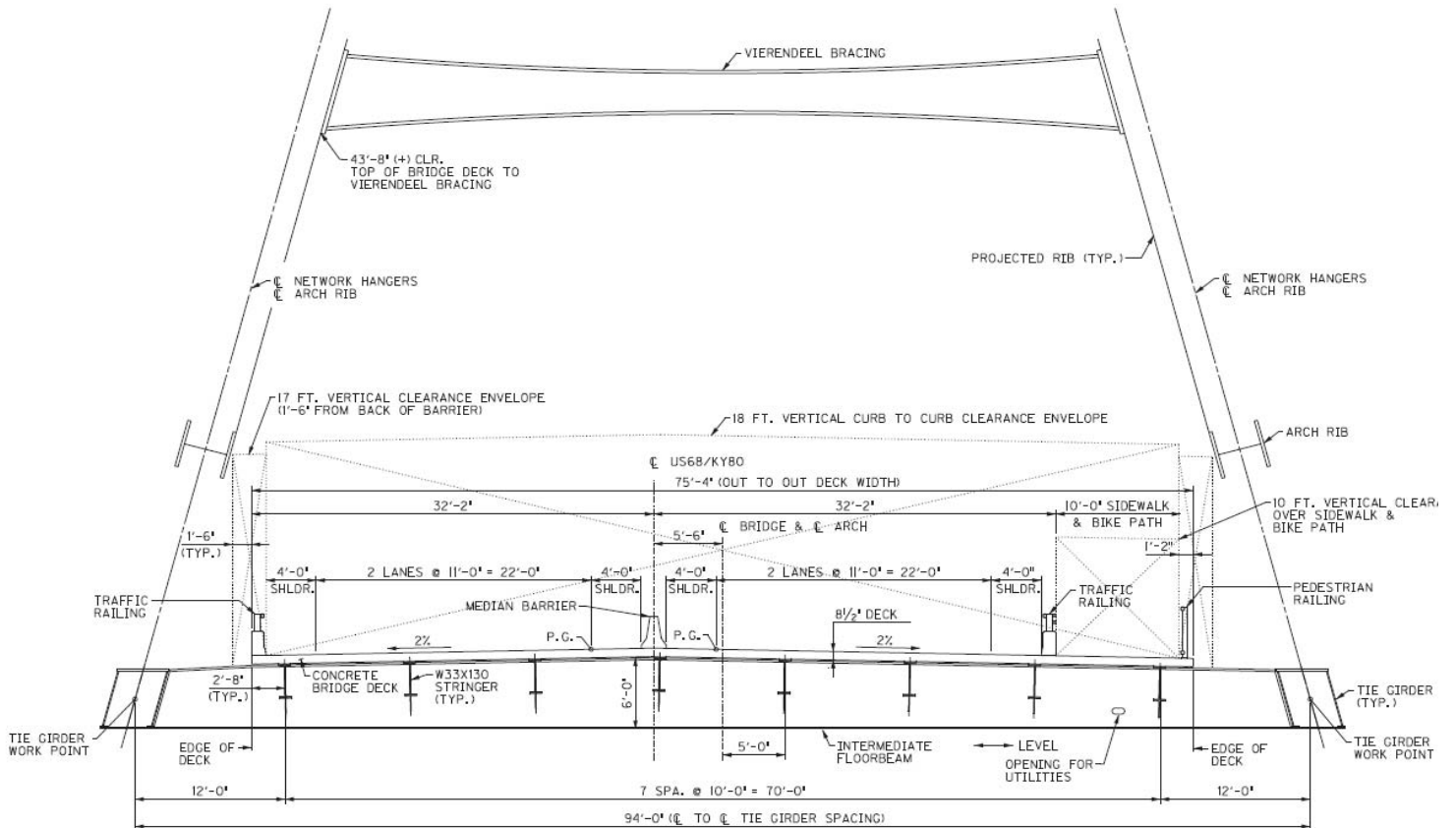
TYPICAL TIE GIRDER SECTION



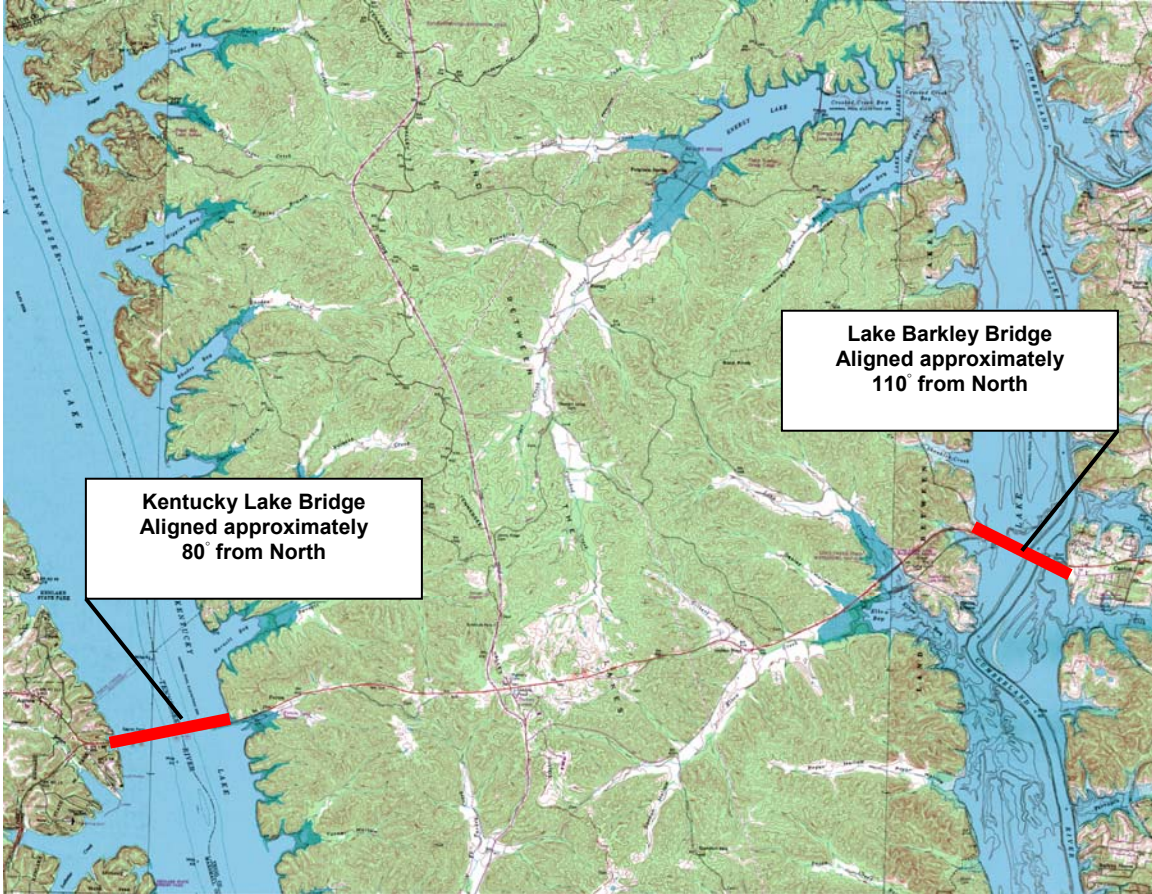
TYPICAL TIE GIRDER SECTION AT FLOORBEAM



VIEW B-B



TYPICAL ARCH SPAN CROSS SECTION
(LOOKING AHEAD STATION)



Plan of bridges sites over Kentucky and Barkley Lakes

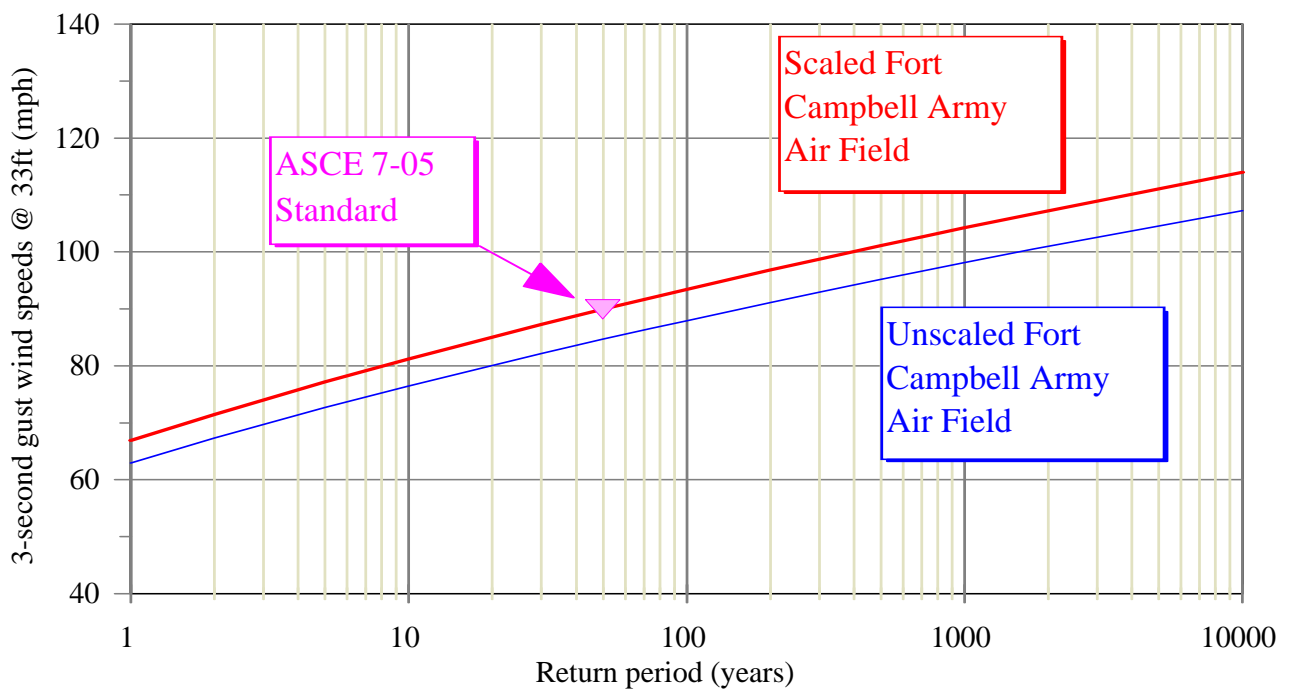
Figure No. 2-1

Lake Bridges – Over Kentucky Lake and Lake Barkley

Project #1301291

Date: May 6, 2013





3-second Gust Speed at 33 ft
Wind speeds vs. return periods in a standard terrain

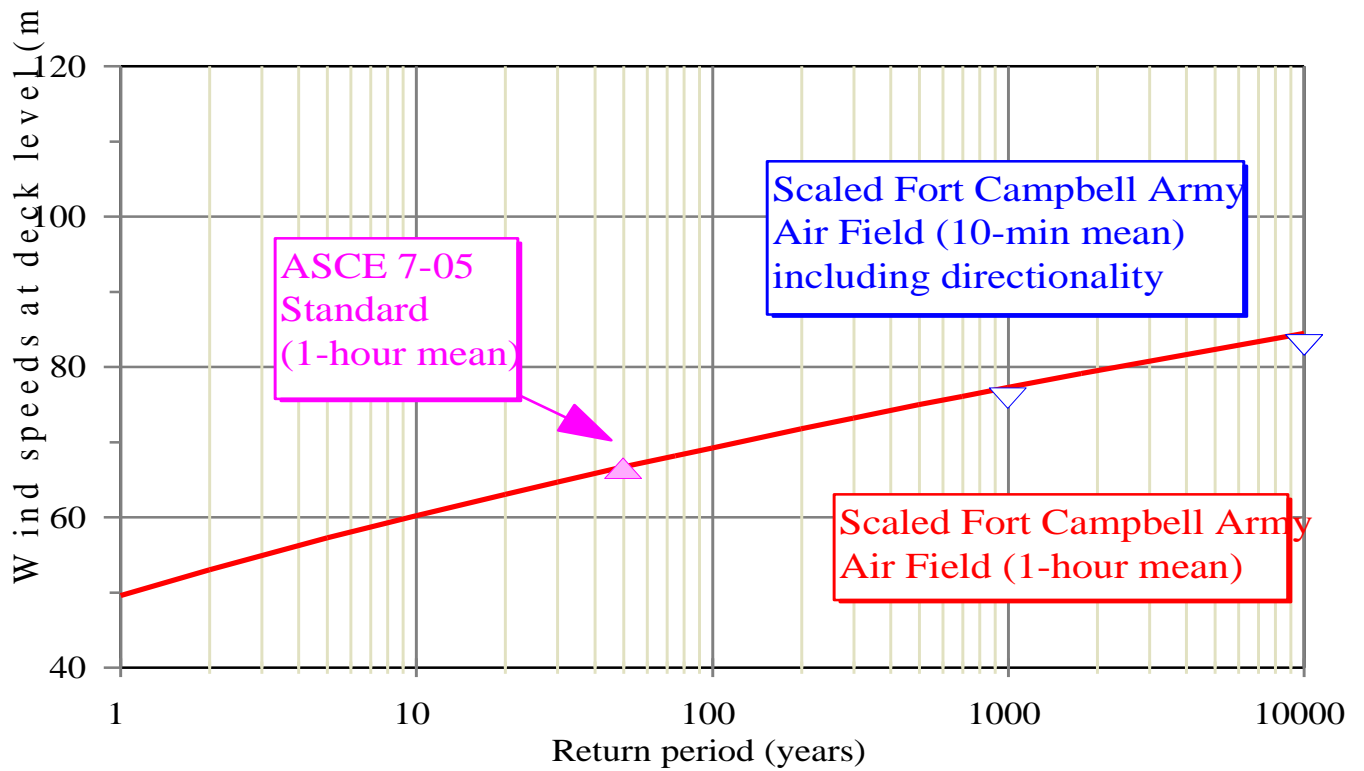
Lake Bridges – Over Kentucky Lake and Lake Barkley

Project #1301291

Figure No. 2-2

Date: May 6, 2013





Mean Wind Speeds at Deck Level (80 ft)

Kentucky Lake Bridge and Lake Barkley Bridge

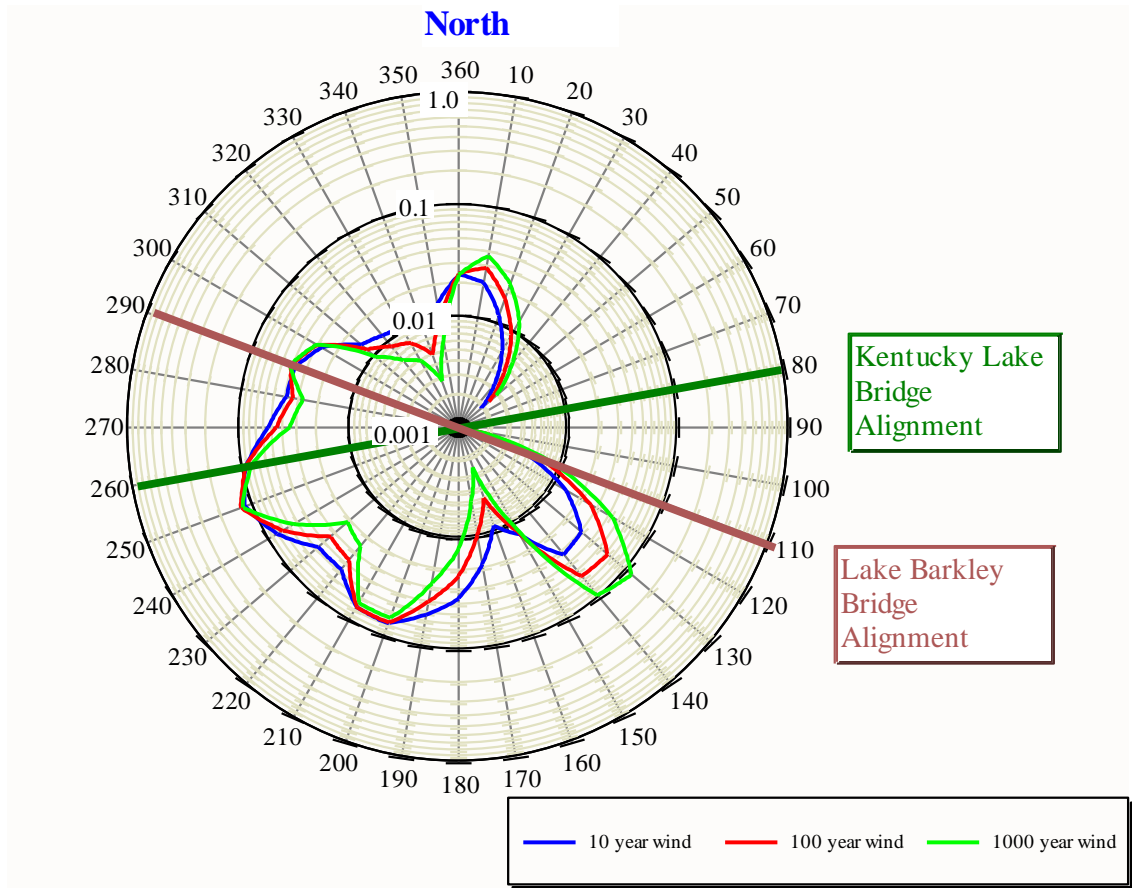
Lake Bridges – Over Kentucky Lake and Lake Barkley

Figure No. 2-3

Date: May 6, 2013

Project #1301291





Wind Directionality at the Bridge Sites

Probability of Exceeding Wind Speed vs. Wind Direction
 Mean Hourly Wind Speed at Deck Height (80 ft)

Lake Bridges – Over Kentucky Lake and Lake Barkley

Figure No. 2-4

Date: May 6, 2013



Project #1301291



a) sectional model & ground plate



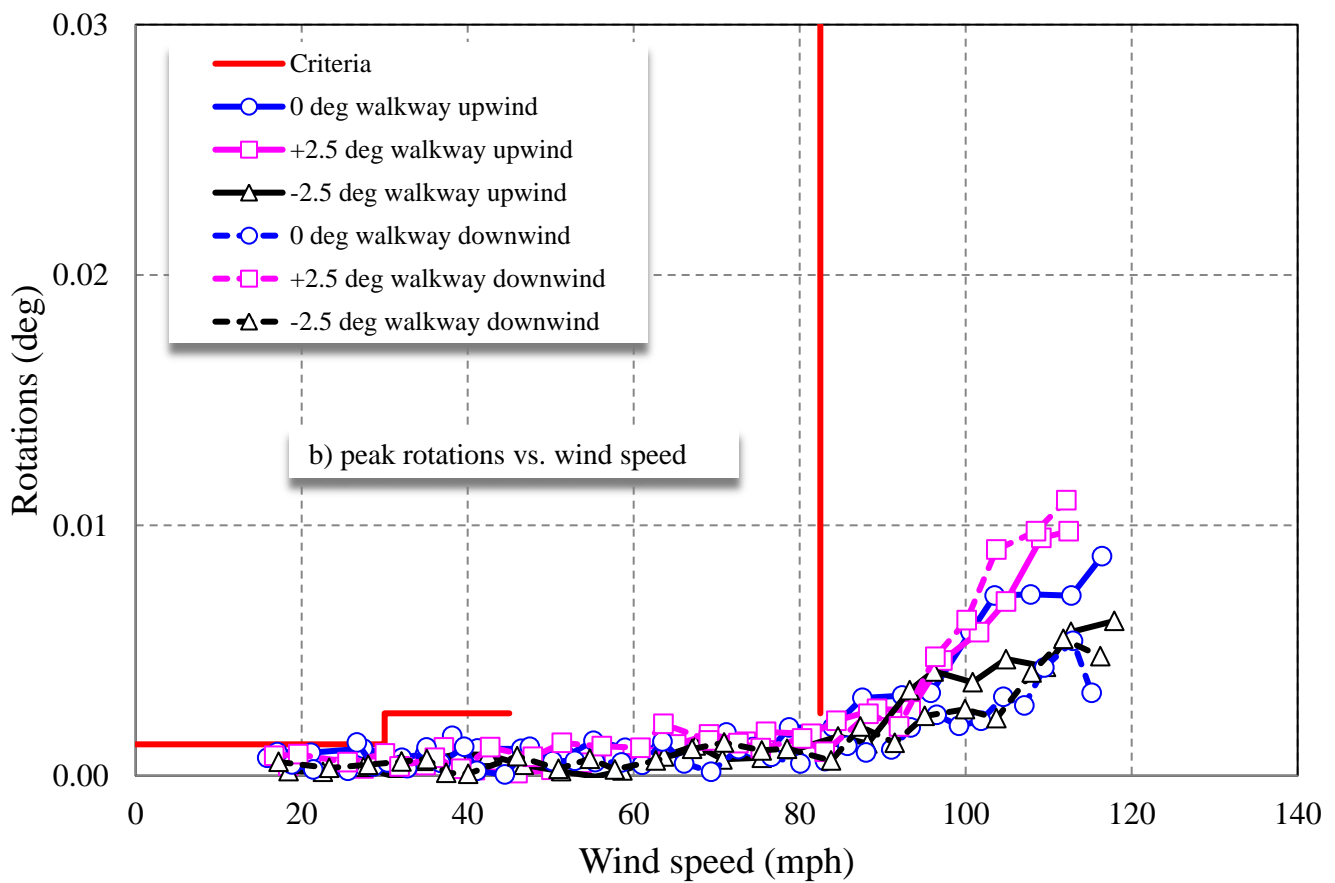
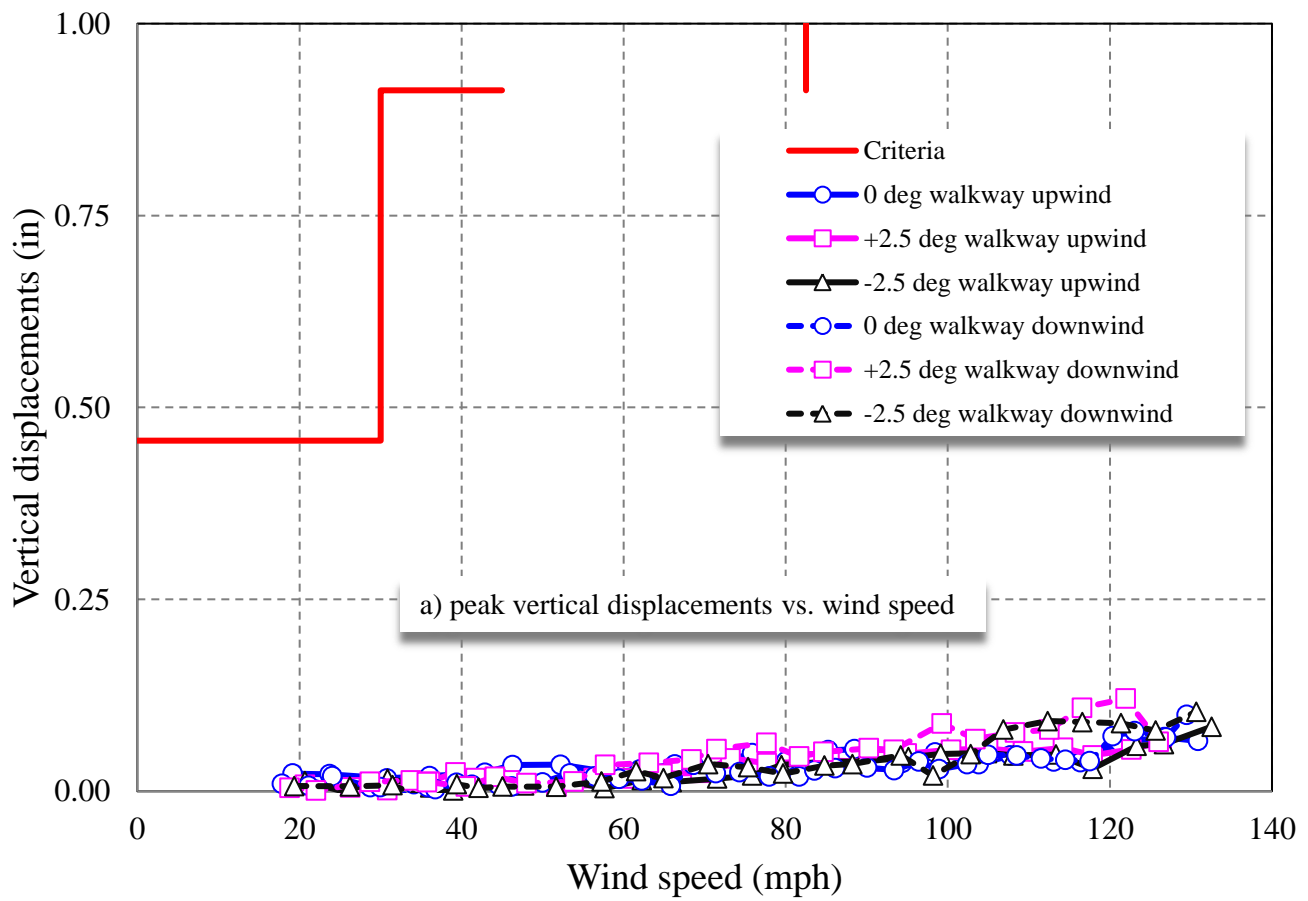
b) external set-up

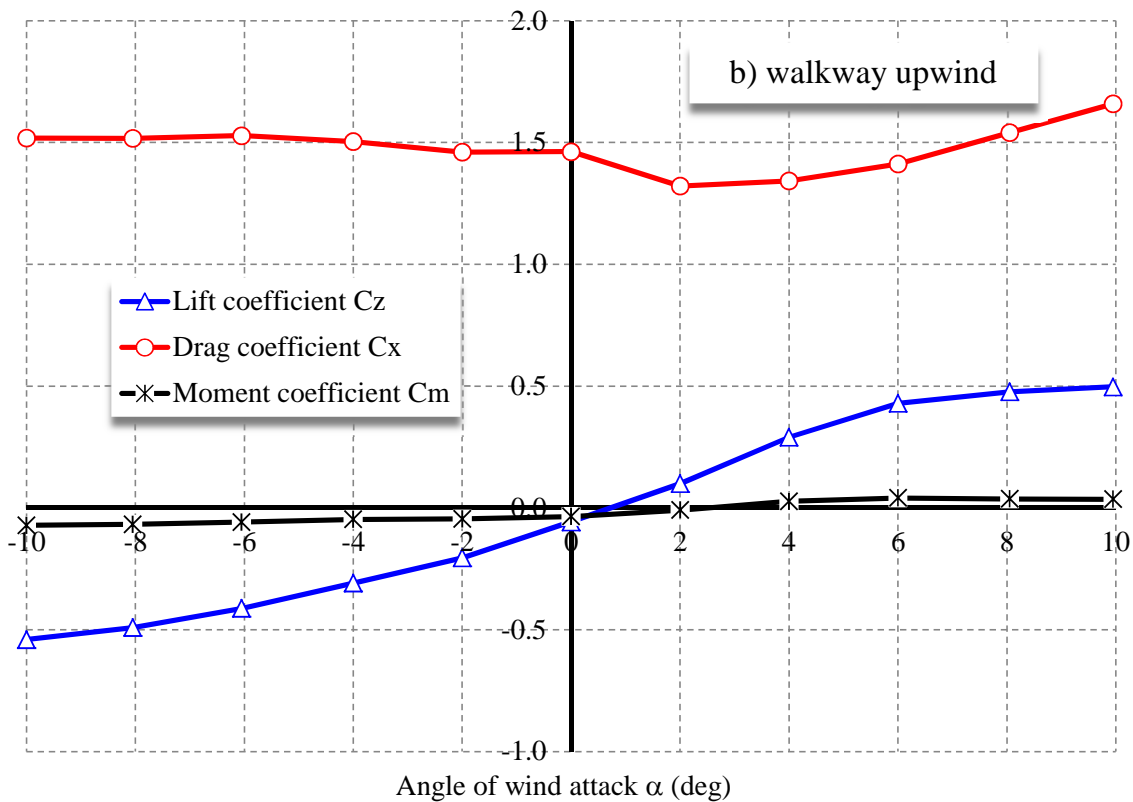
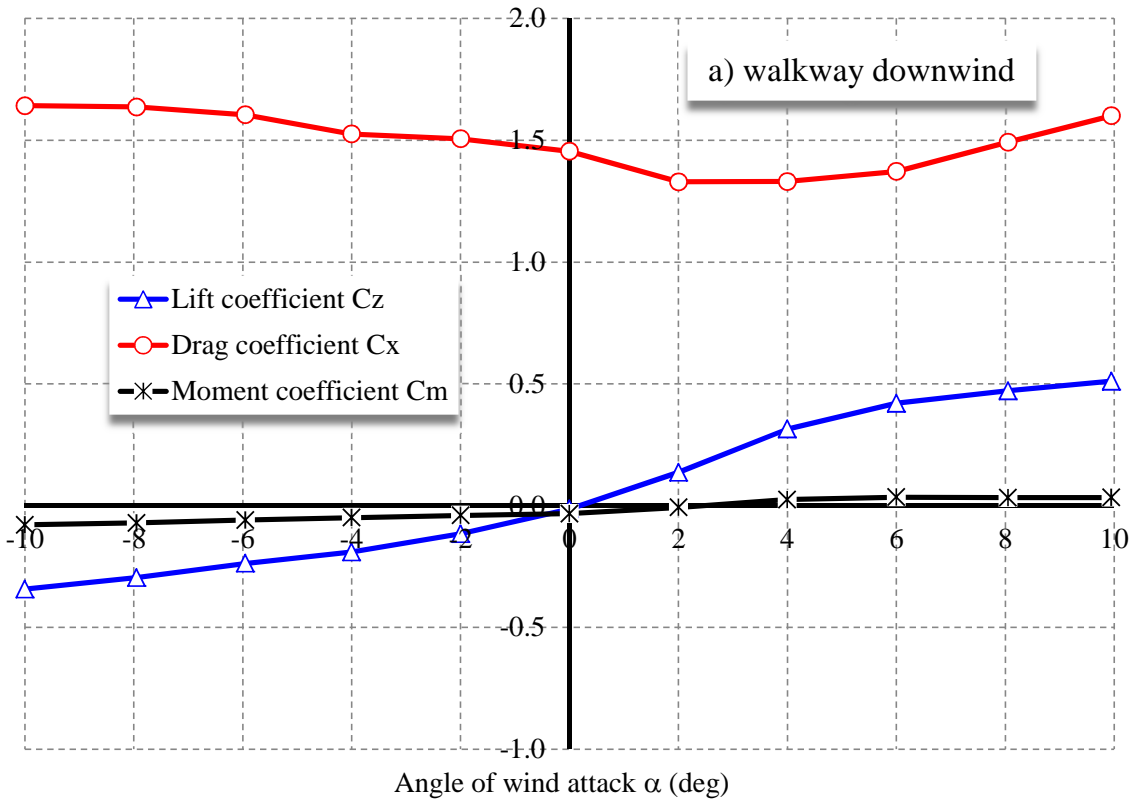


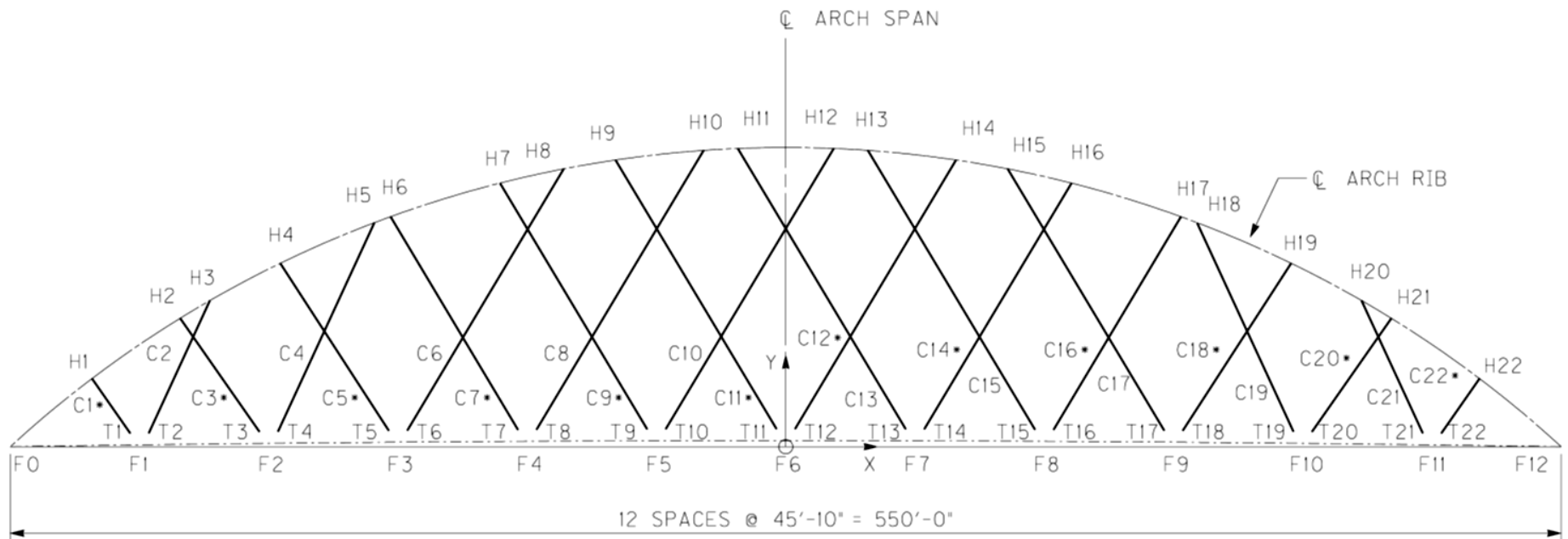
c) walkway upwind top-view



d) view from beneath





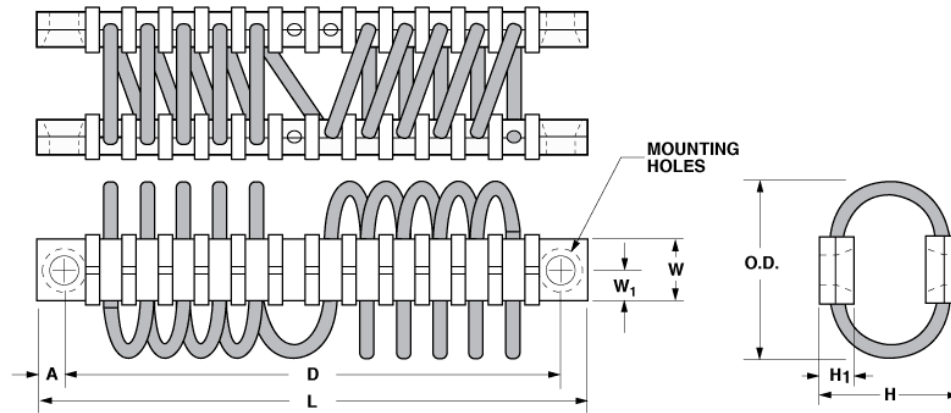


KEY ELEVATION

Notes: * denotes twin parallel cable arrangement.
 Hanger layout for north and south arches are identical.

<p>Hanger Identification System</p> <p>Lake Bridges – Over Kentucky Lake and Lake Barkley</p>	<p>Figure No. 5-1</p>	
	<p>Date: July 22, 2013</p>	

Project #1301291



Wire Rope Isolators

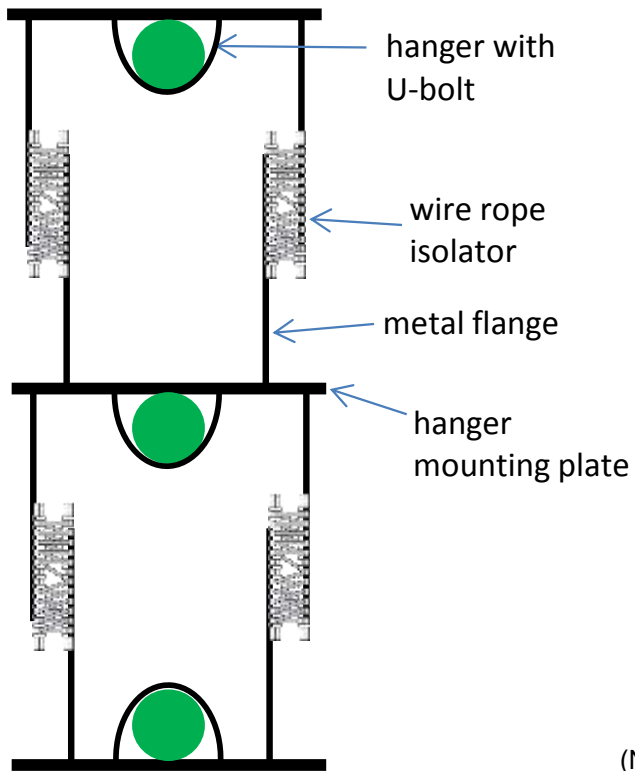
Lake Bridges – Over Kentucky Lake and Lake Barkley

Figure No. 5-2

Date: September 18, 2013

Project #1301291

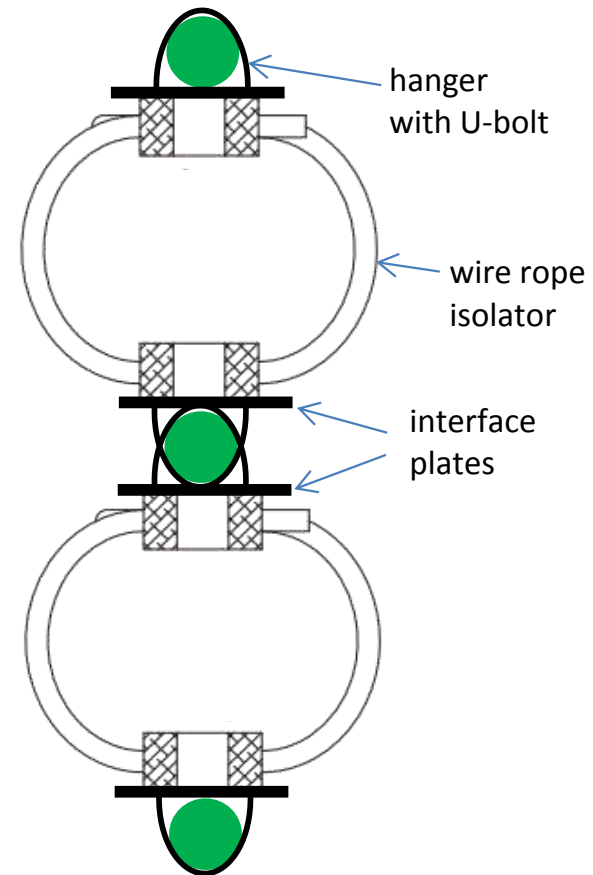




Option 1:

7/8" rods replaced with wire rope isolators with flanges

(Not to scale)



Option 2:

Hangers fastened into wire rope isolator restraining bars via interface plates

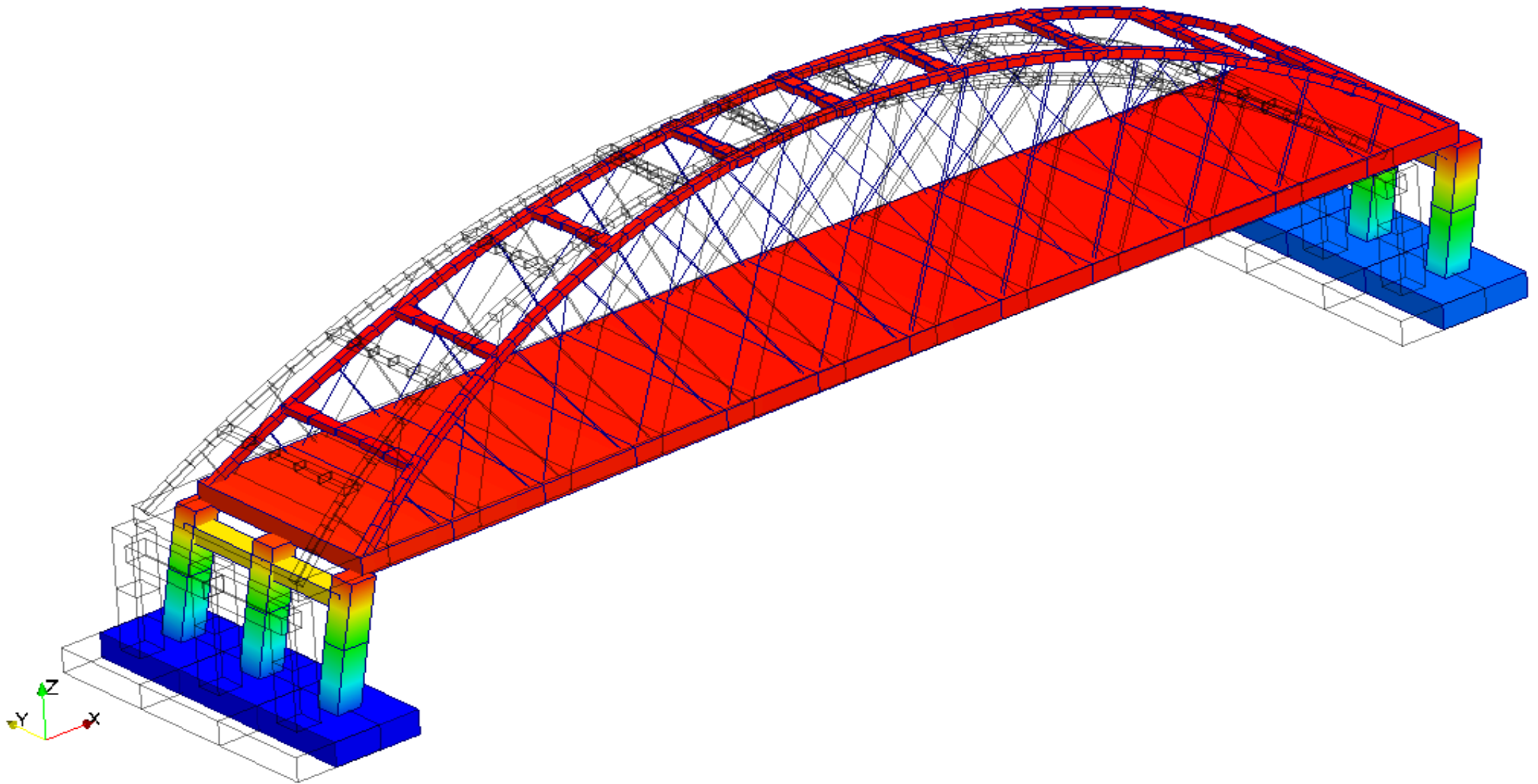
Wire Rope Isolator Connection Options

Figure No. 5-3



APPENDIX A

Kentucky Lake Bridge Dynamic Properties



Dynamic information

Mode 1, $f = 0.257$ Hz

Wind Engineering Study

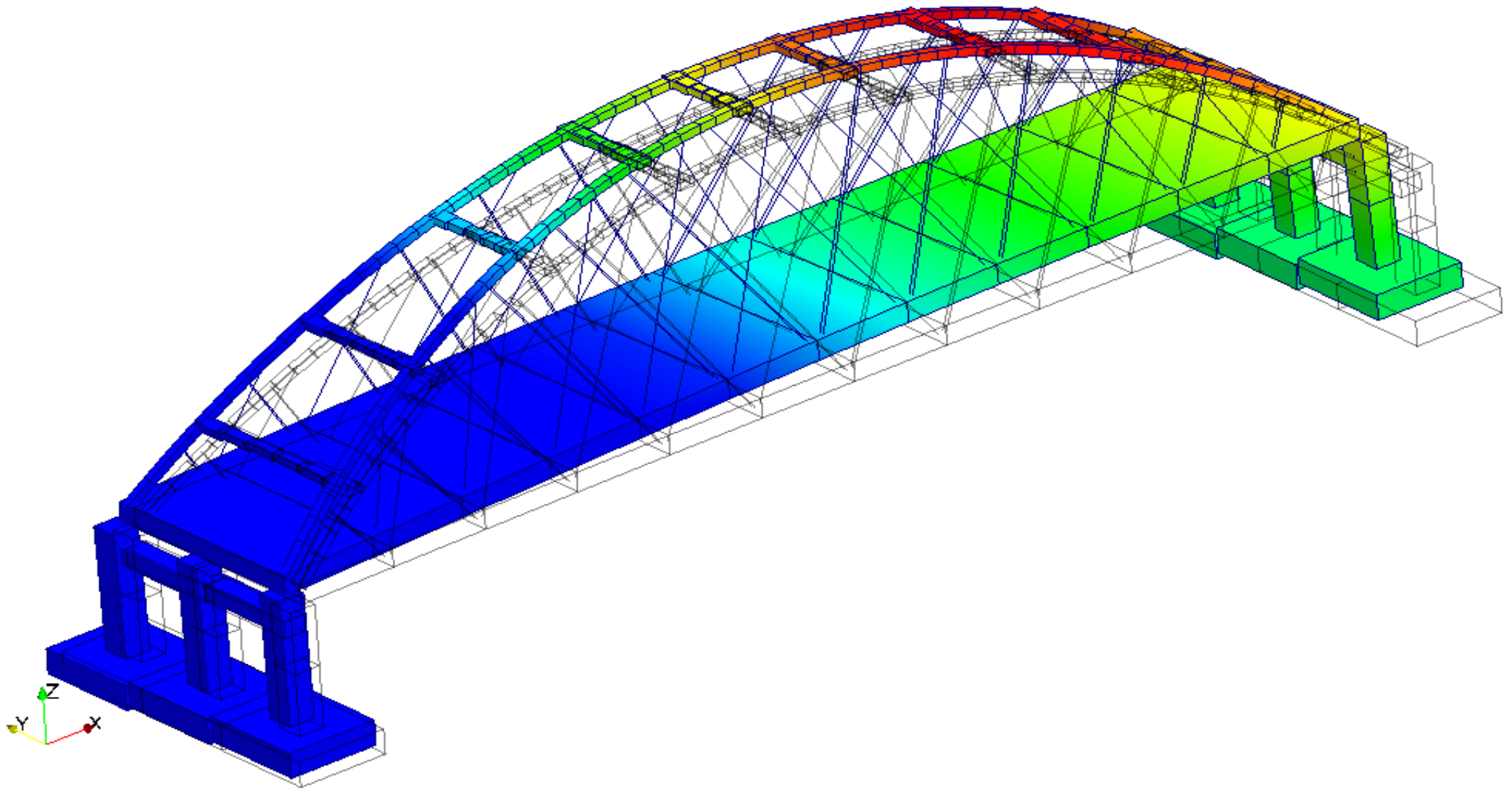
Lake Bridges – Over Kentucky Lake and Lake Barkley

Appendix A-1

May 3, 2013

Project #1301291

RWDI



Dynamic information

Mode 2, $f = 0.351$ Hz

Wind Engineering Study

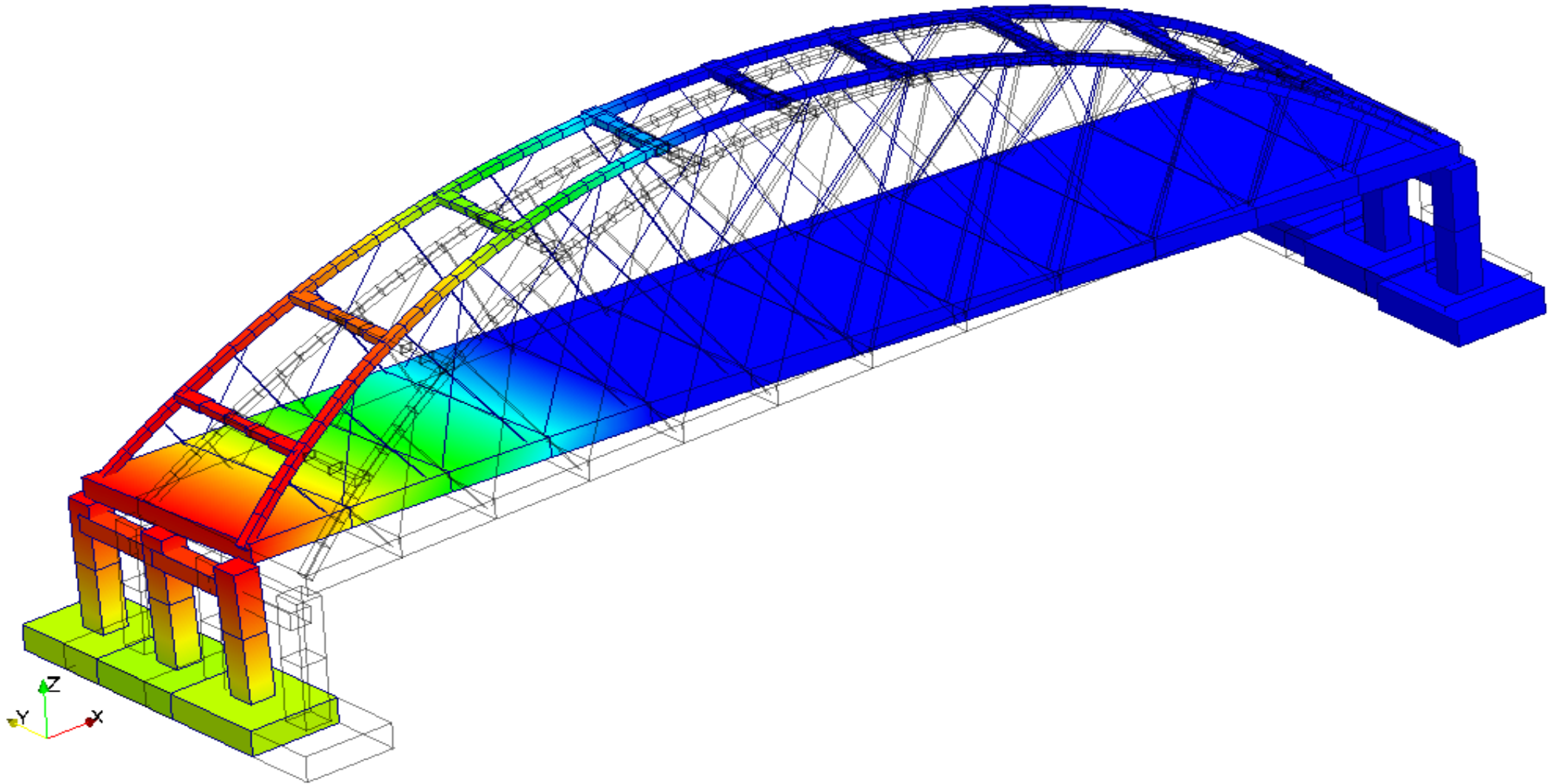
Lake Bridges – Over Kentucky Lake and Lake Barkley

Appendix A-2

May 3, 2013

Project #1301291

RWDI



Dynamic information

Mode 3, $f = 0.415$ Hz

Wind Engineering Study

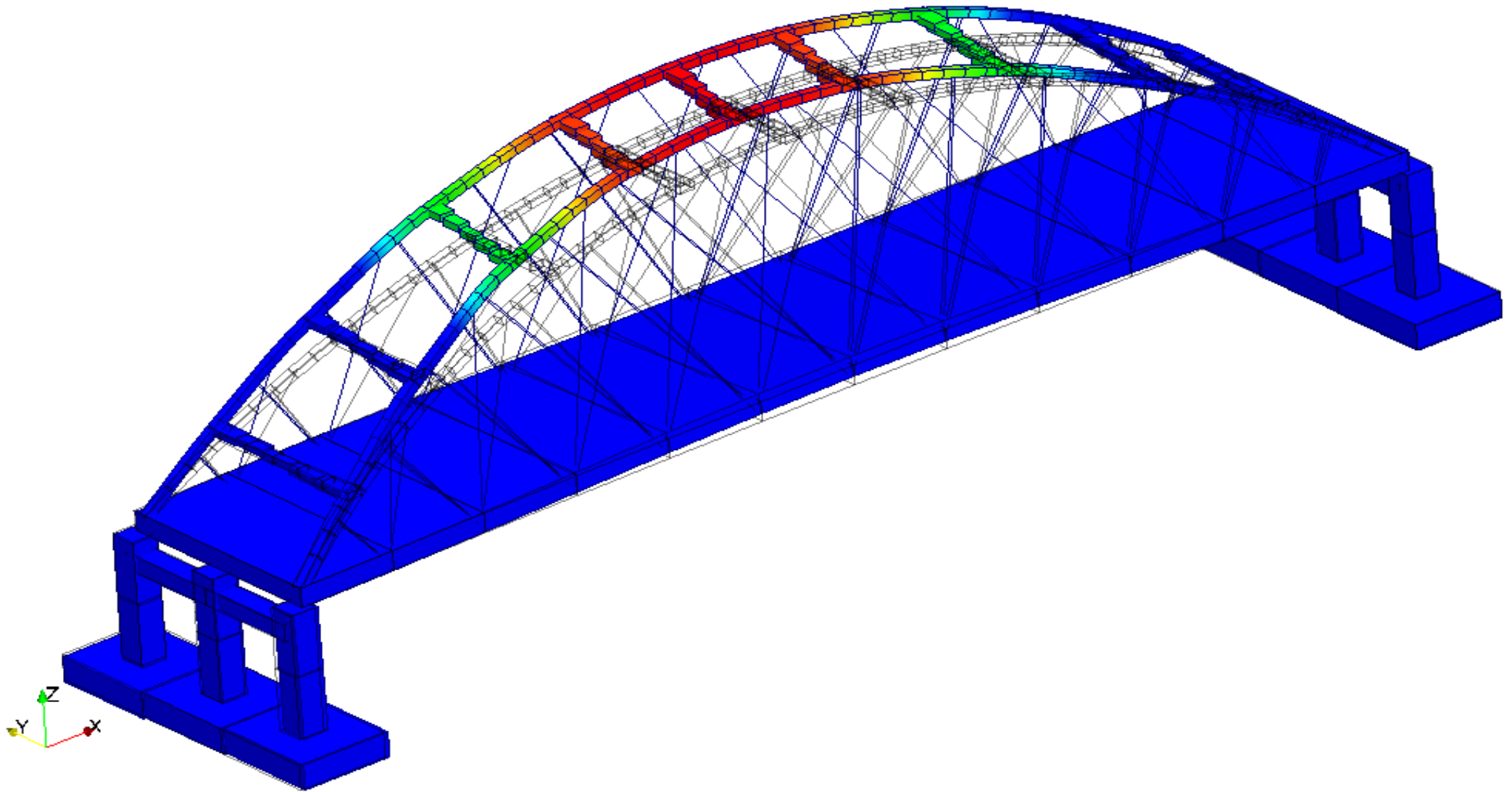
Lake Bridges – Over Kentucky Lake and Lake Barkley

Appendix A-3

May 3, 2013

Project #1301291

RWDI



Dynamic information

Mode 4, $f = 0.882$ Hz

Wind Engineering Study

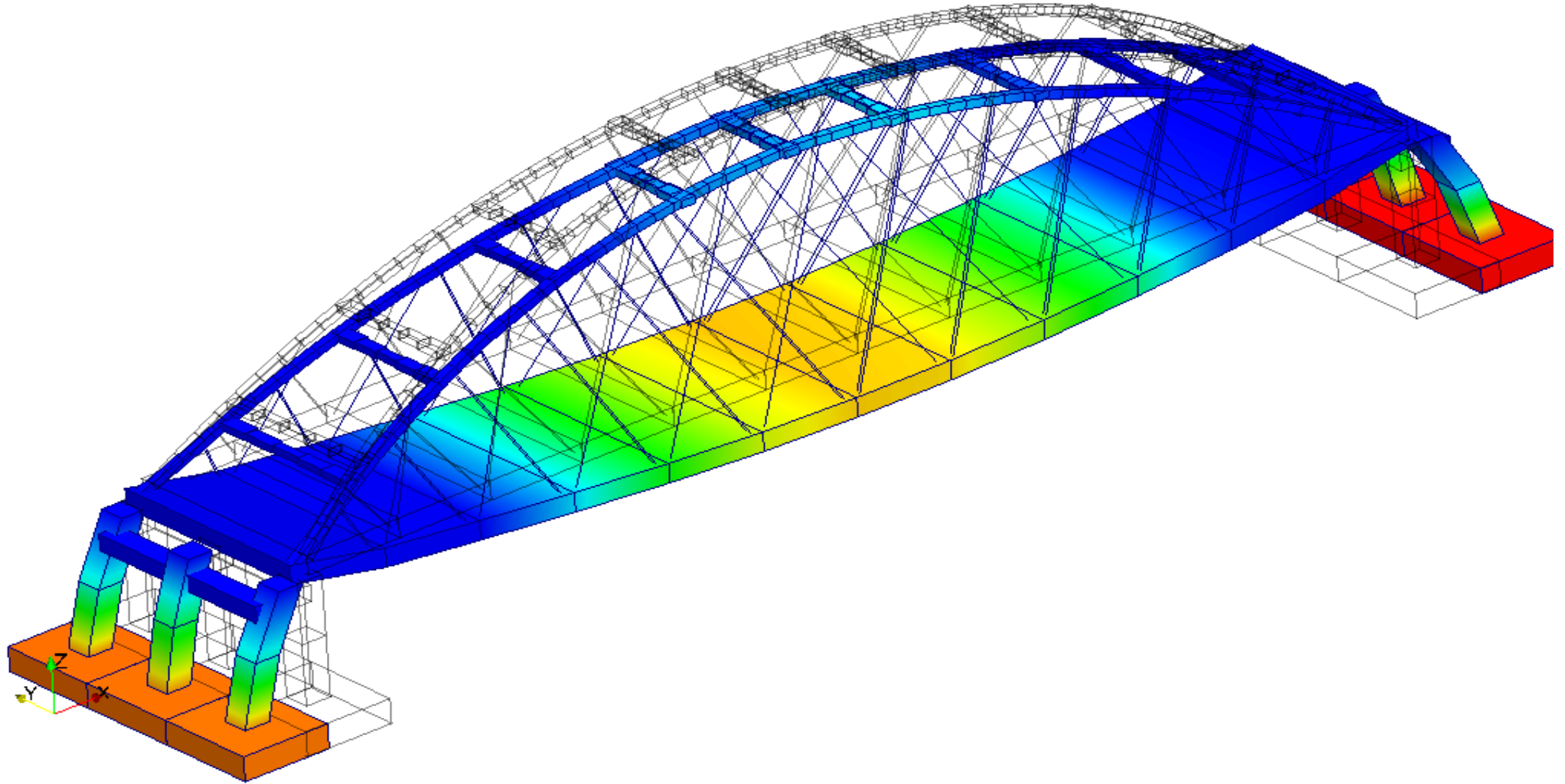
Lake Bridges – Over Kentucky Lake and Lake Barkley

Appendix A-4

May 3, 2013

Project #1301291

RWDI



Dynamic information

Mode 5, $f = 0.897$ Hz

Wind Engineering Study

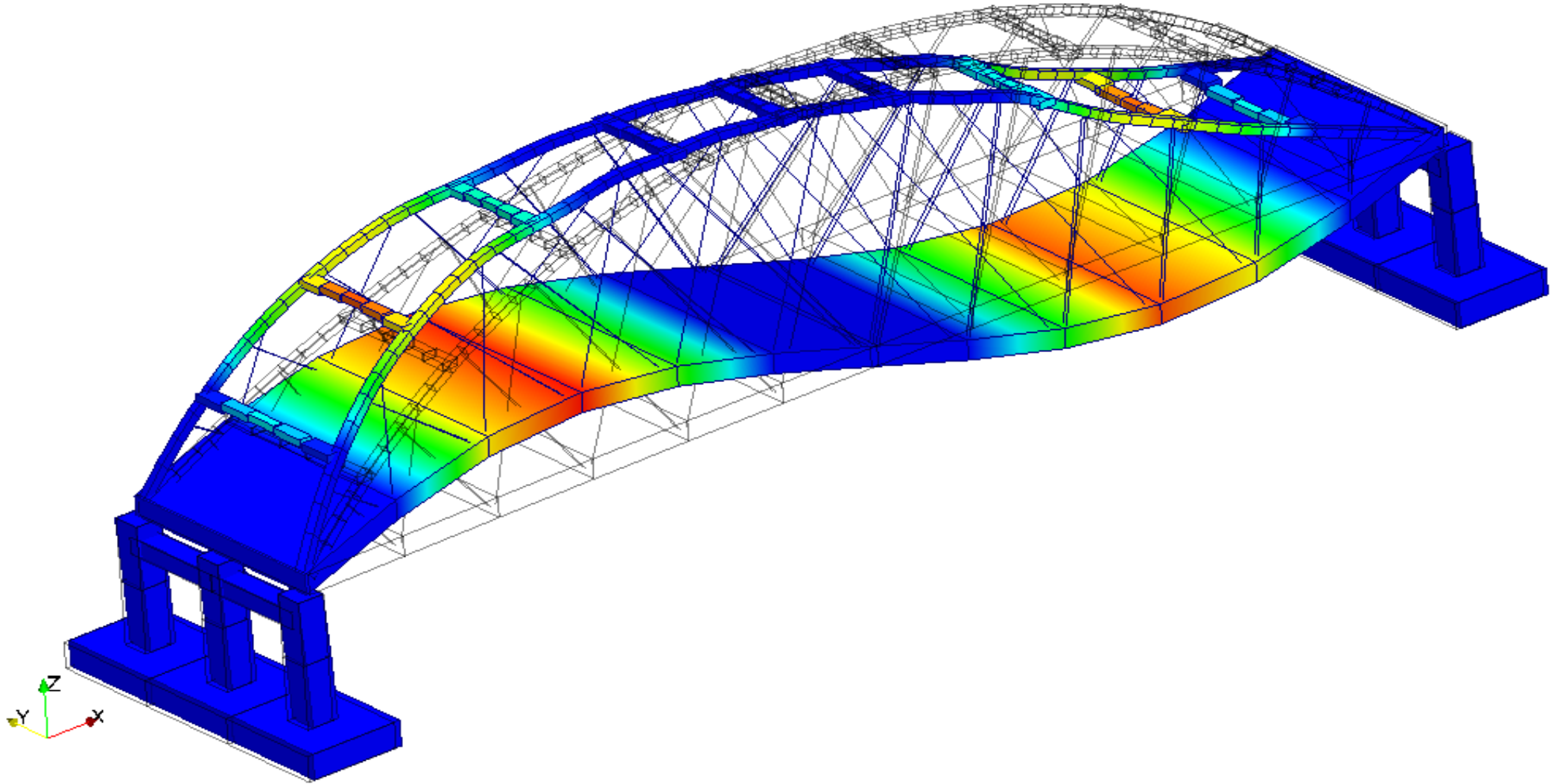
Lake Bridges – Over Kentucky Lake and Lake Barkley

Appendix A-5

May 3, 2013

Project #1301291

RWDI



Dynamic information

Mode 6, $f = 1.035$ Hz

Wind Engineering Study

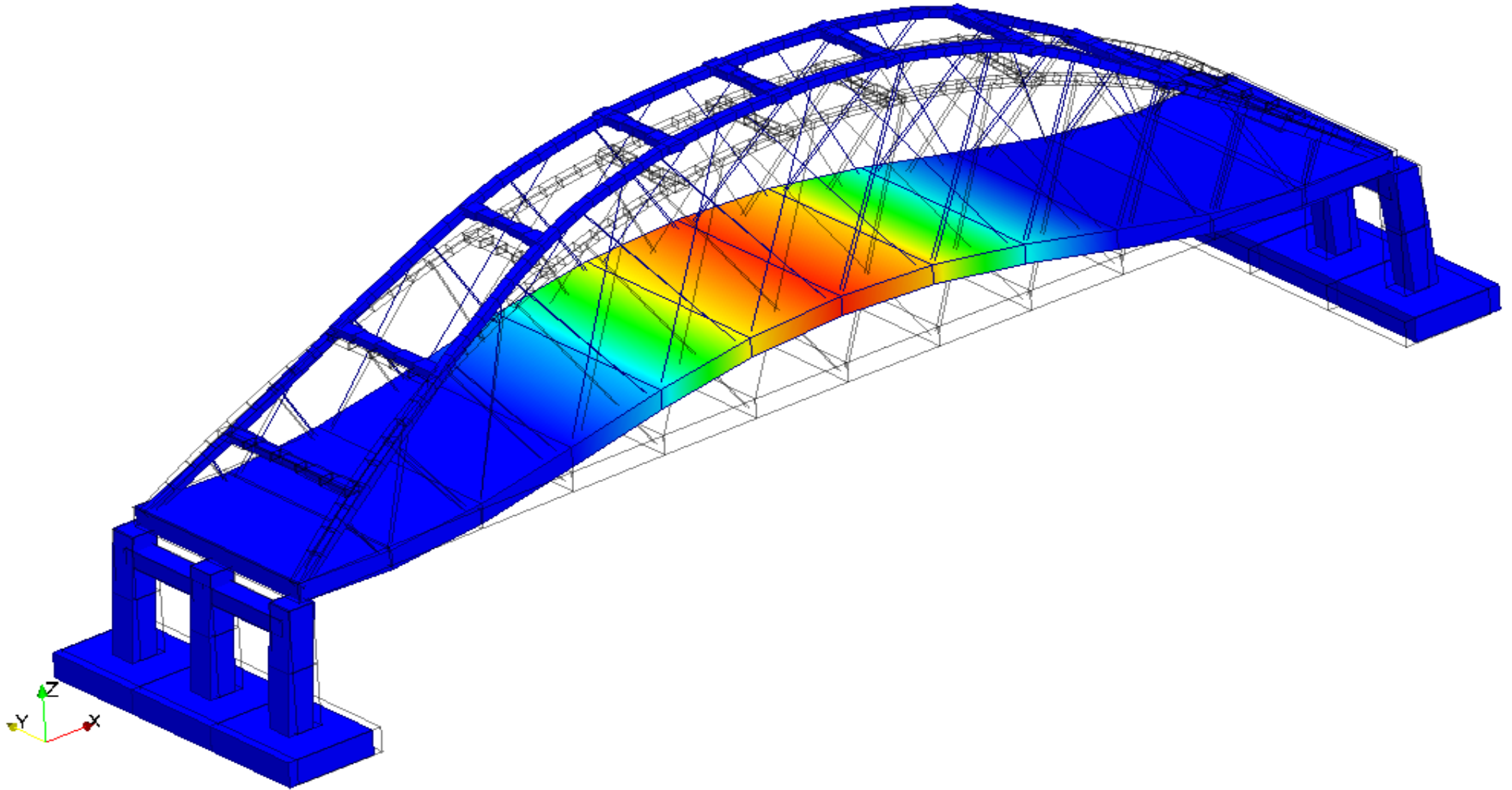
Lake Bridges – Over Kentucky Lake and Lake Barkley

Appendix A-6

May 3, 2013

Project #1301291

RWDI



Dynamic information

Mode 7, $f = 1.085$ Hz

Wind Engineering Study

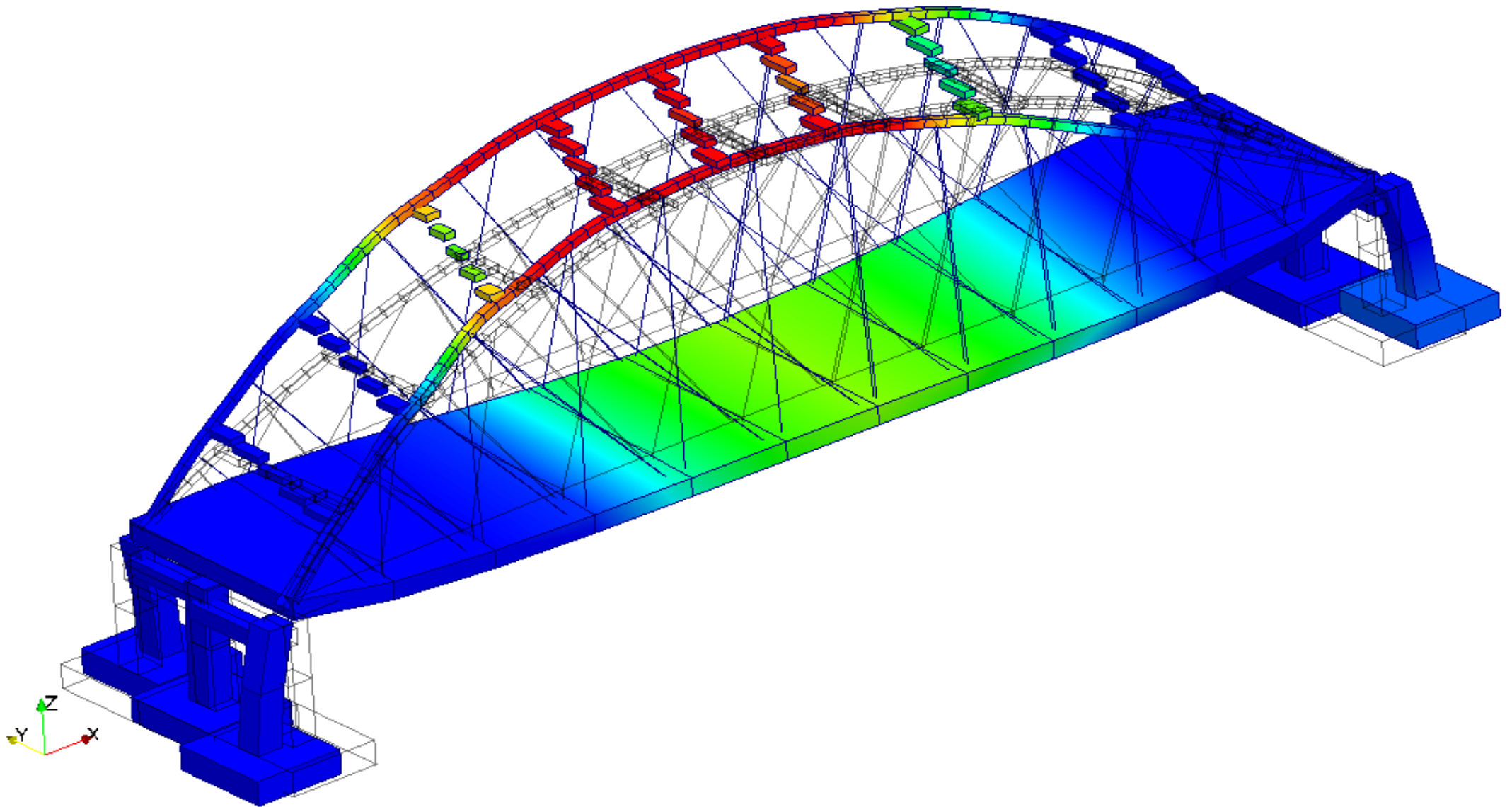
Lake Bridges – Over Kentucky Lake and Lake Barkley

Appendix A-7

May 3, 2013

Project #1301291

RWDI



Dynamic information

Mode 8, $f = 1.147$ Hz

Wind Engineering Study

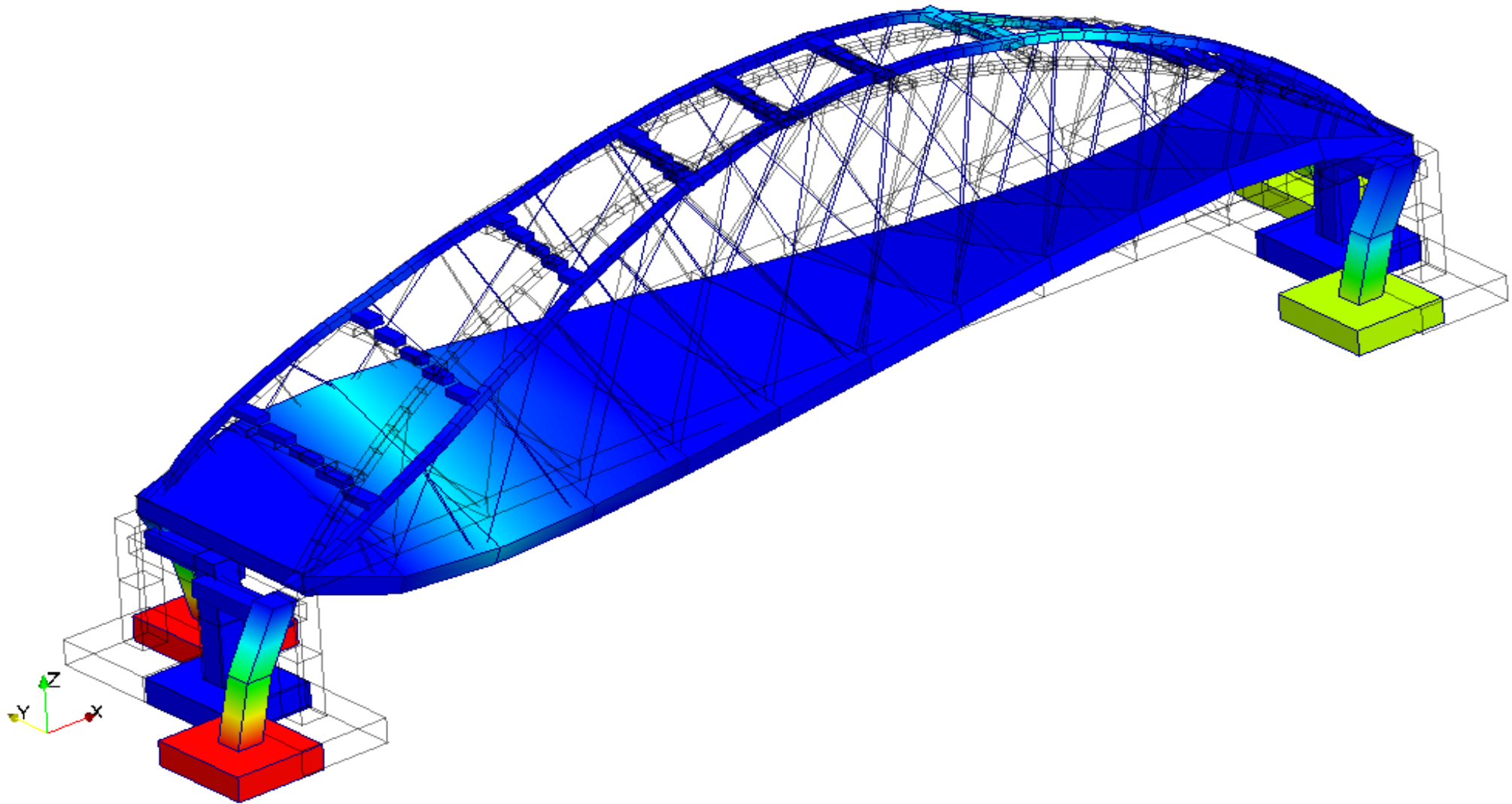
Lake Bridges – Over Kentucky Lake and Lake Barkley

Appendix A-8

May 3, 2013

Project #1301291

RWDI



Dynamic information

Mode 9, $f = 1.226$ Hz

Wind Engineering Study

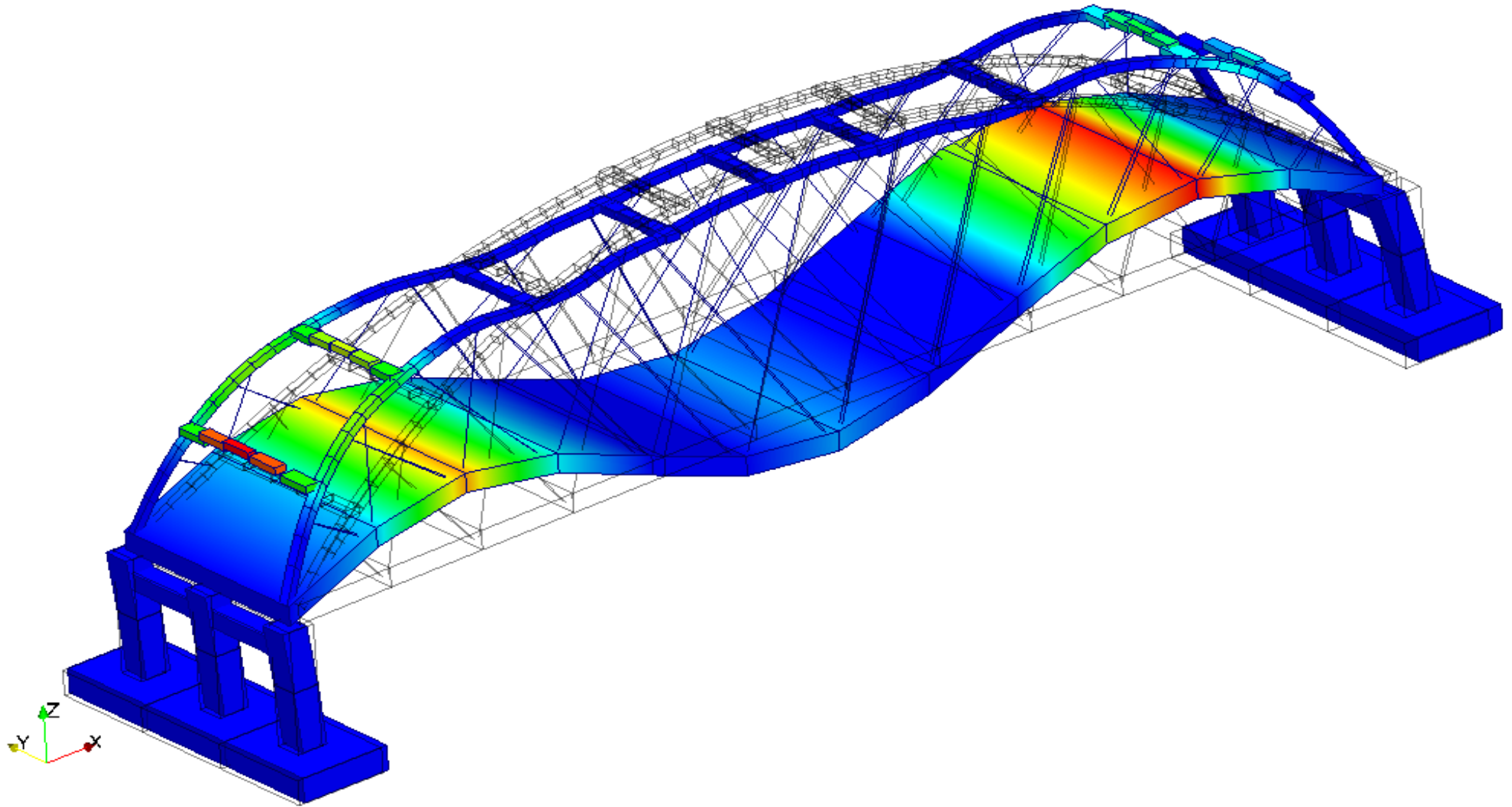
Lake Bridges – Over Kentucky Lake and Lake Barkley

Appendix A-9

May 3, 2013

Project #1301291

RWDI



Dynamic information

Mode 10, $f = 1.336$ Hz

Wind Engineering Study

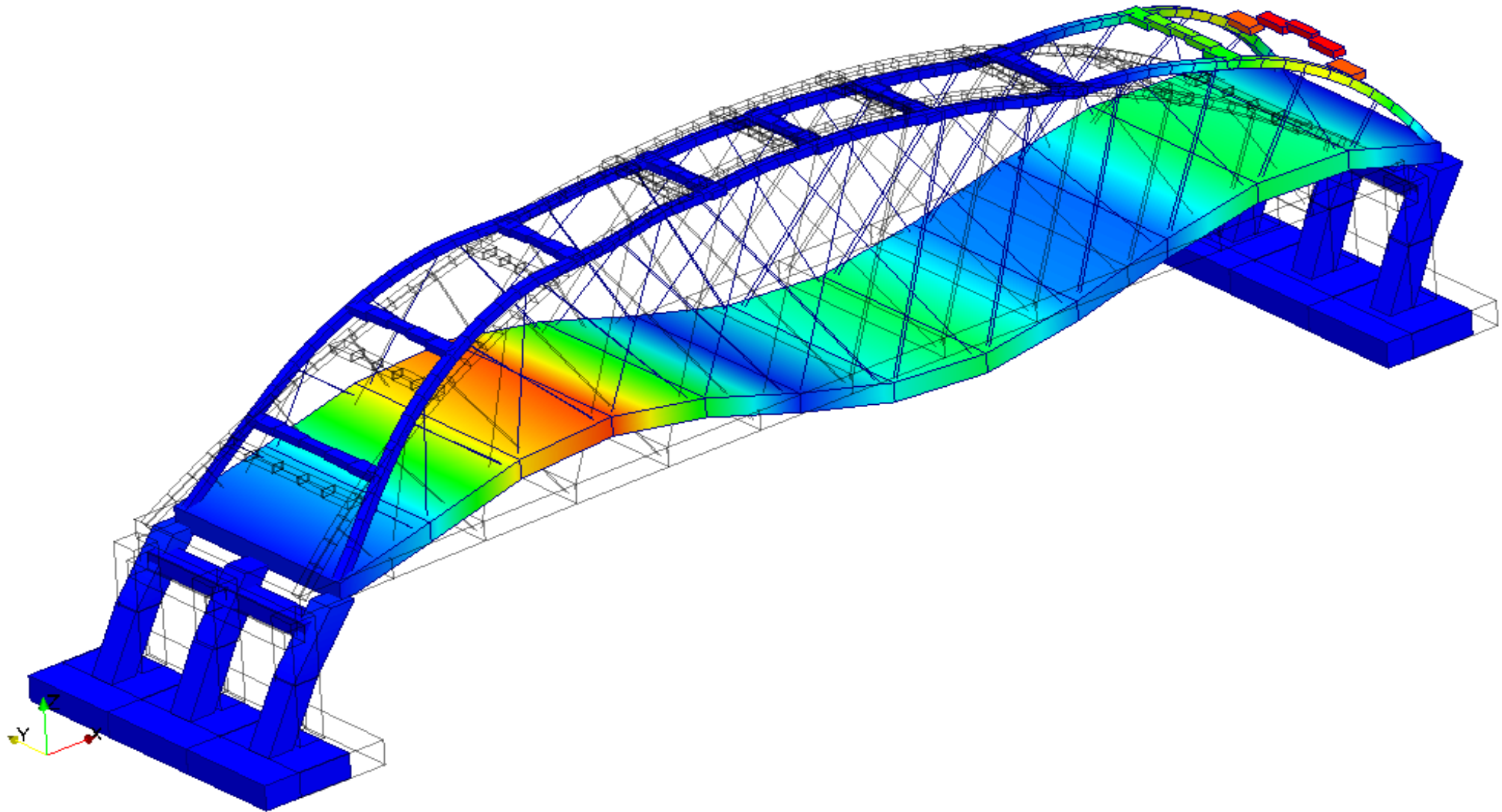
Lake Bridges – Over Kentucky Lake and Lake Barkley

Appendix A-10

May 3, 2013

Project #1301291

RWDI



Dynamic information

Mode 11, $f = 1.350$ Hz

Wind Engineering Study

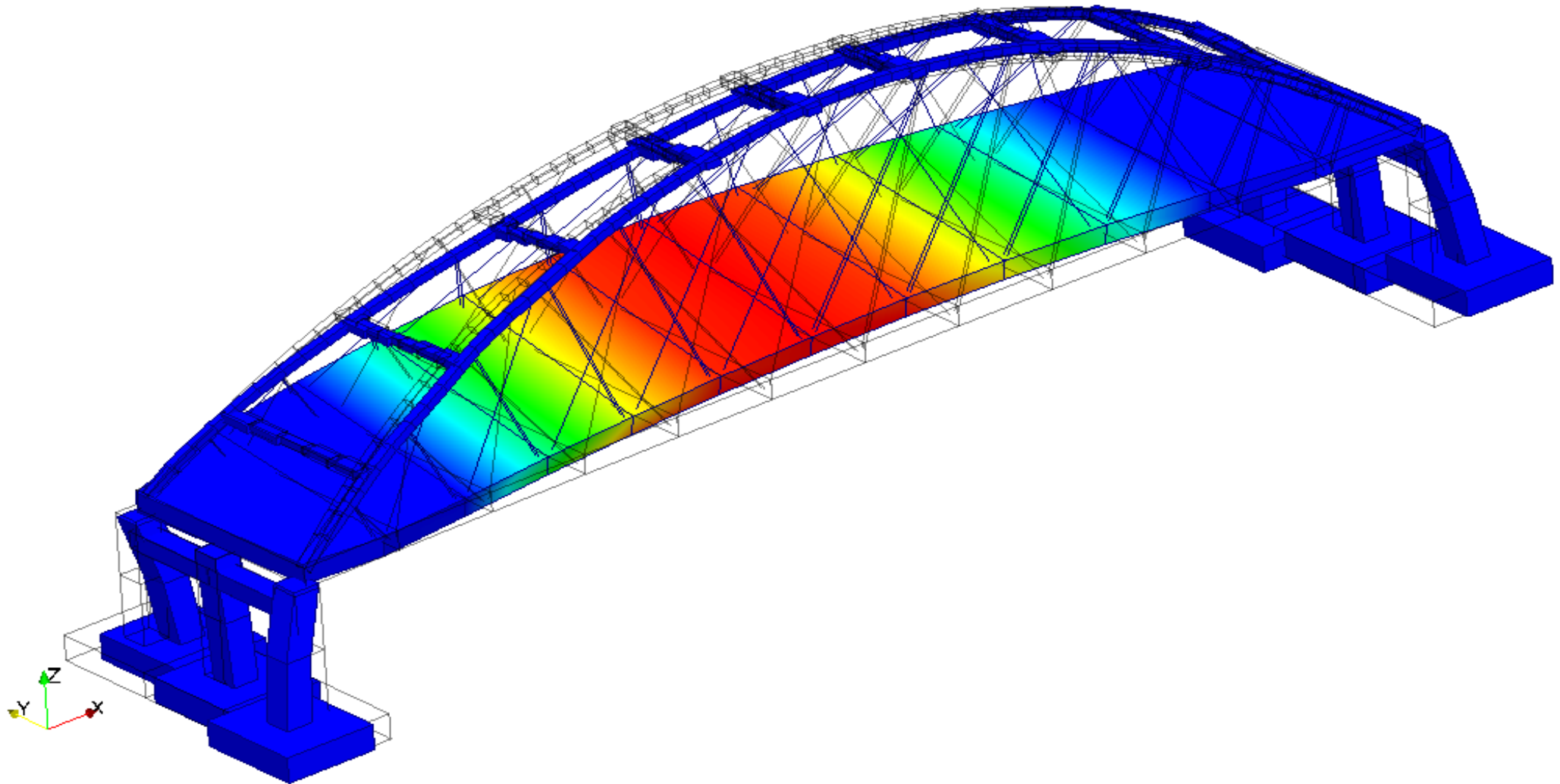
Lake Bridges – Over Kentucky Lake and Lake Barkley

Appendix A-11

May 3, 2013

Project #1301291

RWDI



Dynamic information

Mode 12, $f = 1.395$ Hz

Wind Engineering Study

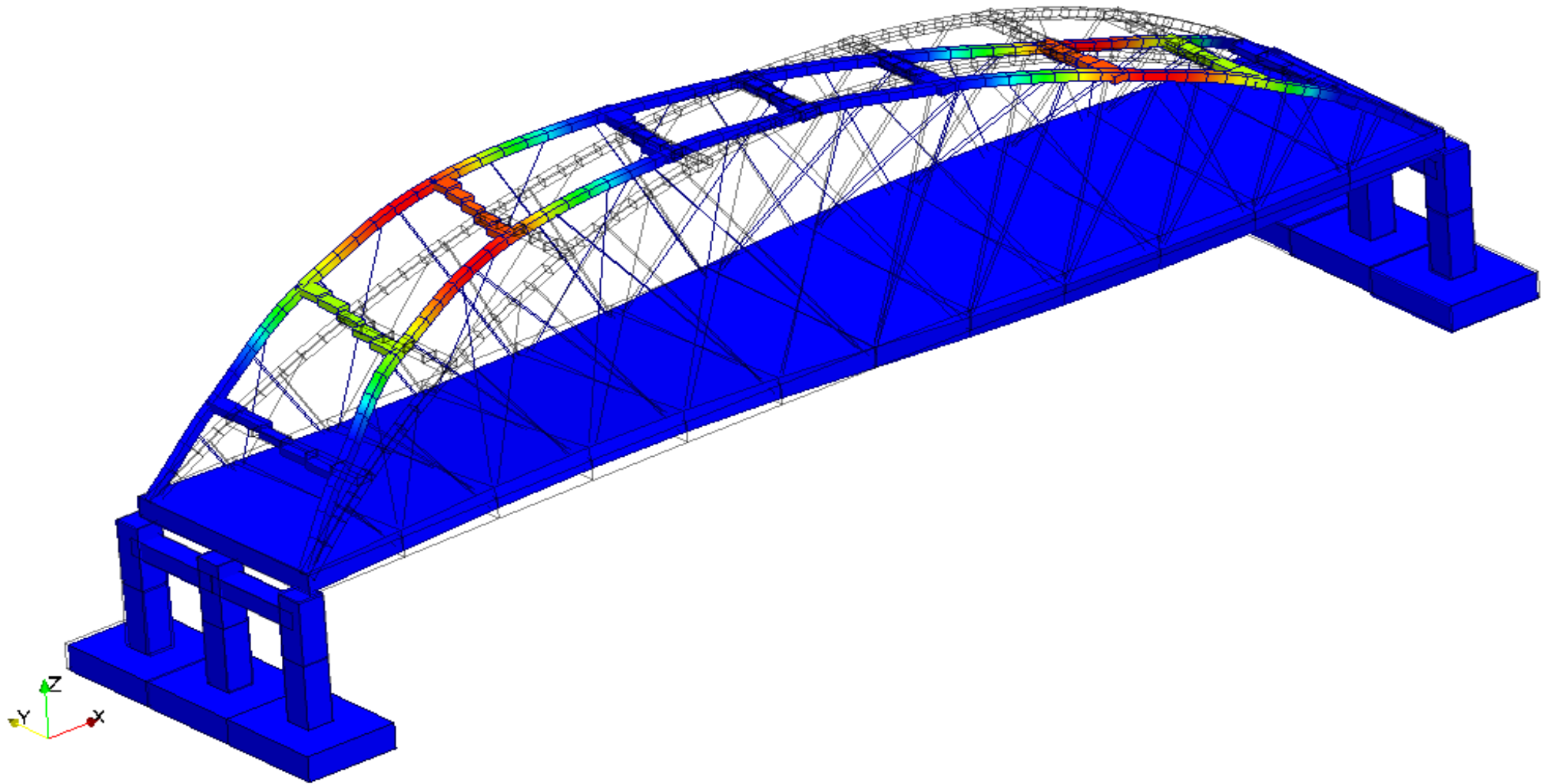
Lake Bridges – Over Kentucky Lake and Lake Barkley

Appendix A-12

May 3, 2013

Project #1301291

RWDI



Dynamic information

Mode 13, $f = 1.484$ Hz

Wind Engineering Study

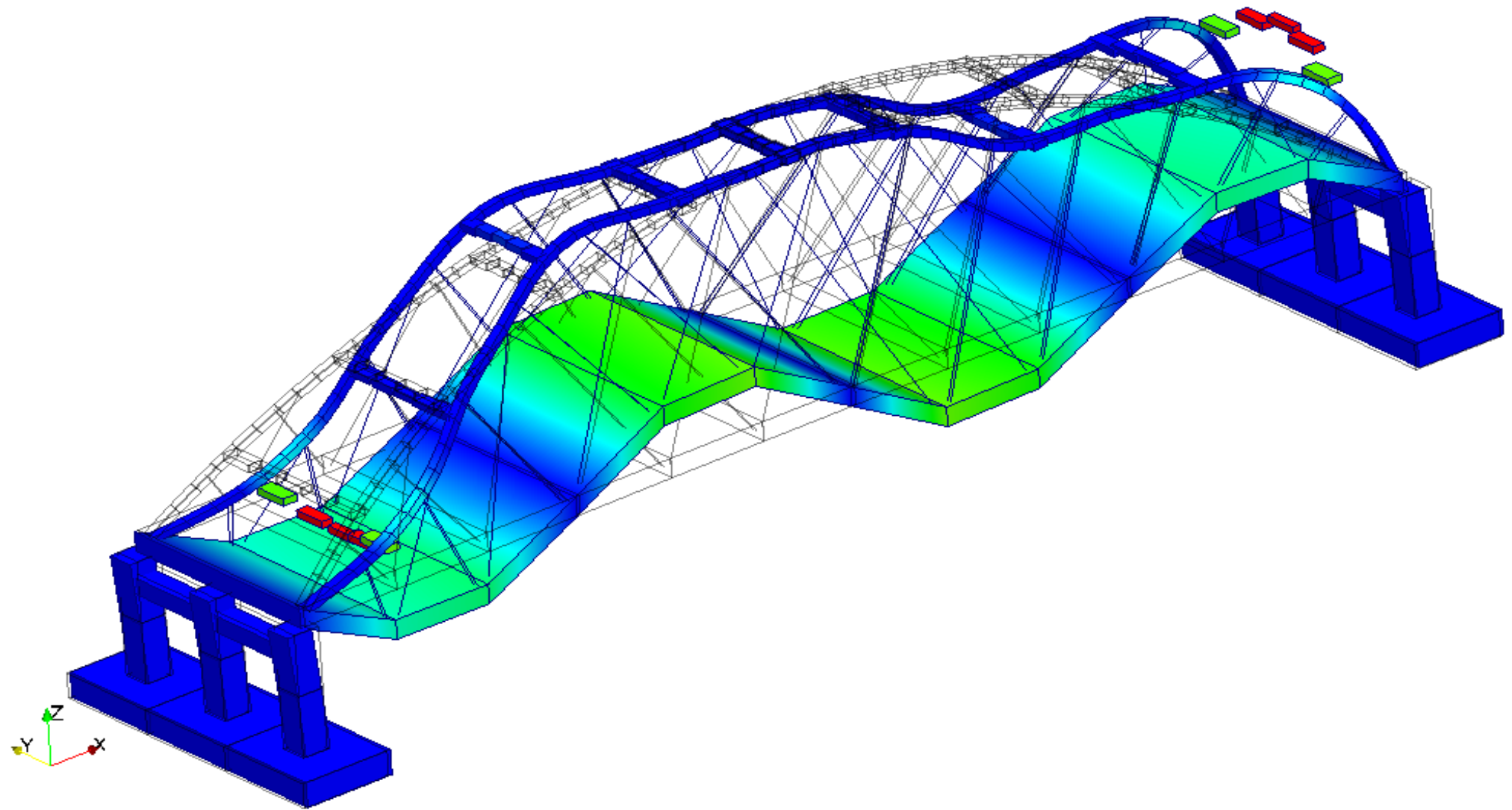
Lake Bridges – Over Kentucky Lake and Lake Barkley

Appendix A-13

May 3, 2013

Project #1301291

RWDI



Dynamic information

Mode 14, $f = 1.652$ Hz

Wind Engineering Study

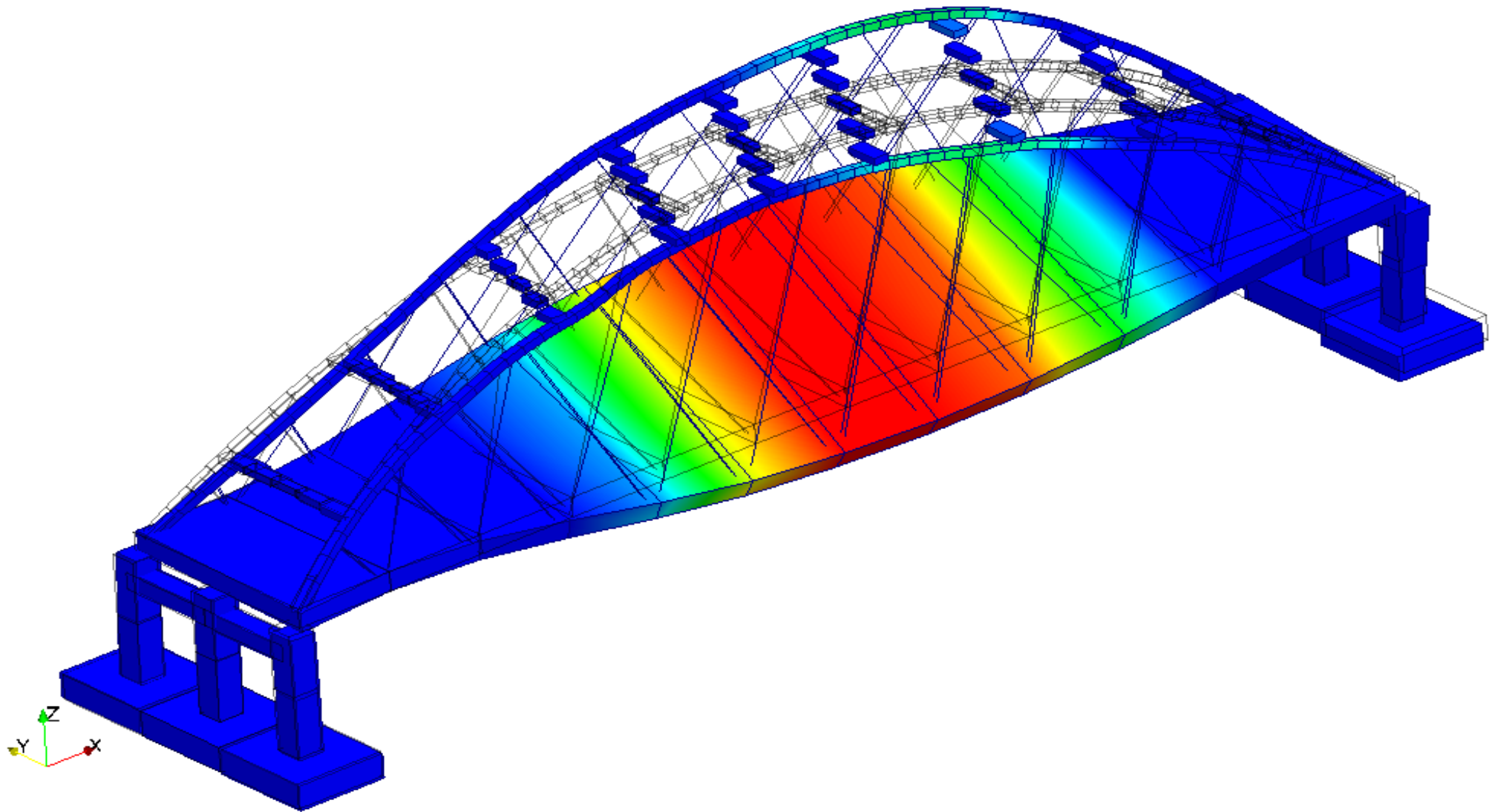
Lake Bridges – Over Kentucky Lake and Lake Barkley

Appendix A-14

May 3, 2013

Project #1301291

RWDI



Dynamic information

Mode 15, $f = 1.851$ Hz

Wind Engineering Study

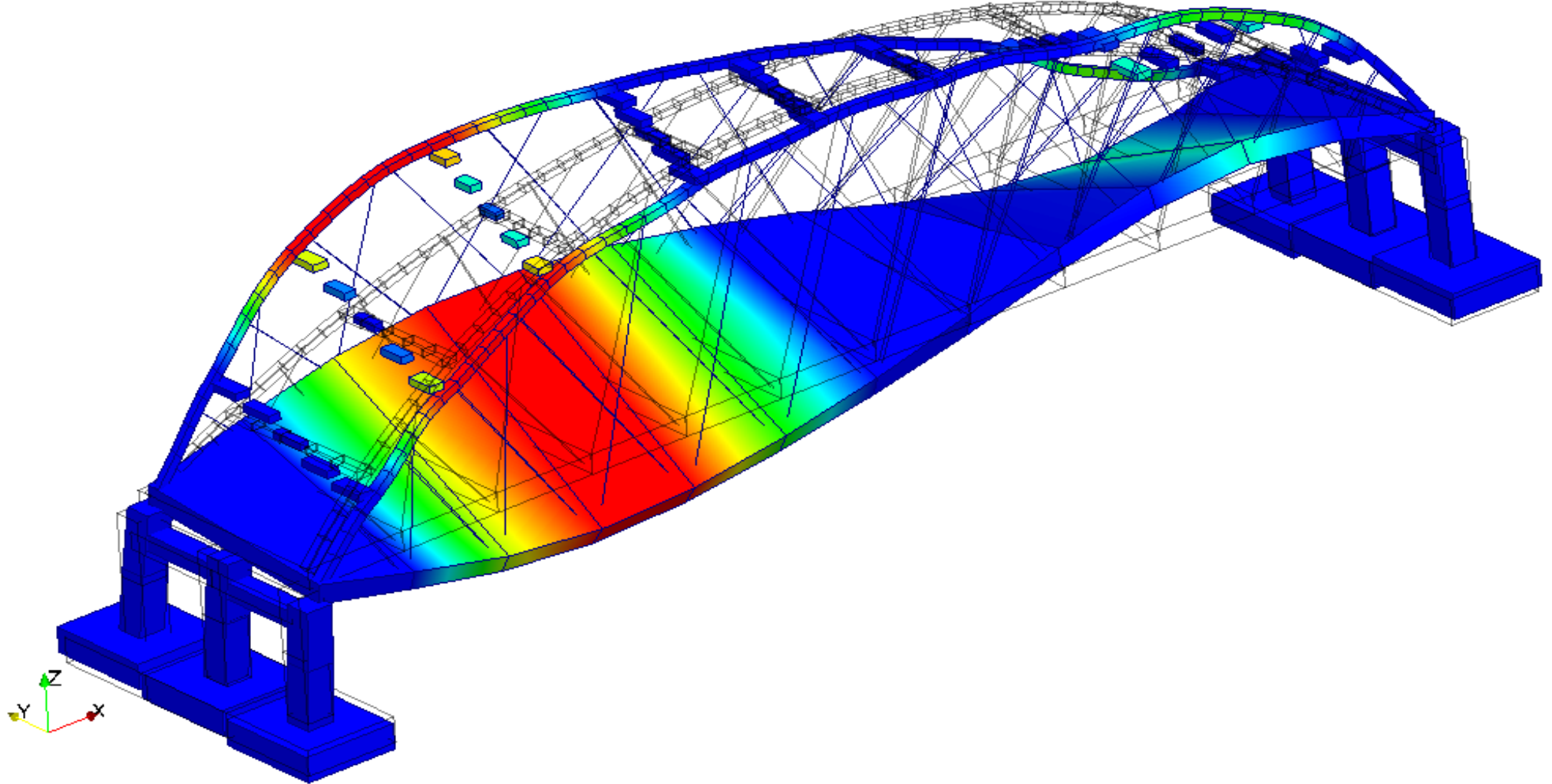
Lake Bridges – Over Kentucky Lake and Lake Barkley

Appendix A-15

May 3, 2013

Project #1301291

RWDI



Dynamic information

Mode 16, $f = 1.915$ Hz

Wind Engineering Study

Lake Bridges – Over Kentucky Lake and Lake Barkley

Appendix A-16

May 3, 2013

Project #1301291

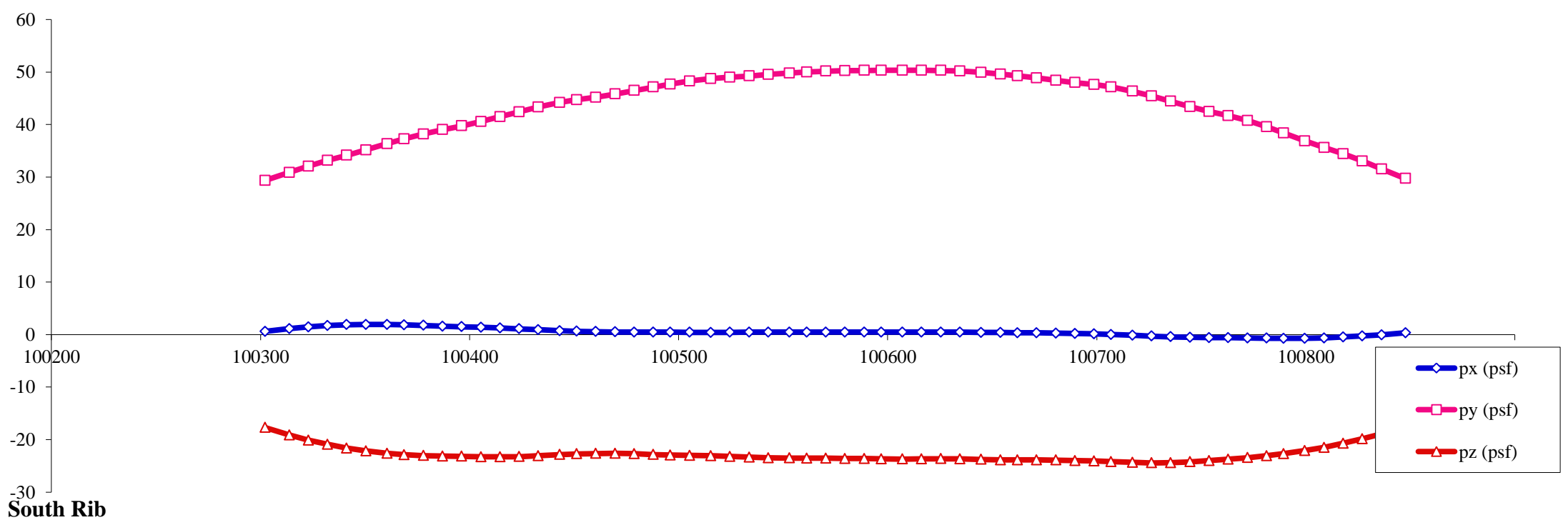
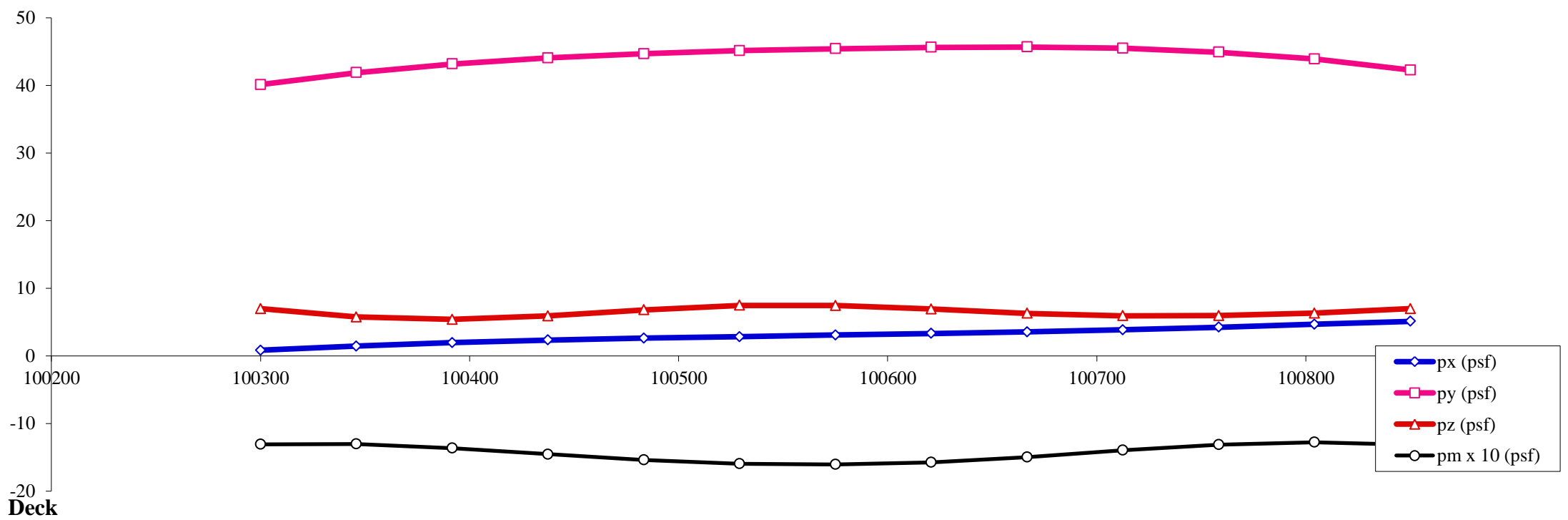
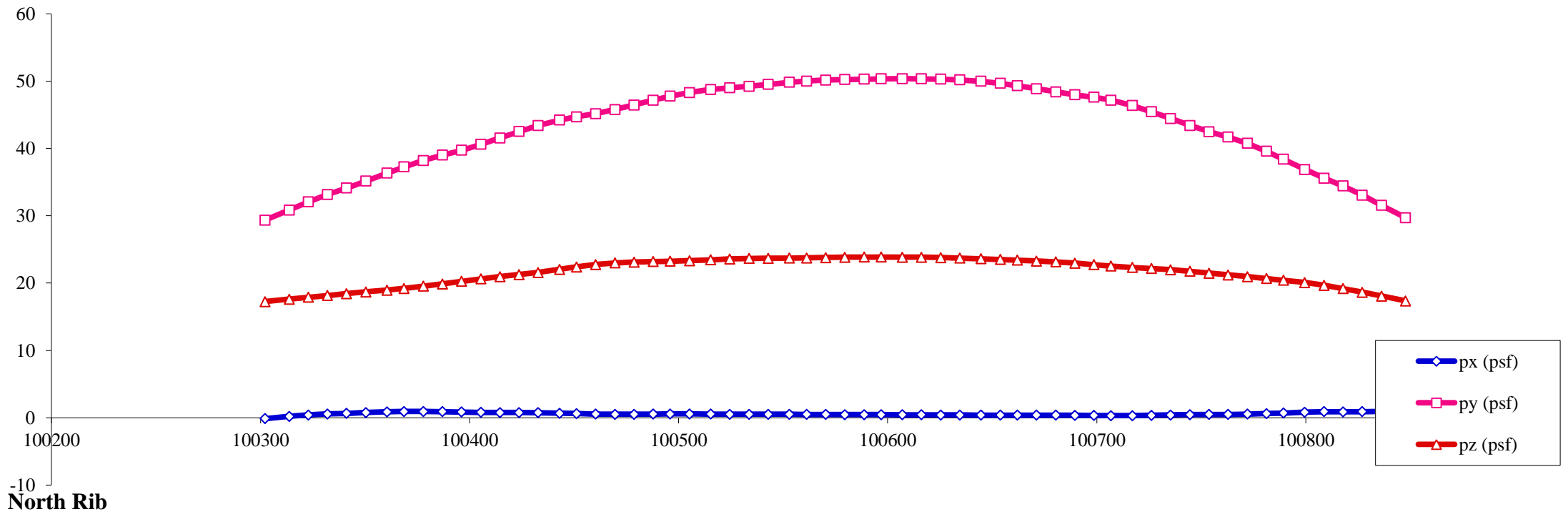
RWDI

APPENDIX B

100-Year Preliminary Design Wind Loads

Load Visualization Page

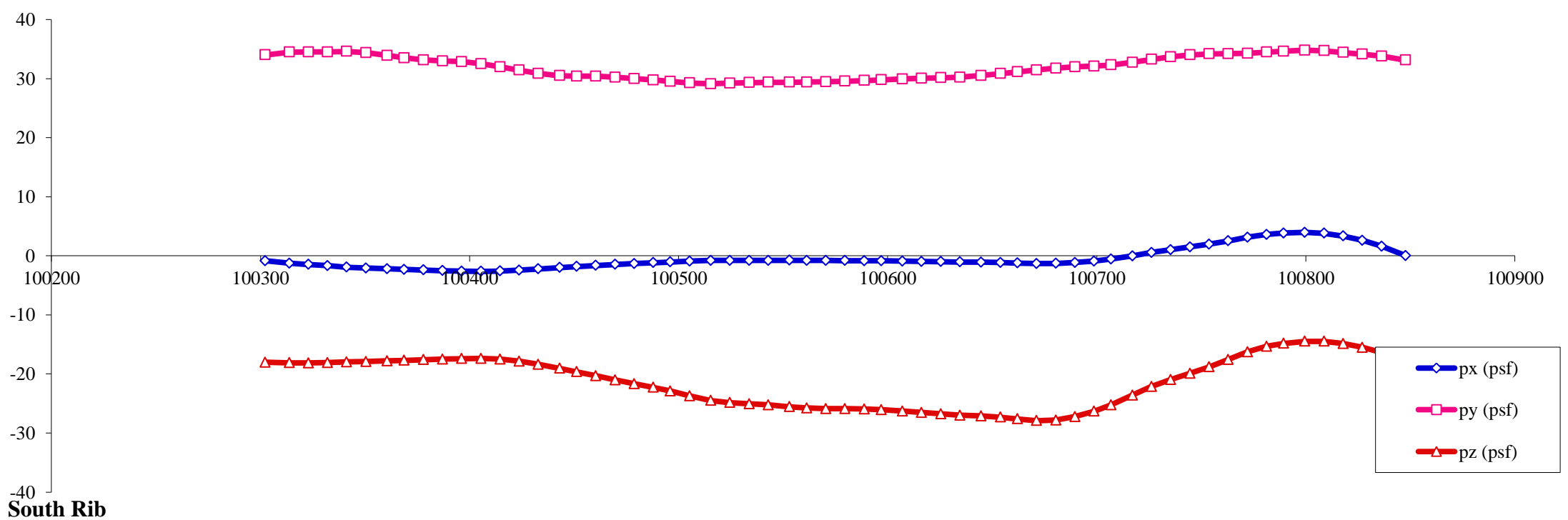
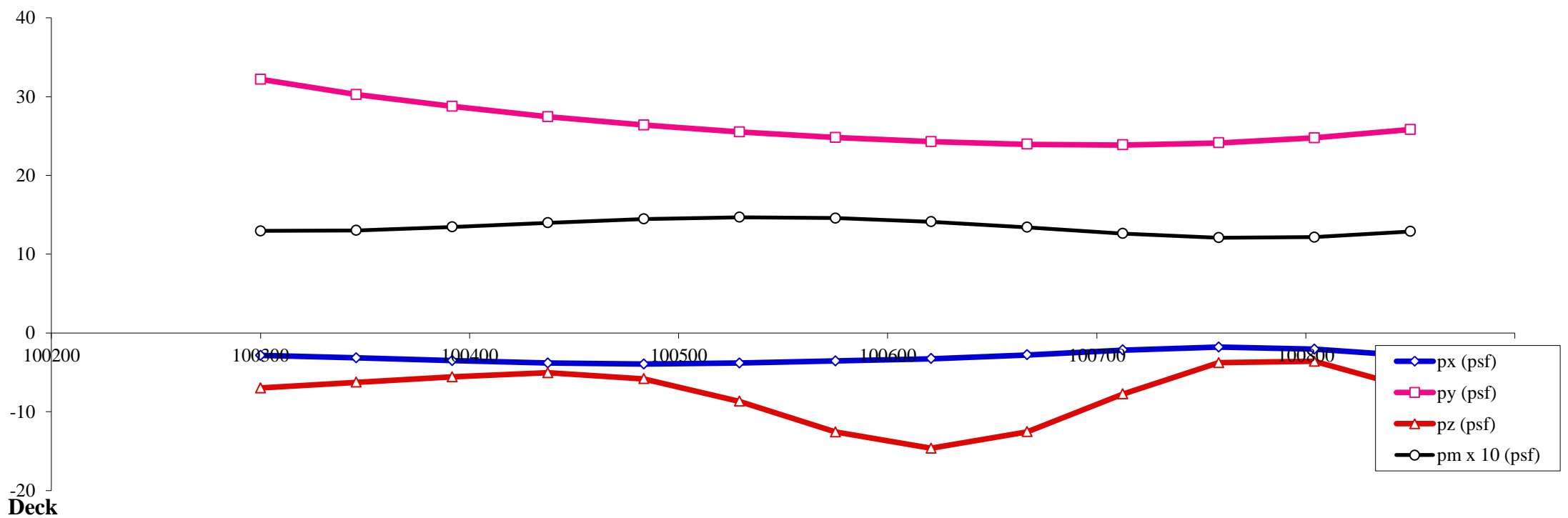
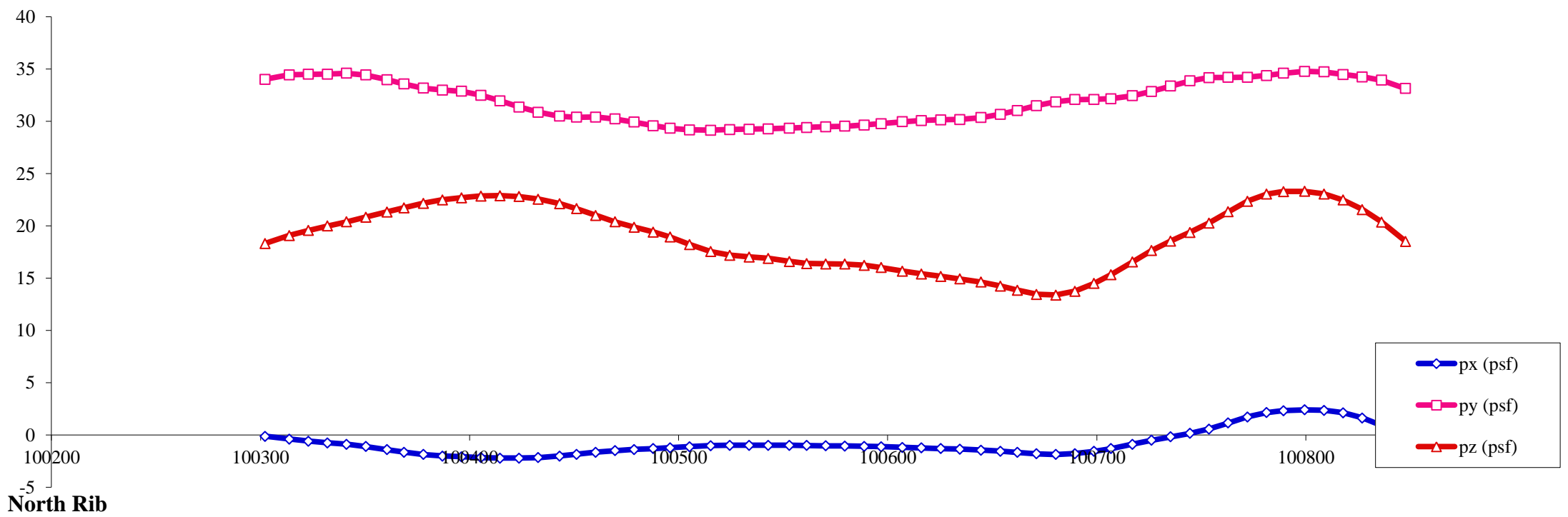
Load case : **1** Objective: Max lateral on deck, middle of the span



- Notes:
1. All pressures in (psf)
 2. All coordinates/elevations in (ft)
 3. Loads for hangers, arch bracings, columns, pier caps and footings are not presented here

Load Visualization Page

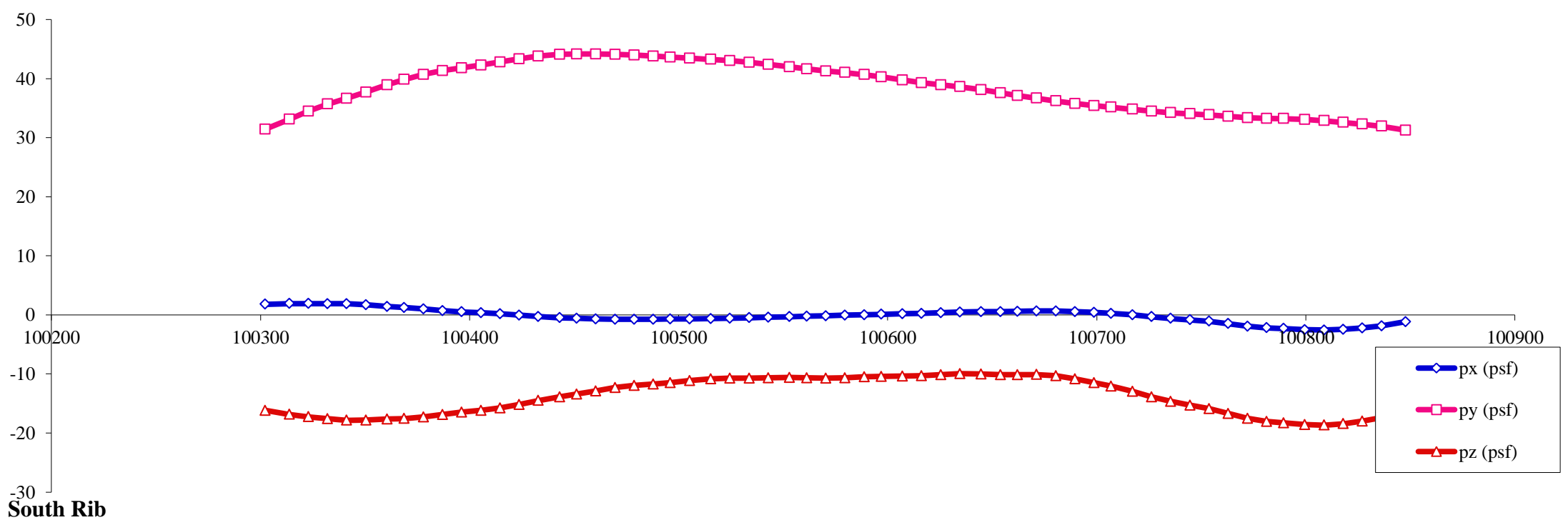
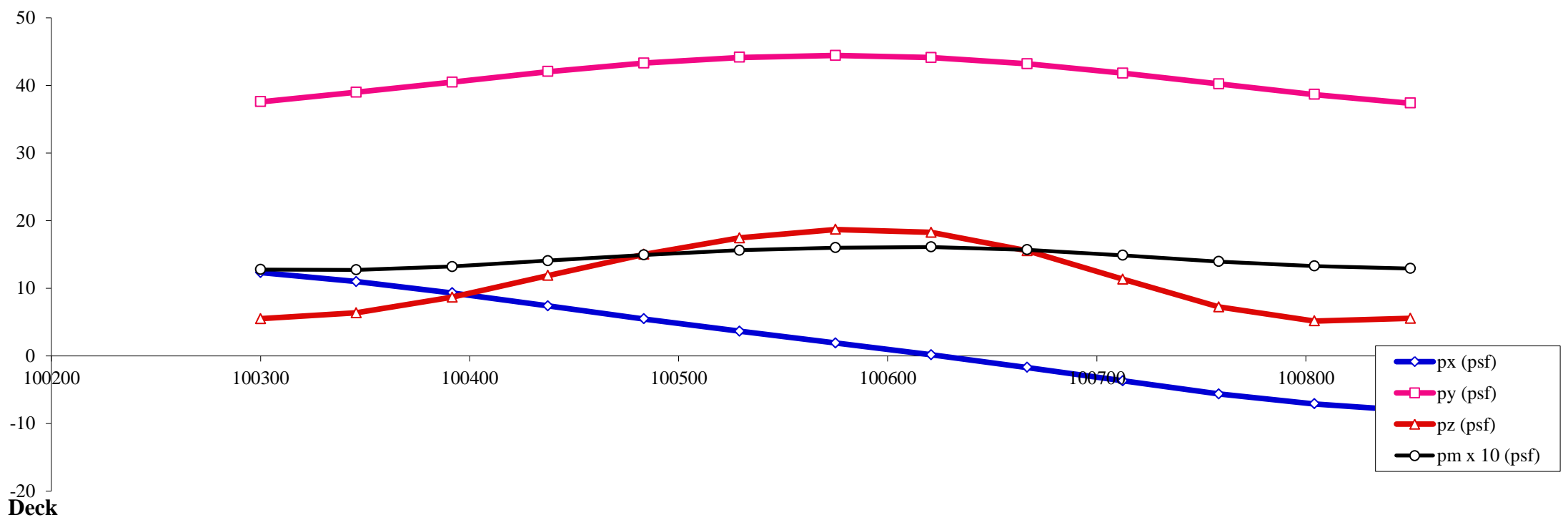
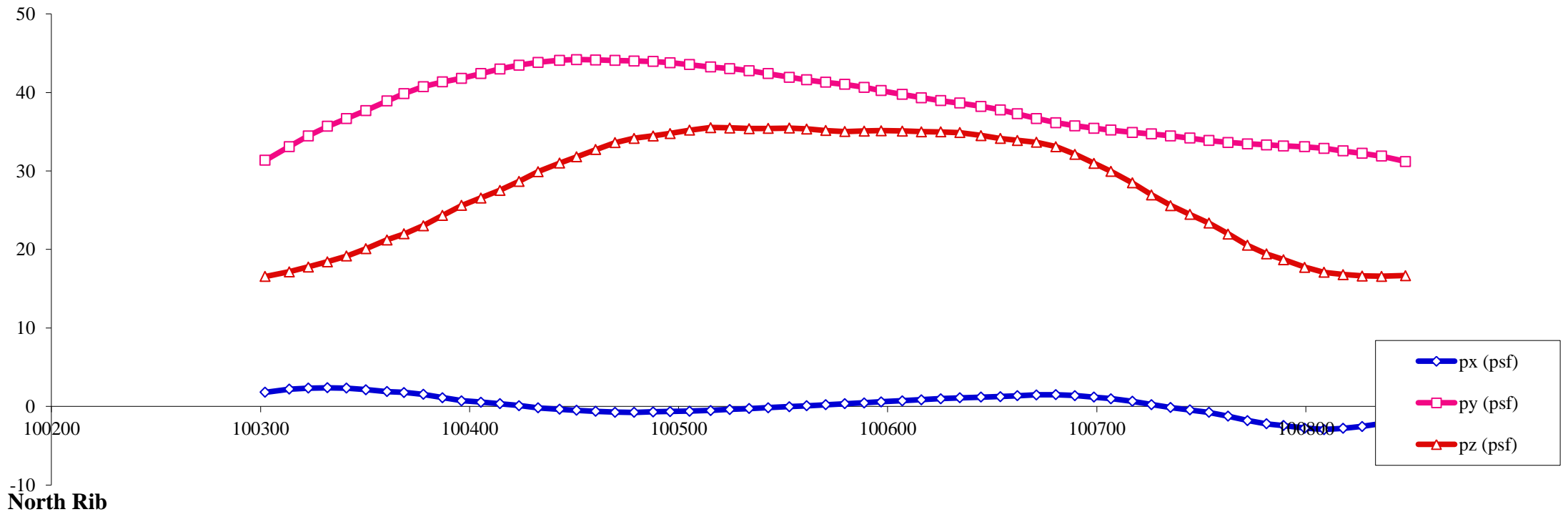
Load case : **2** Objective: Peak lateral with reversed dynamic component on deck, middle of the span



- Notes:
1. All pressures in (psf)
 2. All coordinates/elevations in (ft)
 3. Loads for hangers, arch bracings, columns, pier caps and footings are not presented here

Load Visualization Page

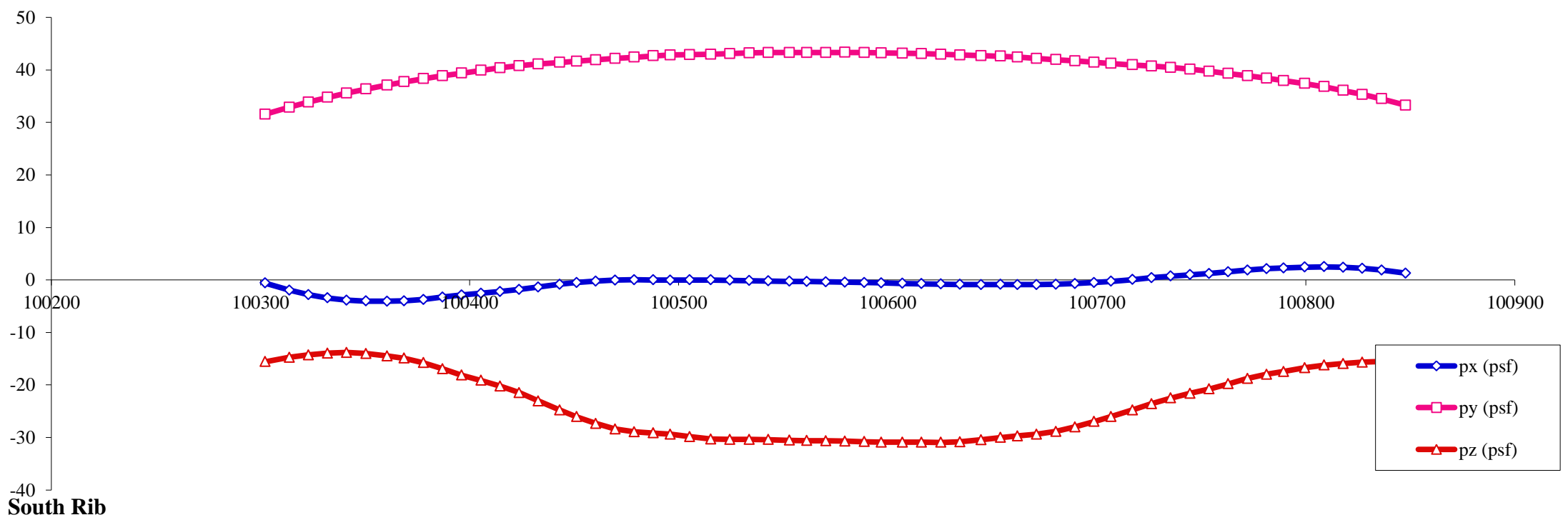
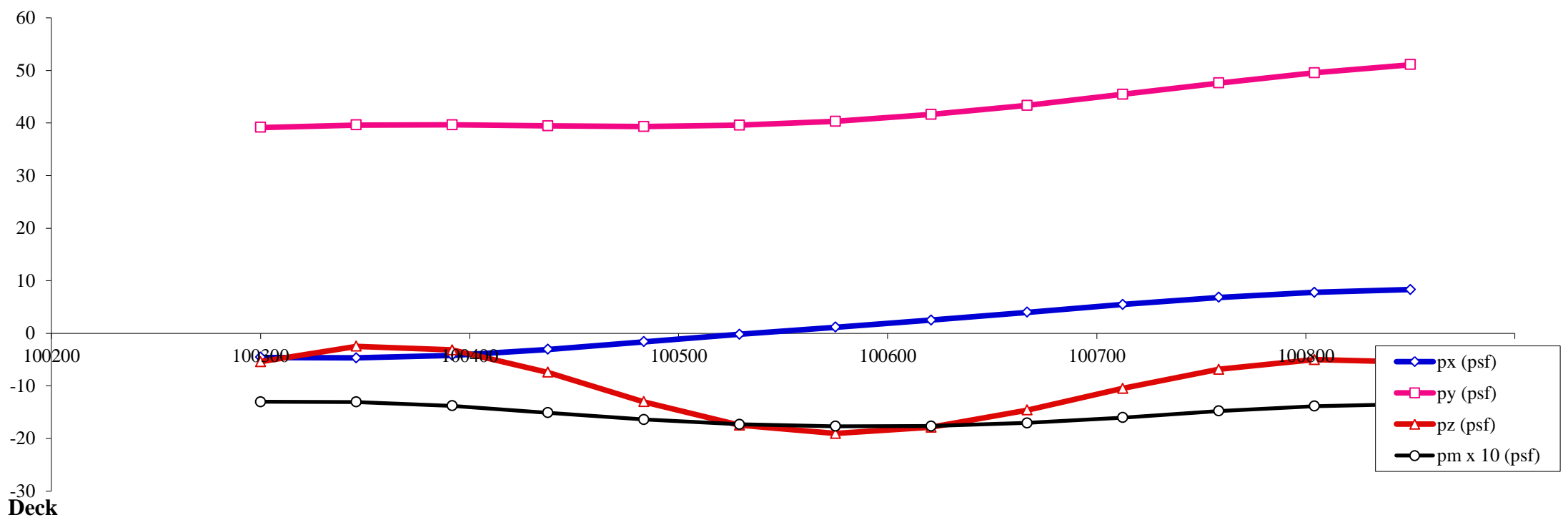
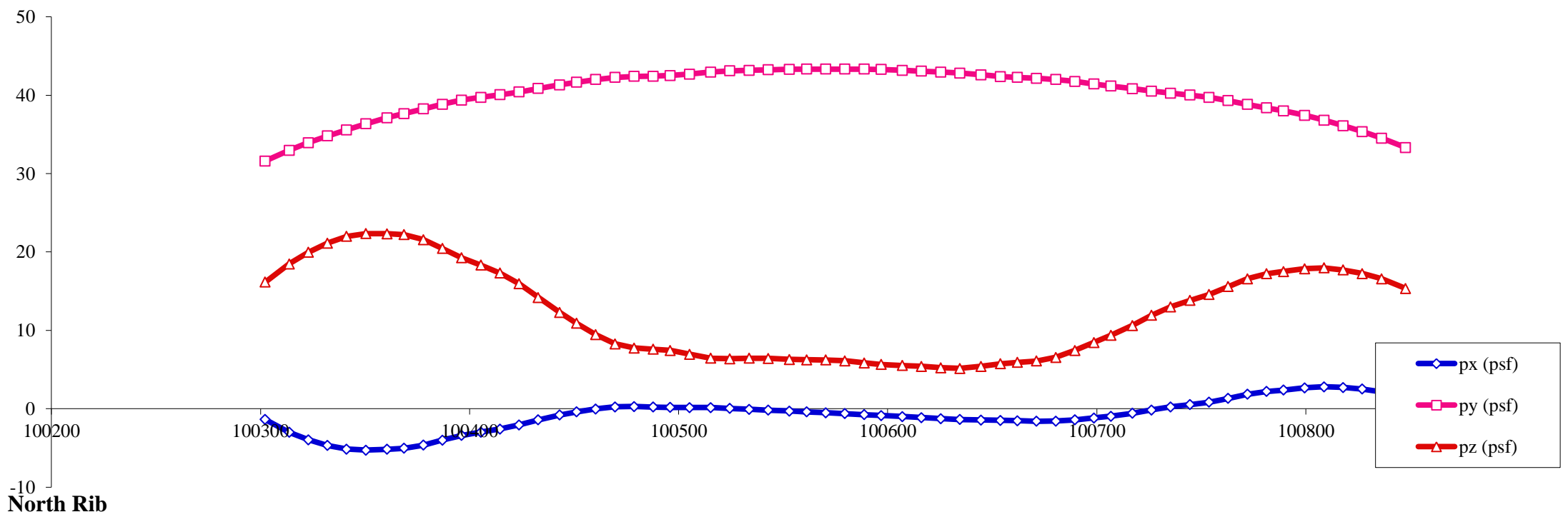
Load case : **3** Objective: Max uplift on deck, middle of the span



- Notes:
1. All pressures in (psf)
 2. All coordinates/elevations in (ft)
 3. Loads for hangers, arch bracings, columns, pier caps and footings are not presented here

Load Visualization Page

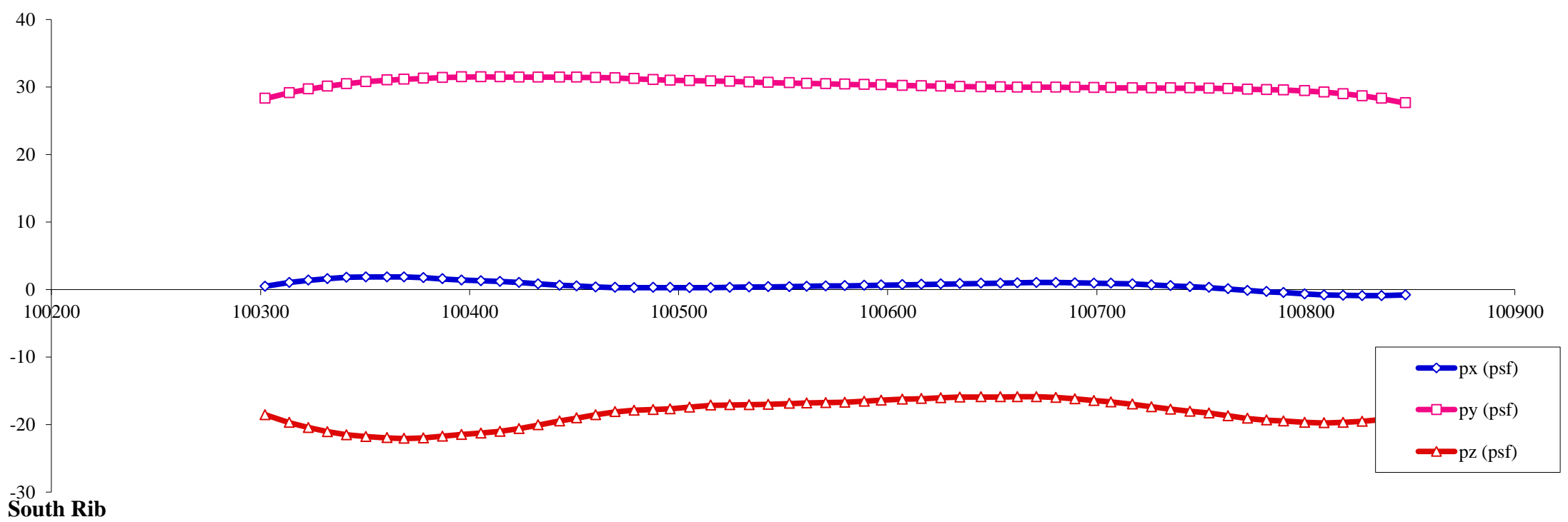
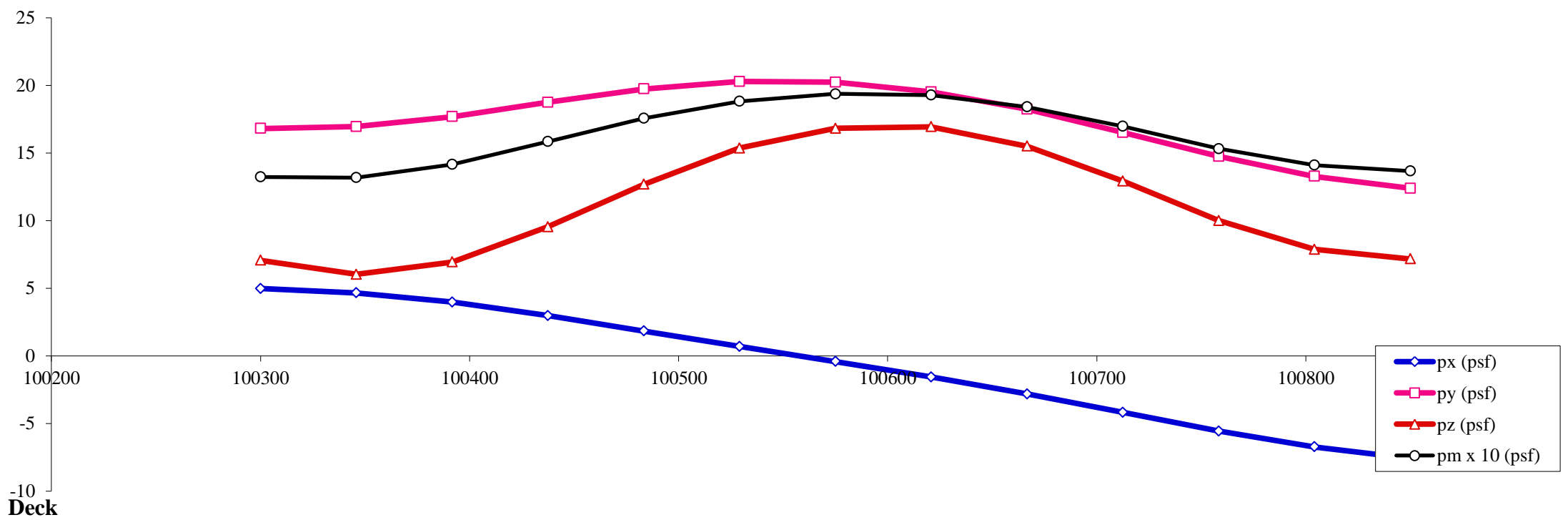
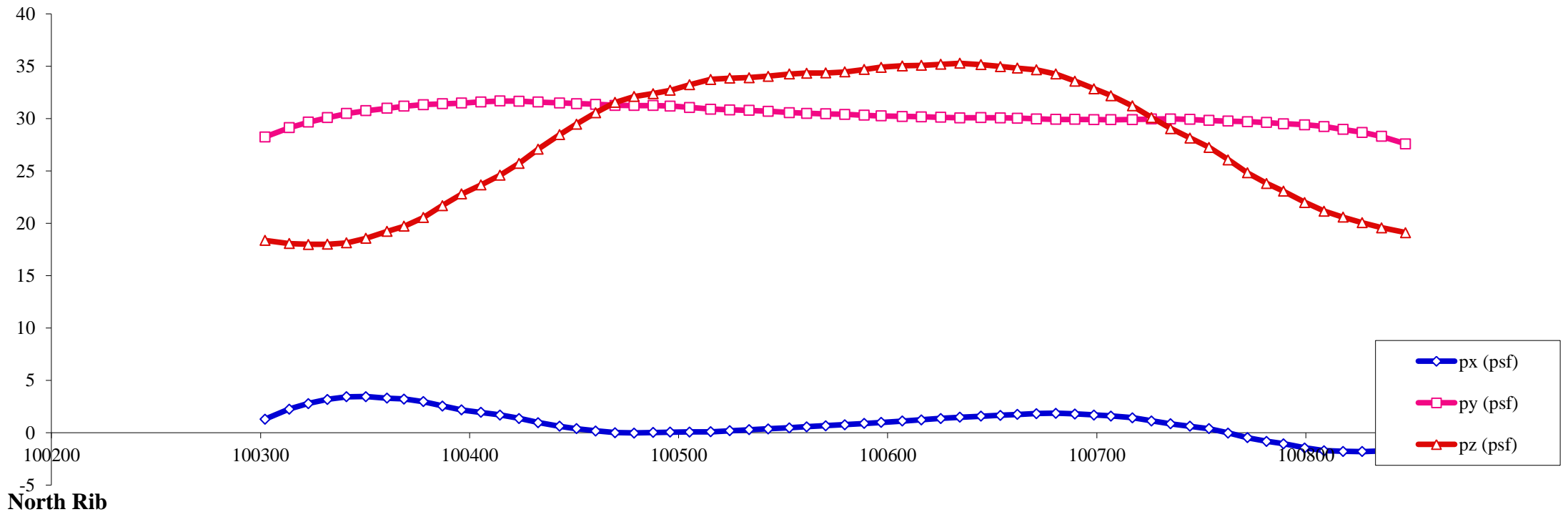
Load case : **4** Objective: Max down force on deck, middle of the span



- Notes:
1. All pressures in (psf)
 2. All coordinates/elevations in (ft)
 3. Loads for hangers, arch bracings, columns, pier caps and footings are not presented here

Load Visualization Page

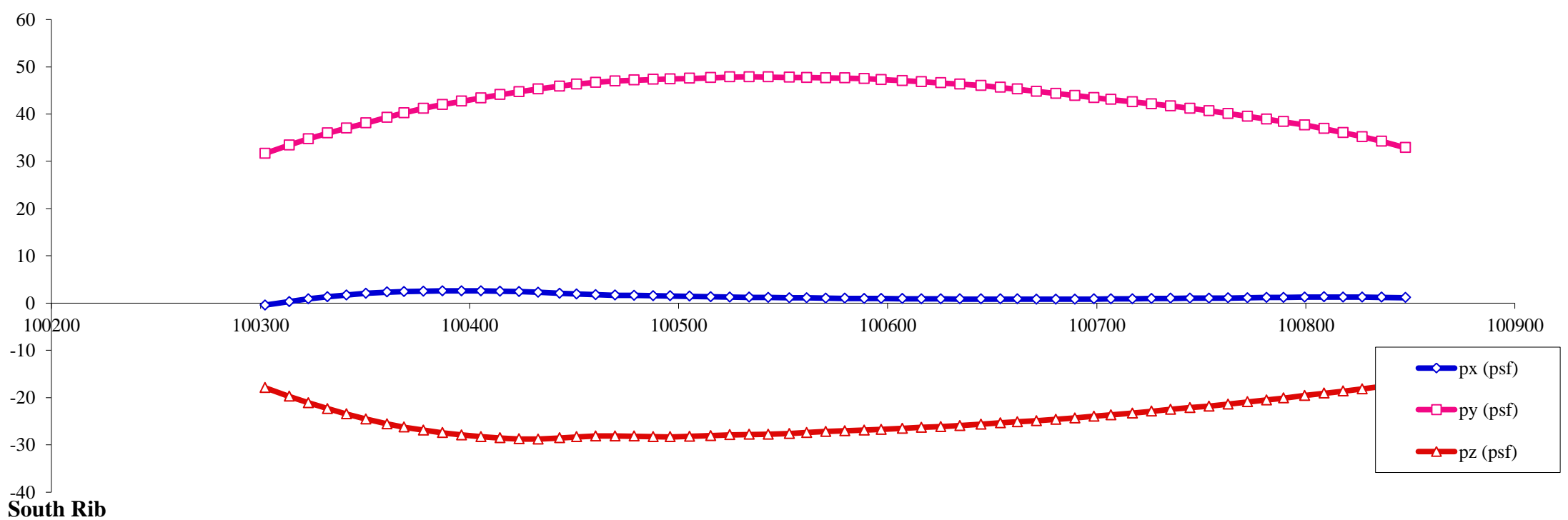
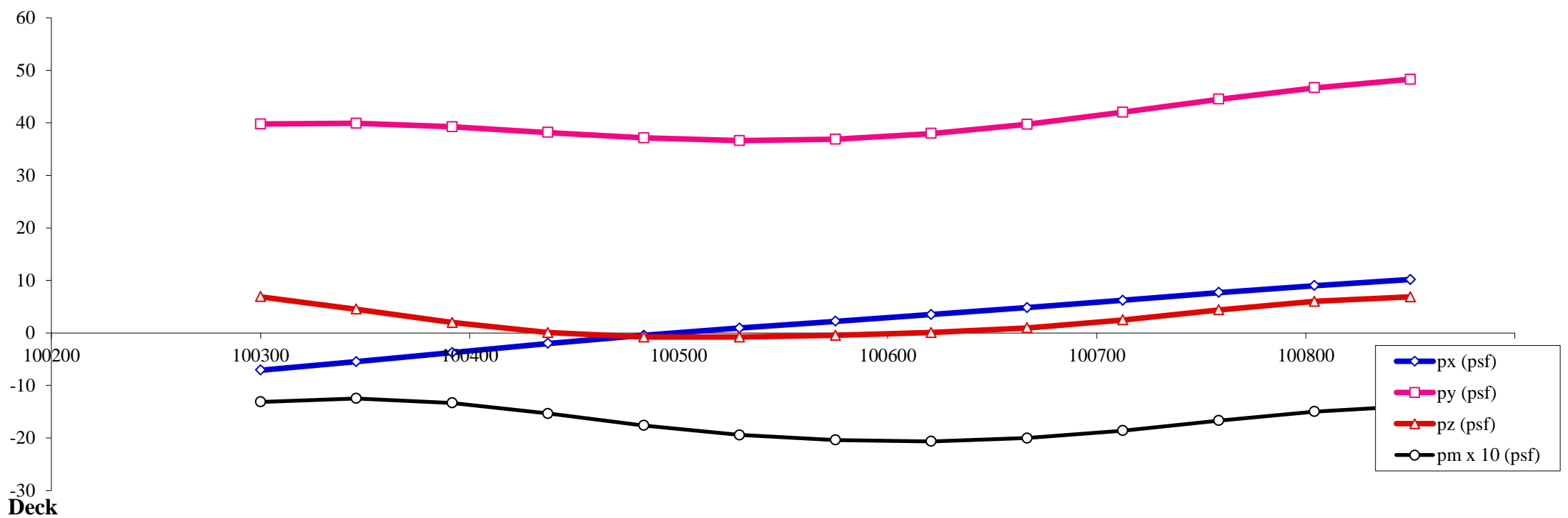
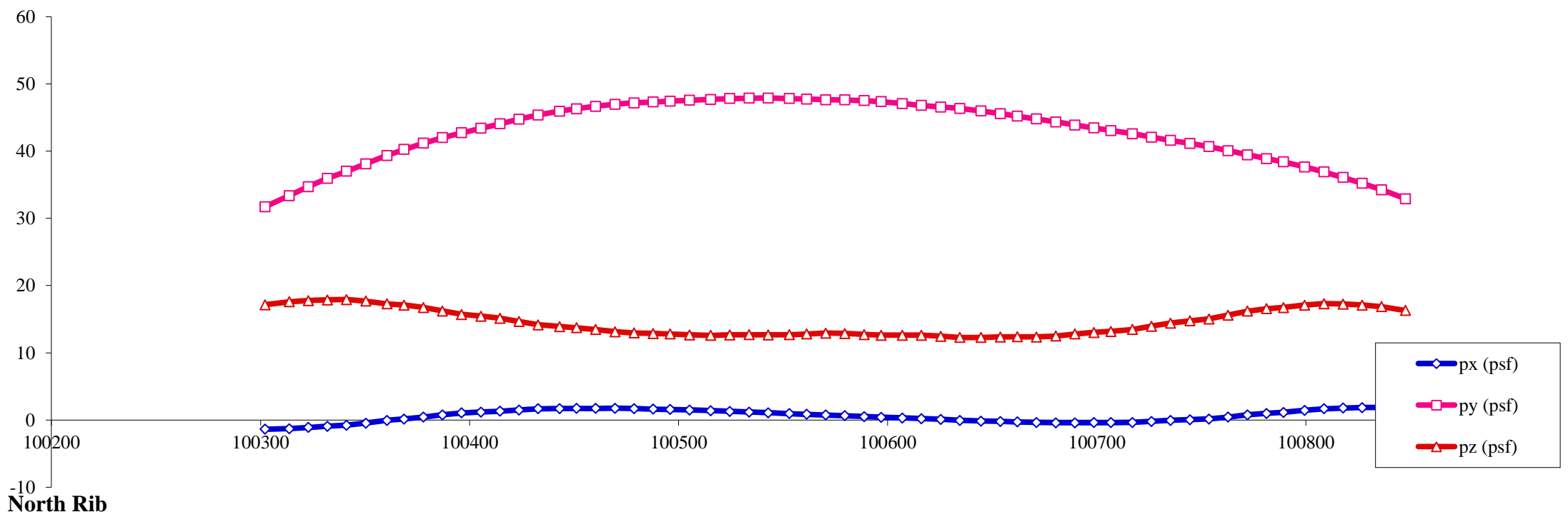
Load case : **5** Objective: Max positive moment on deck, middle of the span



- Notes:
1. All pressures in (psf)
 2. All coordinates/elevations in (ft)
 3. Loads for hangers, arch bracings, columns, pier caps and footings are not presented here

Load Visualization Page

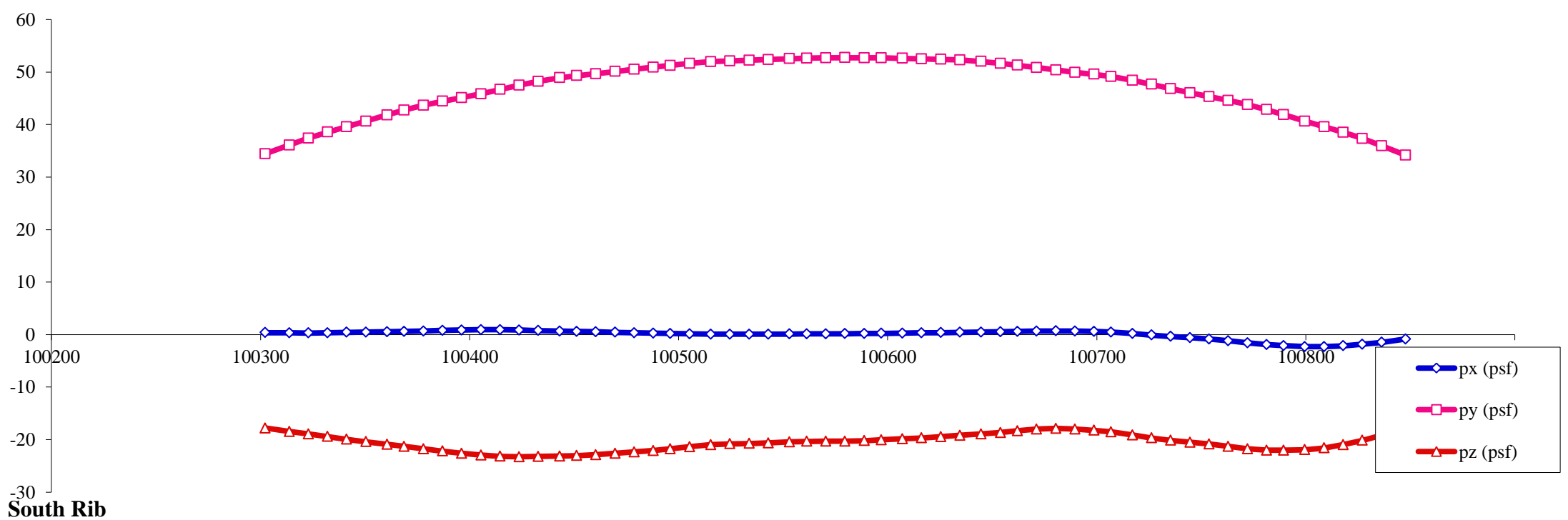
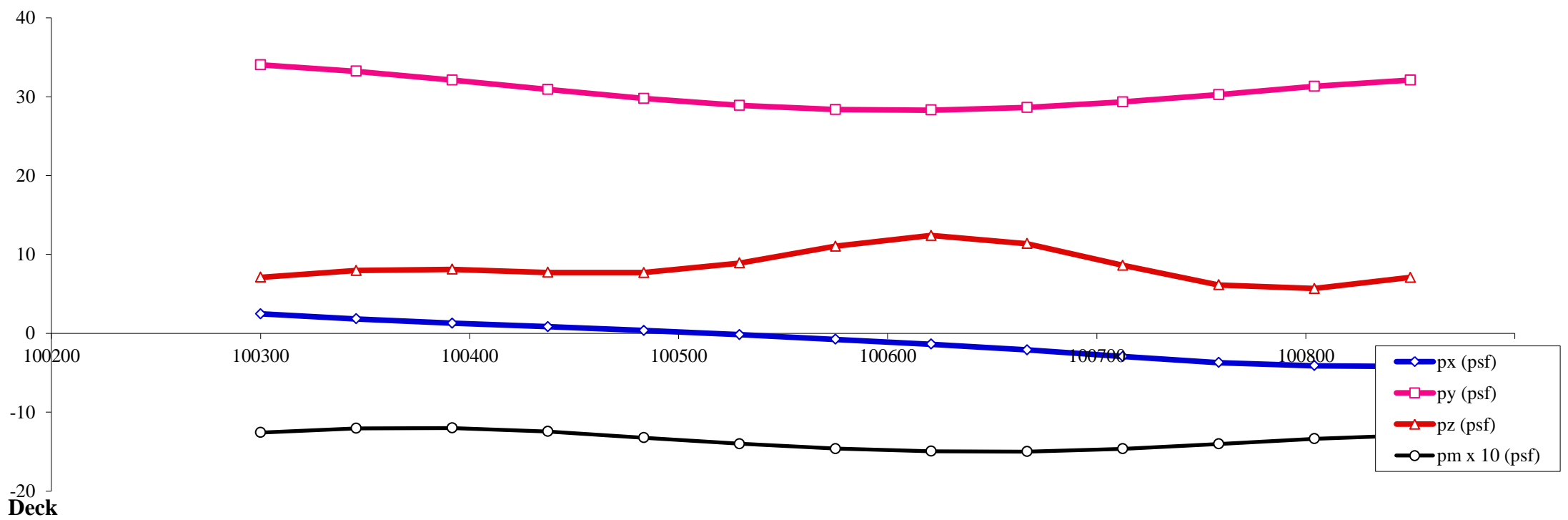
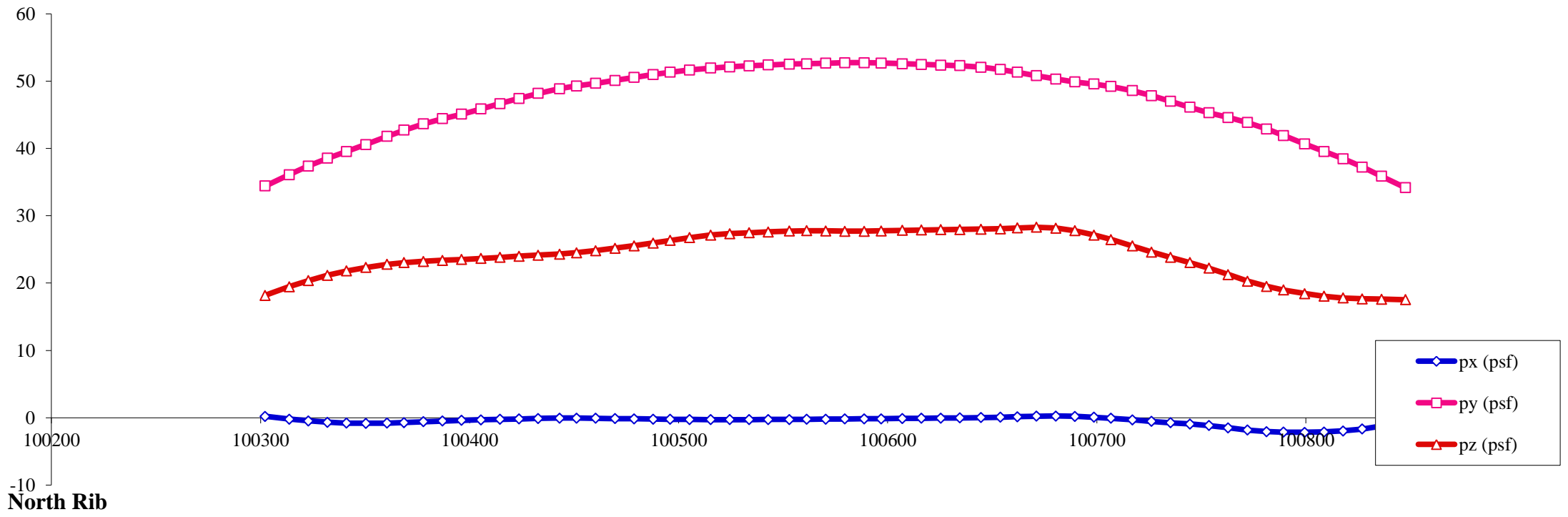
Load case : **6** Objective: Max negative moment on deck, middle of the span



- Notes:
1. All pressures in (psf)
 2. All coordinates/elevations in (ft)
 3. Loads for hangers, arch bracings, columns, pier caps and footings are not presented here

Load Visualization Page

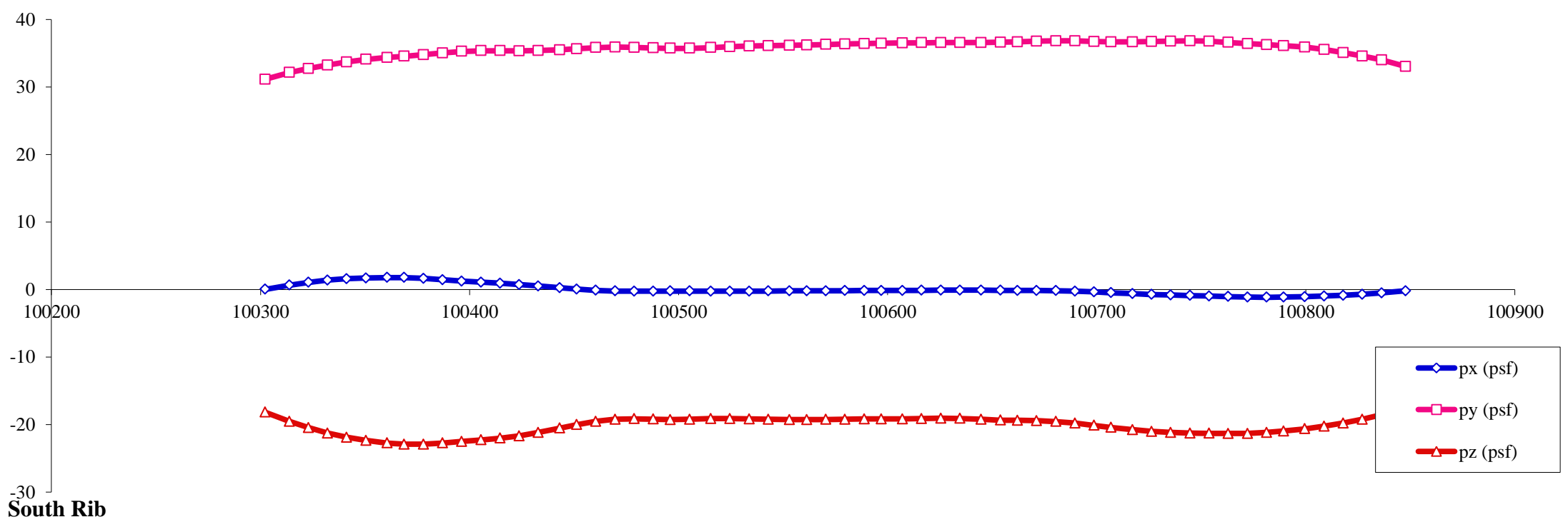
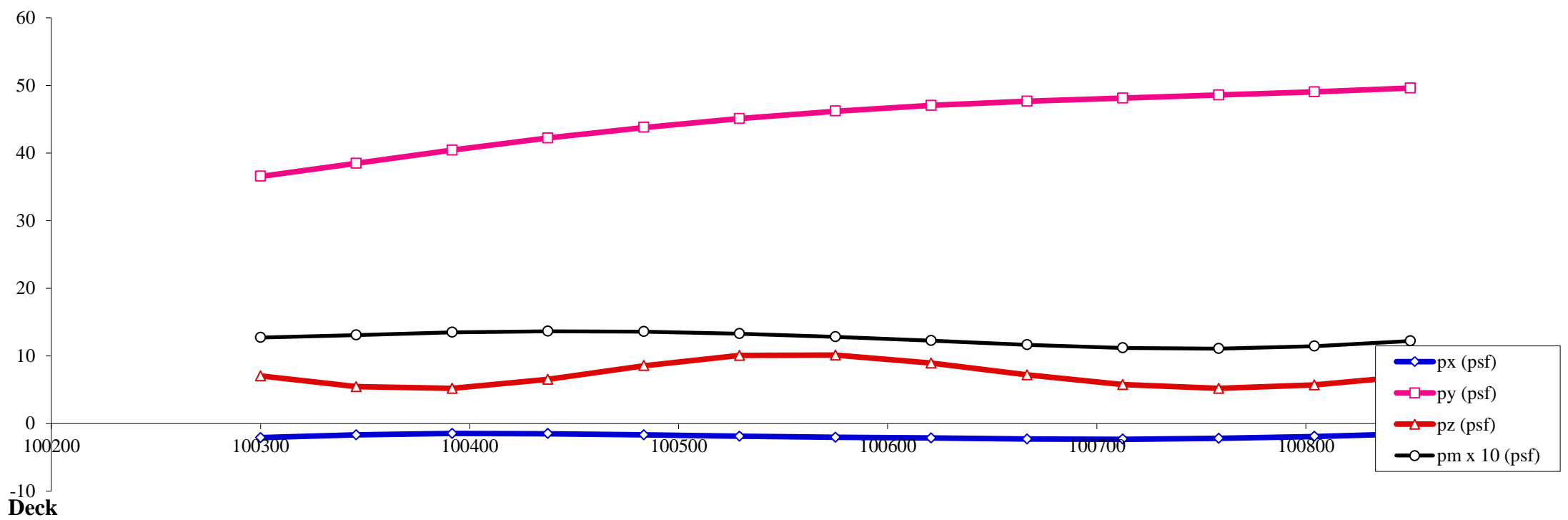
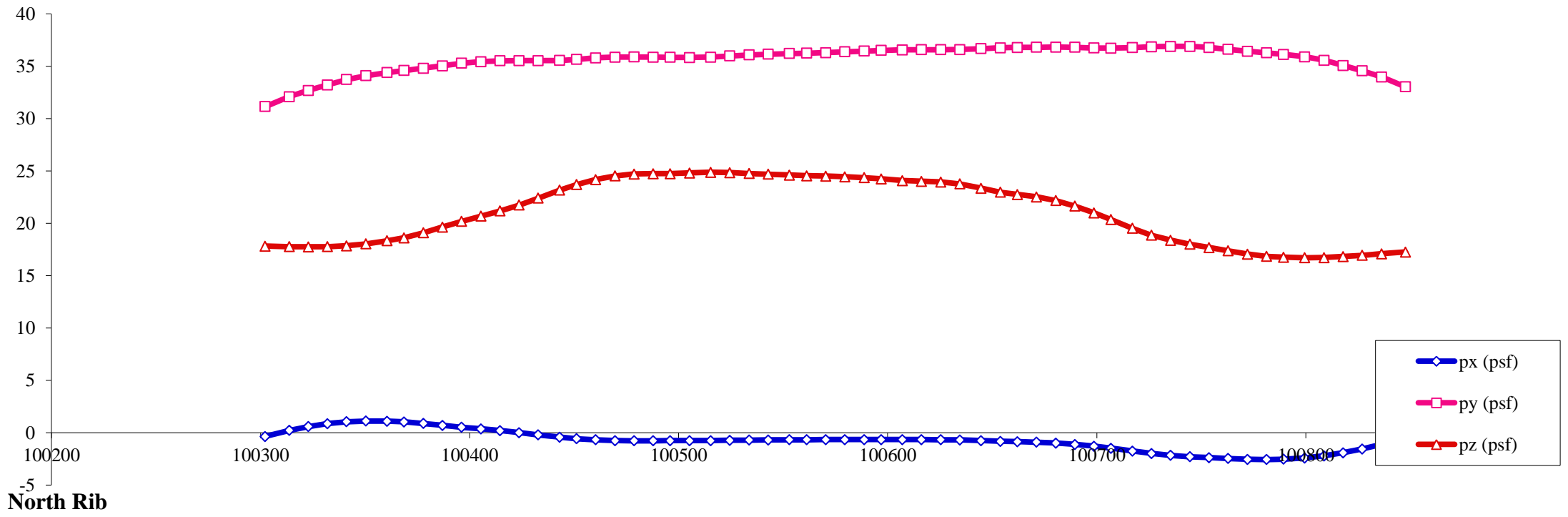
Load case : **7** Objective: Max lateral, middle of the span, differential between deck and arch



- Notes:**
1. All pressures in (psf)
 2. All coordinates/elevations in (ft)
 3. Loads for hangers, arch bracings, columns, pier caps and footings are not presented here

Load Visualization Page

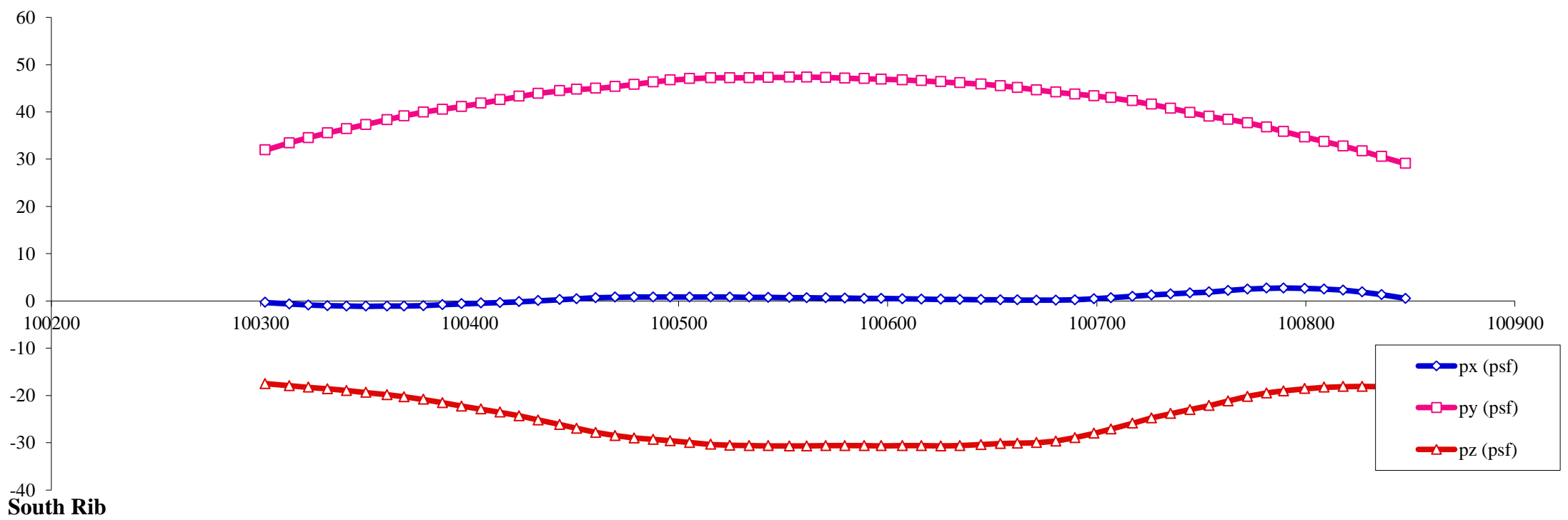
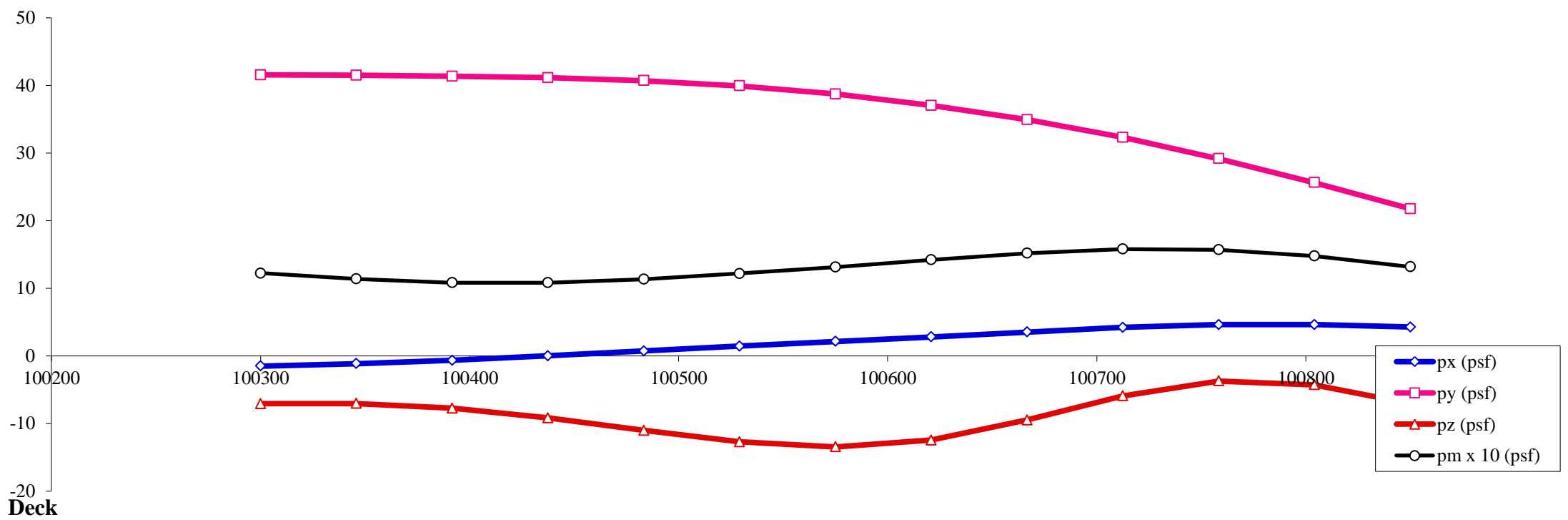
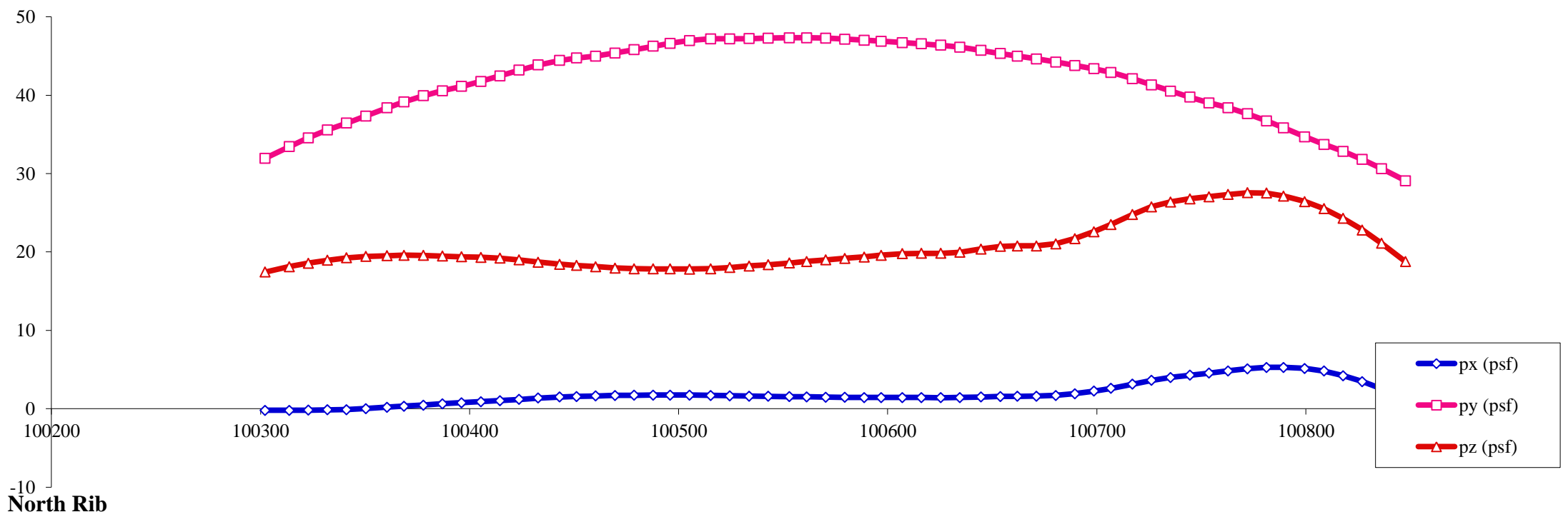
Load case : **8** Objective: Max lateral, middle of the span, differential between deck and arch



- Notes:**
1. All pressures in (psf)
 2. All coordinates/elevations in (ft)
 3. Loads for hangers, arch bracings, columns, pier caps and footings are not presented here

Load Visualization Page

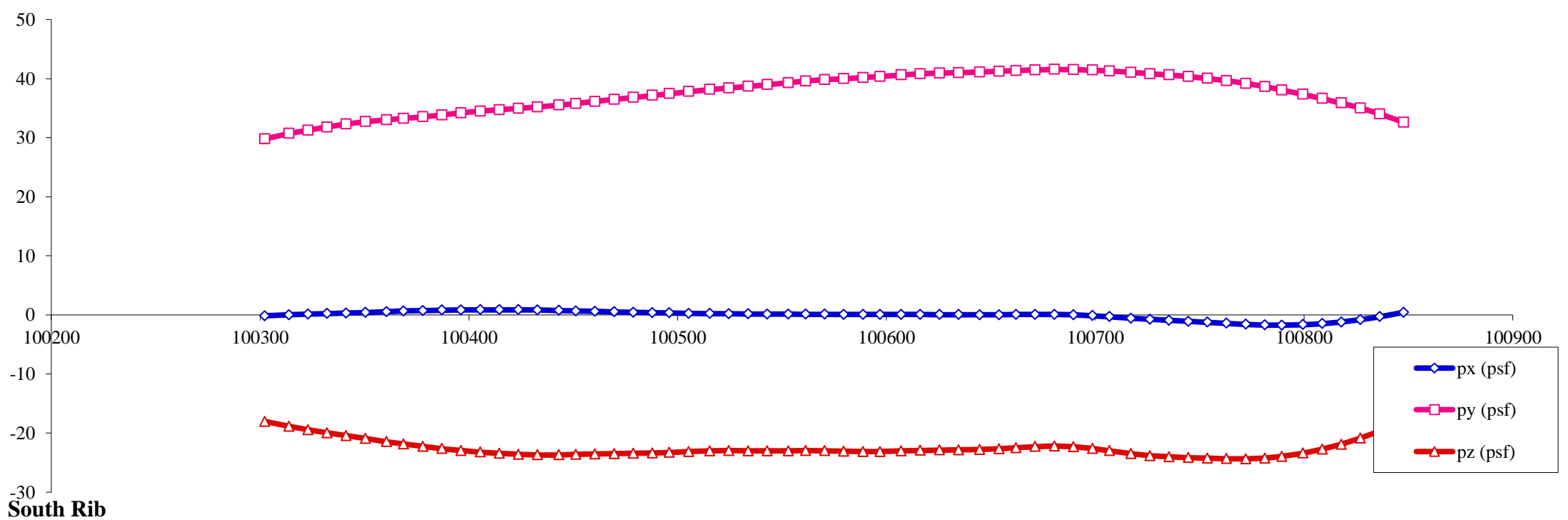
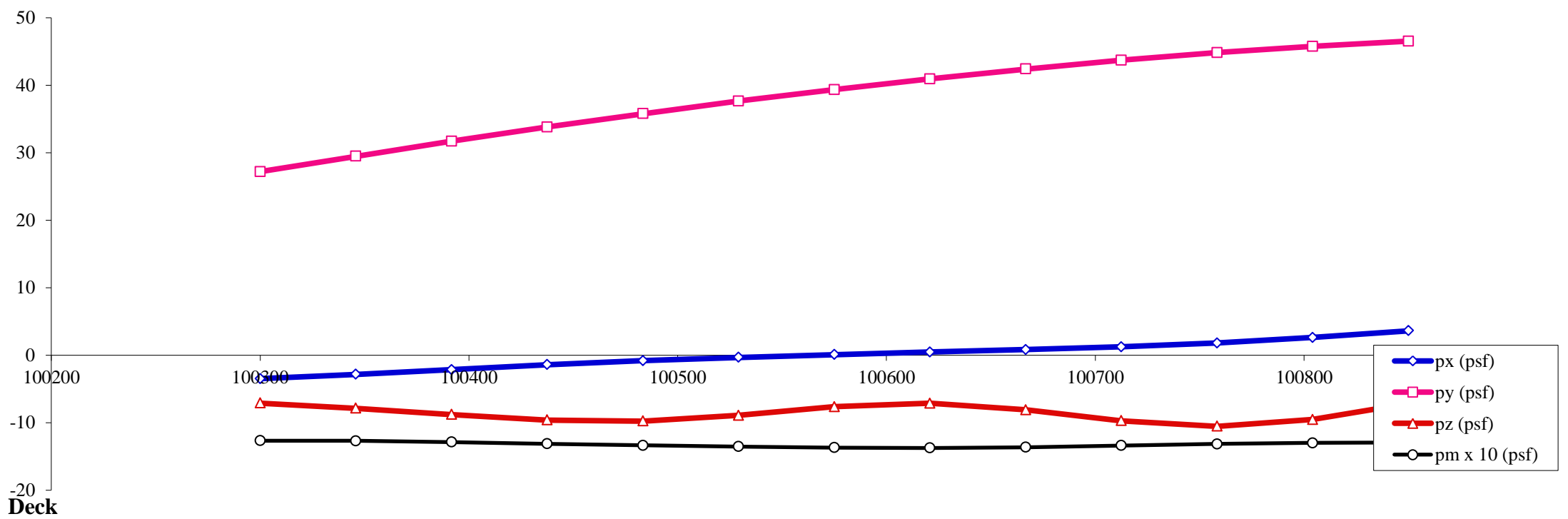
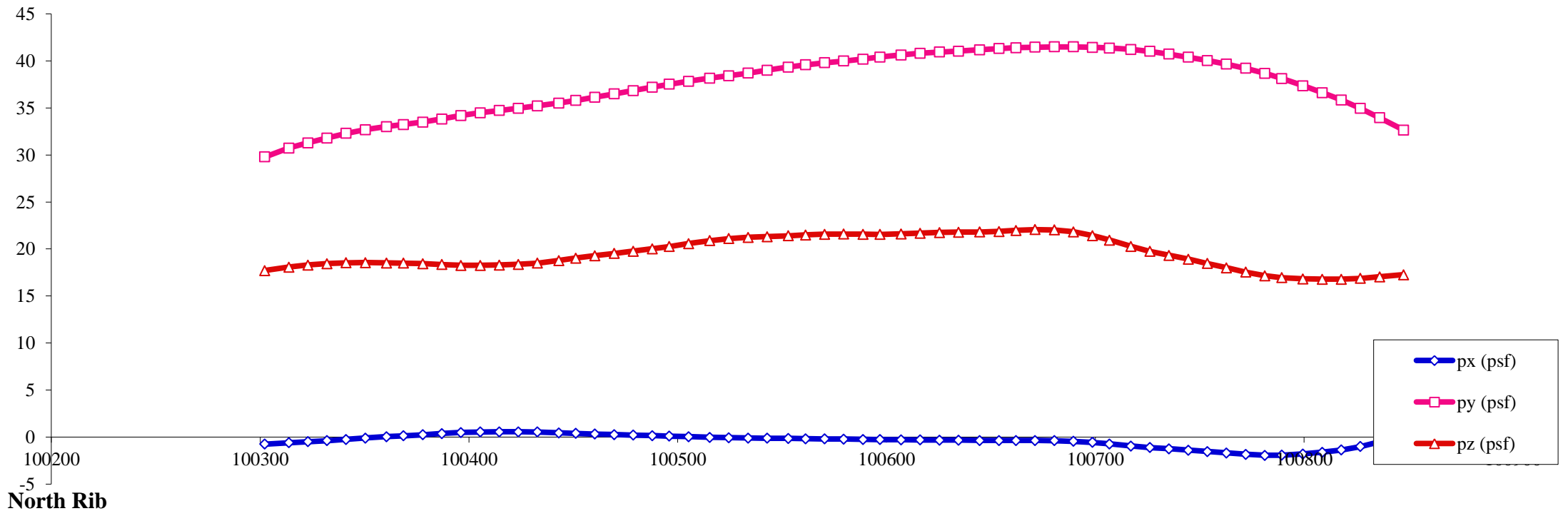
Load case : **9** Objective: Max lateral on deck, differential between 1/4 and 3/4 span



- Notes:
1. All pressures in (psf)
 2. All coordinates/elevations in (ft)
 3. Loads for hangers, arch bracings, columns, pier caps and footings are not presented here

Load Visualization Page

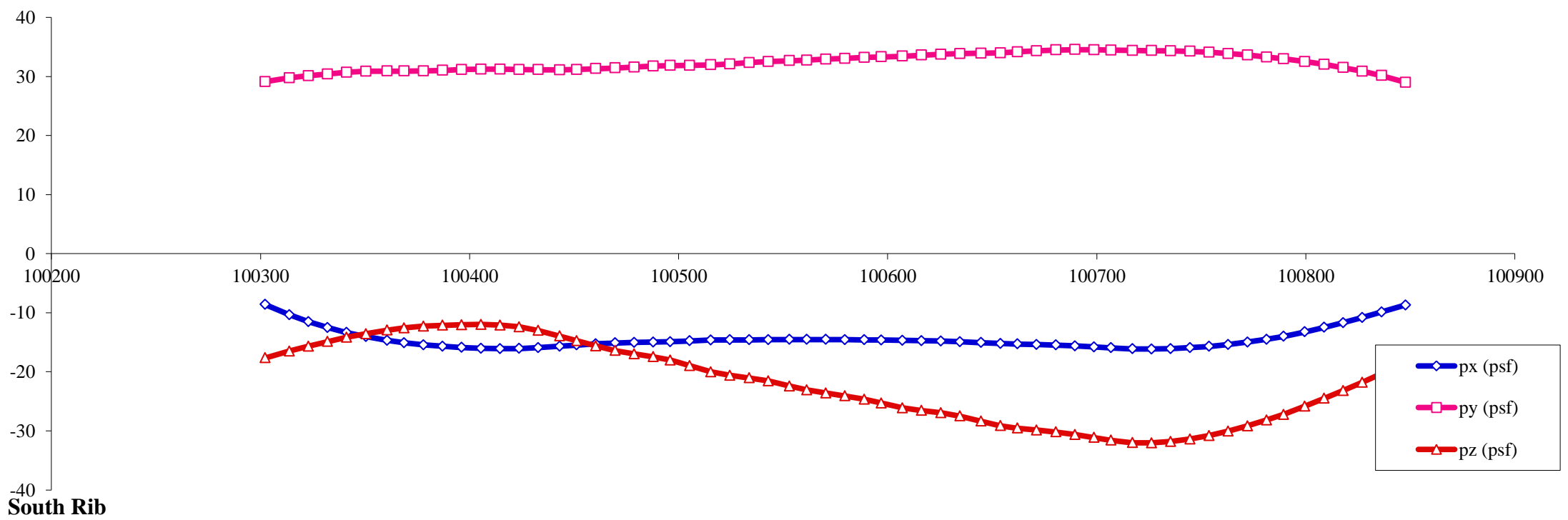
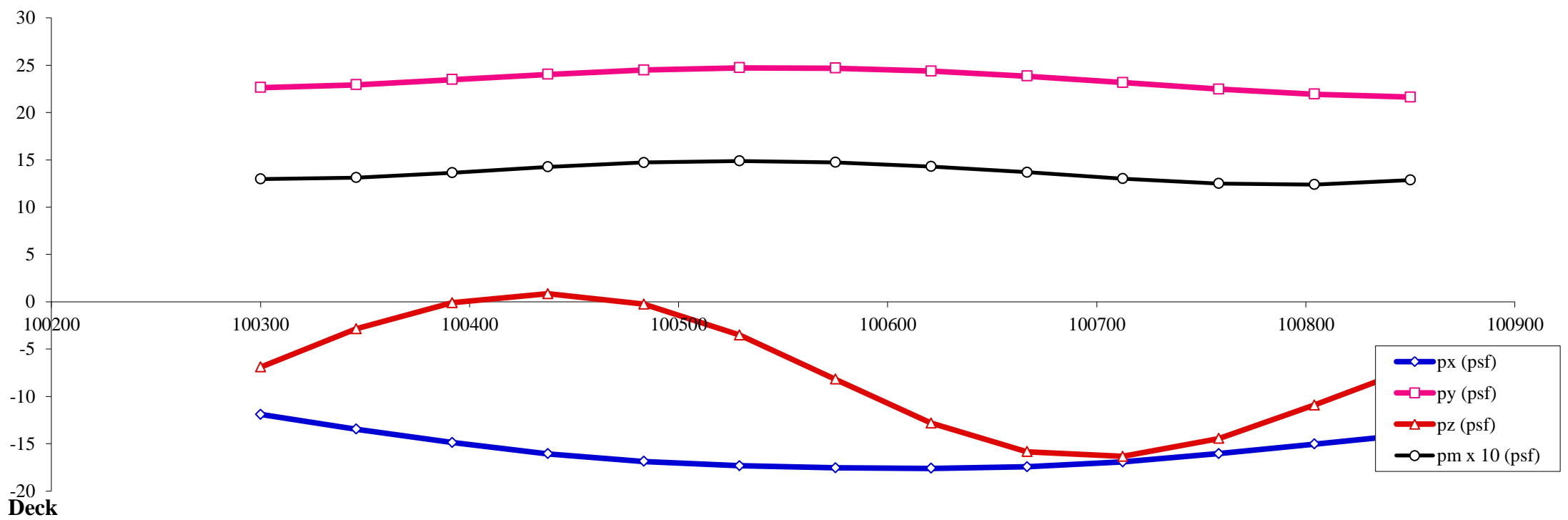
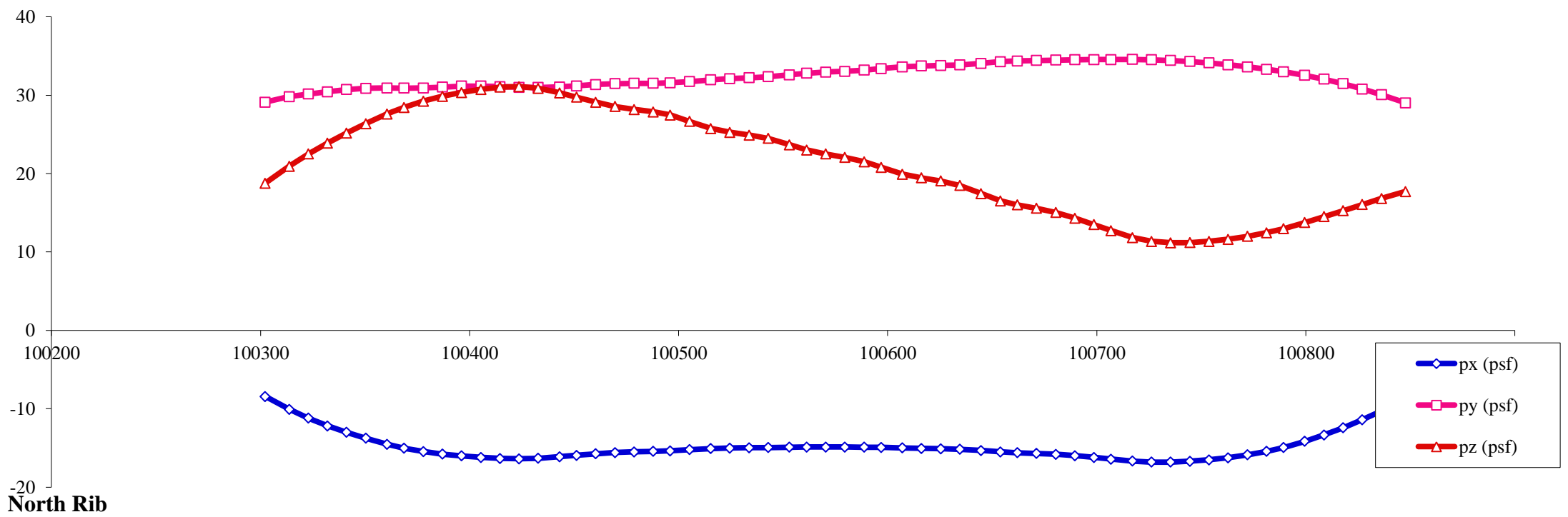
Load case : **10** Objective: Max lateral on deck, differential between 1/4 and 3/4 span



- Notes:**
1. All pressures in (psf)
 2. All coordinates/elevations in (ft)
 3. Loads for hangers, arch bracings, columns, pier caps and footings are not presented here

Load Visualization Page

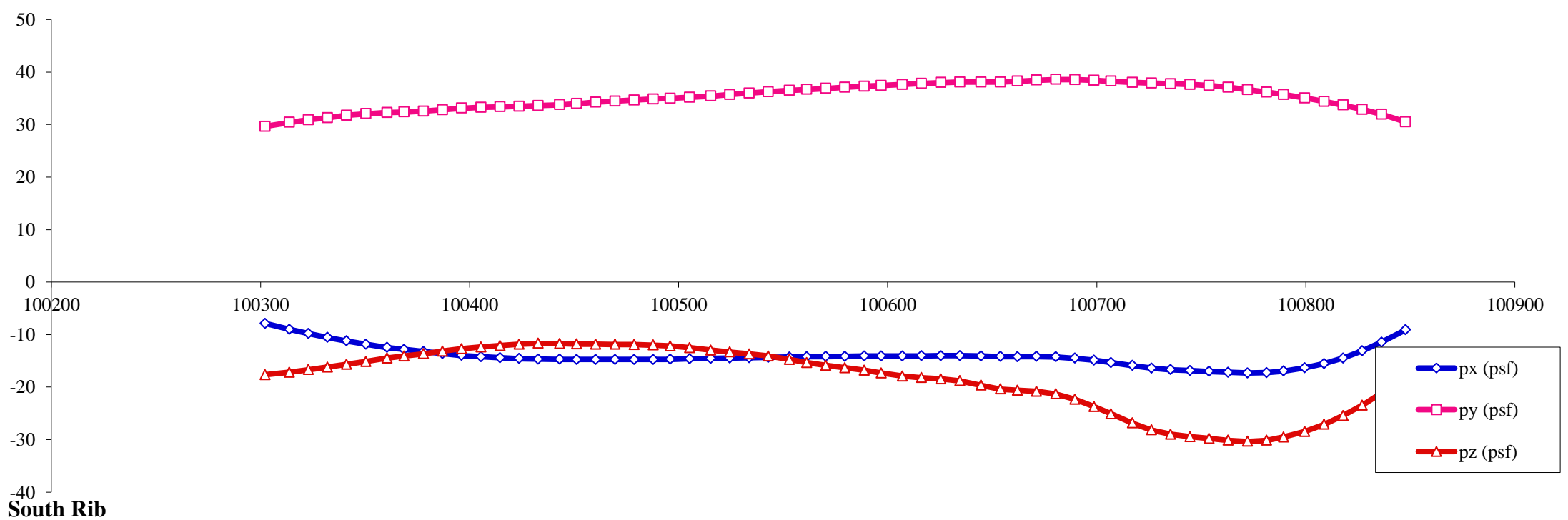
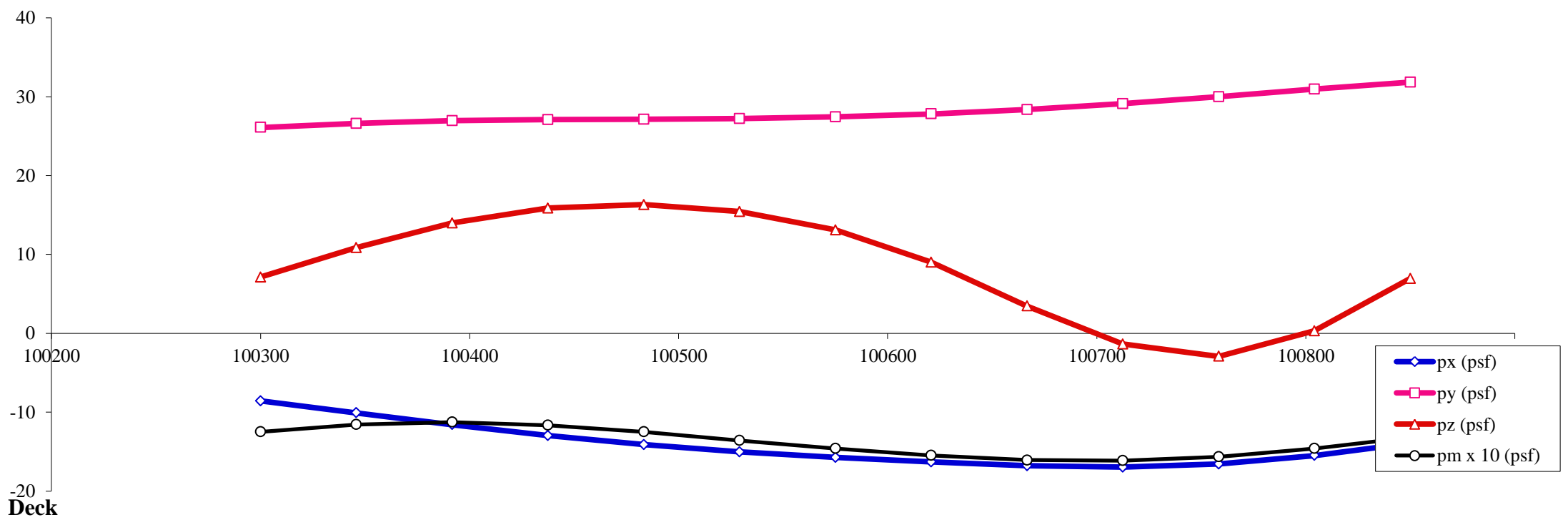
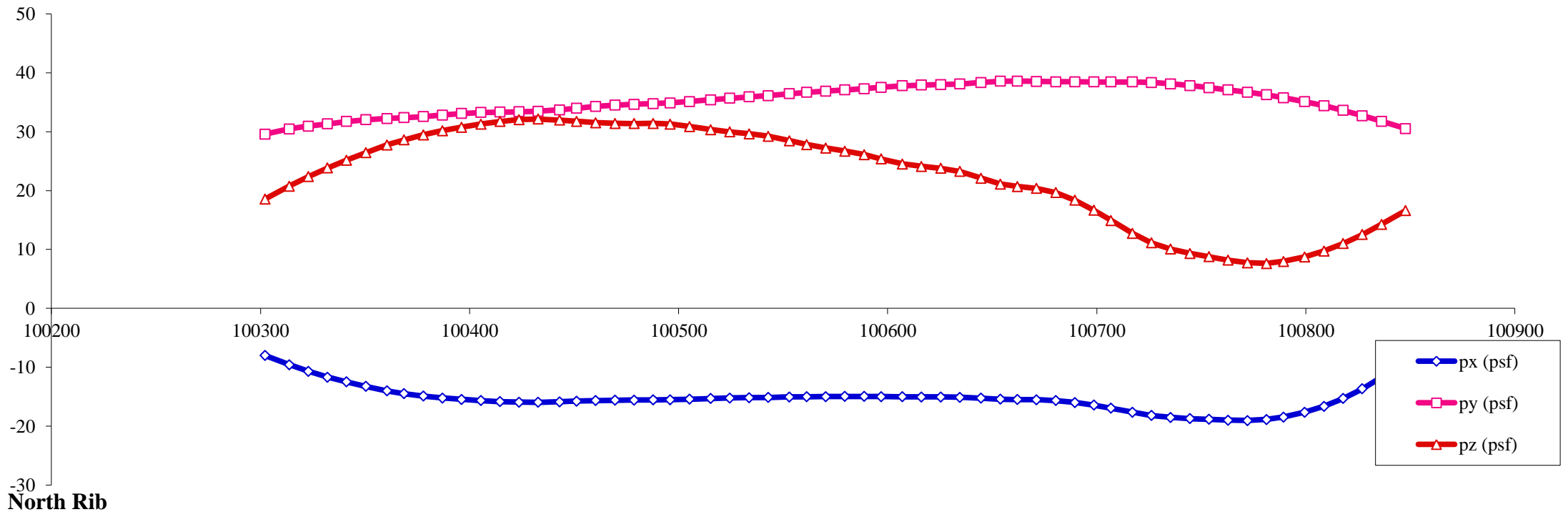
Load case : **11** Objective: Max uplift on deck, differential between 1/4 and 3/4 span



- Notes:**
1. All pressures in (psf)
 2. All coordinates/elevations in (ft)
 3. Loads for hangers, arch bracings, columns, pier caps and footings are not presented here

Load Visualization Page

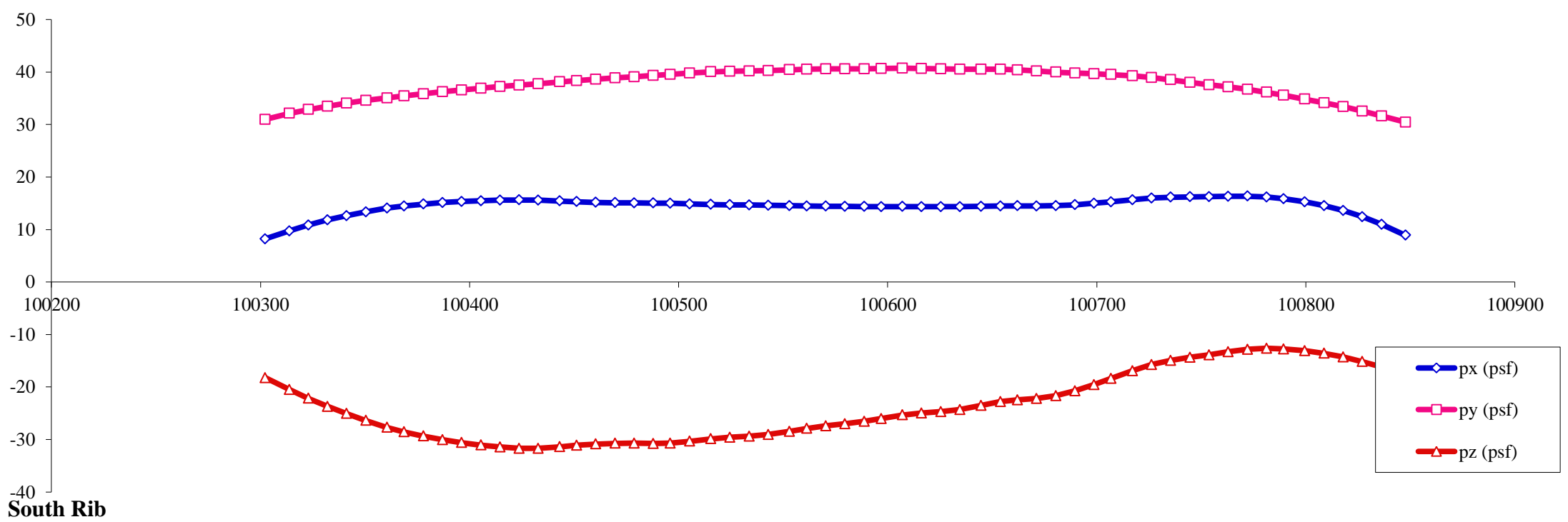
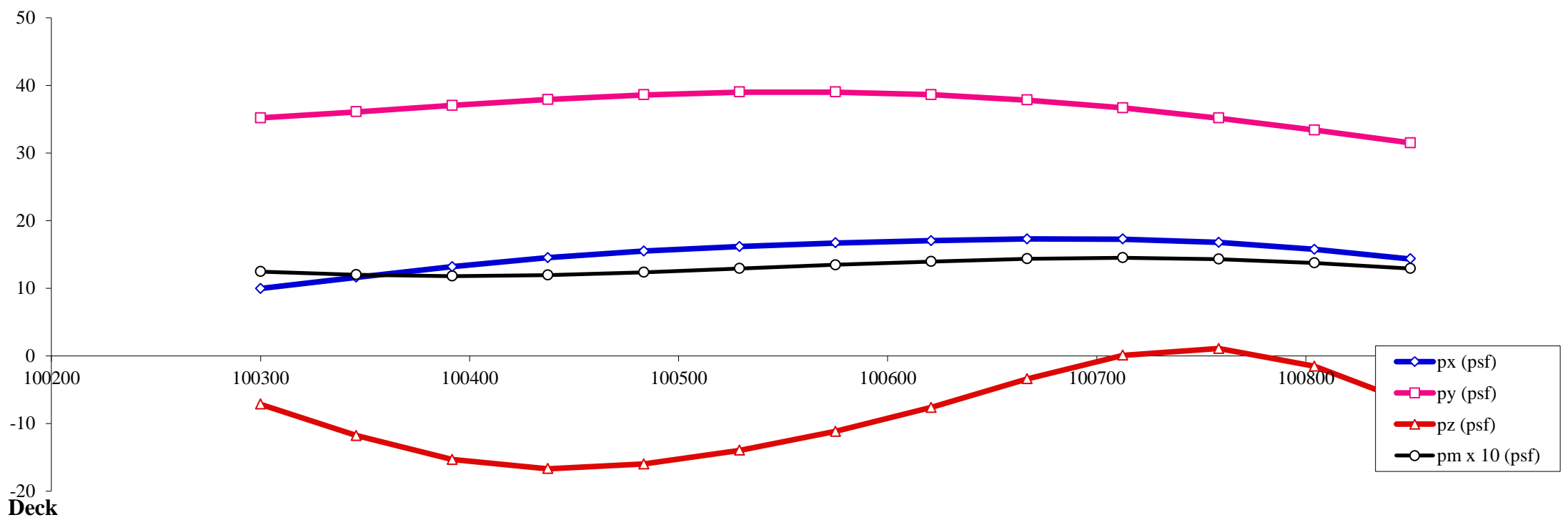
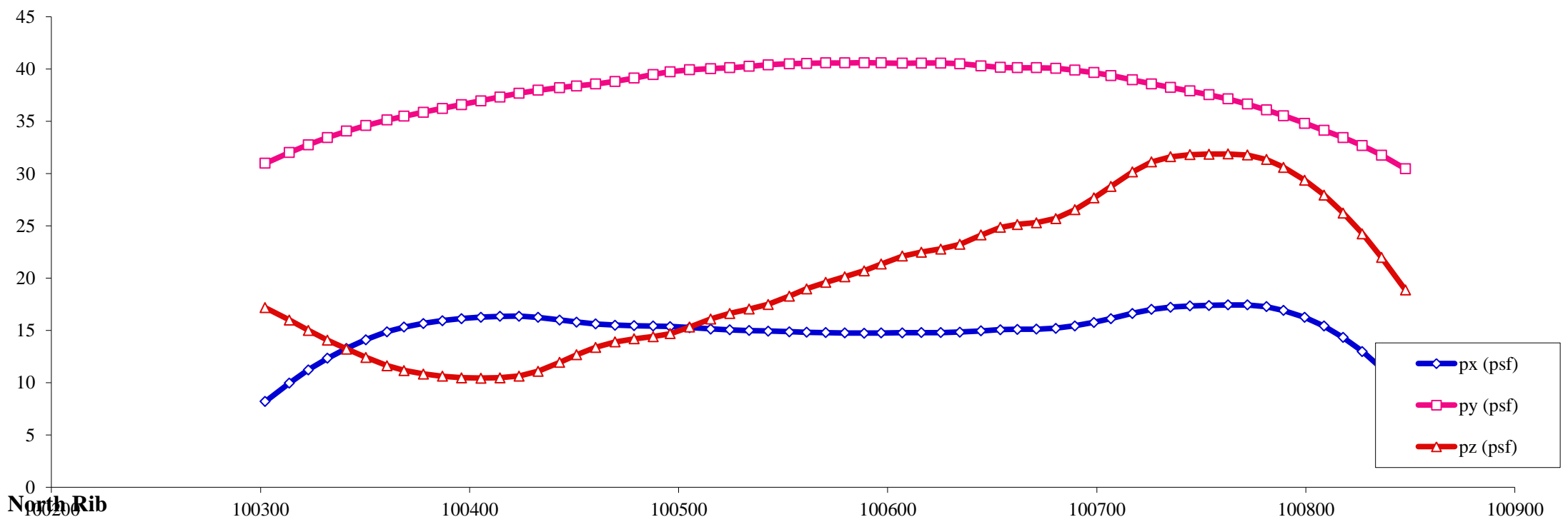
Load case : **12** Objective: Max uplift on deck, differential between 1/4 and 3/4 span



- Notes:
1. All pressures in (psf)
 2. All coordinates/elevations in (ft)
 3. Loads for hangers, arch bracings, columns, pier caps and footings are not presented here

Load Visualization Page

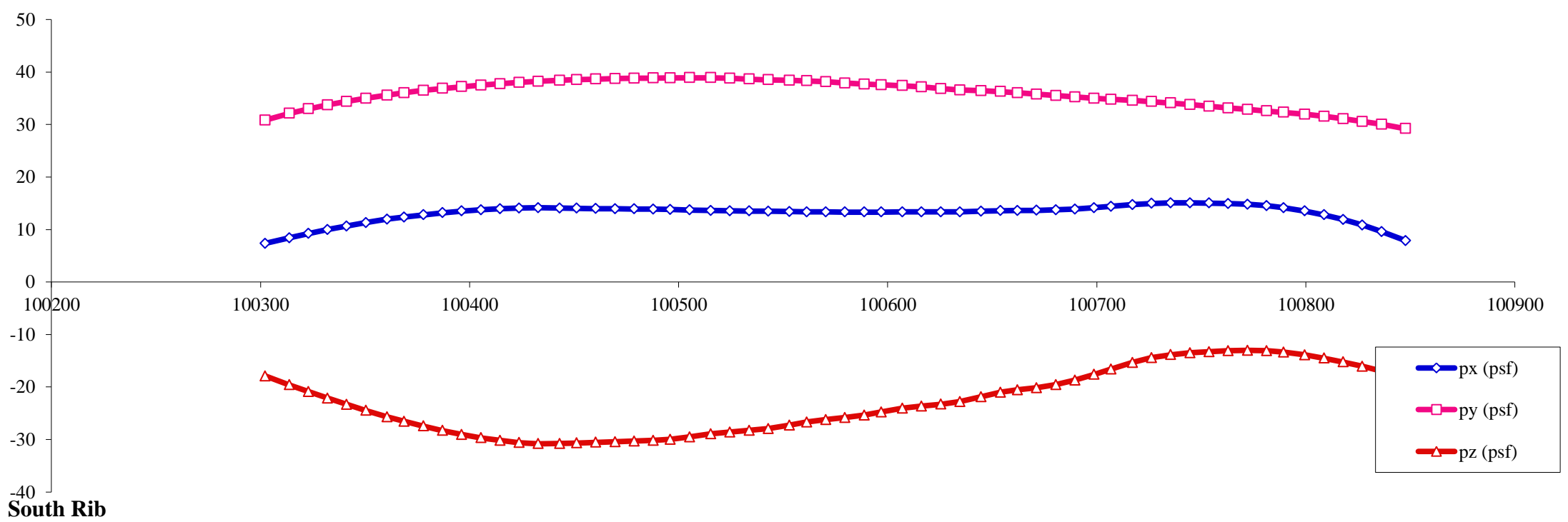
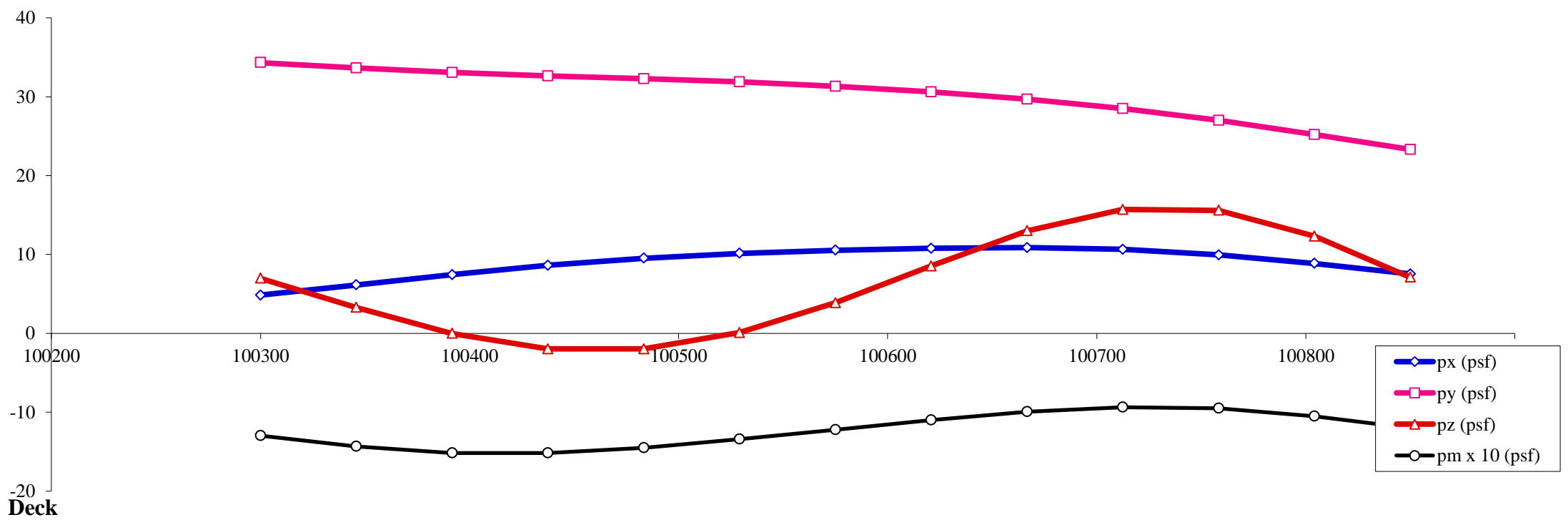
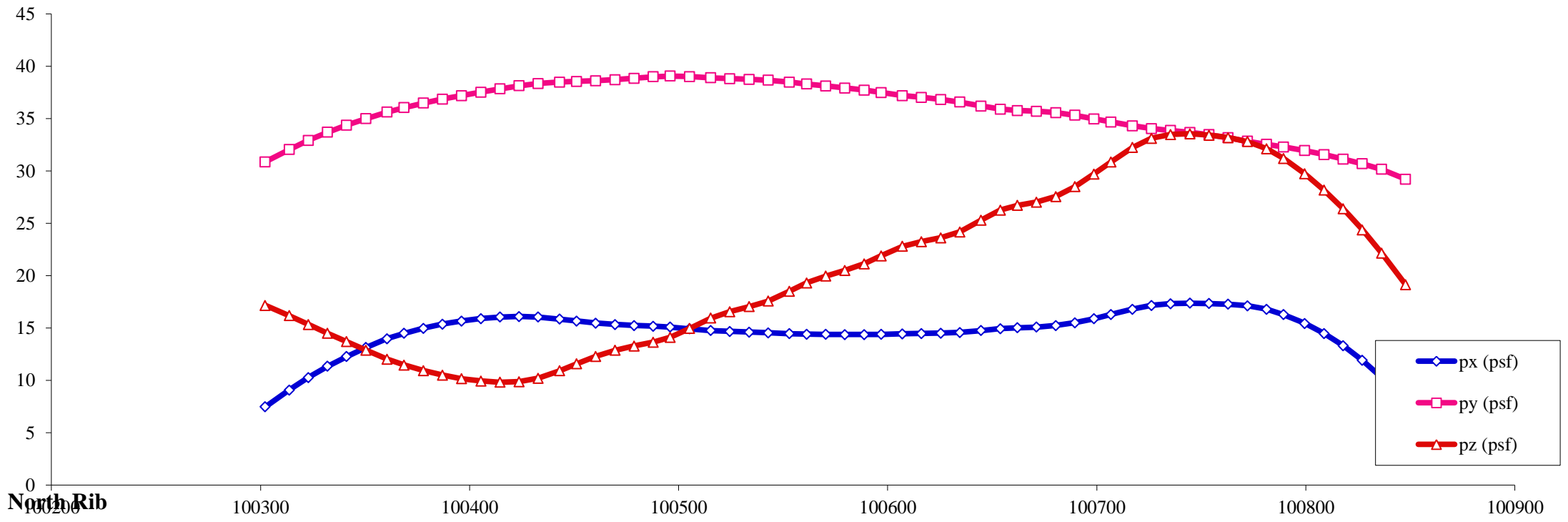
Load case : **13** Objective: Max uplift on deck, differential between 1/4 and 3/4 span



- Notes:
1. All pressures in (psf)
 2. All coordinates/elevations in (ft)
 3. Loads for hangers, arch bracings, columns, pier caps and footings are not presented here

Load Visualization Page

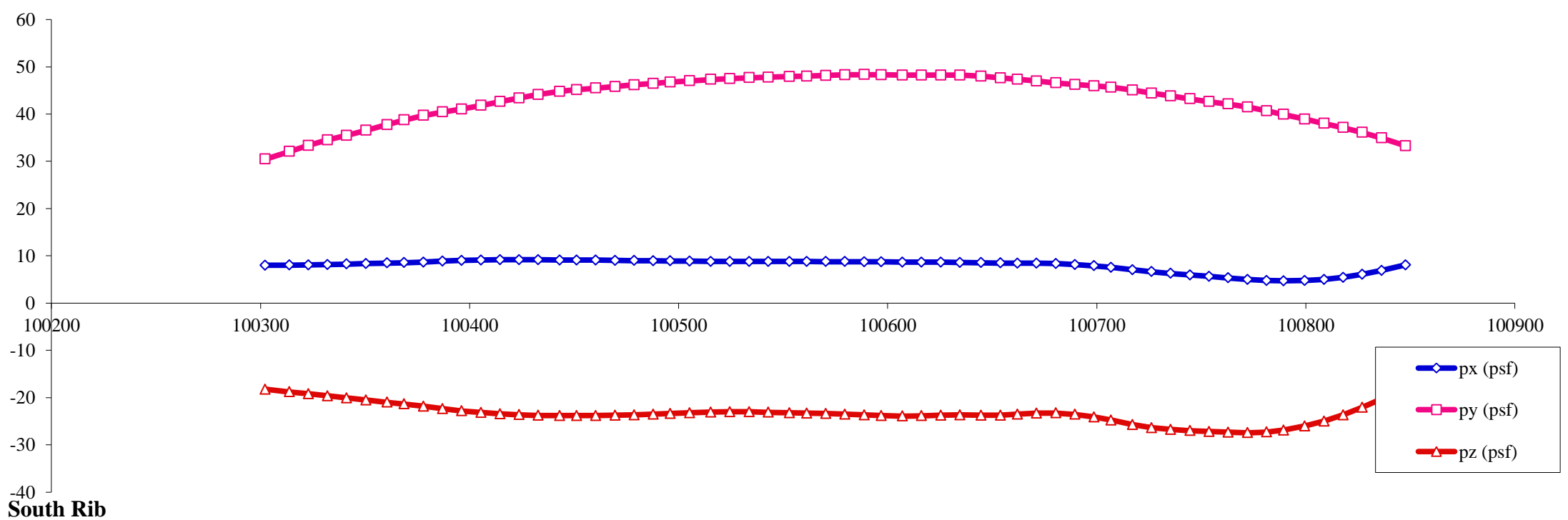
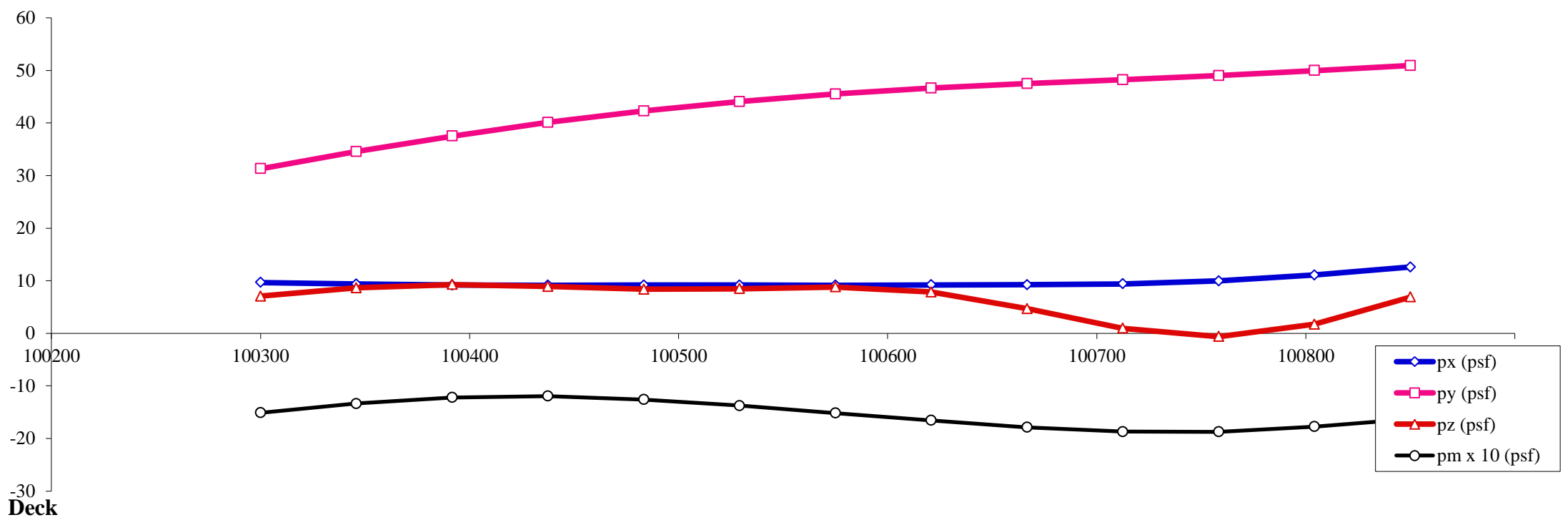
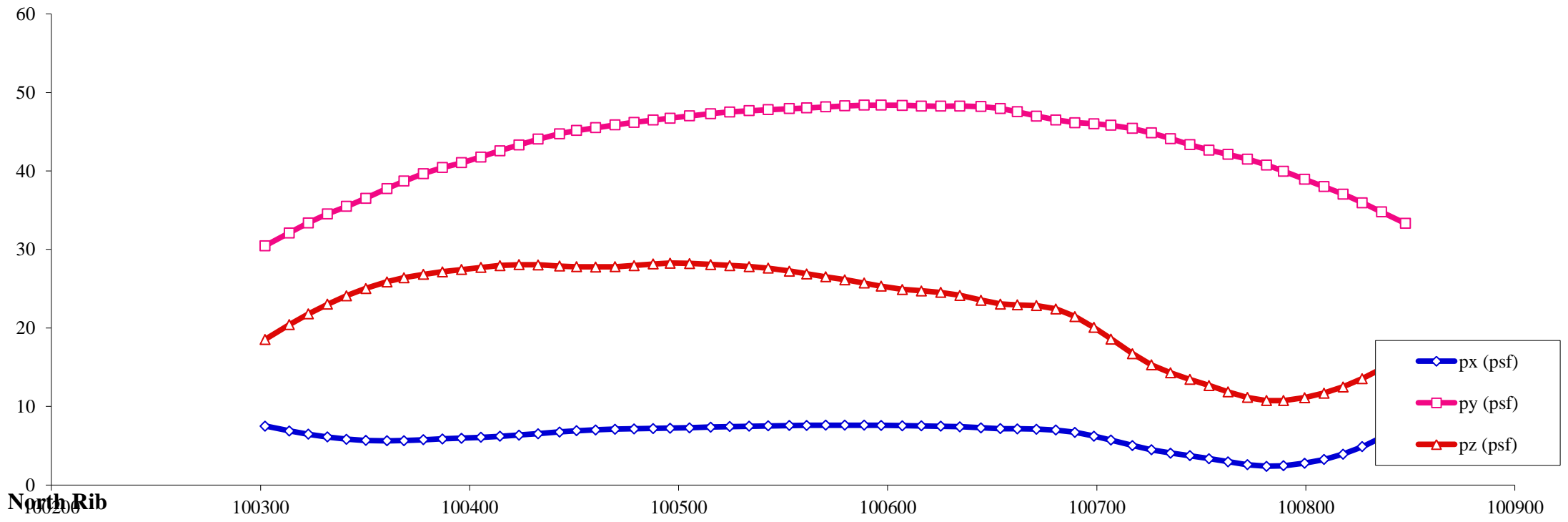
Load case : **14** Objective: Max uplift on deck, differential between 1/4 and 3/4 span



- Notes:
1. All pressures in (psf)
 2. All coordinates/elevations in (ft)
 3. Loads for hangers, arch bracings, columns, pier caps and footings are not presented here

Load Visualization Page

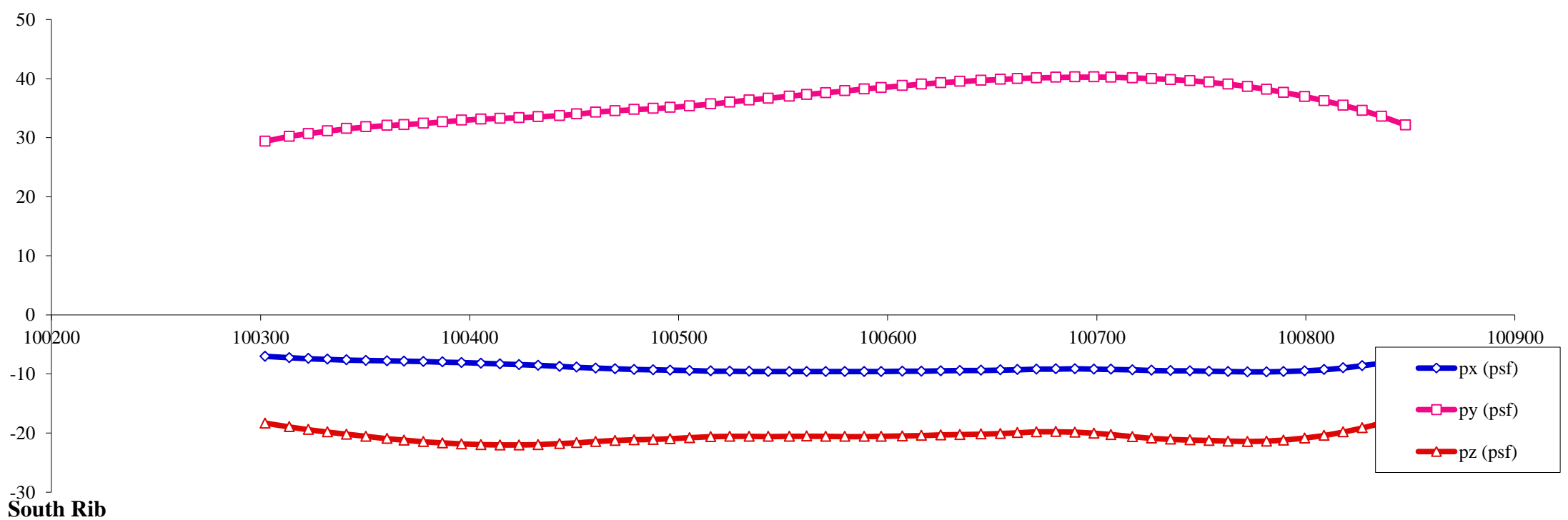
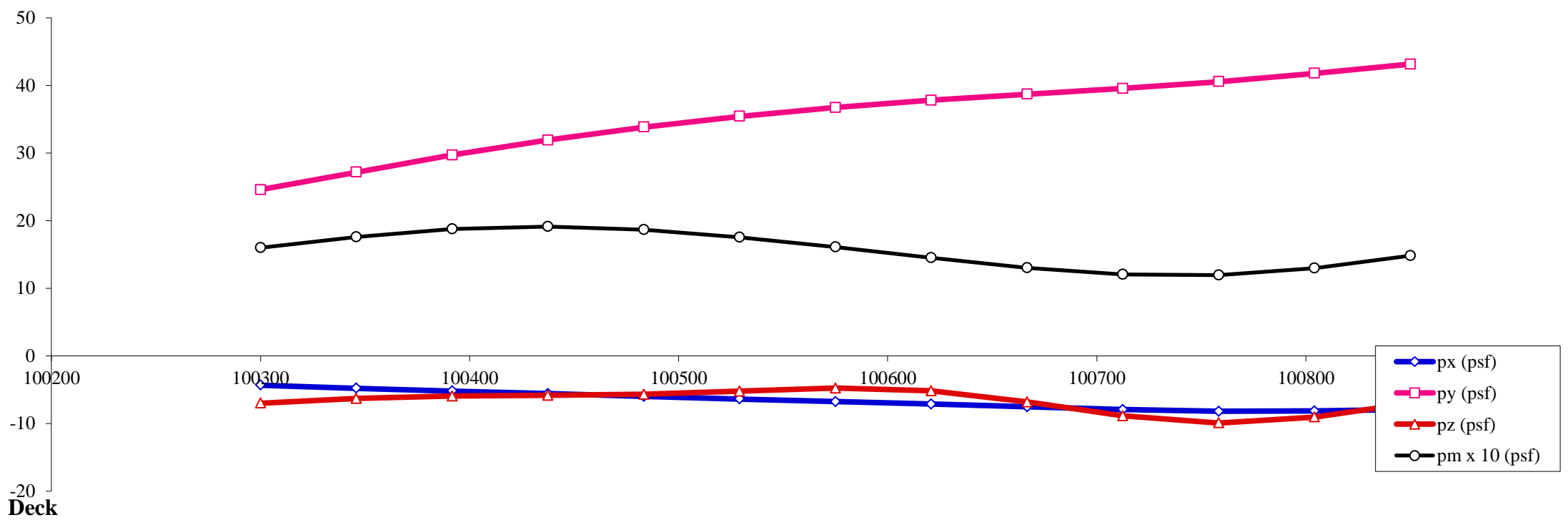
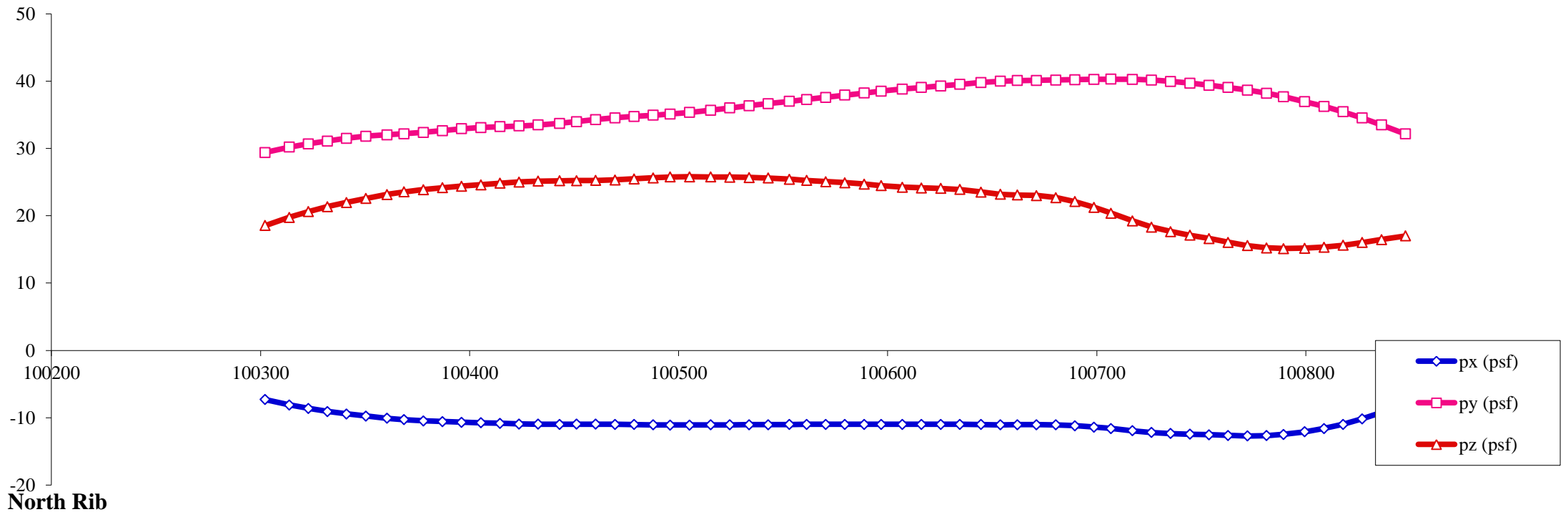
Load case : **15** Objective: Max moment on deck, differential between 1/4 and 3/4 span



- Notes:
1. All pressures in (psf)
 2. All coordinates/elevations in (ft)
 3. Loads for hangers, arch bracings, columns, pier caps and footings are not presented here

Load Visualization Page

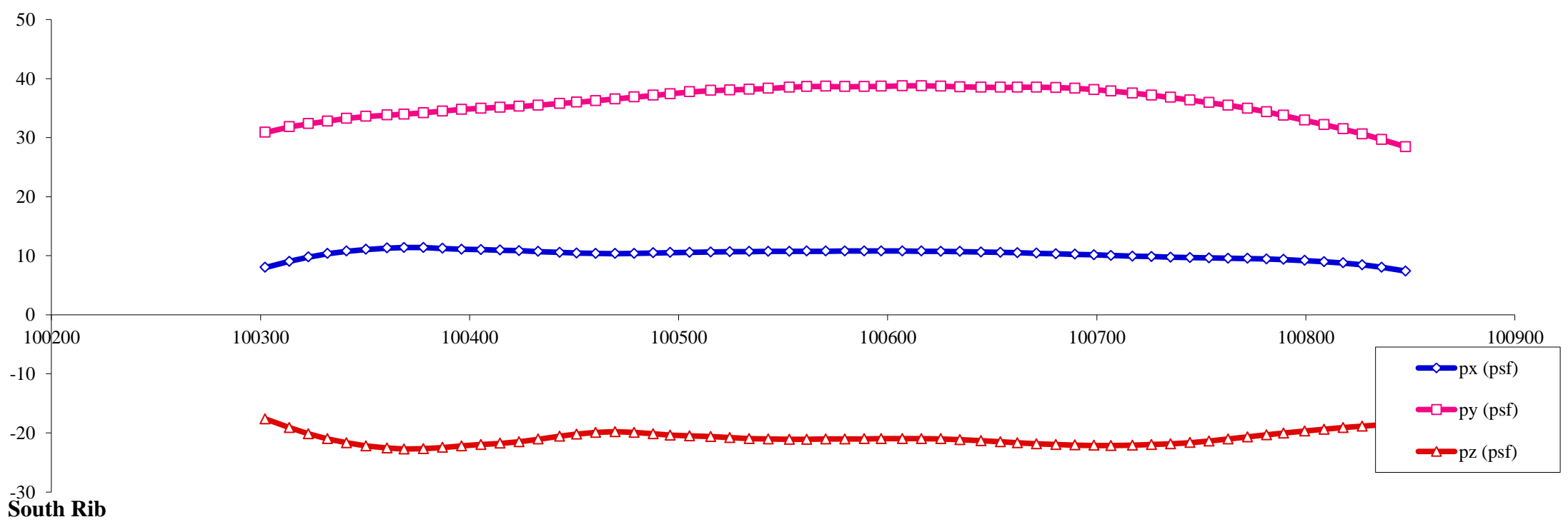
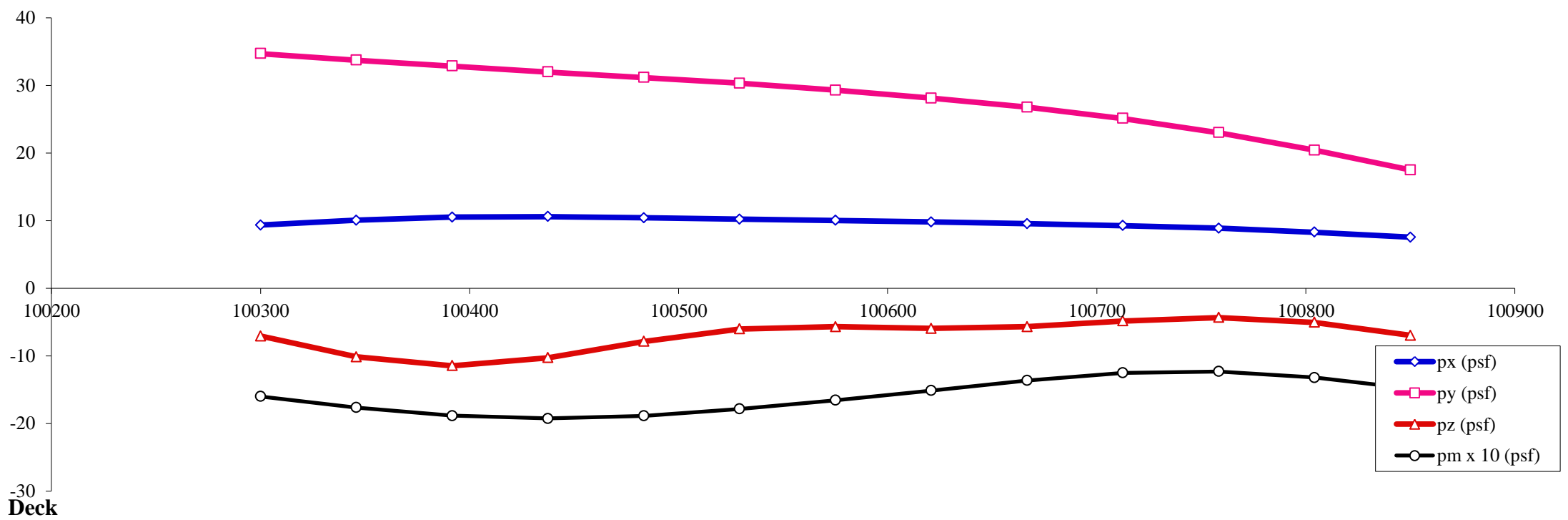
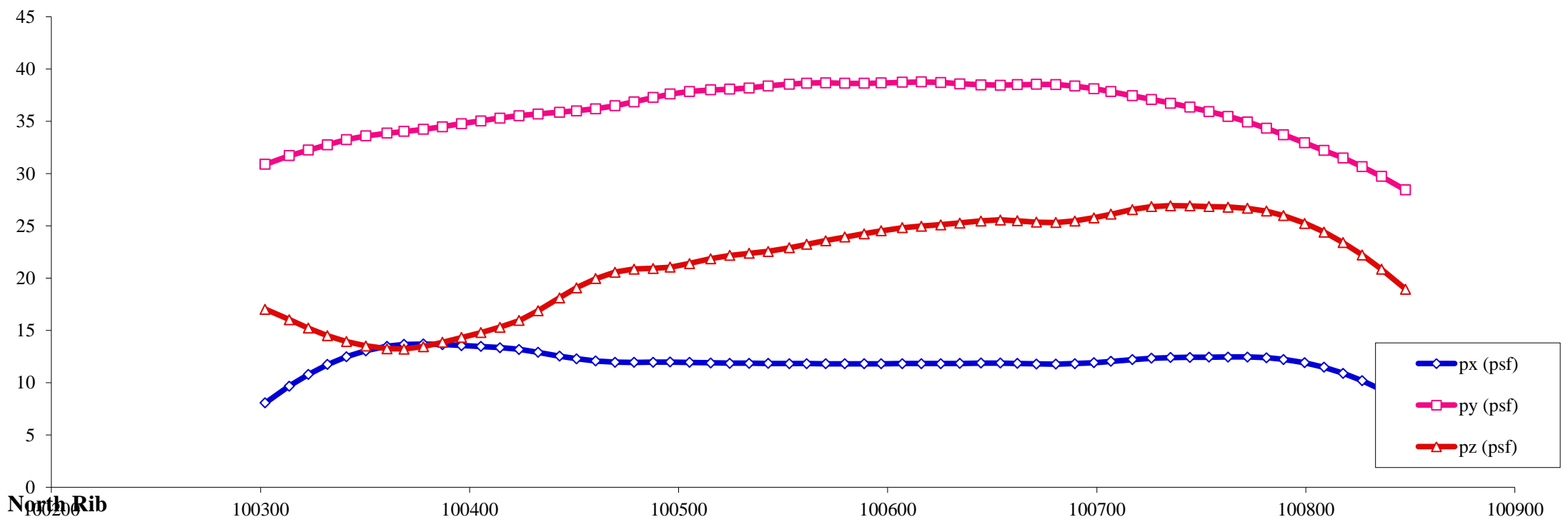
Load case : **16** Objective: Max moment on deck, differential between 1/4 and 3/4 span



- Notes:
1. All pressures in (psf)
 2. All coordinates/elevations in (ft)
 3. Loads for hangers, arch bracings, columns, pier caps and footings are not presented here

Load Visualization Page

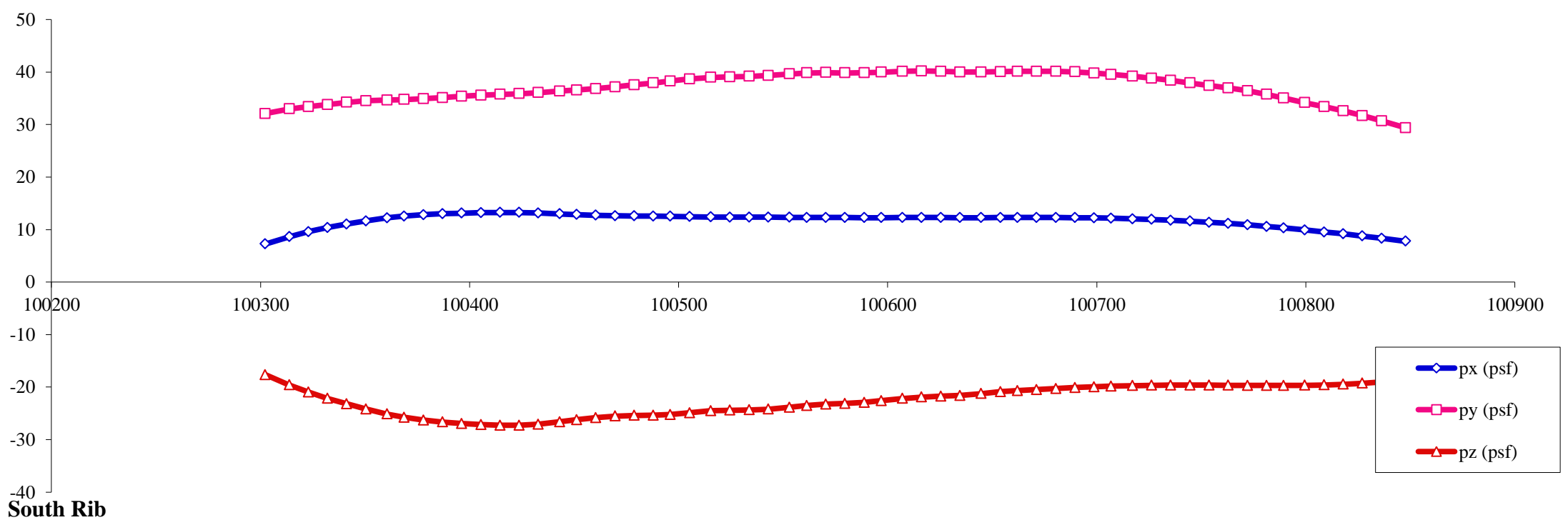
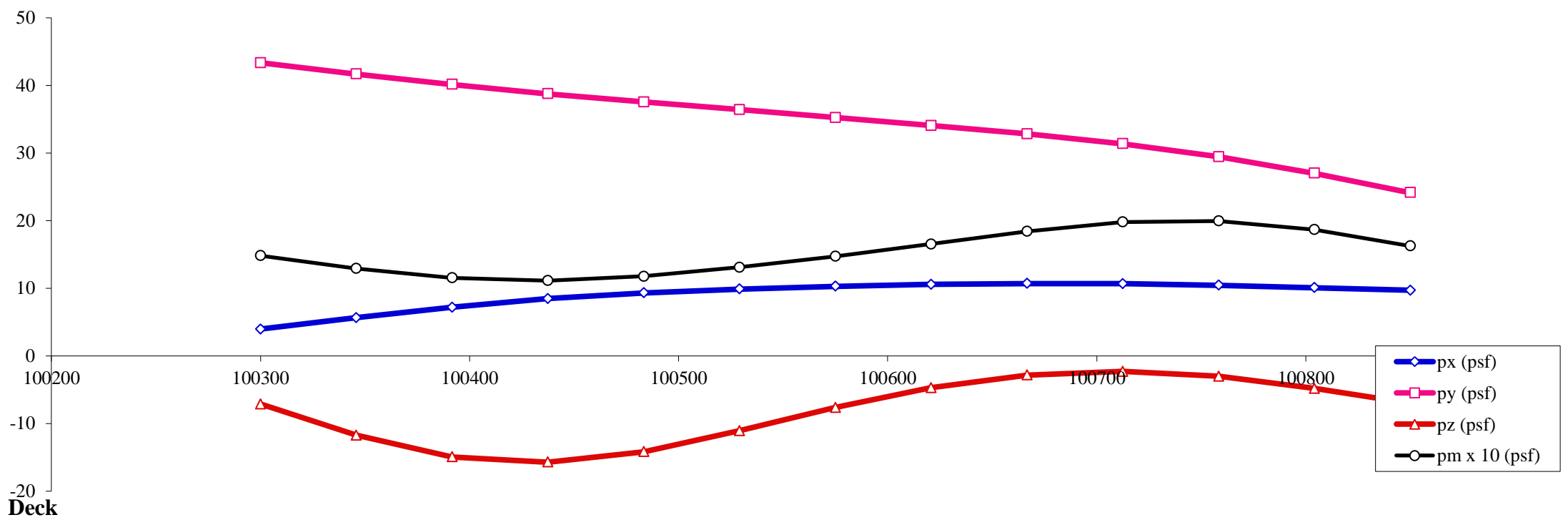
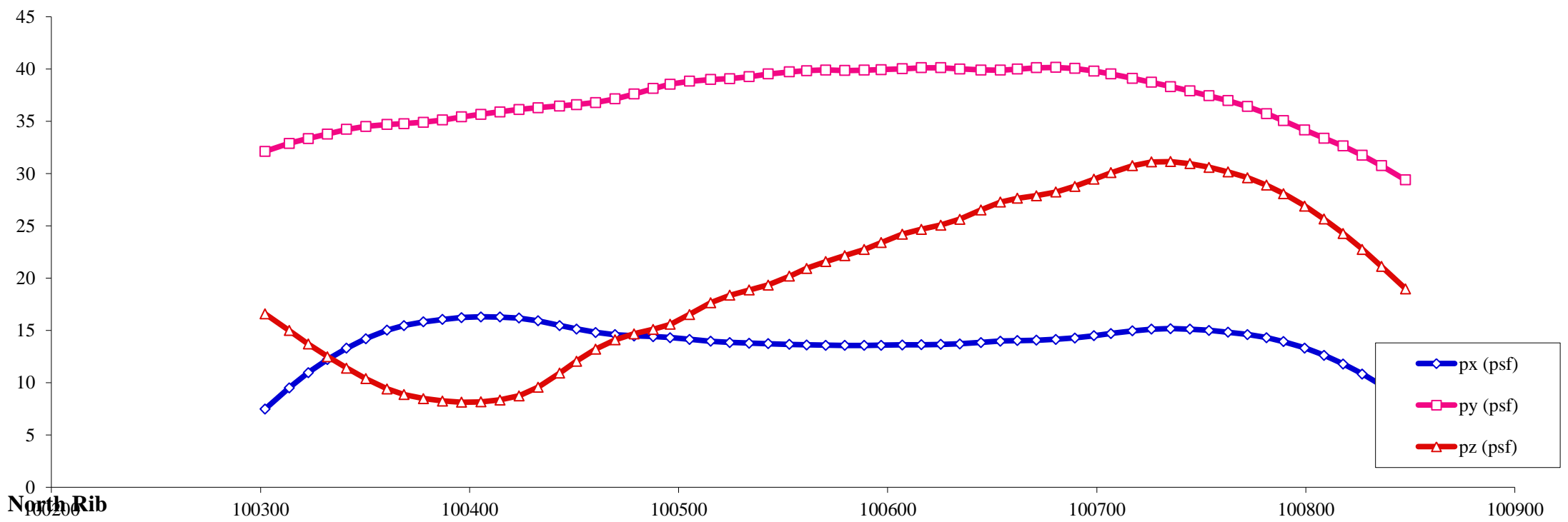
Load case : **17** Objective: Max moment on deck, differential between 1/4 and 3/4 span



- Notes:
1. All pressures in (psf)
 2. All coordinates/elevations in (ft)
 3. Loads for hangers, arch bracings, columns, pier caps and footings are not presented here

Load Visualization Page

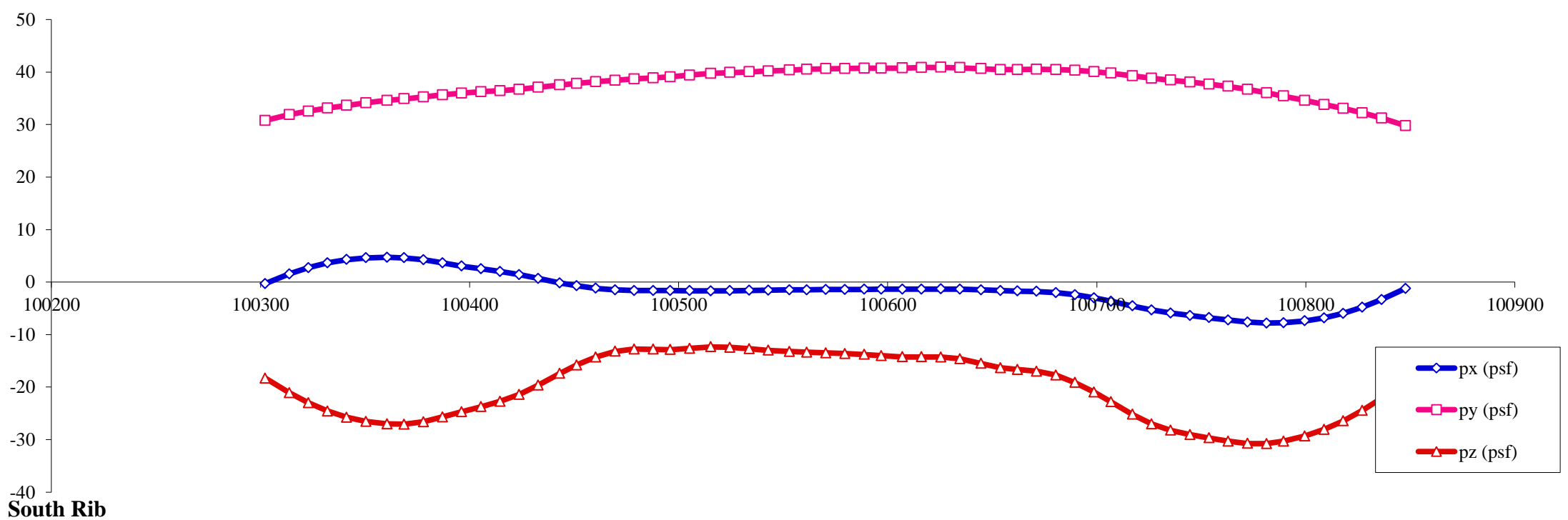
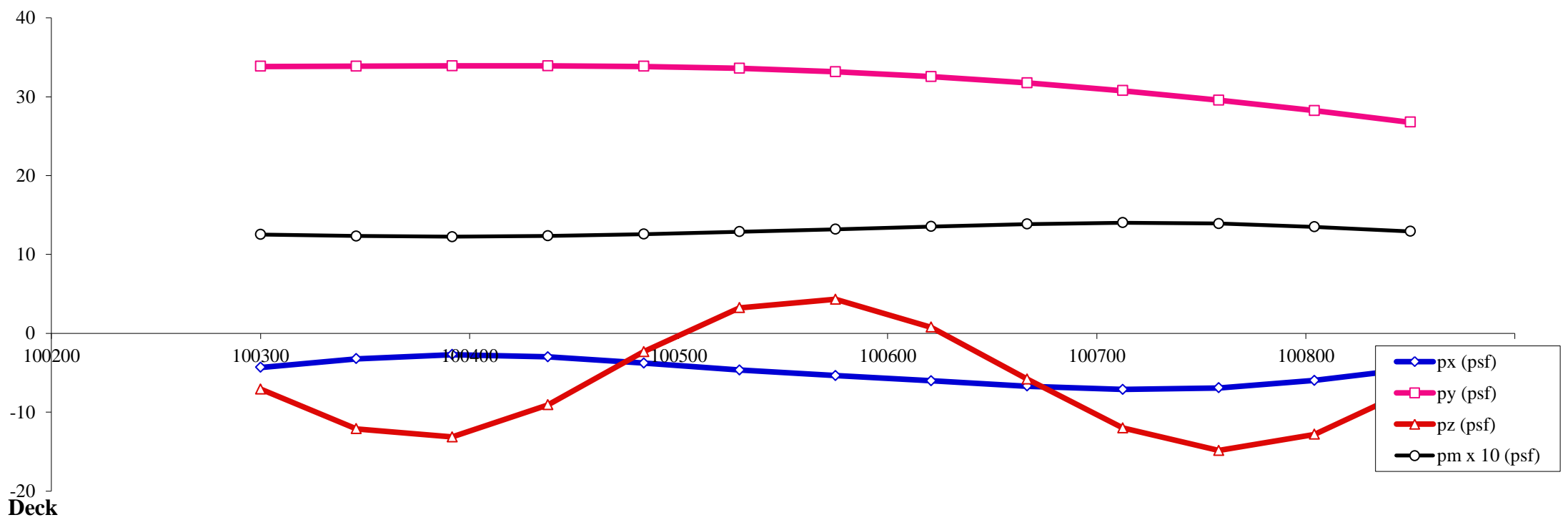
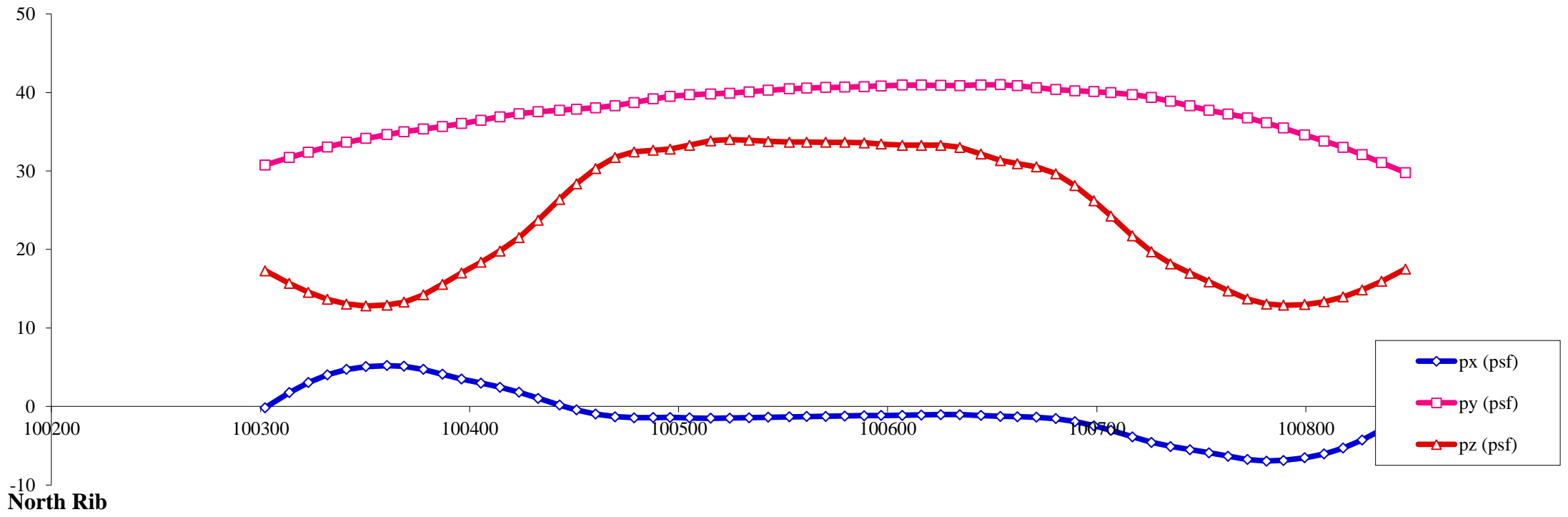
Load case : **18** Objective: Max moment on deck, differential between 1/4 and 3/4 span



- Notes:
1. All pressures in (psf)
 2. All coordinates/elevations in (ft)
 3. Loads for hangers, arch bracings, columns, pier caps and footings are not presented here

Load Visualization Page

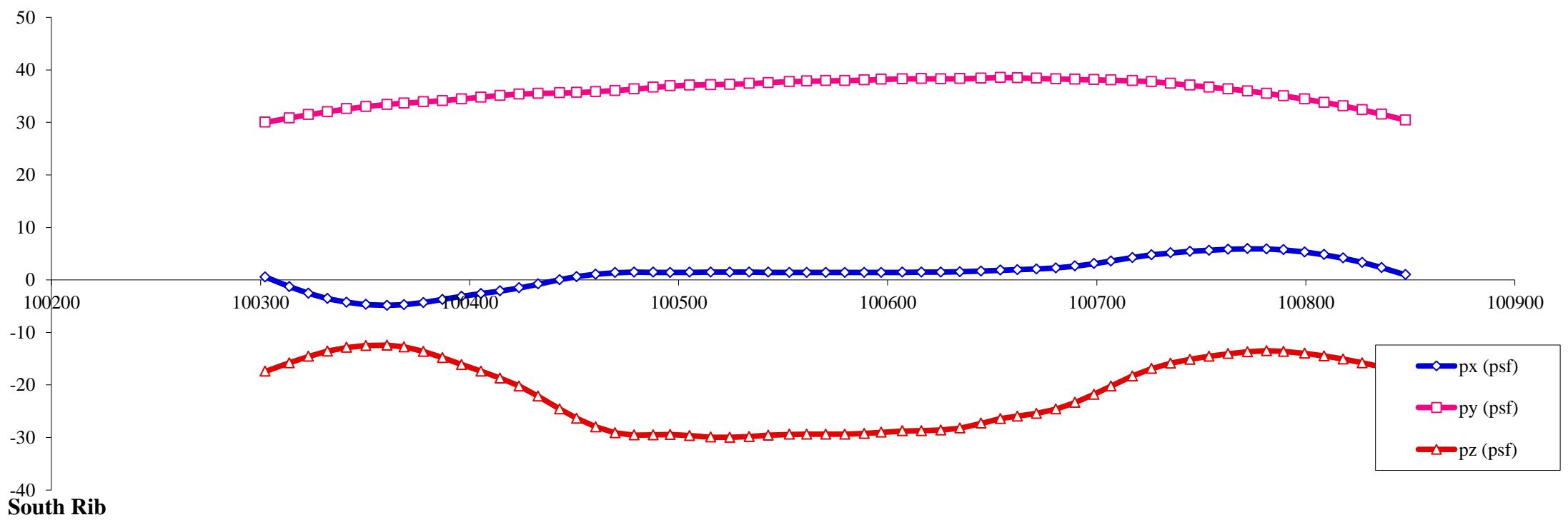
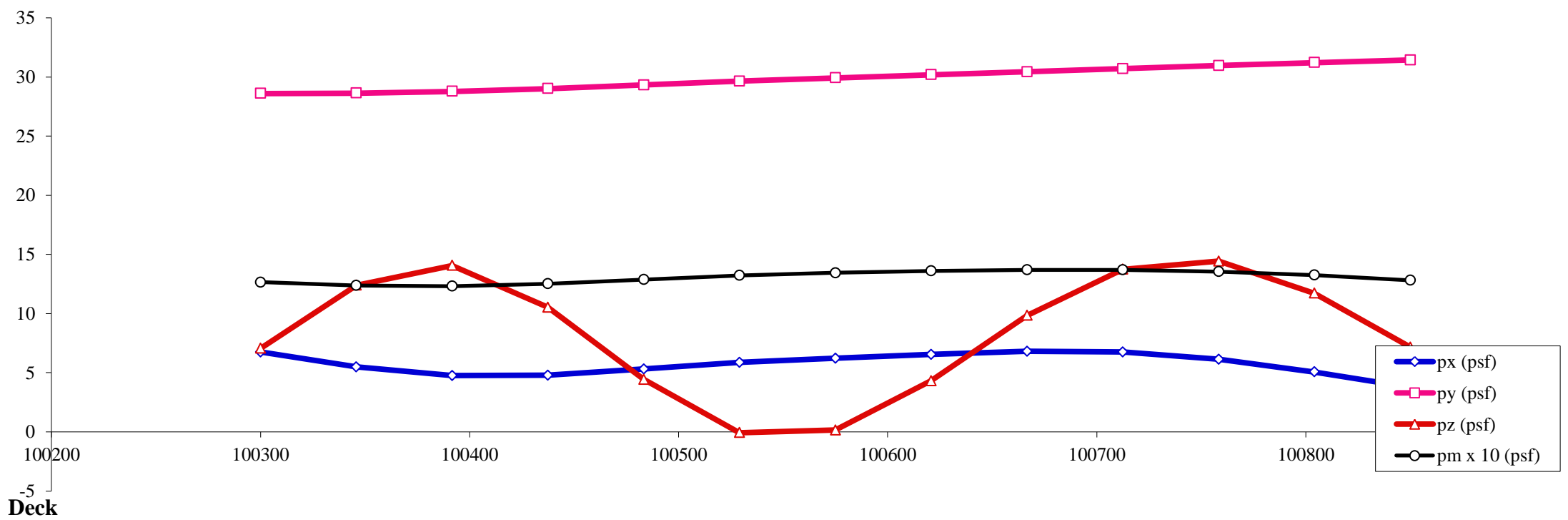
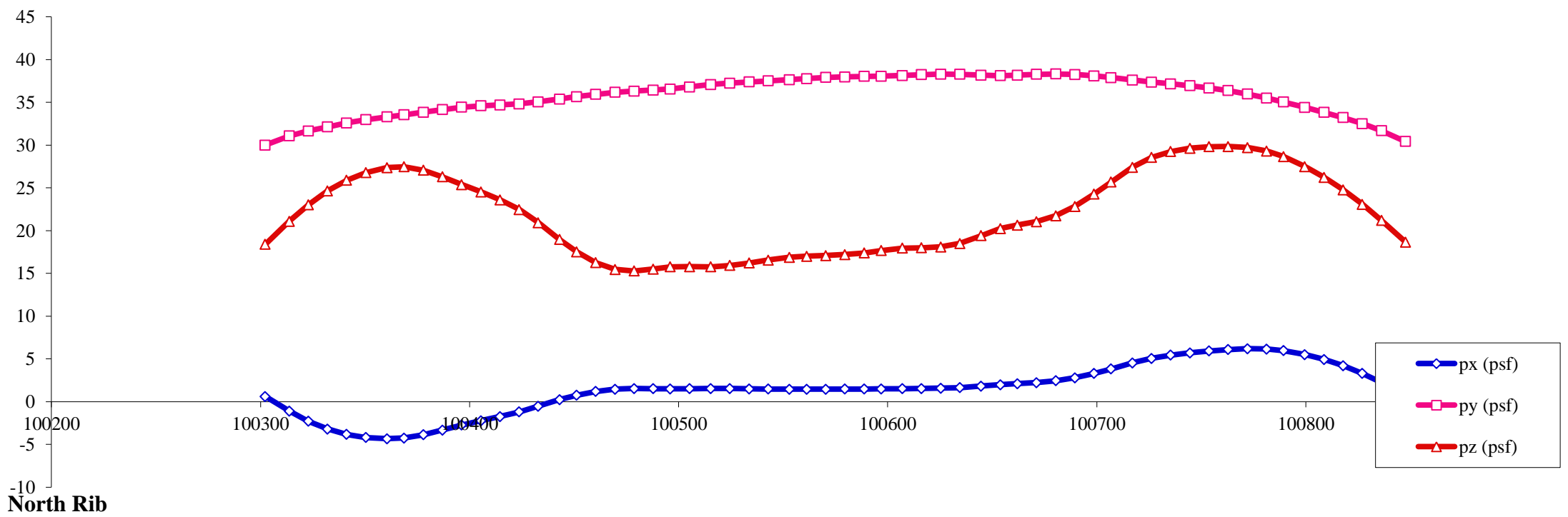
Load case : **19** Objective: Max uplift on deck, differential between middle and 1/4 & 3/4 span



- Notes:
1. All pressures in (psf)
 2. All coordinates/elevations in (ft)
 3. Loads for hangers, arch bracings, columns, pier caps and footings are not presented here

Load Visualization Page

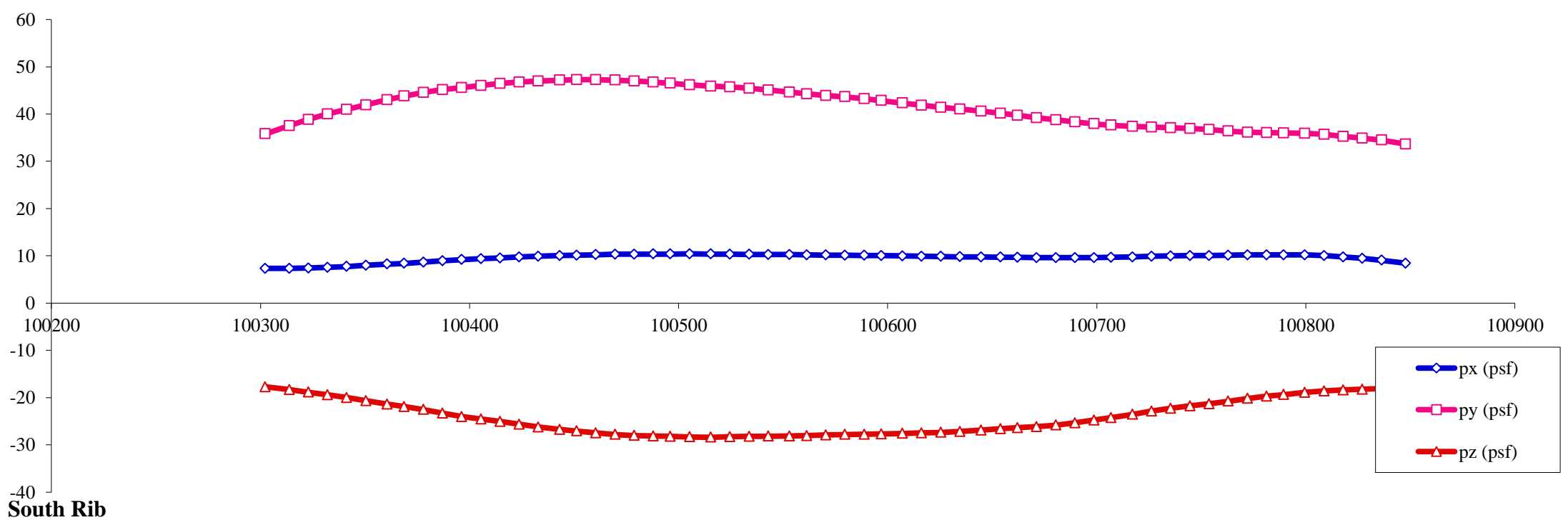
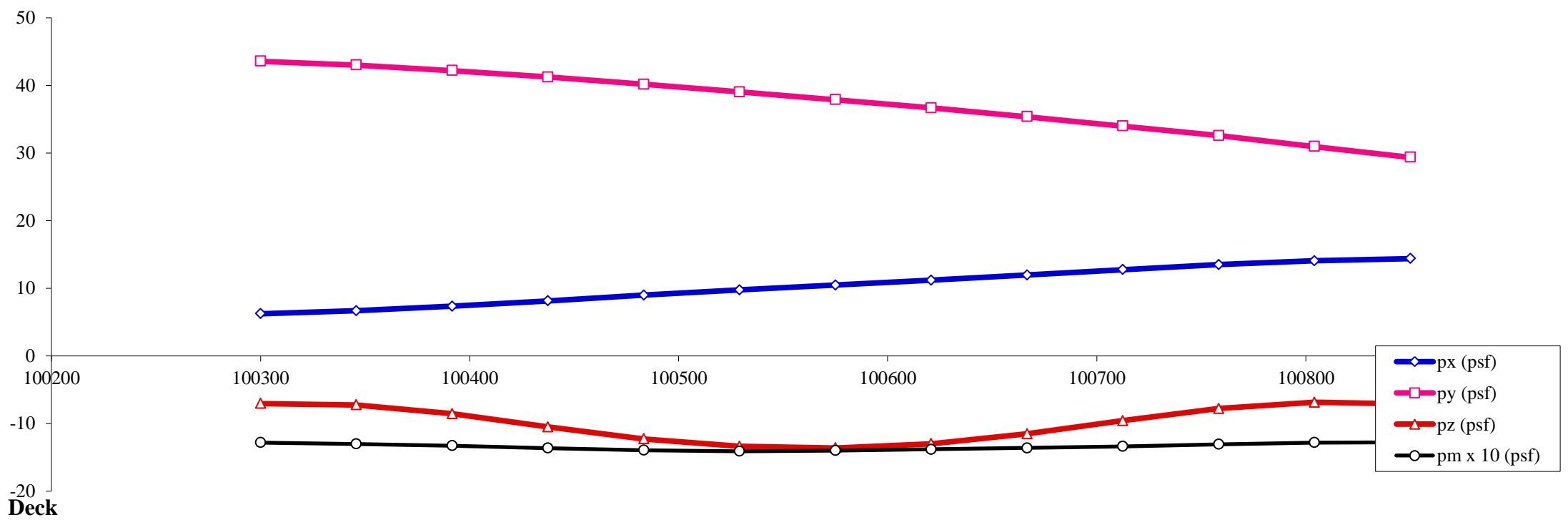
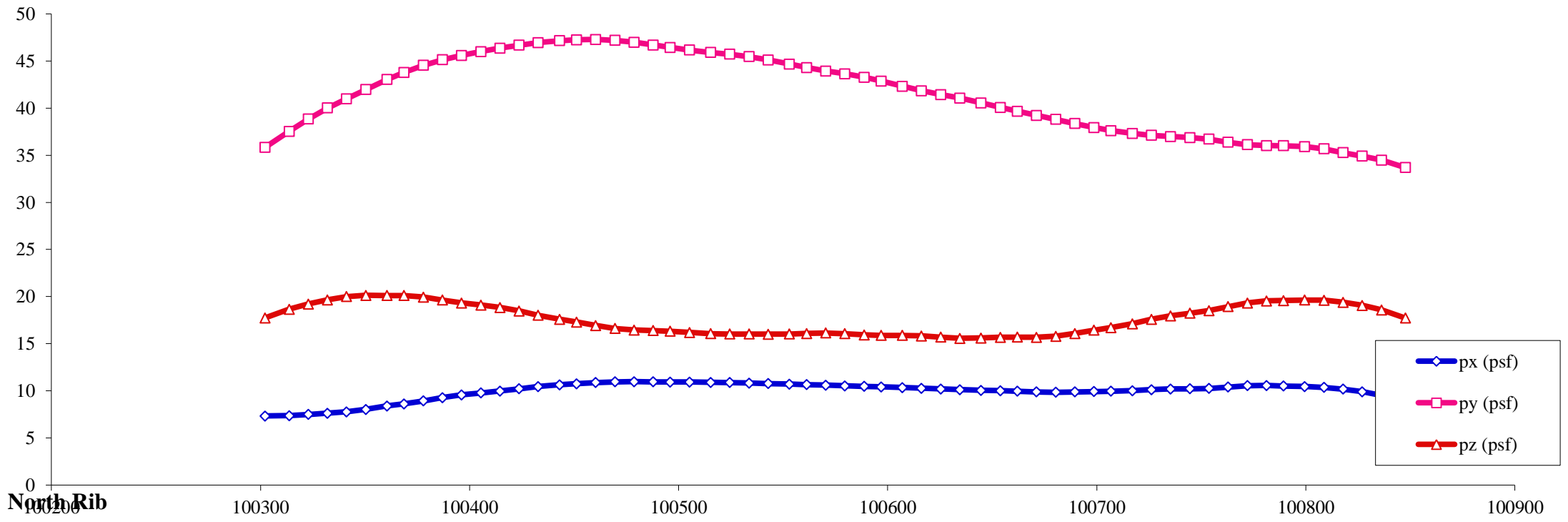
Load case : **20** Objective: Max uplift on deck, differential between middle and 1/4 & 3/4 span



- Notes:
1. All pressures in (psf)
 2. All coordinates/elevations in (ft)
 3. Loads for hangers, arch bracings, columns, pier caps and footings are not presented here

Load Visualization Page

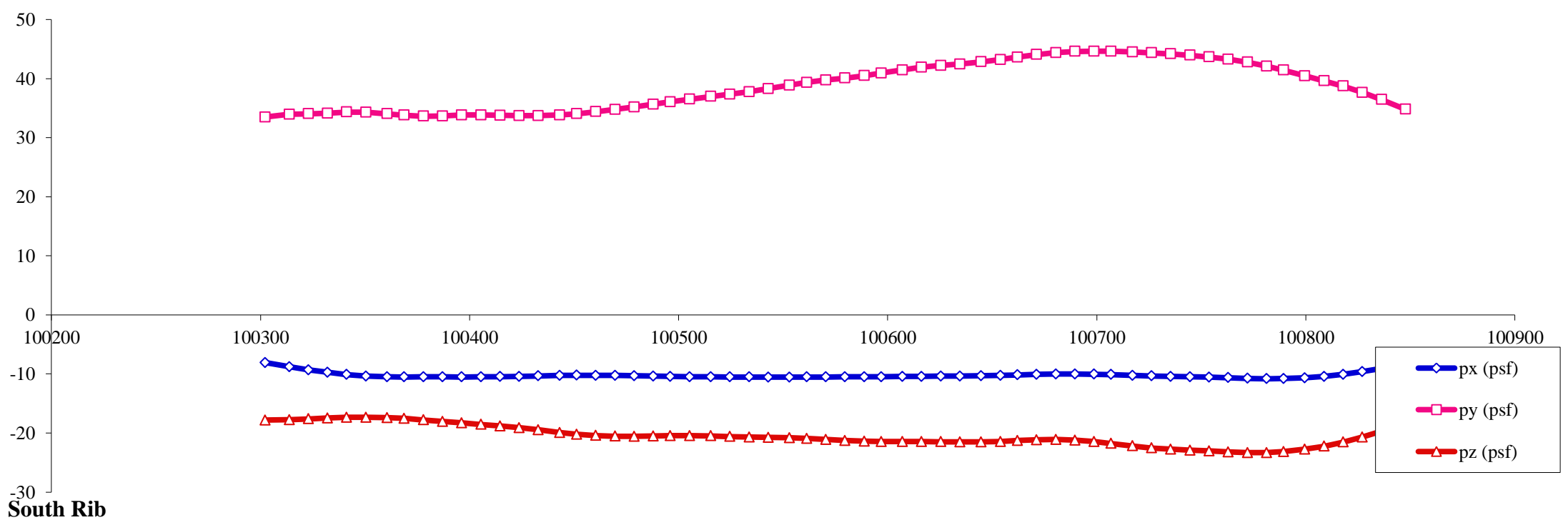
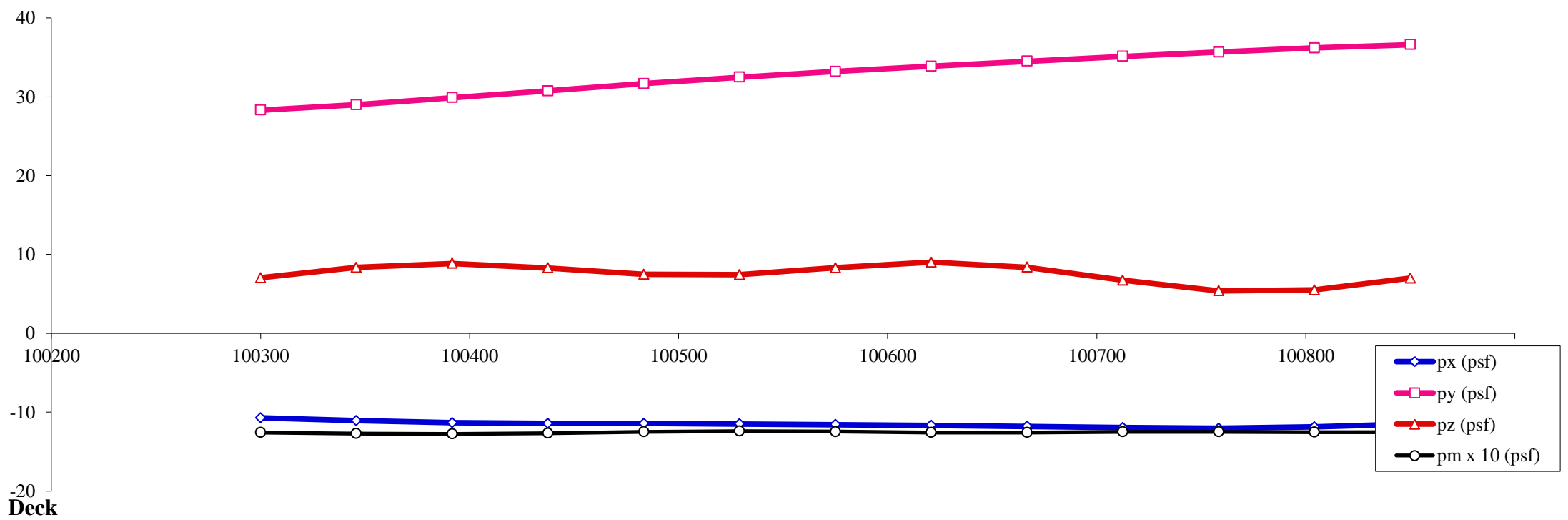
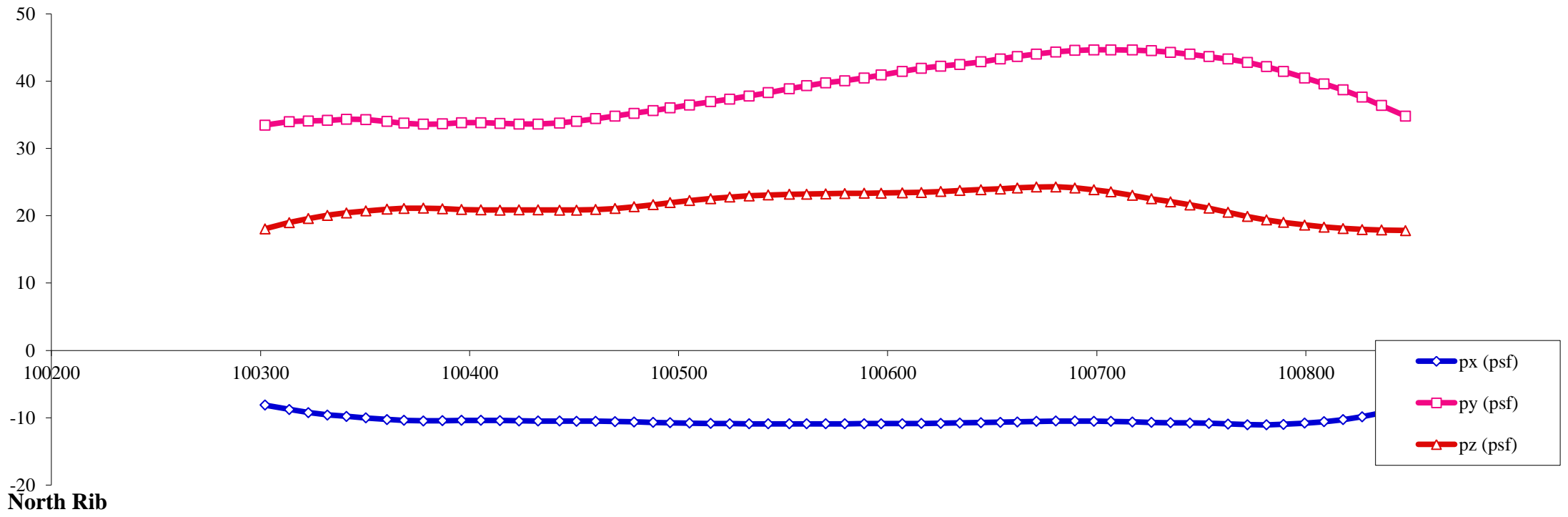
Load case : **21** Objective: Max lateral on arch ribs, differential between 1/4 and 3/4 span



- Notes:
1. All pressures in (psf)
 2. All coordinates/elevations in (ft)
 3. Loads for hangers, arch bracings, columns, pier caps and footings are not presented here

Load Visualization Page

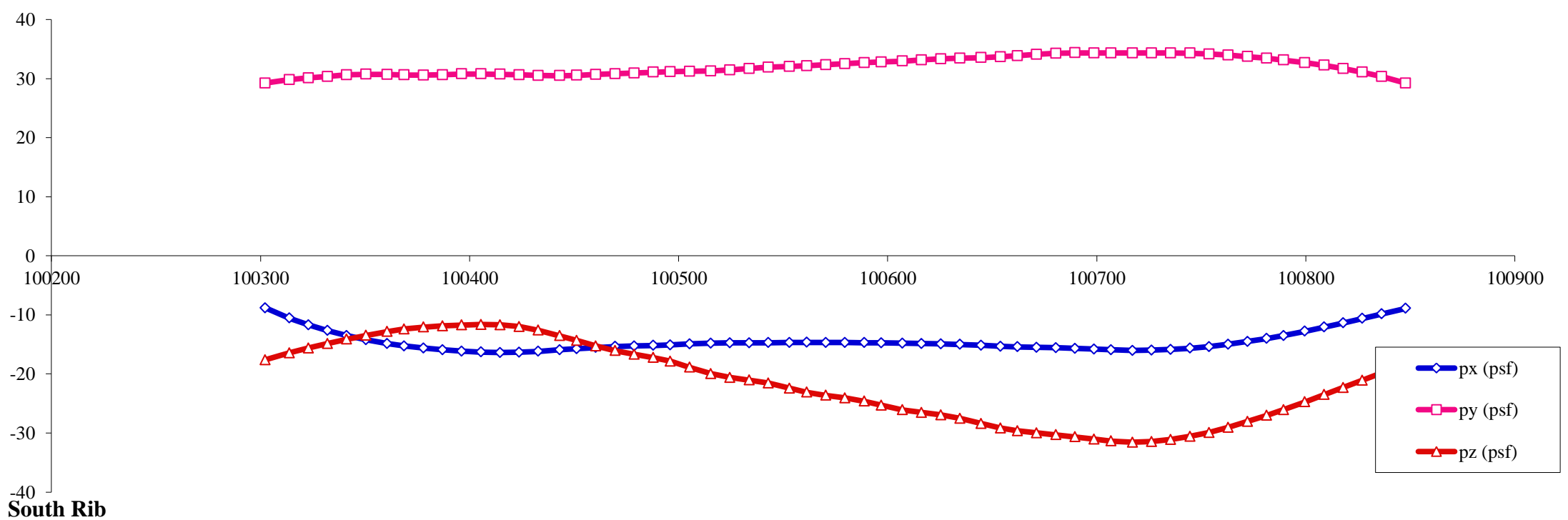
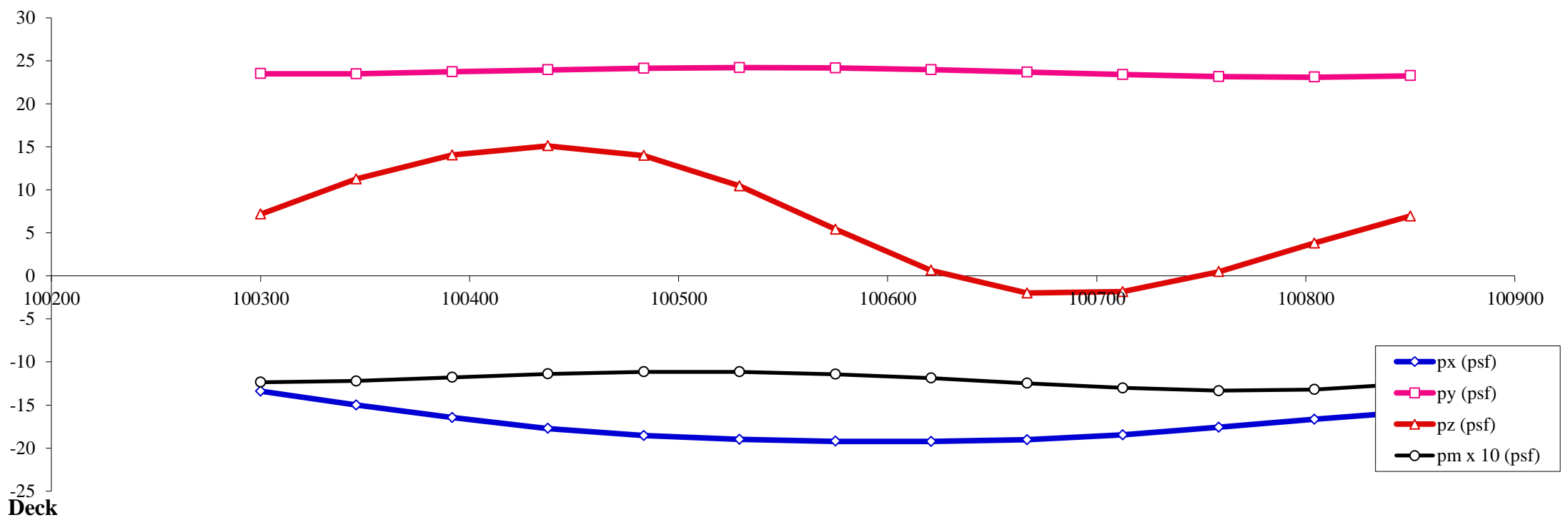
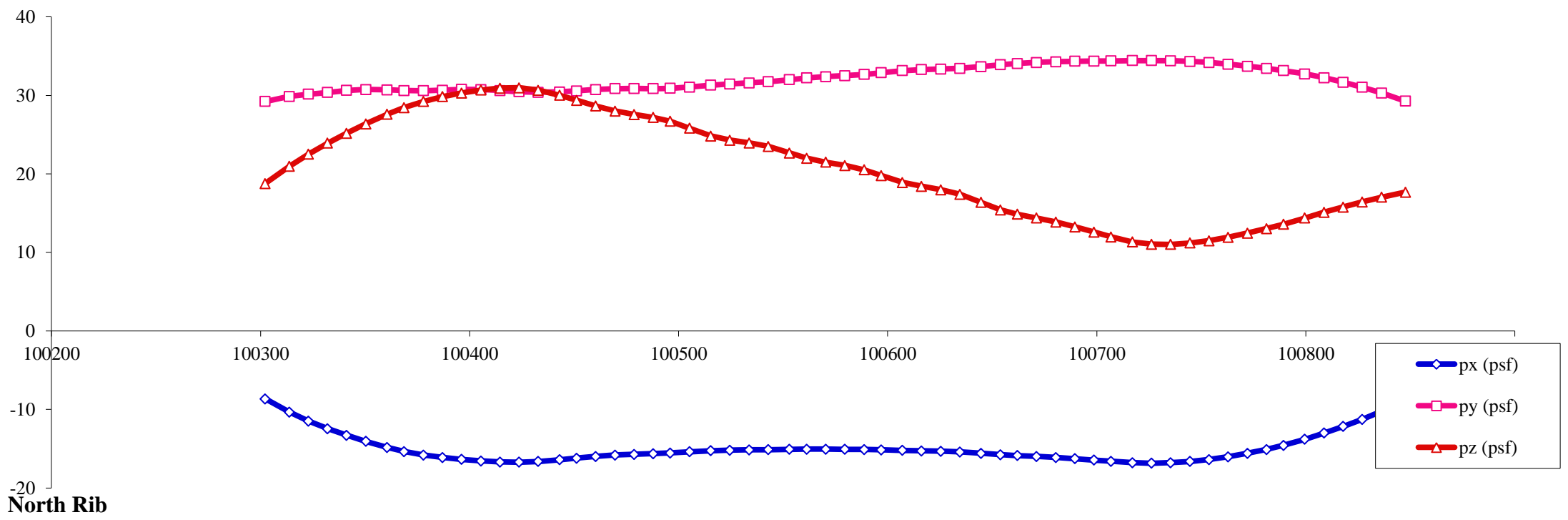
Load case : **22** Objective: Max lateral on arch ribs, differential between 1/4 and 3/4 span



- Notes:
1. All pressures in (psf)
 2. All coordinates/elevations in (ft)
 3. Loads for hangers, arch bracings, columns, pier caps and footings are not presented here

Load Visualization Page

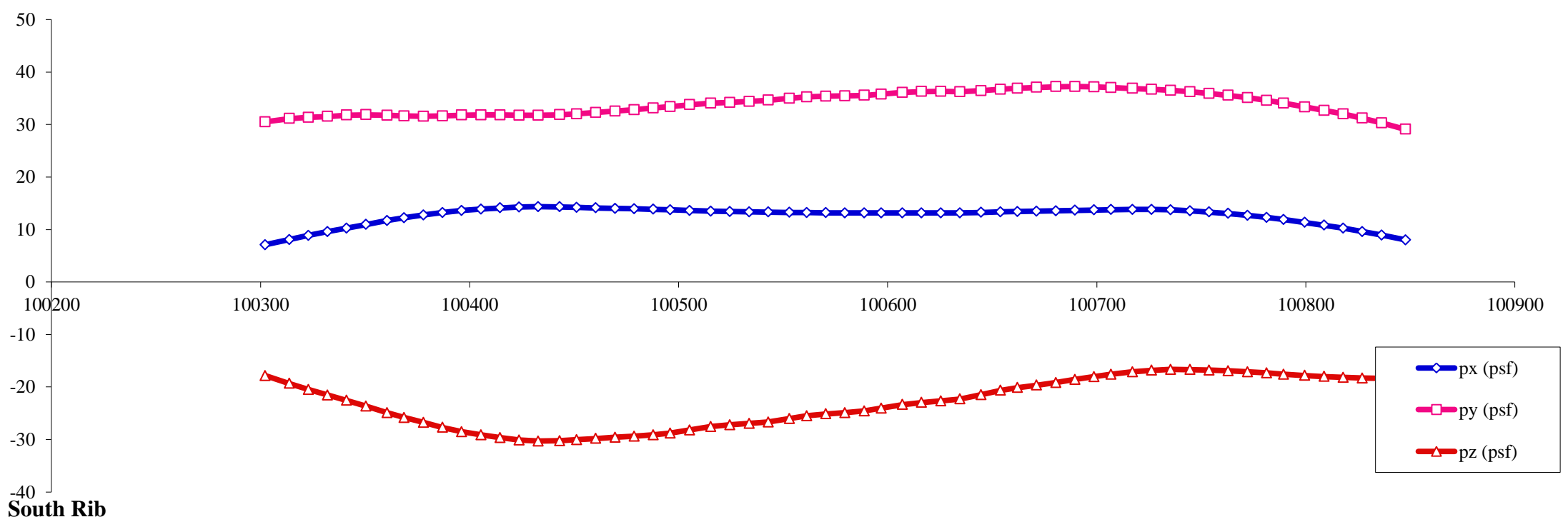
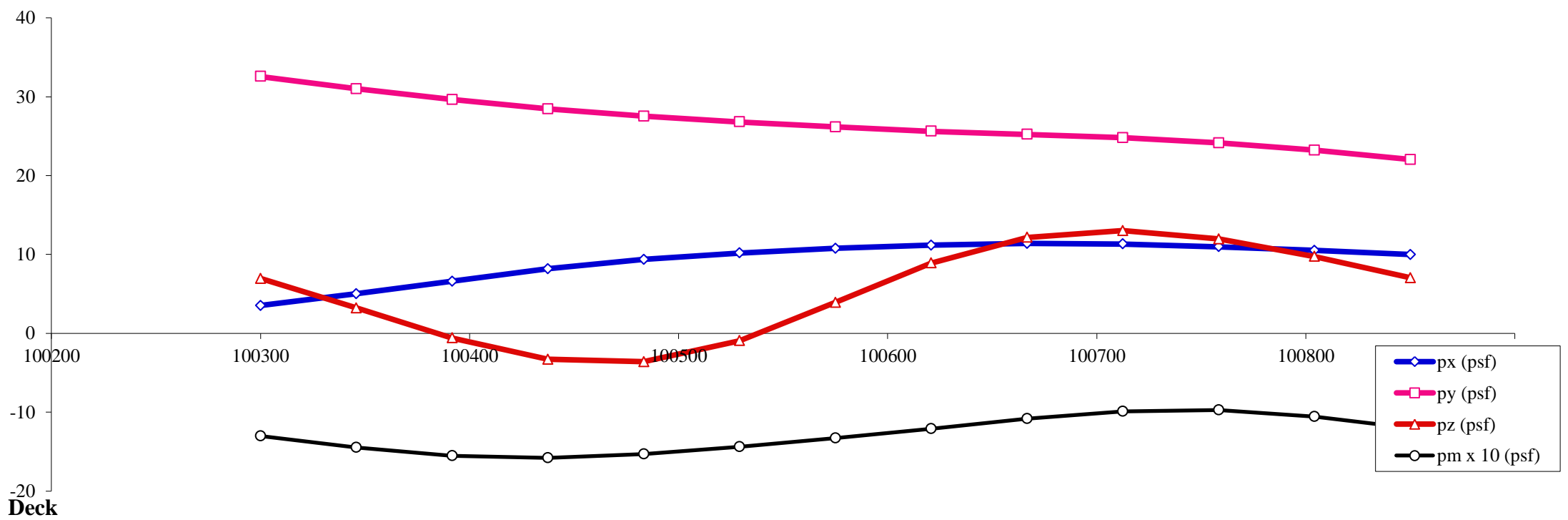
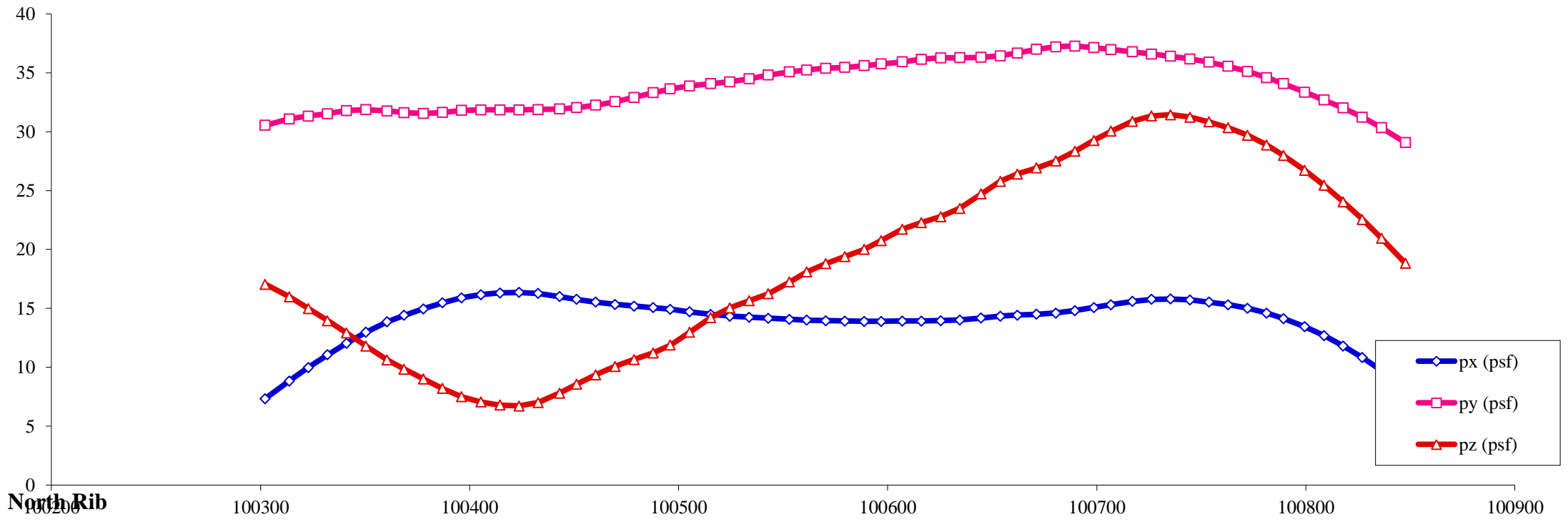
Load case : **23** Objective: Max uplift on arch ribs, differential between 1/4 and 3/4 span



- Notes:
1. All pressures in (psf)
 2. All coordinates/elevations in (ft)
 3. Loads for hangers, arch bracings, columns, pier caps and footings are not presented here

Load Visualization Page

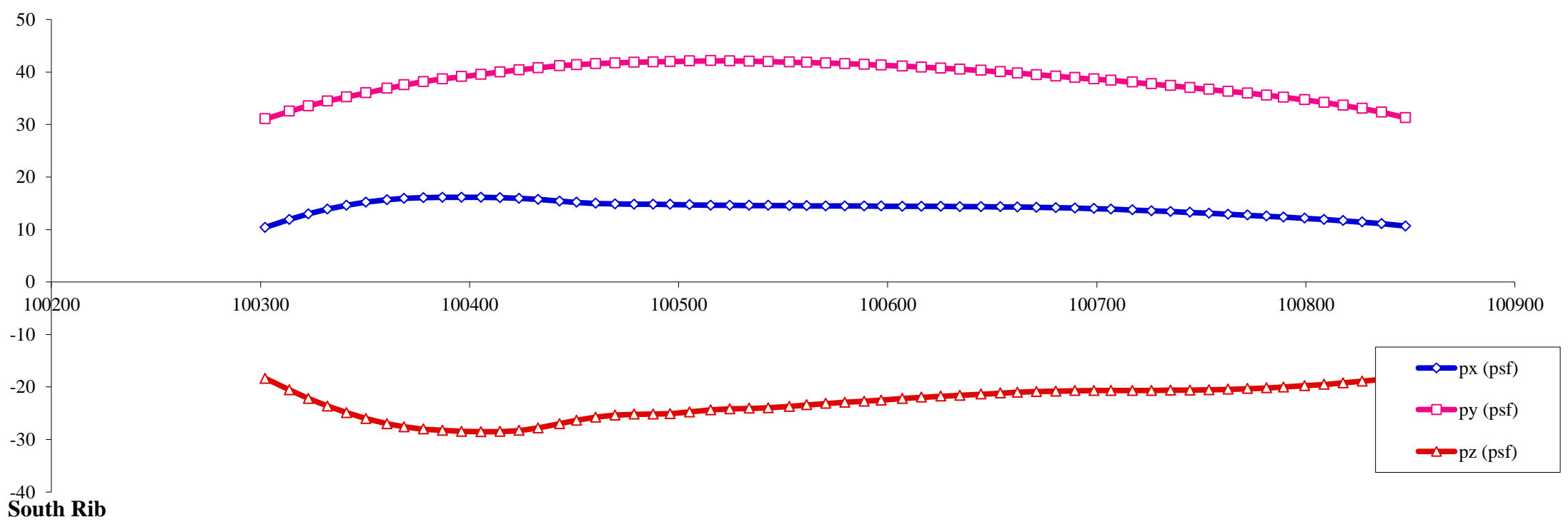
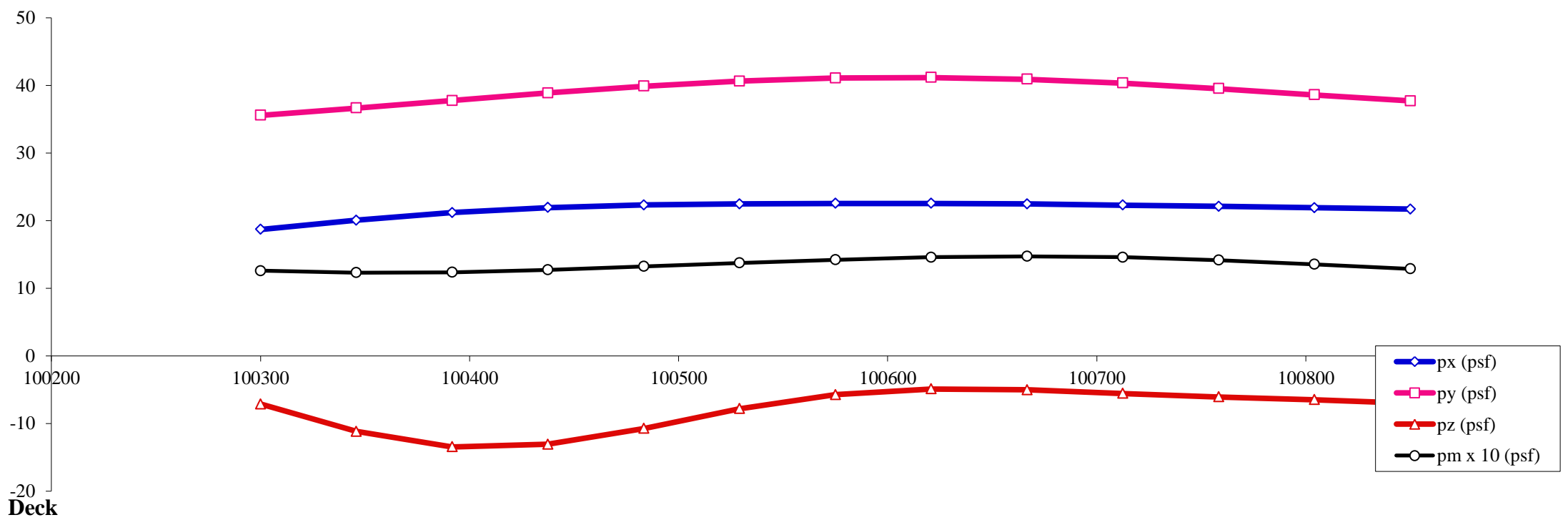
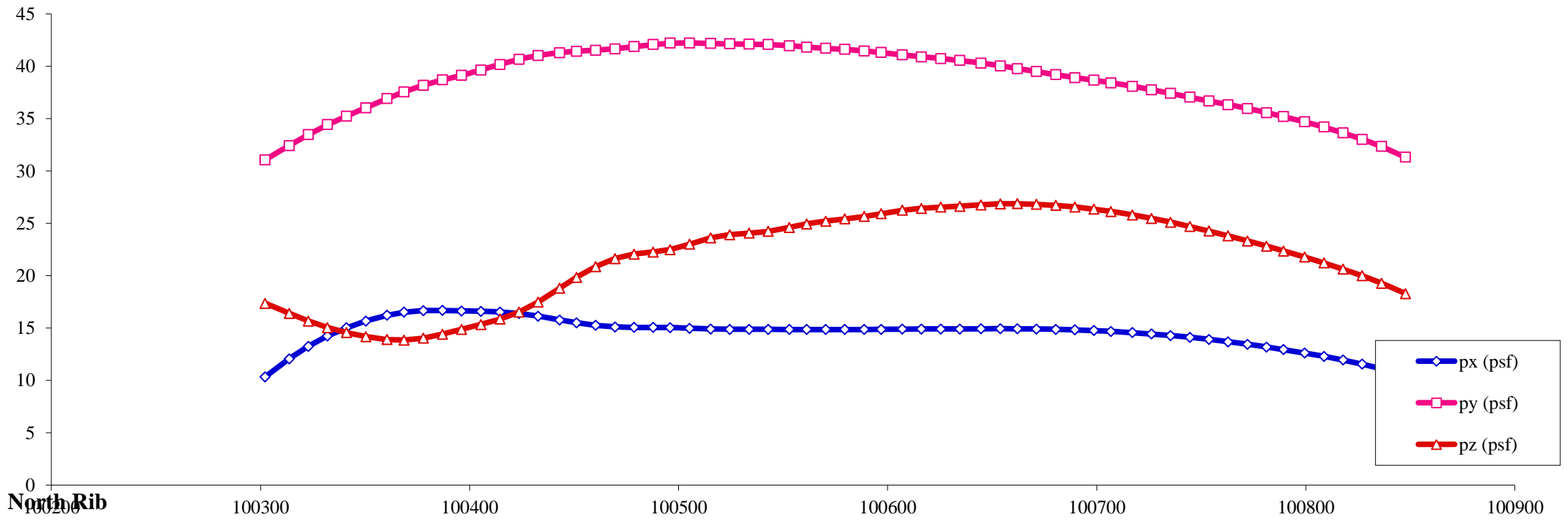
Load case : **24** Objective: Max uplift on arch ribs, differential between 1/4 and 3/4 span



- Notes:
1. All pressures in (psf)
 2. All coordinates/elevations in (ft)
 3. Loads for hangers, arch bracings, columns, pier caps and footings are not presented here

Load Visualization Page

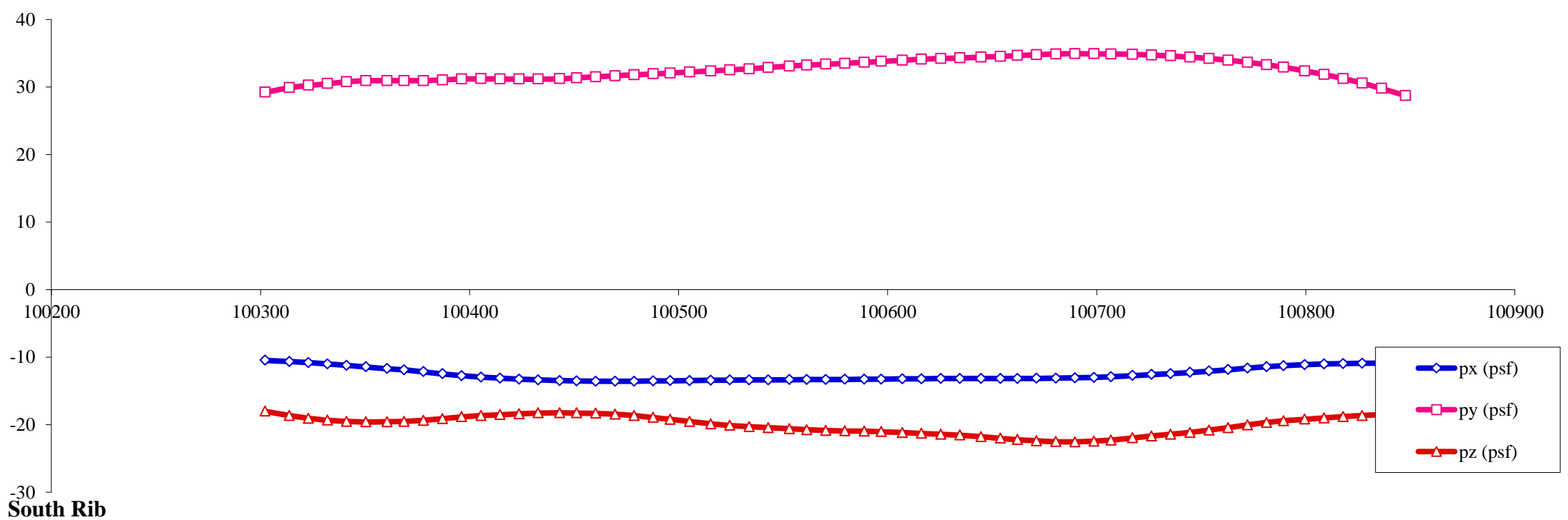
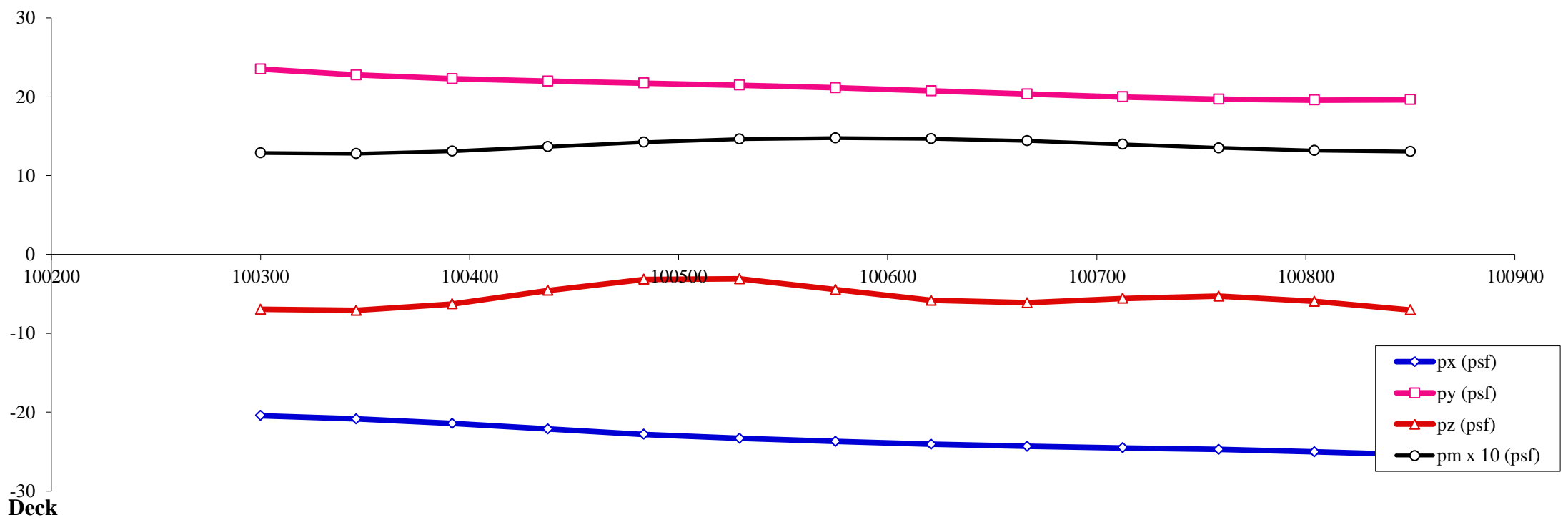
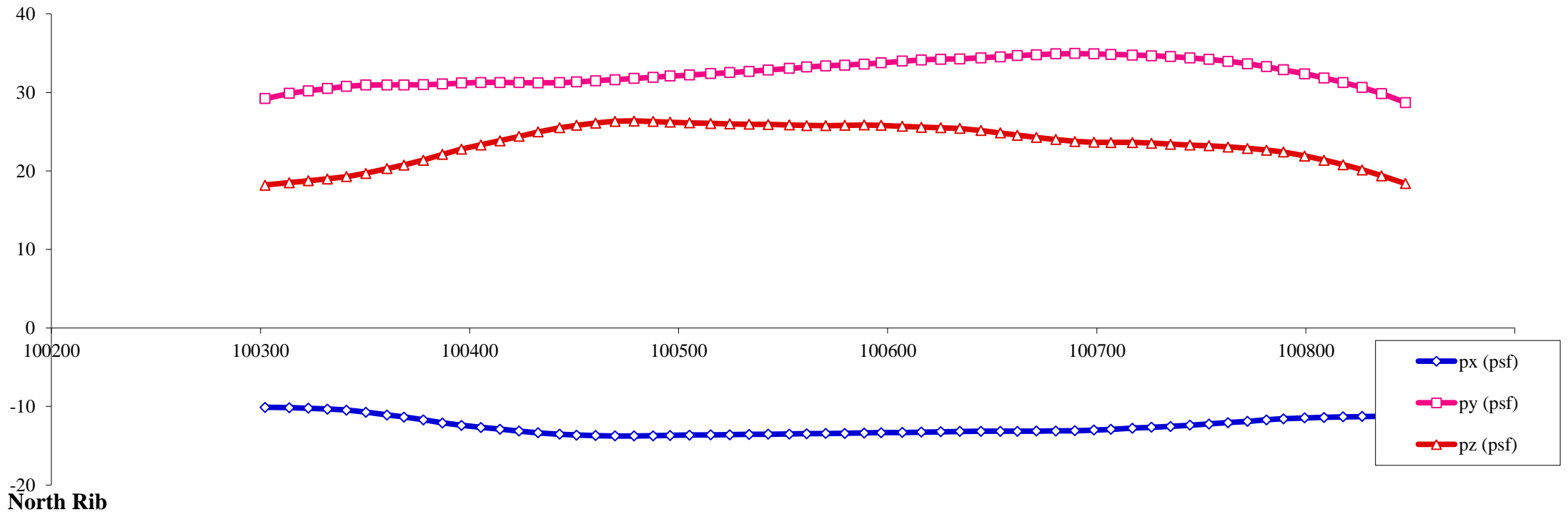
Load case : **25** Objective: Max positive longitudinal



- Notes:
1. All pressures in (psf)
 2. All coordinates/elevations in (ft)
 3. Loads for hangers, arch bracings, columns, pier caps and footings are not presented here

Load Visualization Page

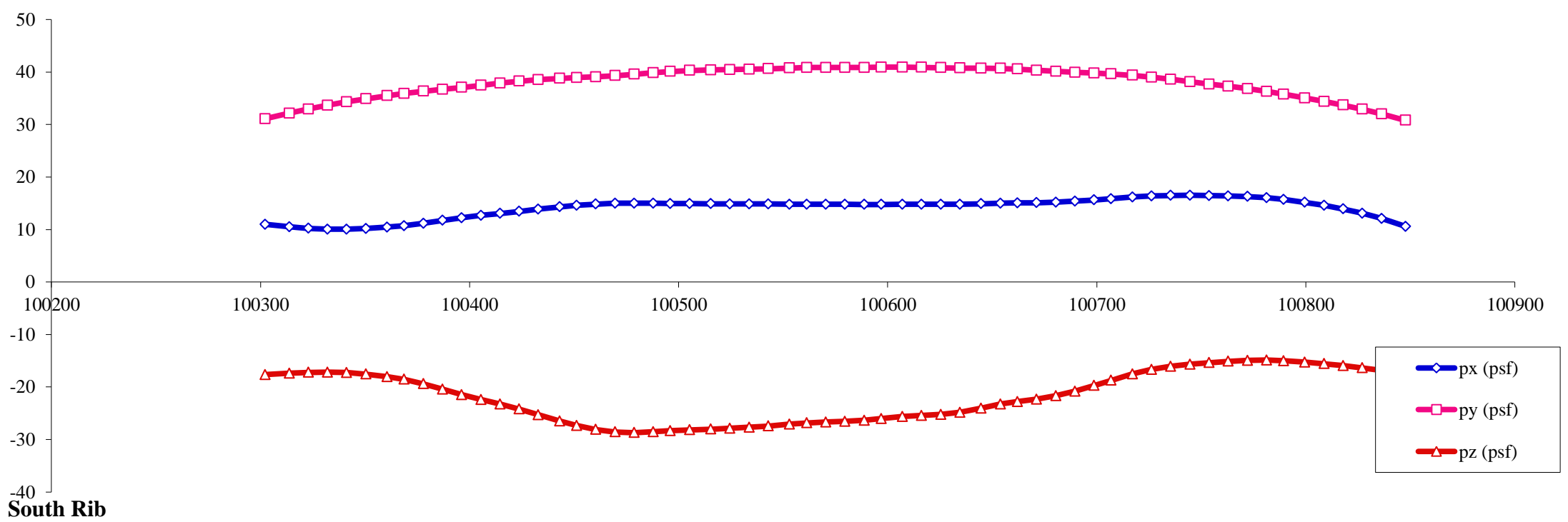
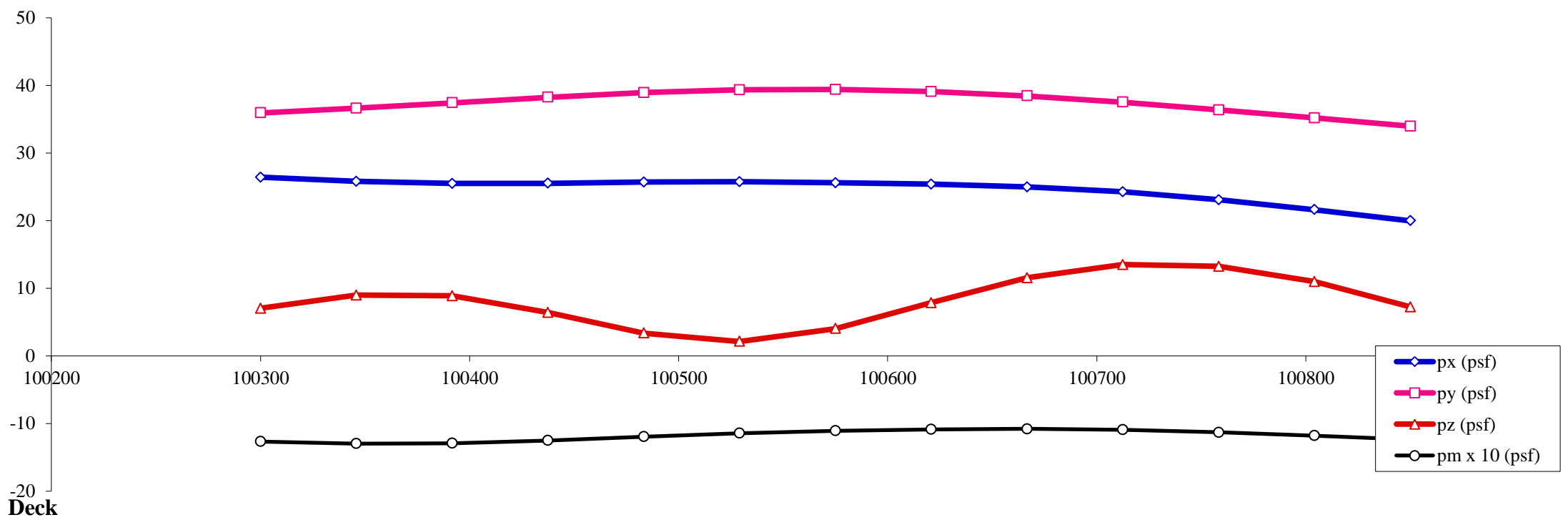
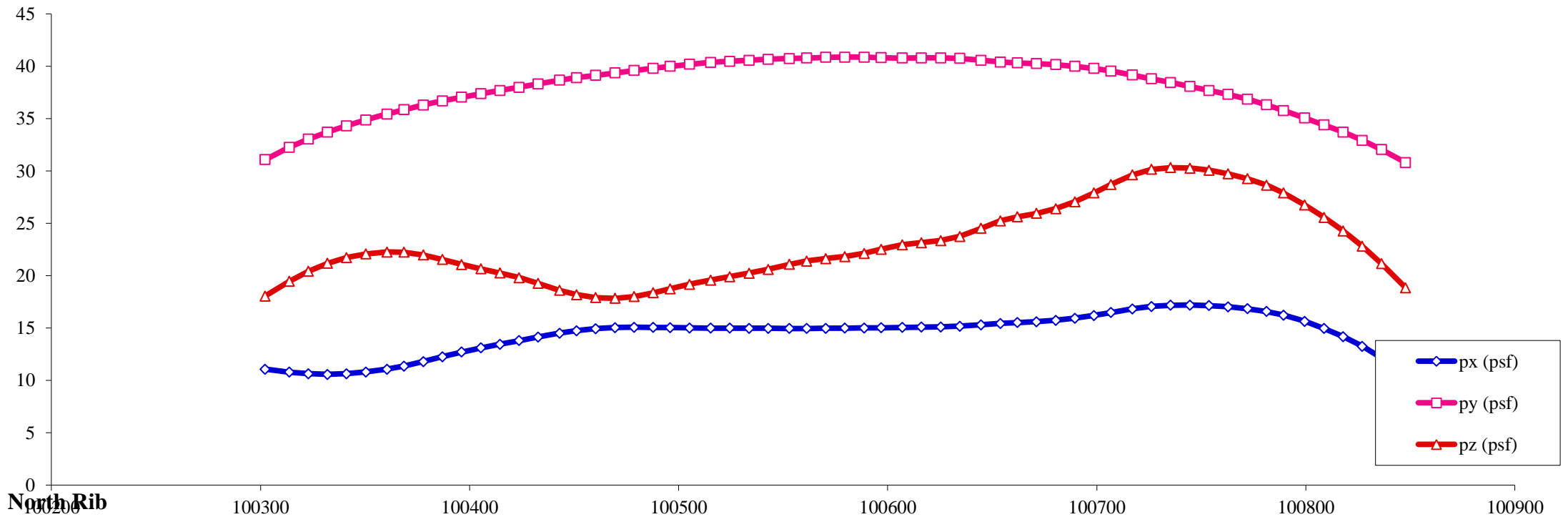
Load case : **26** Objective: Max negative longitudinal



- Notes:
1. All pressures in (psf)
 2. All coordinates/elevations in (ft)
 3. Loads for hangers, arch bracings, columns, pier caps and footings are not presented here

Load Visualization Page

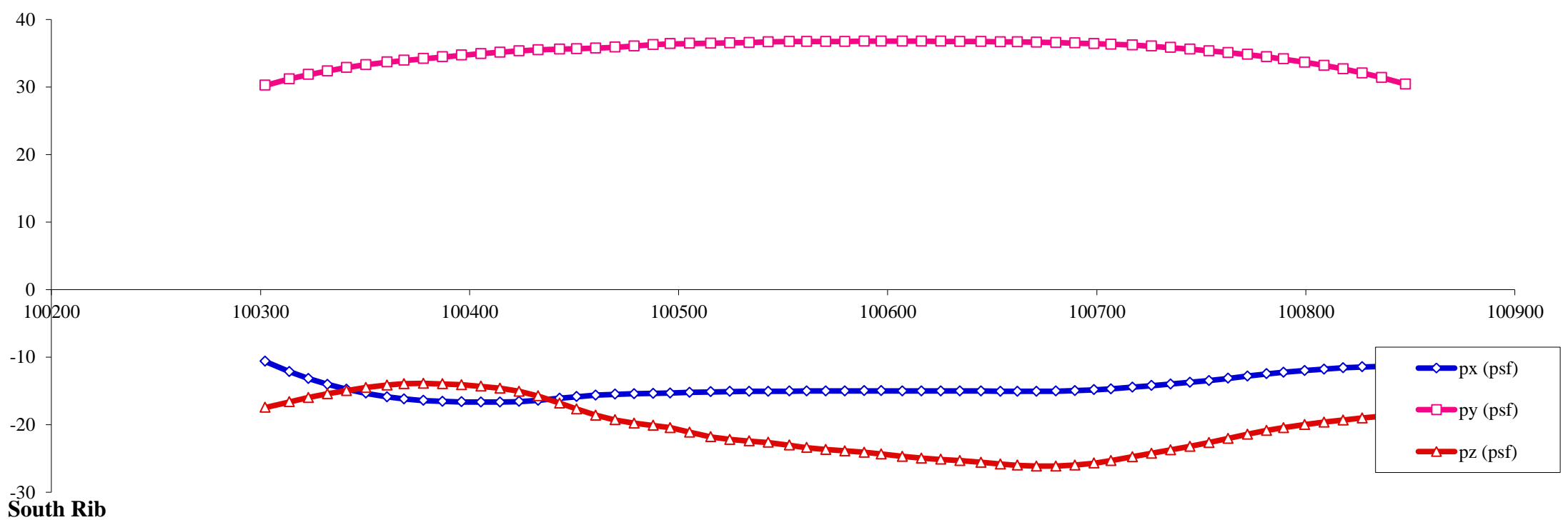
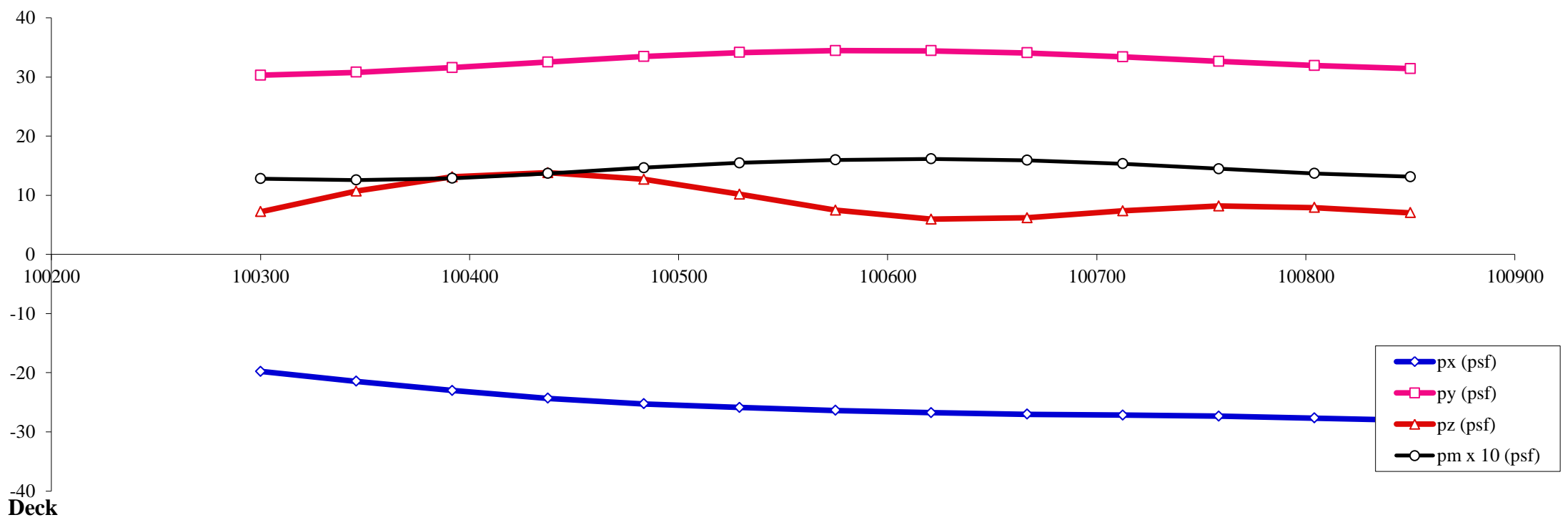
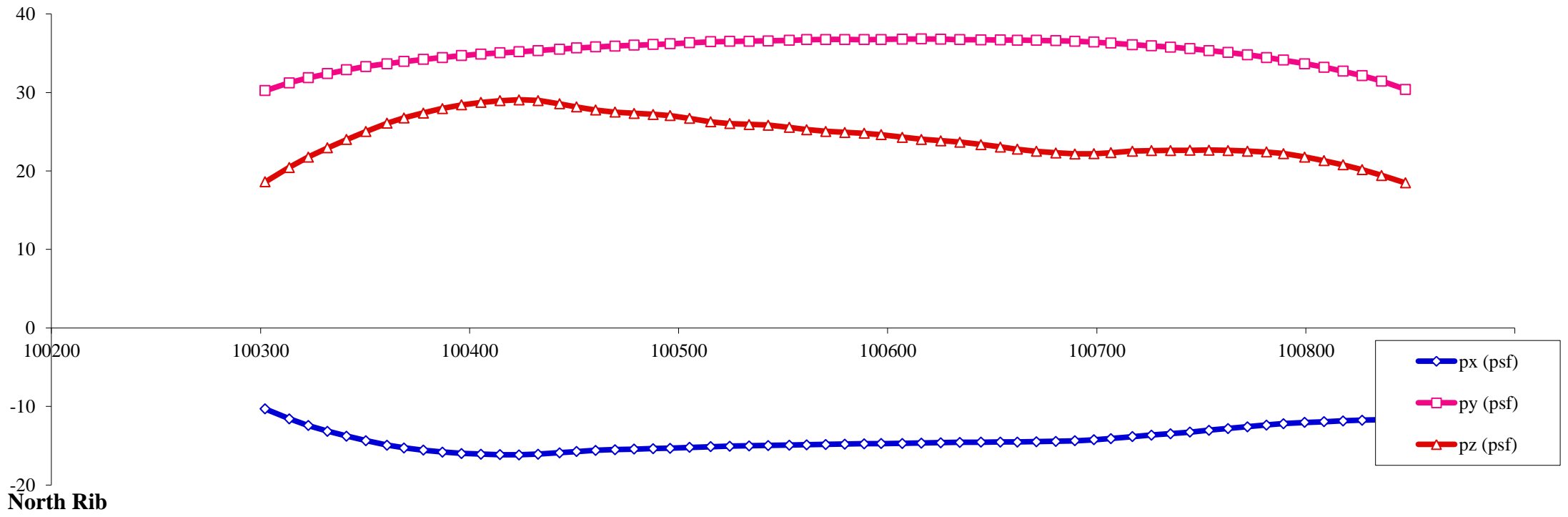
Load case : **27** Objective: Max positive longitudinal, differential between piers and deck



- Notes:
1. All pressures in (psf)
 2. All coordinates/elevations in (ft)
 3. Loads for hangers, arch bracings, columns, pier caps and footings are not presented here

Load Visualization Page

Load case : **28** Objective: Max positive longitudinal, differential between piers and deck



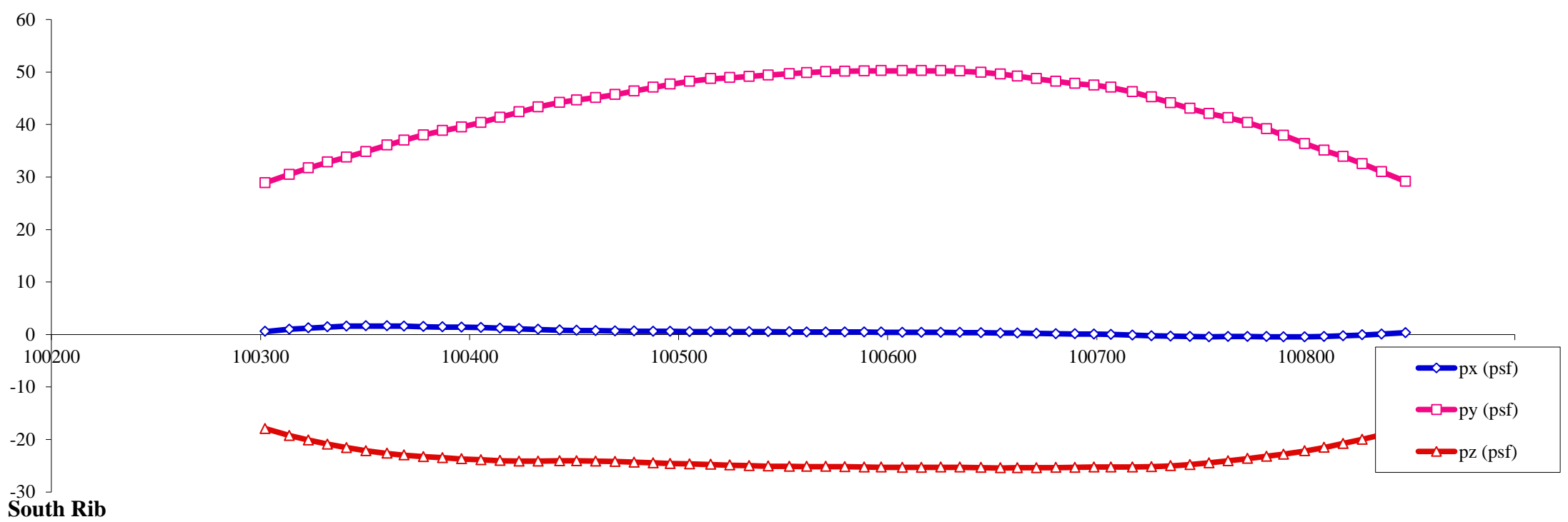
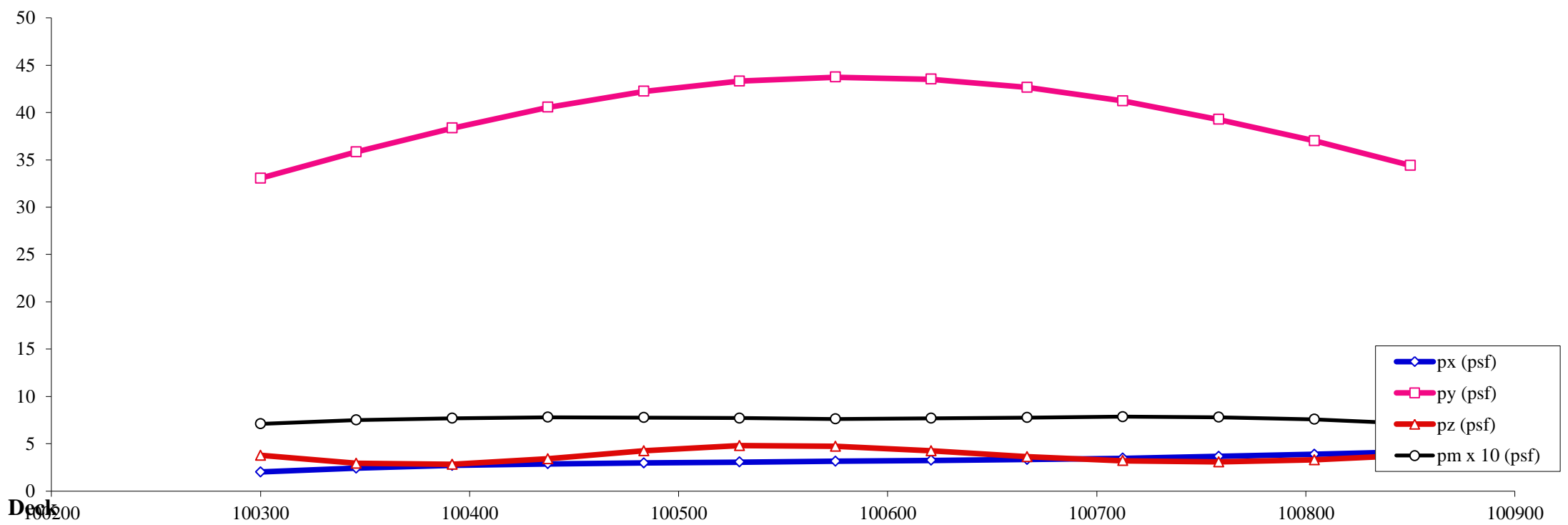
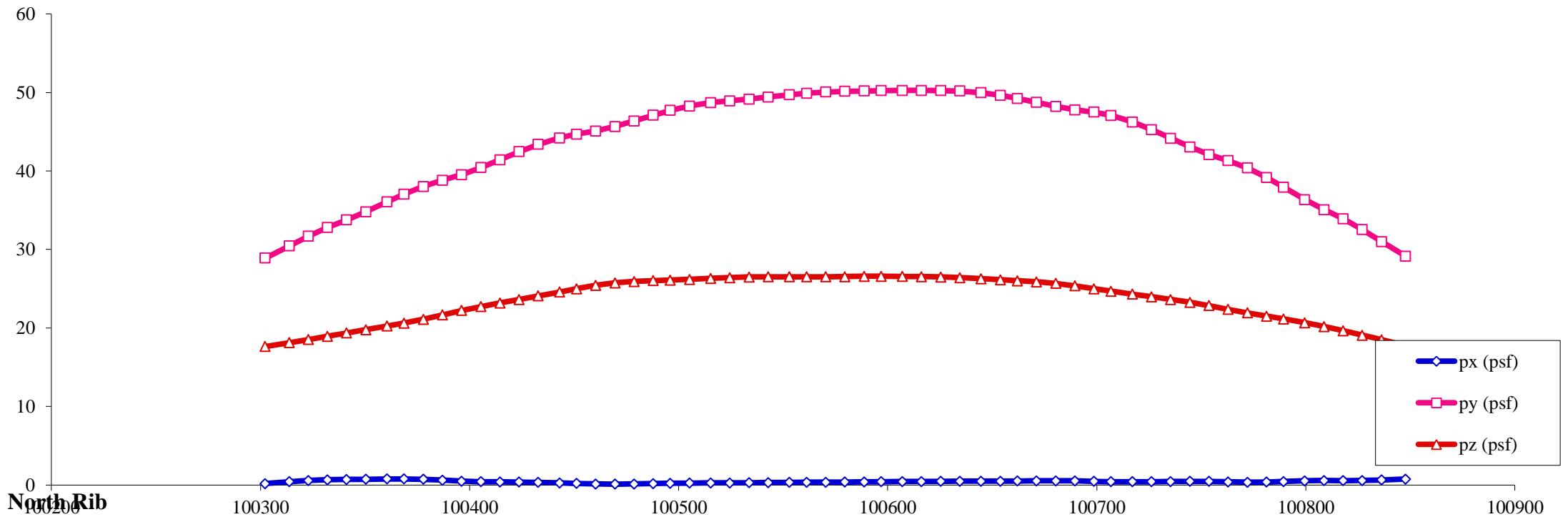
- Notes:
1. All pressures in (psf)
 2. All coordinates/elevations in (ft)
 3. Loads for hangers, arch bracings, columns, pier caps and footings are not presented here

APPENDIX C

100-Year Final Design Wind Loads

Load Visualization Page

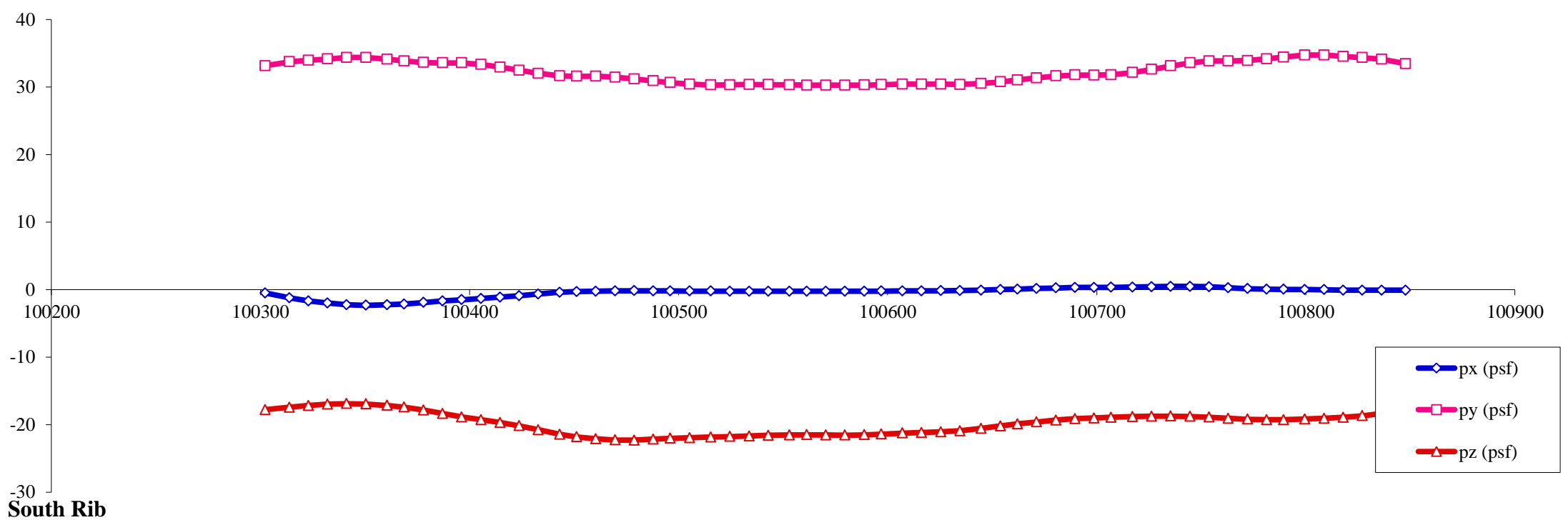
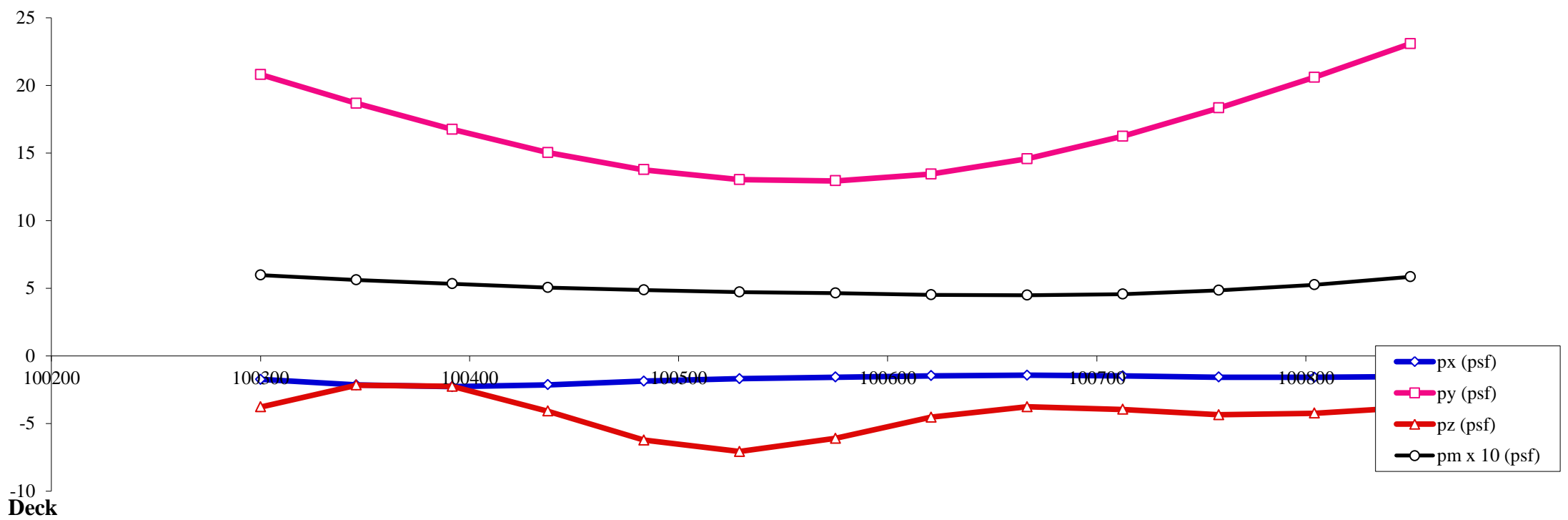
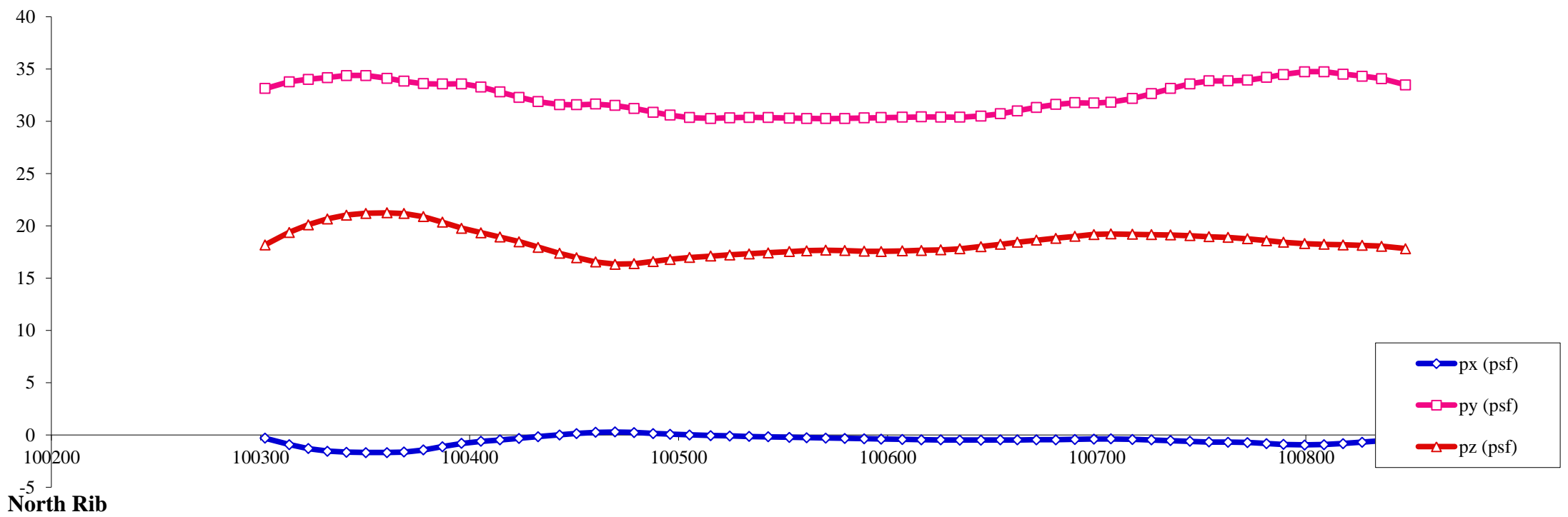
Load case : **1** Objective: Max lateral on deck, middle of the span



- Notes:**
1. All pressures in (psf)
 2. All coordinates/elevations in (ft)
 3. Loads for hangers, arch bracings, columns, pier caps and footings are not presented here

Load Visualization Page

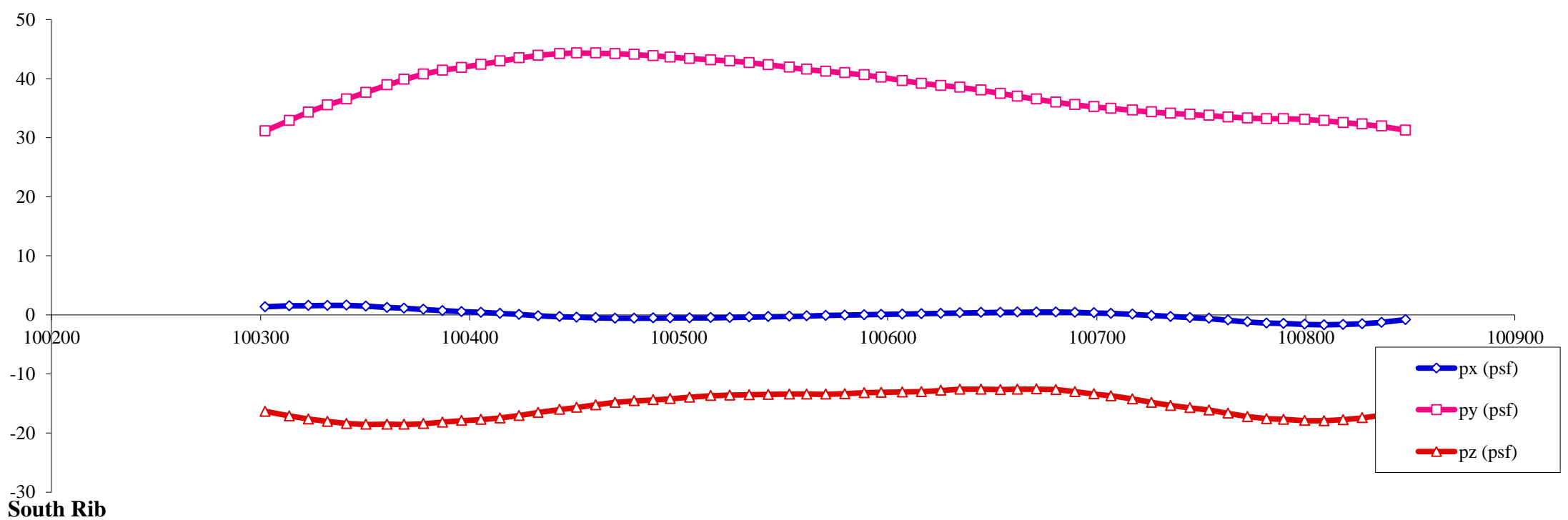
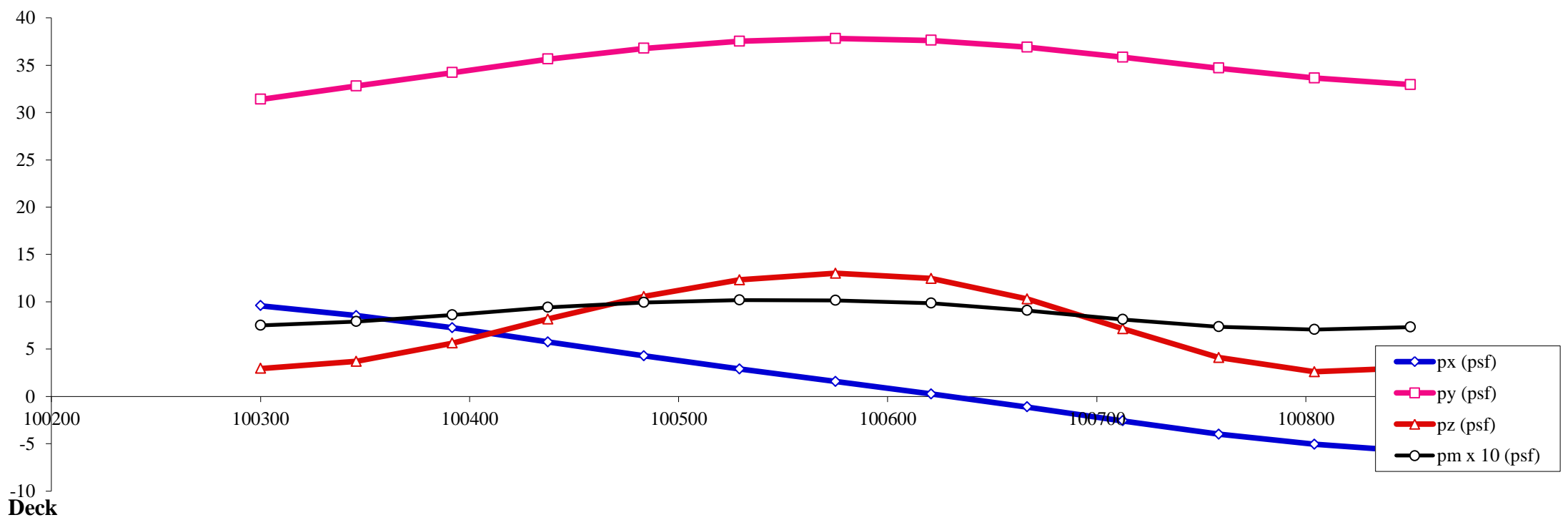
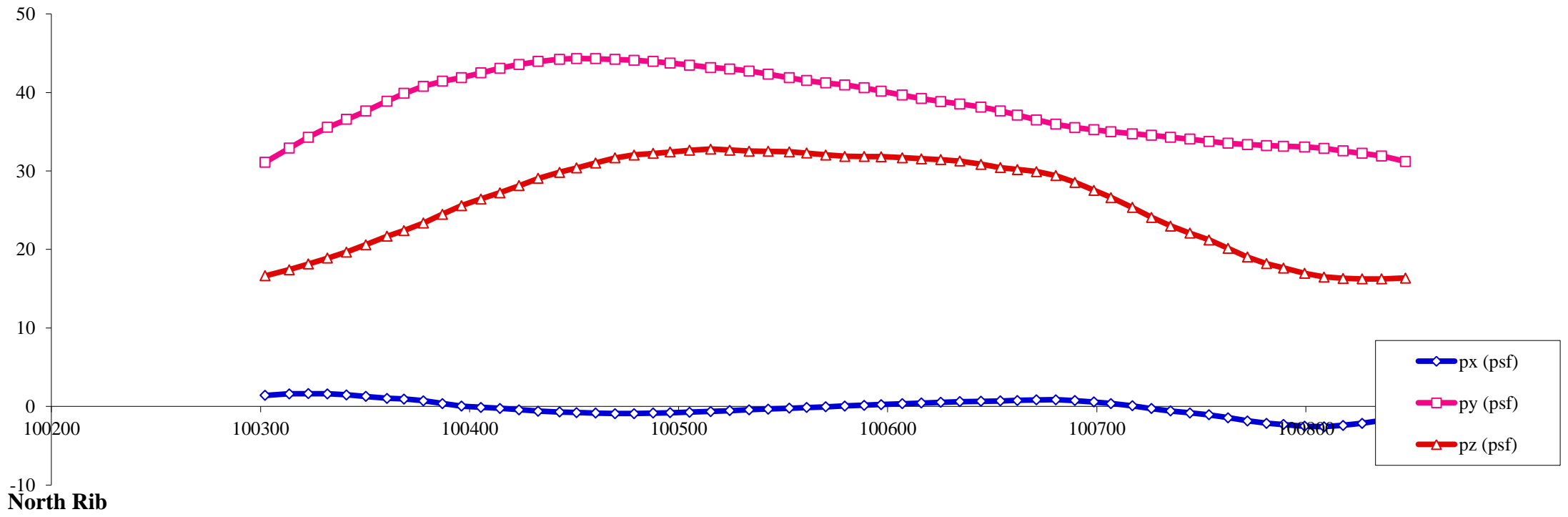
Load case : **2** Objective: Peak lateral with reversed dynamic component on deck, middle of the span



- Notes:
1. All pressures in (psf)
 2. All coordinates/elevations in (ft)
 3. Loads for hangers, arch bracings, columns, pier caps and footings are not presented here

Load Visualization Page

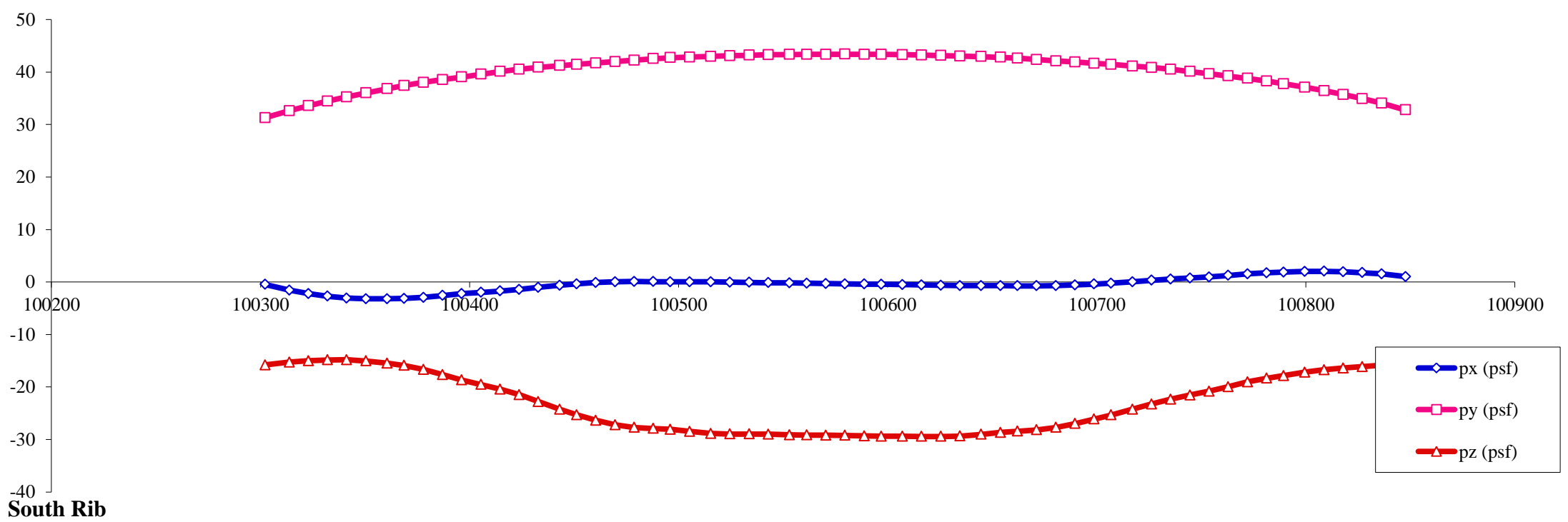
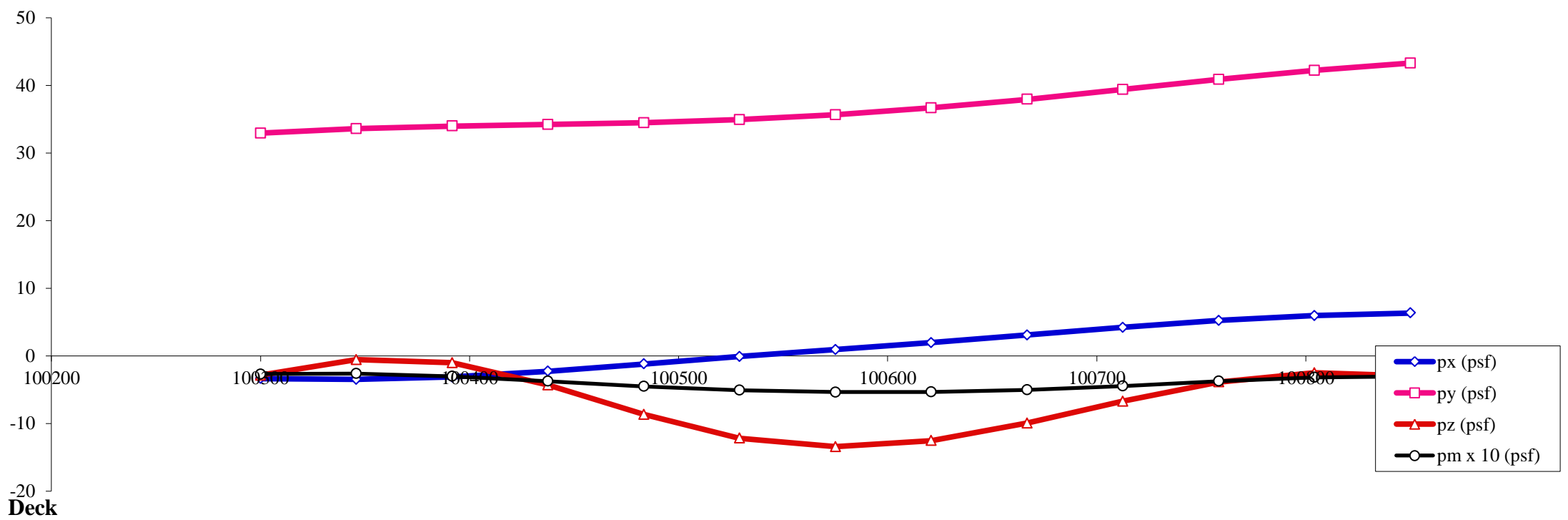
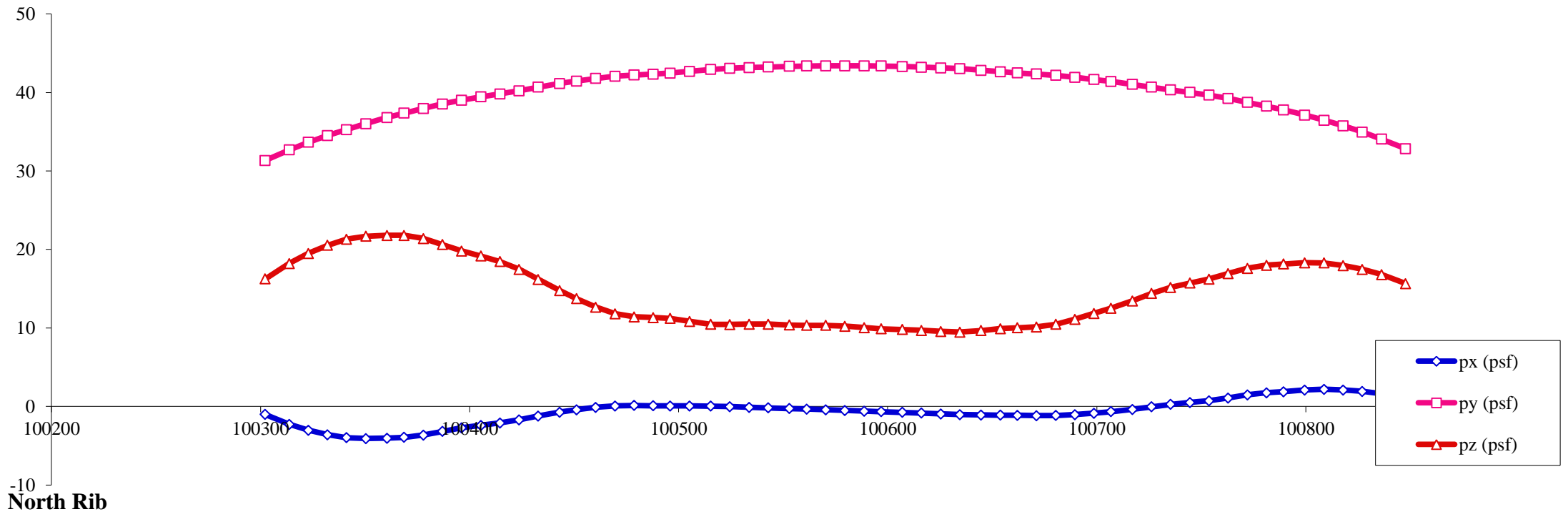
Load case : **3** Objective: Max uplift on deck, middle of the span



- Notes:
1. All pressures in (psf)
 2. All coordinates/elevations in (ft)
 3. Loads for hangers, arch bracings, columns, pier caps and footings are not presented here

Load Visualization Page

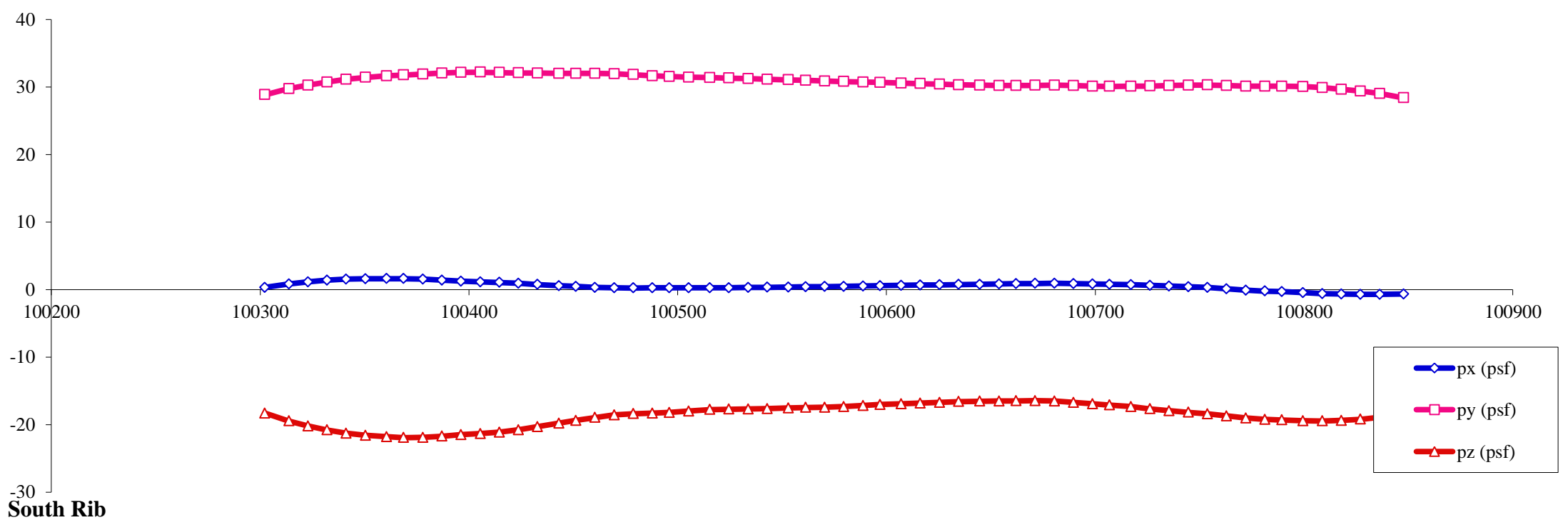
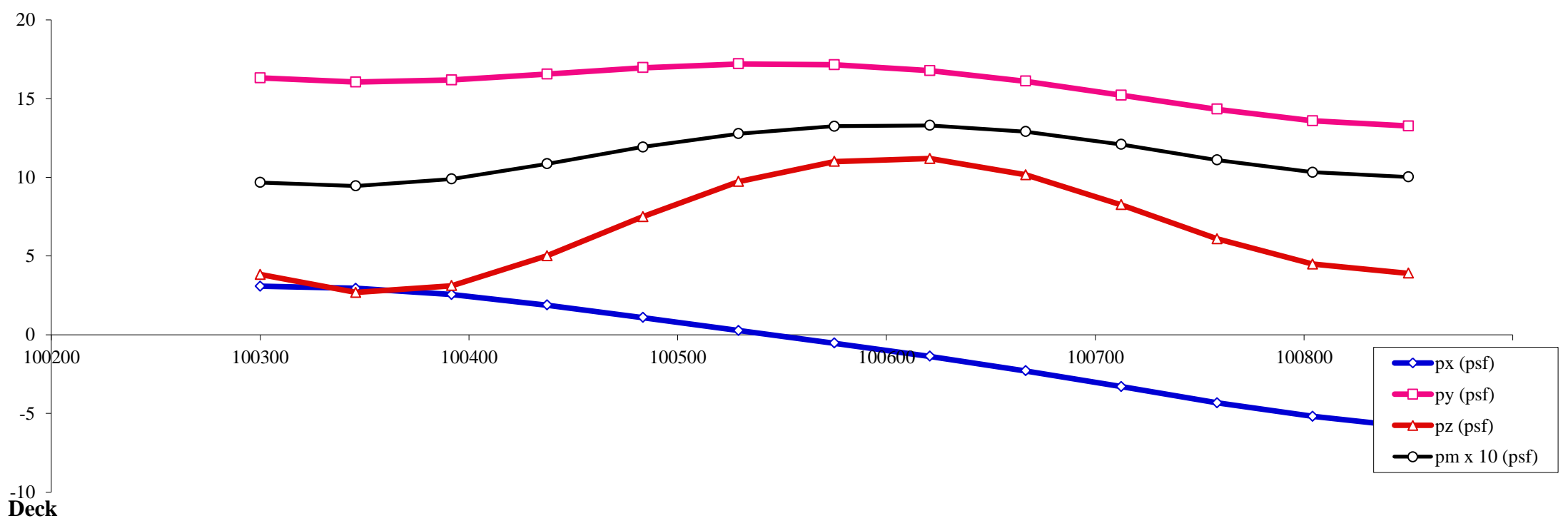
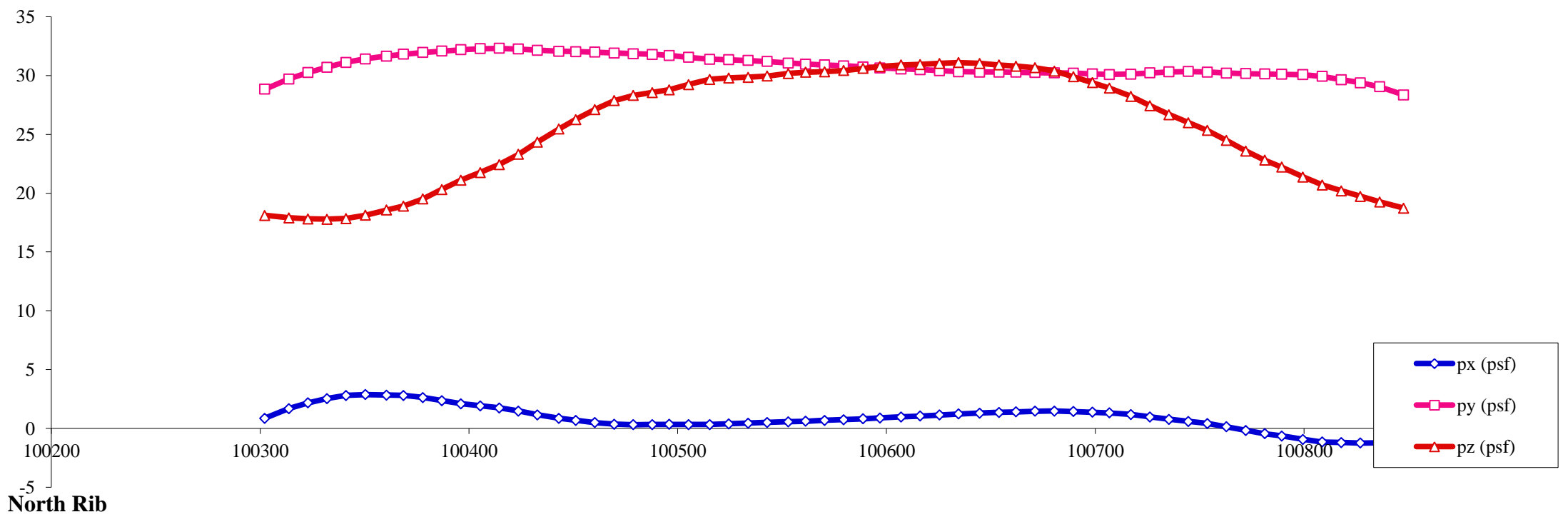
Load case : **4** Objective: Max down force on deck, middle of the span



- Notes:
1. All pressures in (psf)
 2. All coordinates/elevations in (ft)
 3. Loads for hangers, arch bracings, columns, pier caps and footings are not presented here

Load Visualization Page

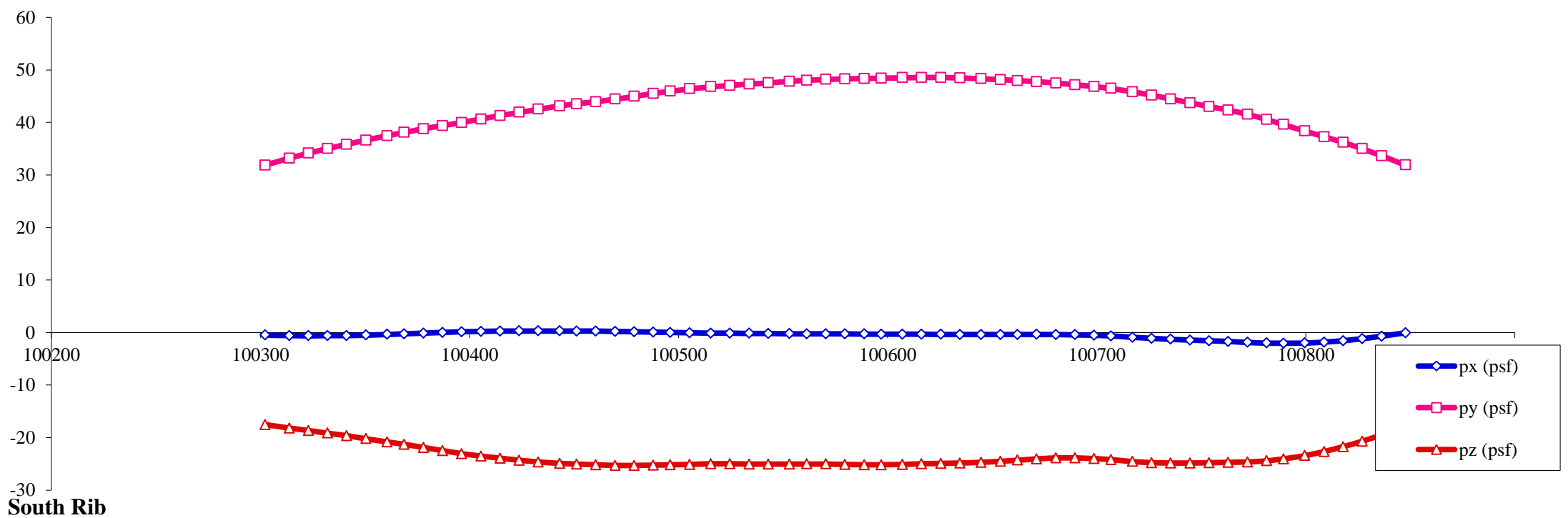
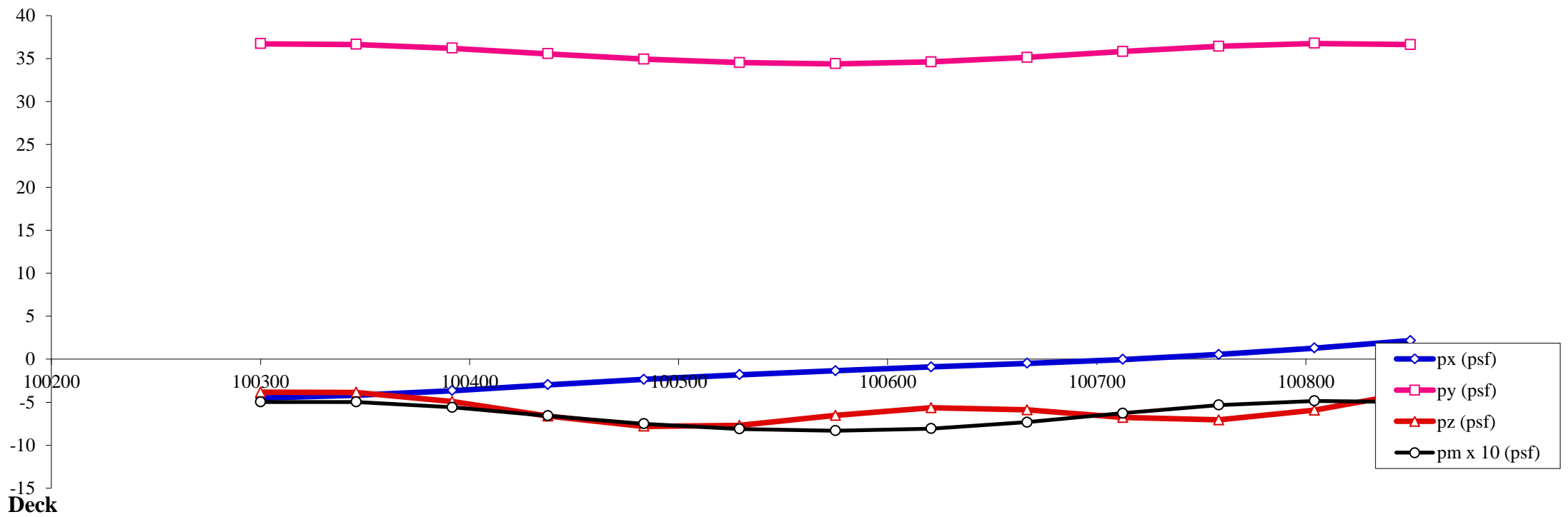
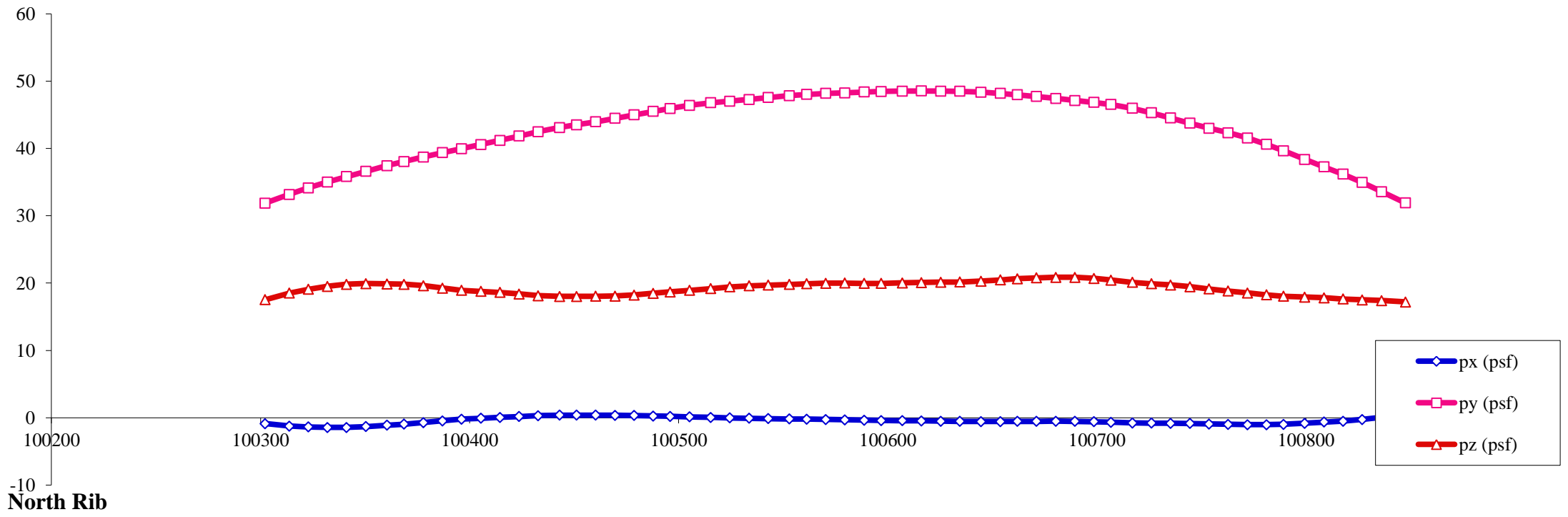
Load case : **5** Objective: Max positive moment on deck, middle of the span



- Notes:
1. All pressures in (psf)
 2. All coordinates/elevations in (ft)
 3. Loads for hangers, arch bracings, columns, pier caps and footings are not presented here

Load Visualization Page

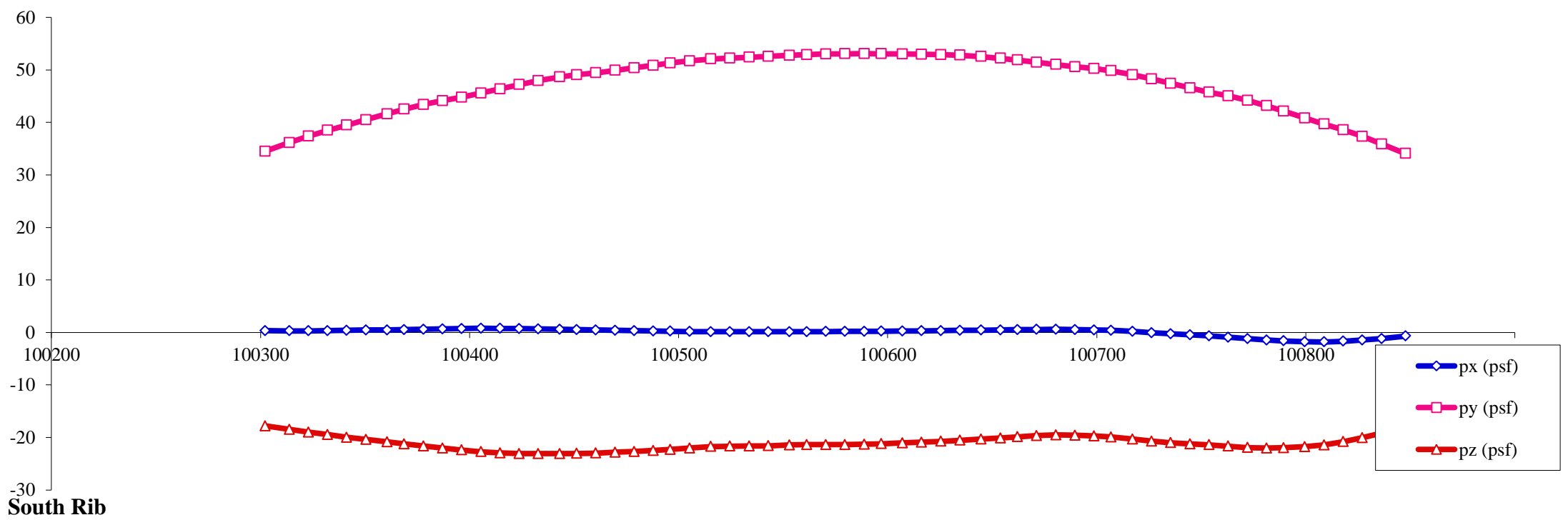
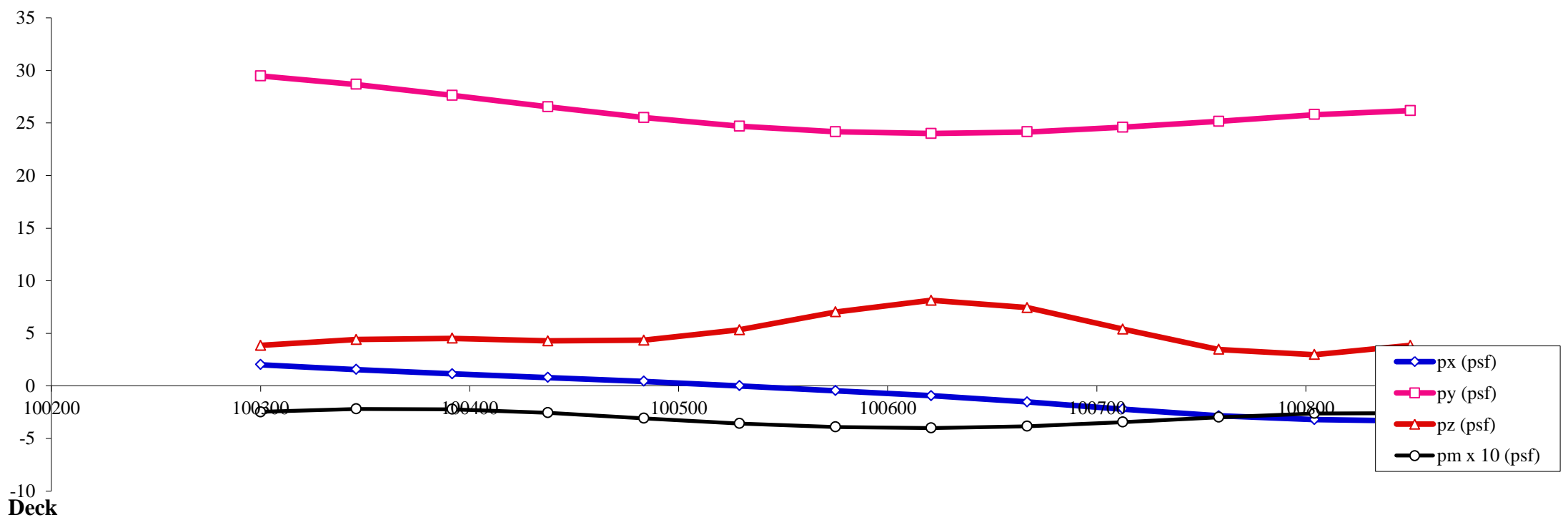
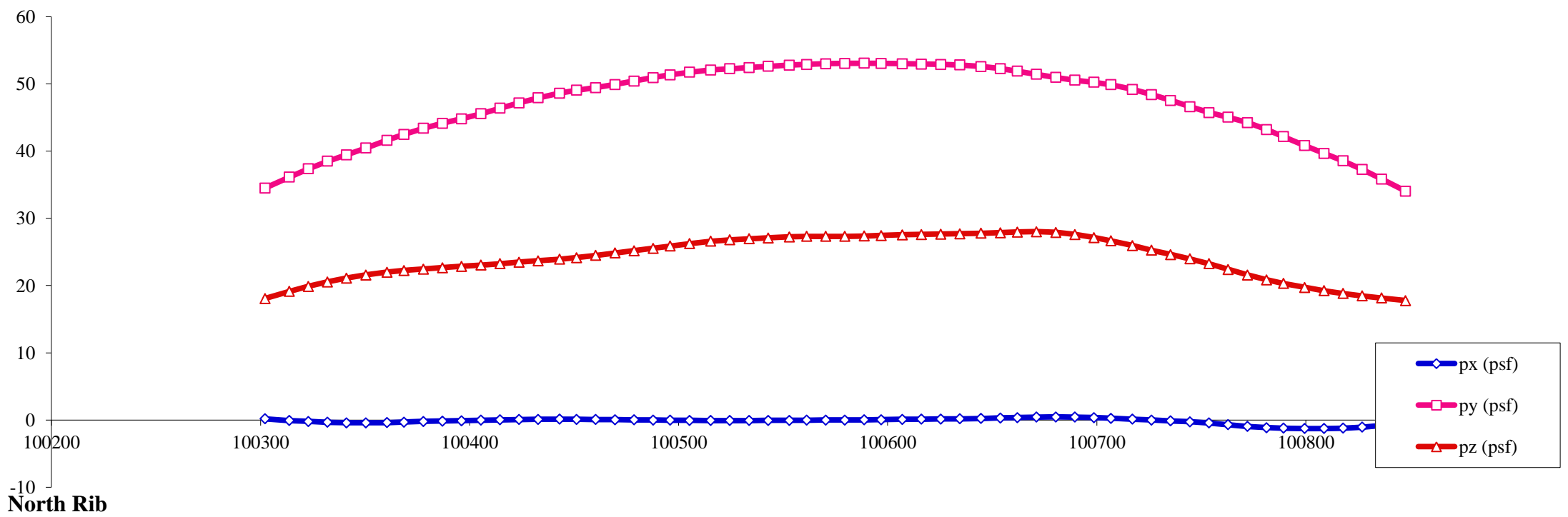
Load case : **6** Objective: Max negative moment on deck, middle of the span



- Notes:
1. All pressures in (psf)
 2. All coordinates/elevations in (ft)
 3. Loads for hangers, arch bracings, columns, pier caps and footings are not presented here

Load Visualization Page

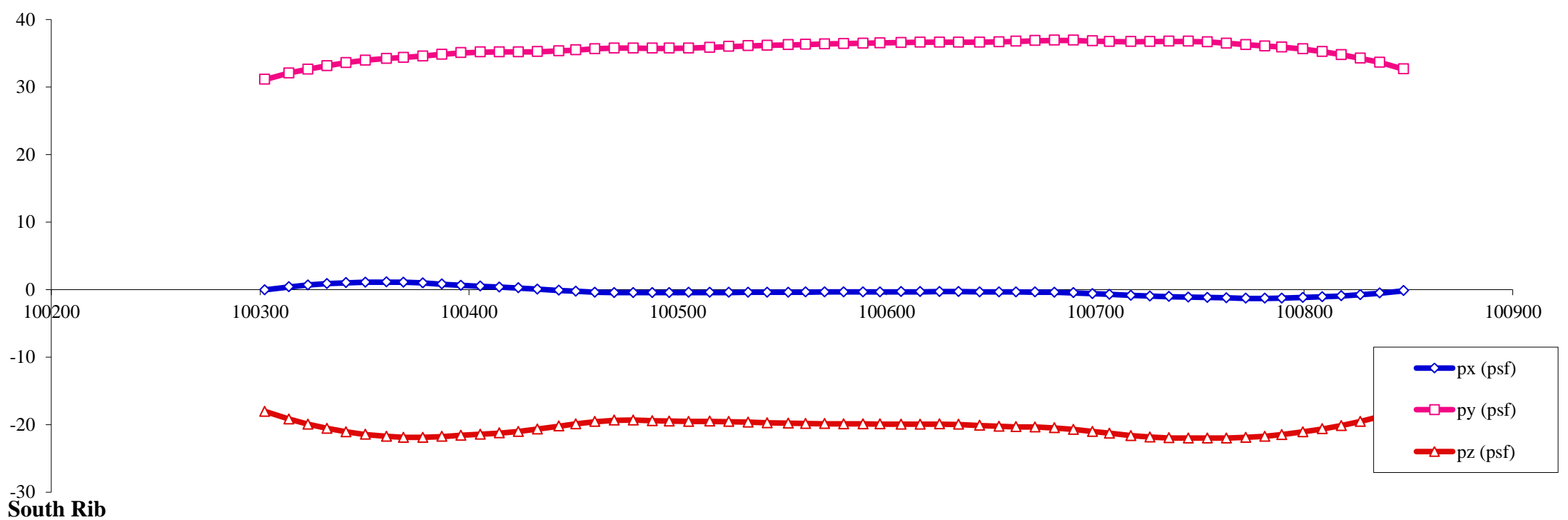
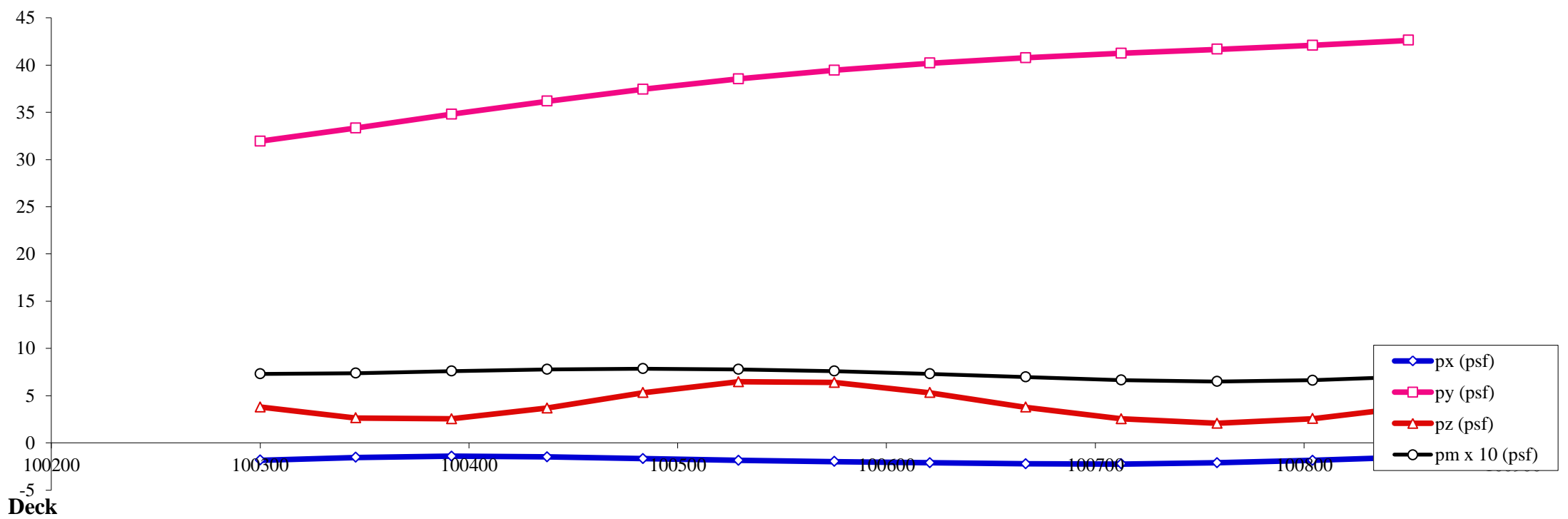
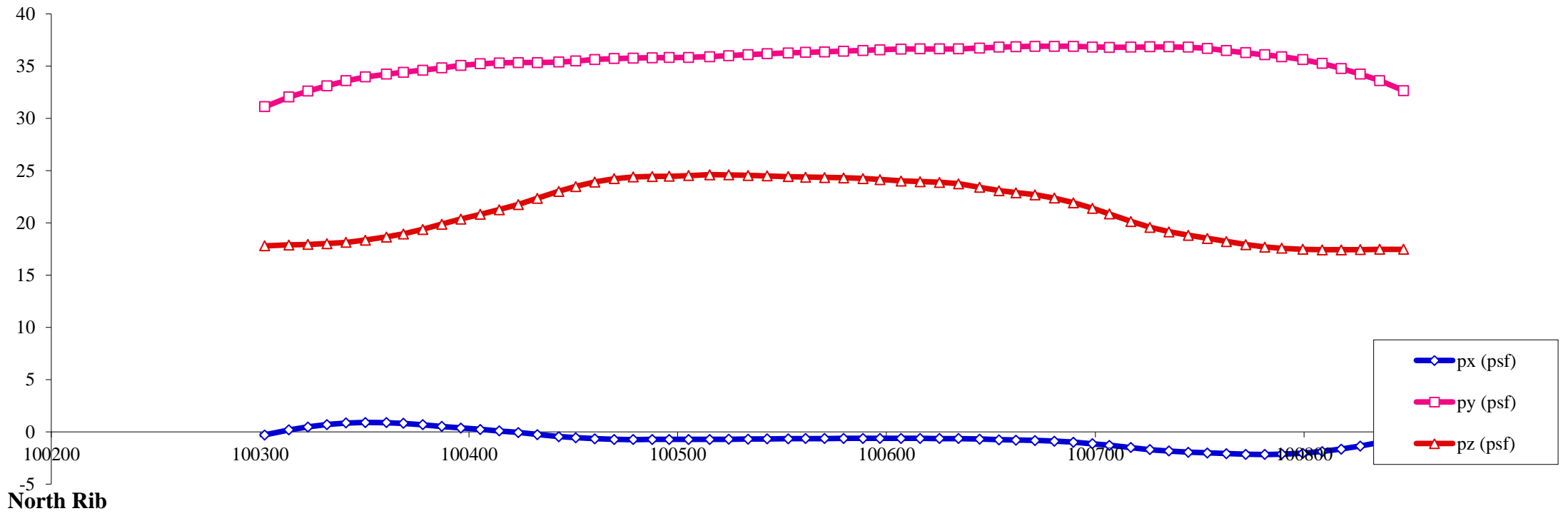
Load case : **7** Objective: Max lateral, middle of the span, differential between deck and arch



- Notes:**
1. All pressures in (psf)
 2. All coordinates/elevations in (ft)
 3. Loads for hangers, arch bracings, columns, pier caps and footings are not presented here

Load Visualization Page

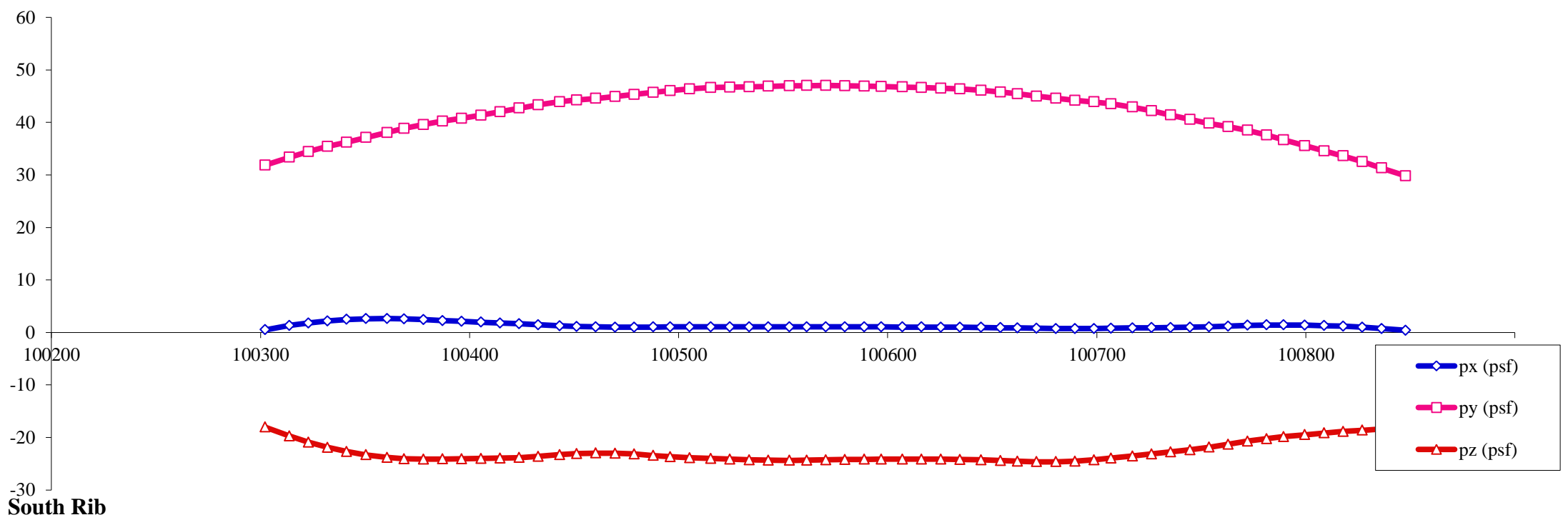
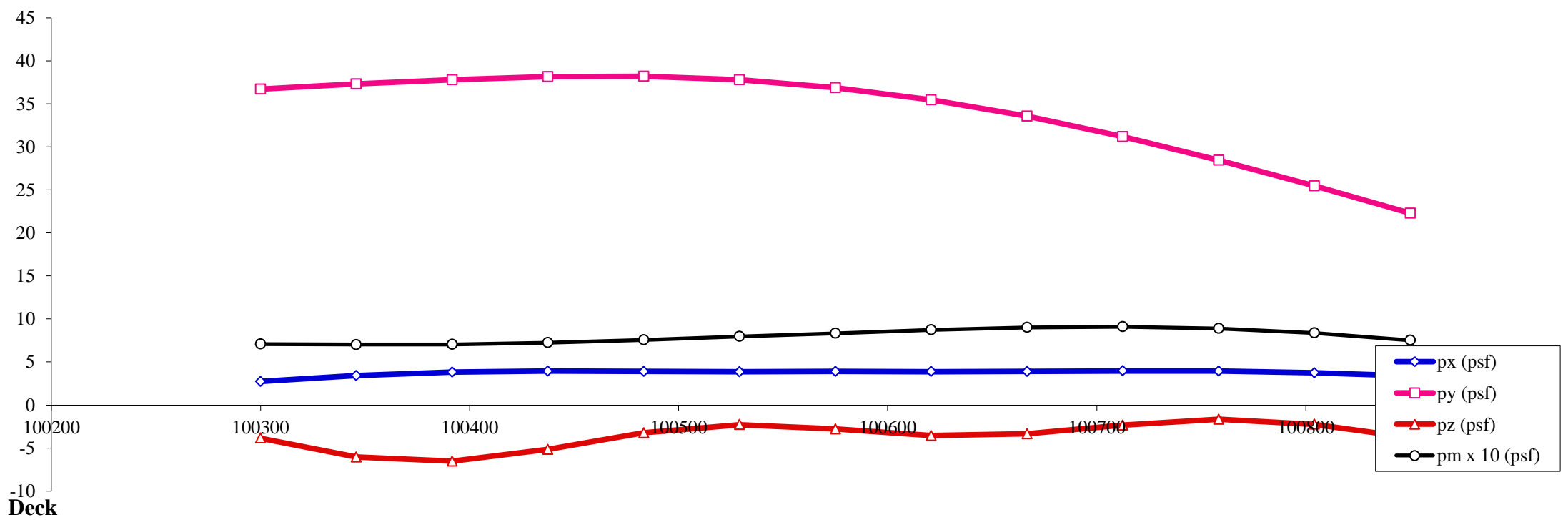
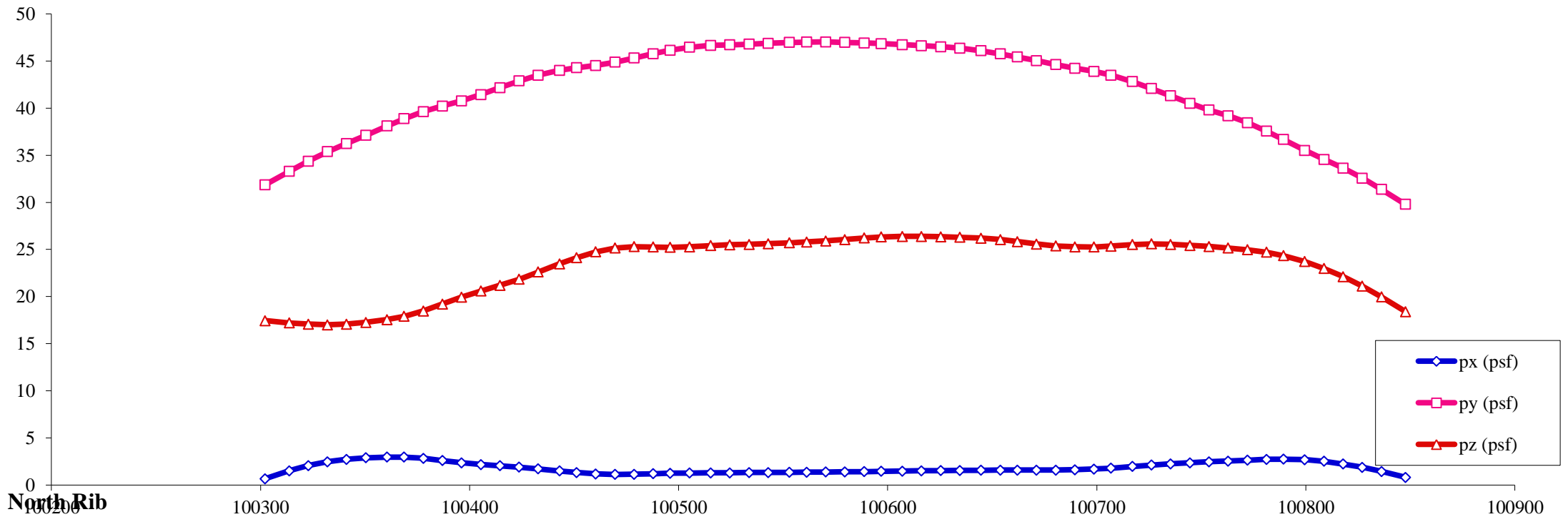
Load case : **8** Objective: Max lateral, middle of the span, differential between deck and arch



- Notes:
1. All pressures in (psf)
 2. All coordinates/elevations in (ft)
 3. Loads for hangers, arch bracings, columns, pier caps and footings are not presented here

Load Visualization Page

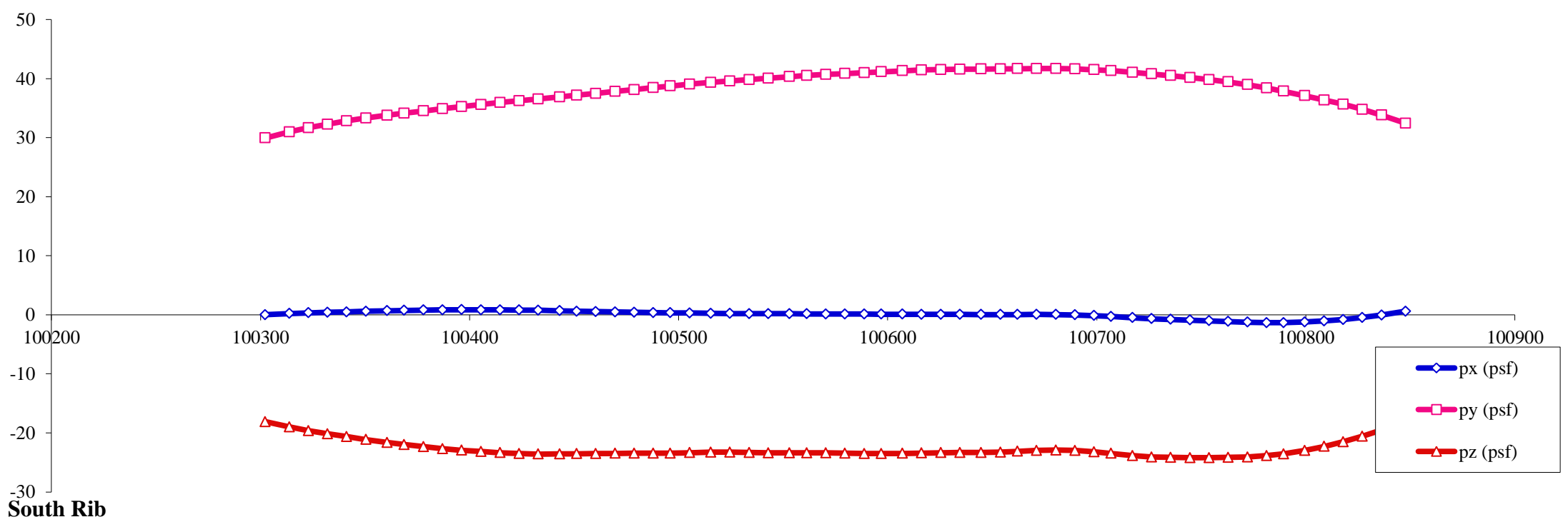
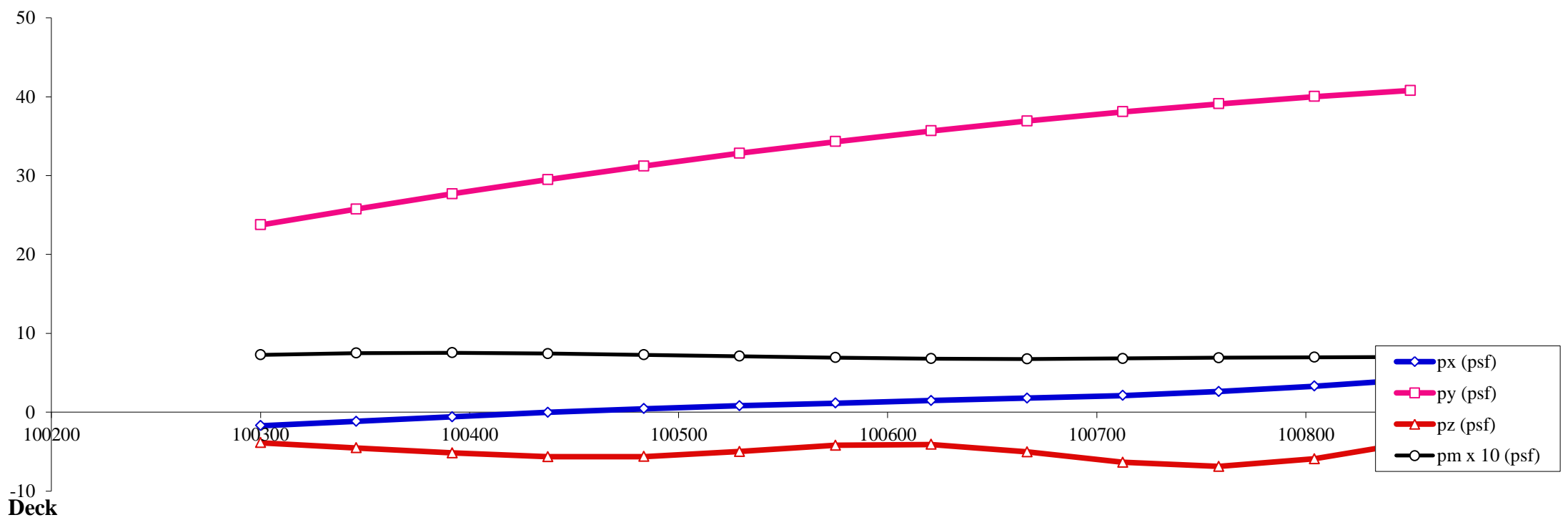
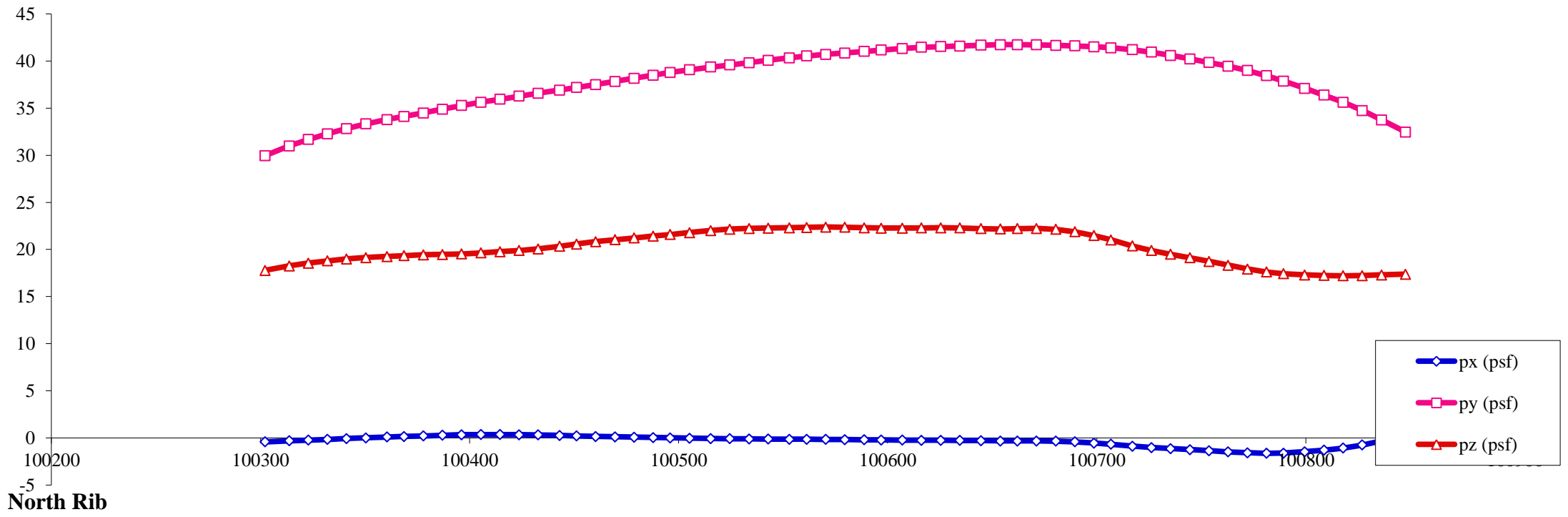
Load case : **9** Objective: Max lateral on deck, differential between 1/4 and 3/4 span



- Notes:
1. All pressures in (psf)
 2. All coordinates/elevations in (ft)
 3. Loads for hangers, arch bracings, columns, pier caps and footings are not presented here

Load Visualization Page

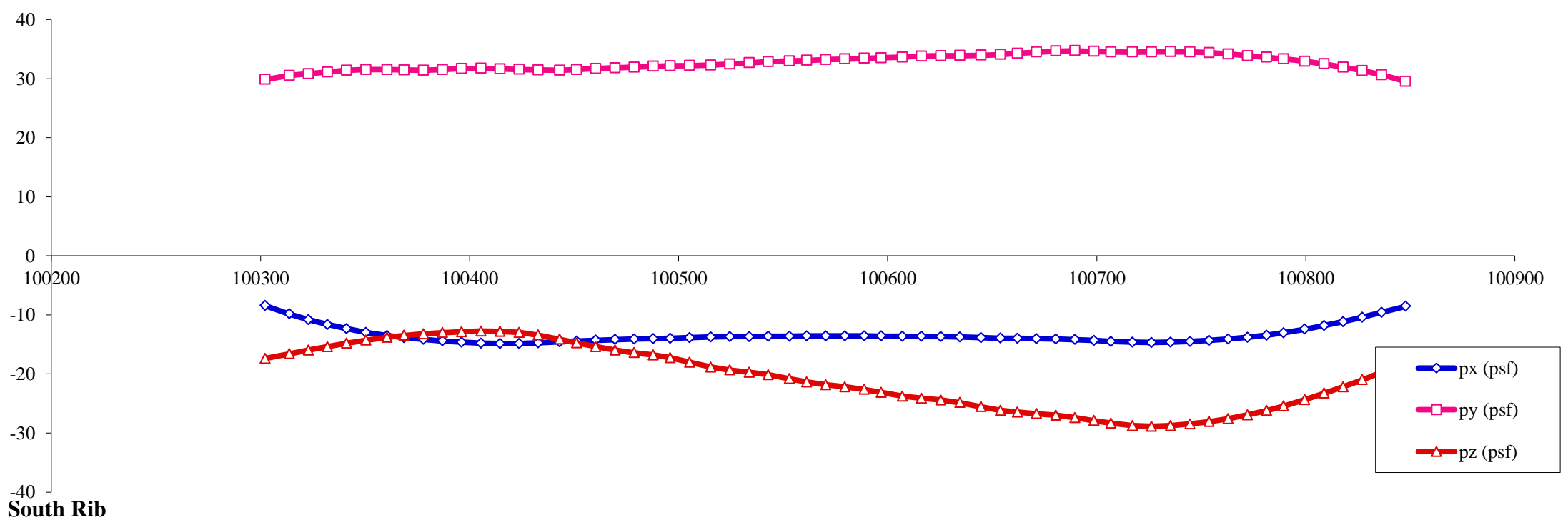
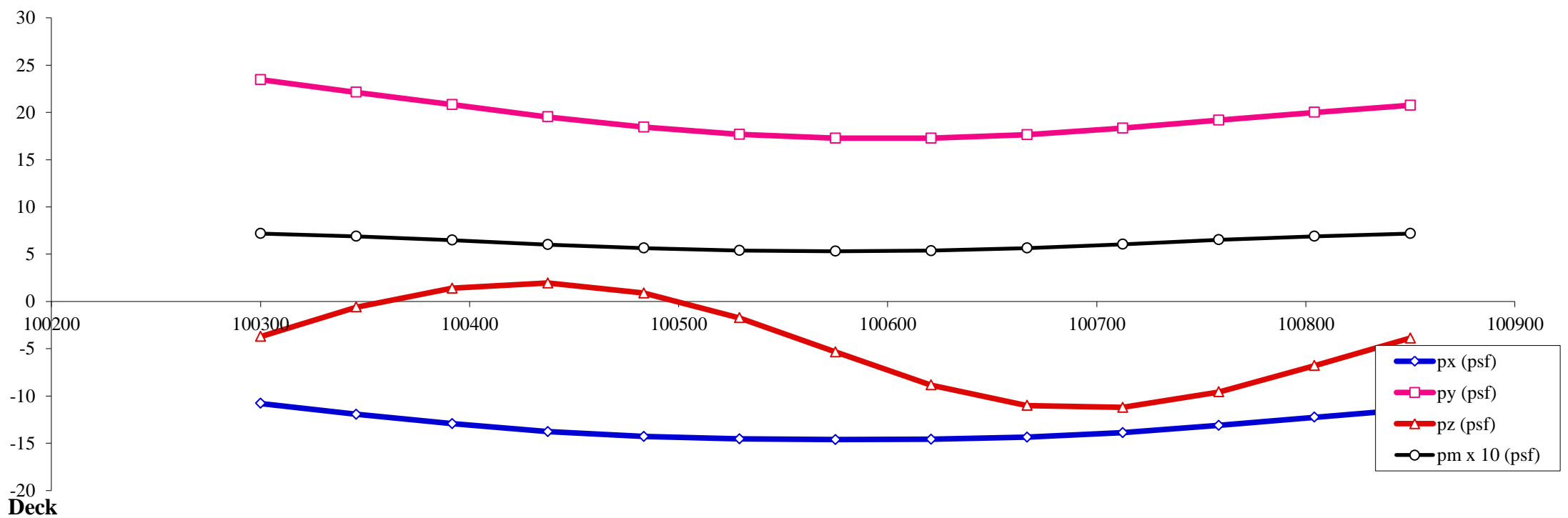
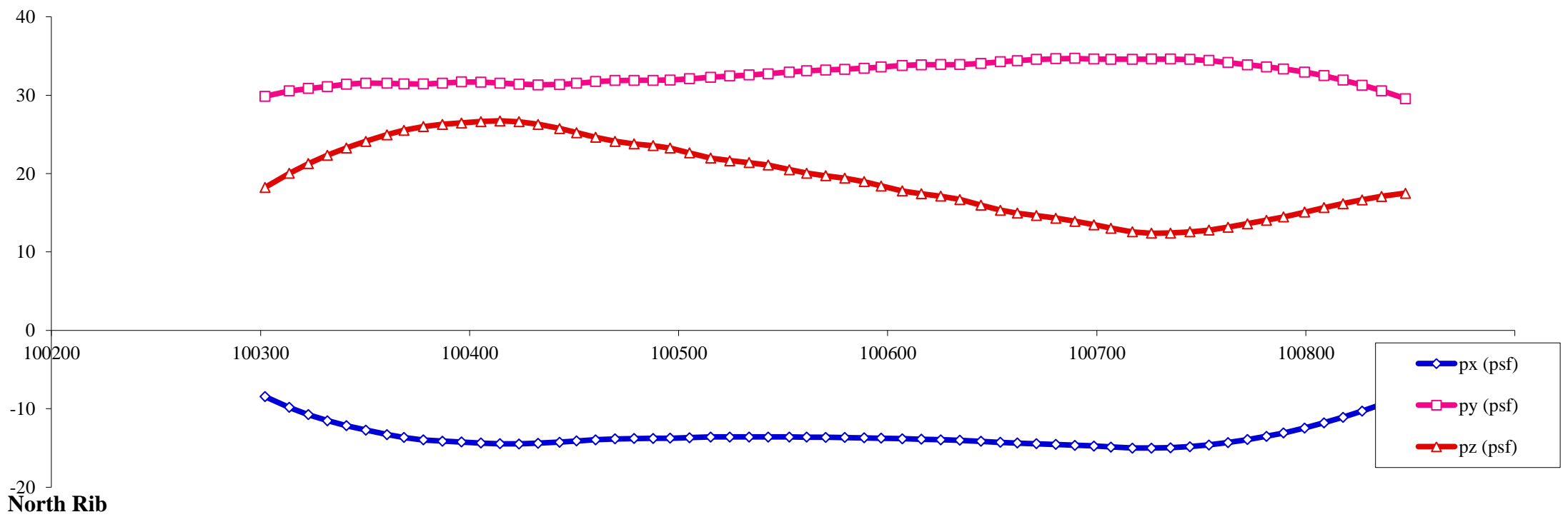
Load case : **10** Objective: Max lateral on deck, differential between 1/4 and 3/4 span



- Notes:
1. All pressures in (psf)
 2. All coordinates/elevations in (ft)
 3. Loads for hangers, arch bracings, columns, pier caps and footings are not presented here

Load Visualization Page

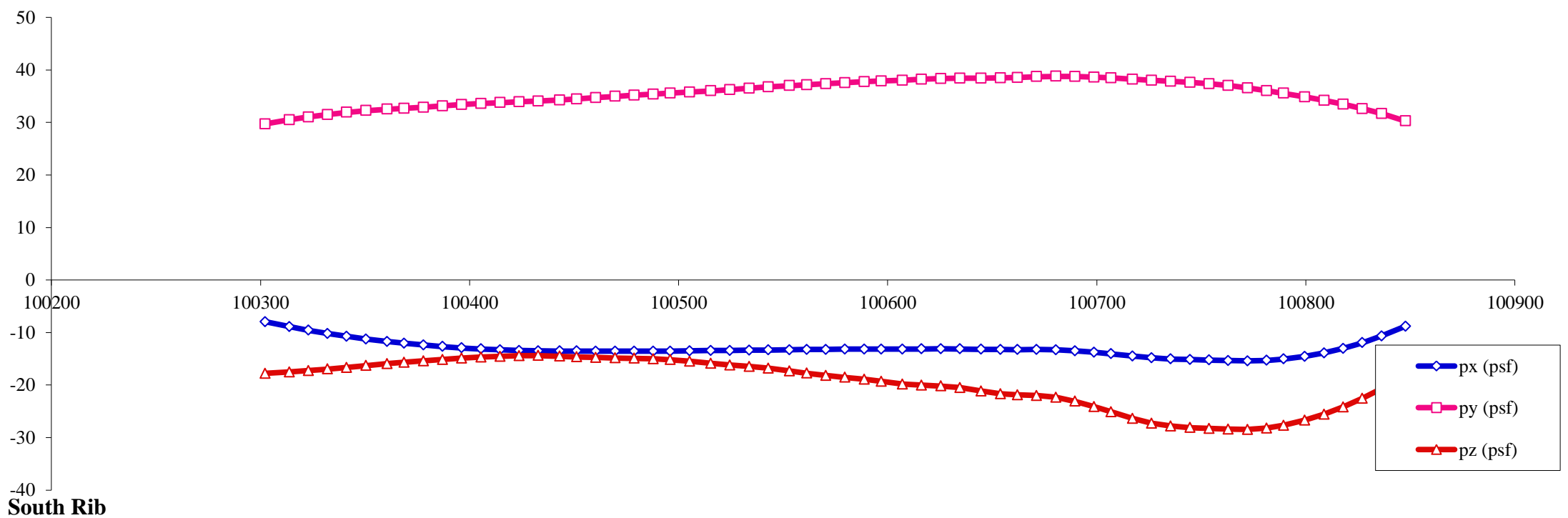
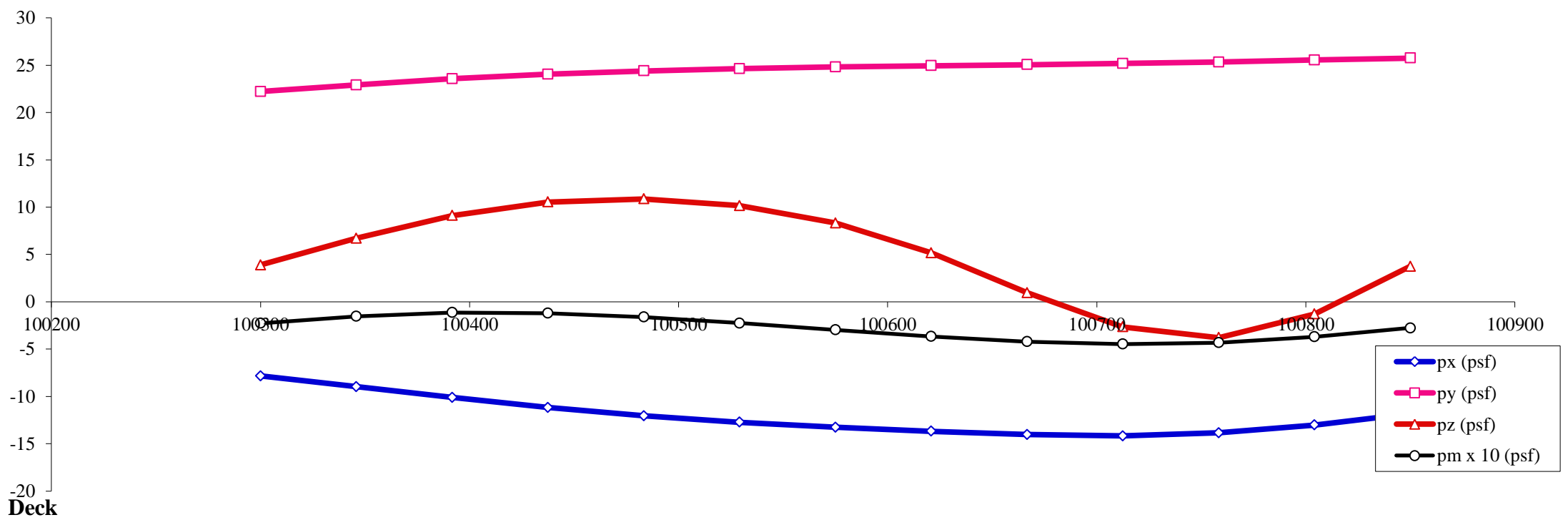
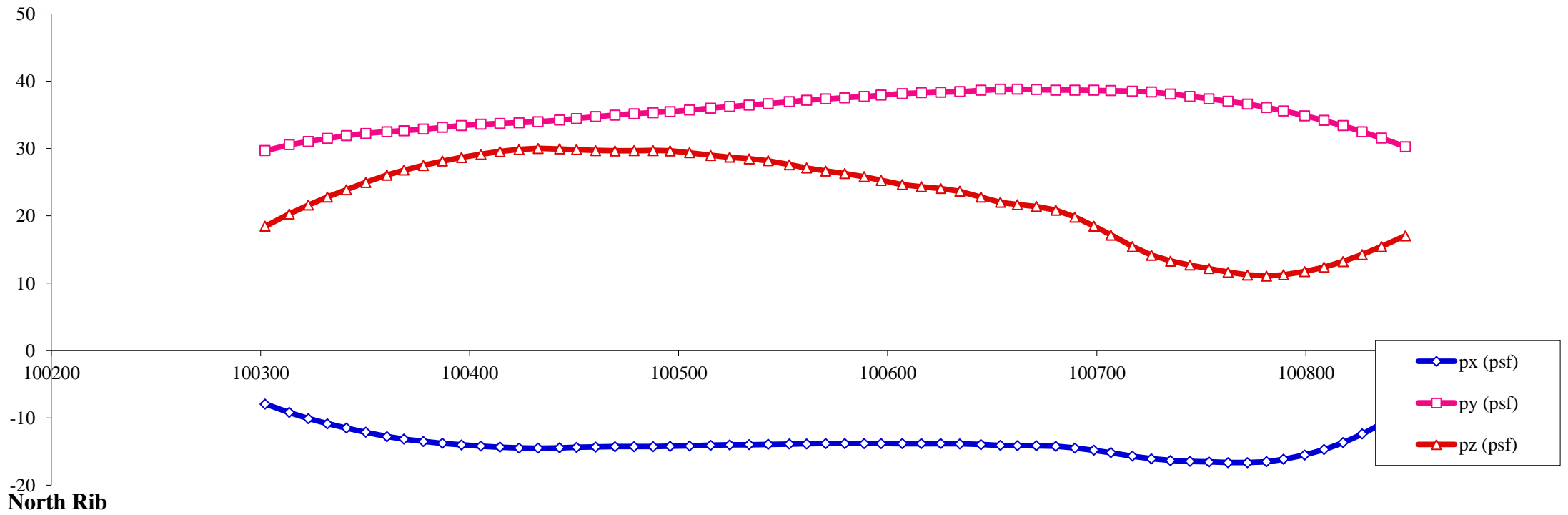
Load case : **11** Objective: Max uplift on deck, differential between 1/4 and 3/4 span



- Notes:
1. All pressures in (psf)
 2. All coordinates/elevations in (ft)
 3. Loads for hangers, arch bracings, columns, pier caps and footings are not presented here

Load Visualization Page

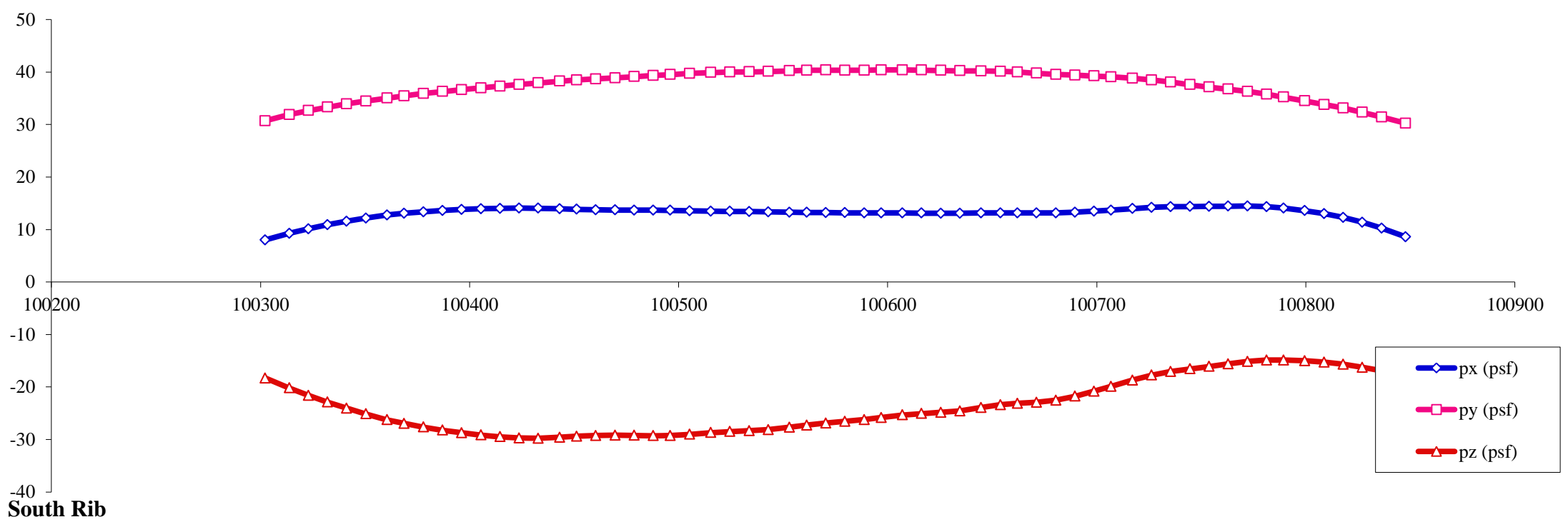
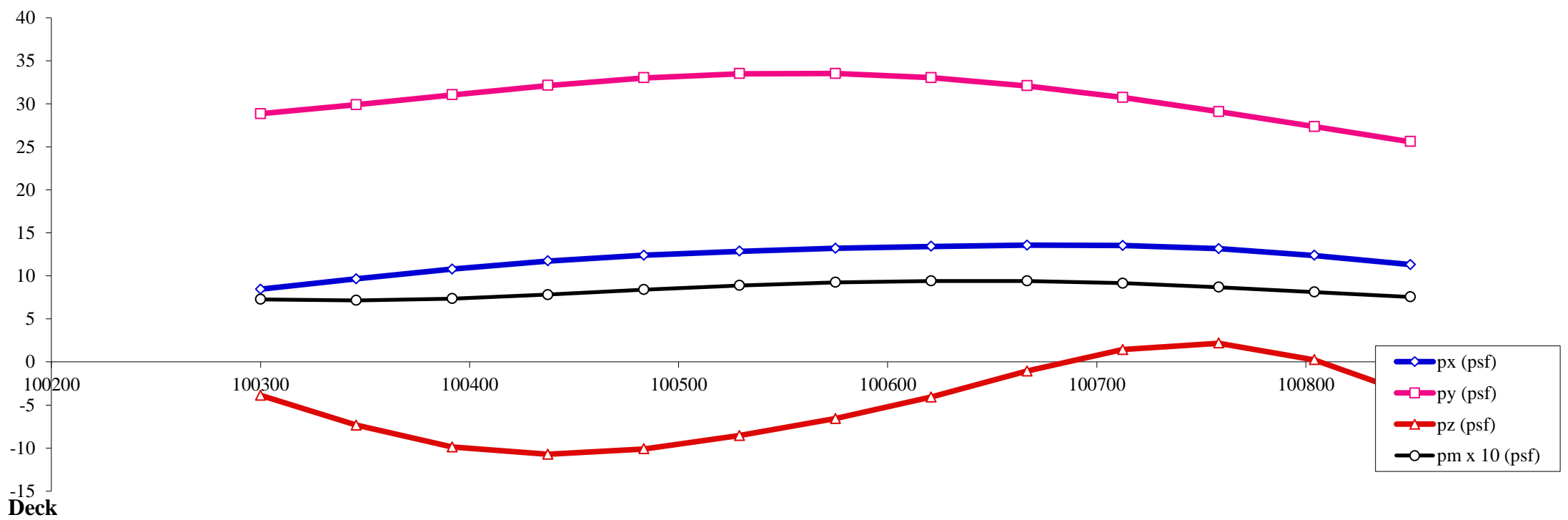
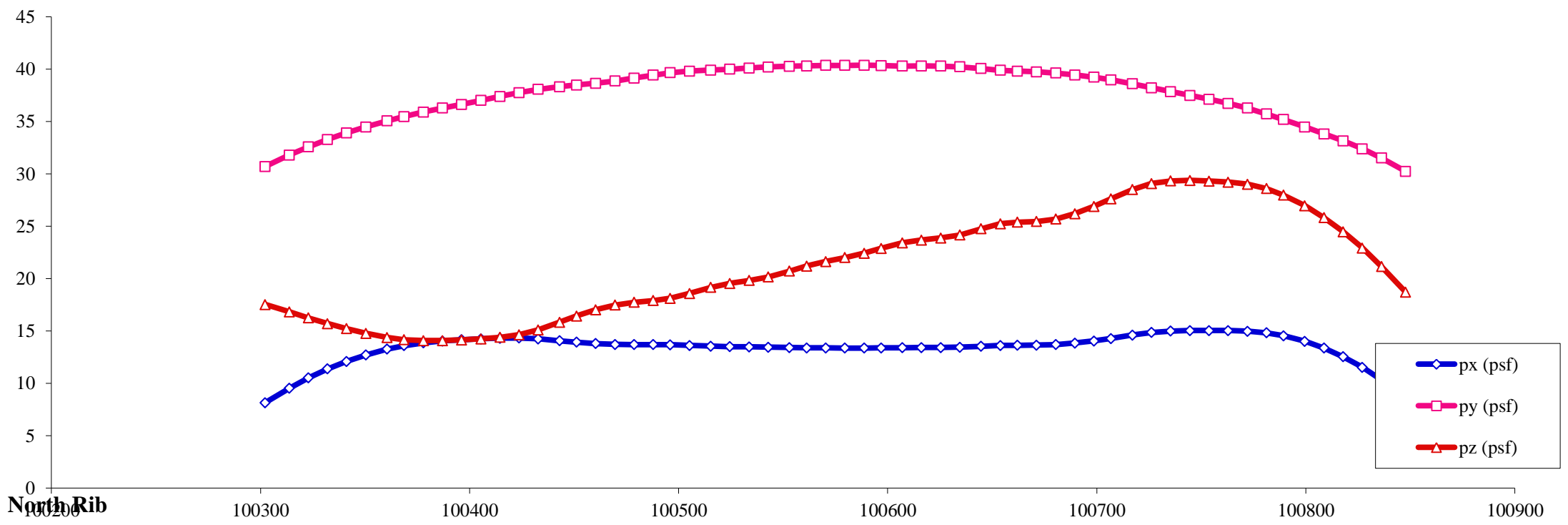
Load case : **12** Objective: Max uplift on deck, differential between 1/4 and 3/4 span



- Notes:
1. All pressures in (psf)
 2. All coordinates/elevations in (ft)
 3. Loads for hangers, arch bracings, columns, pier caps and footings are not presented here

Load Visualization Page

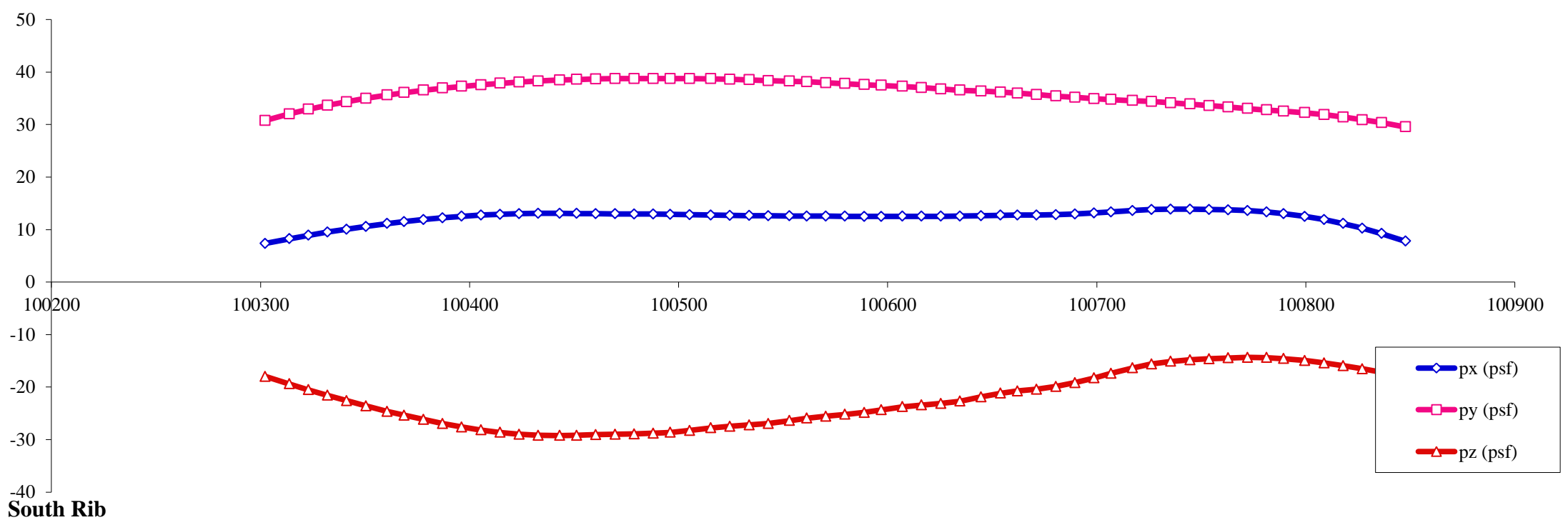
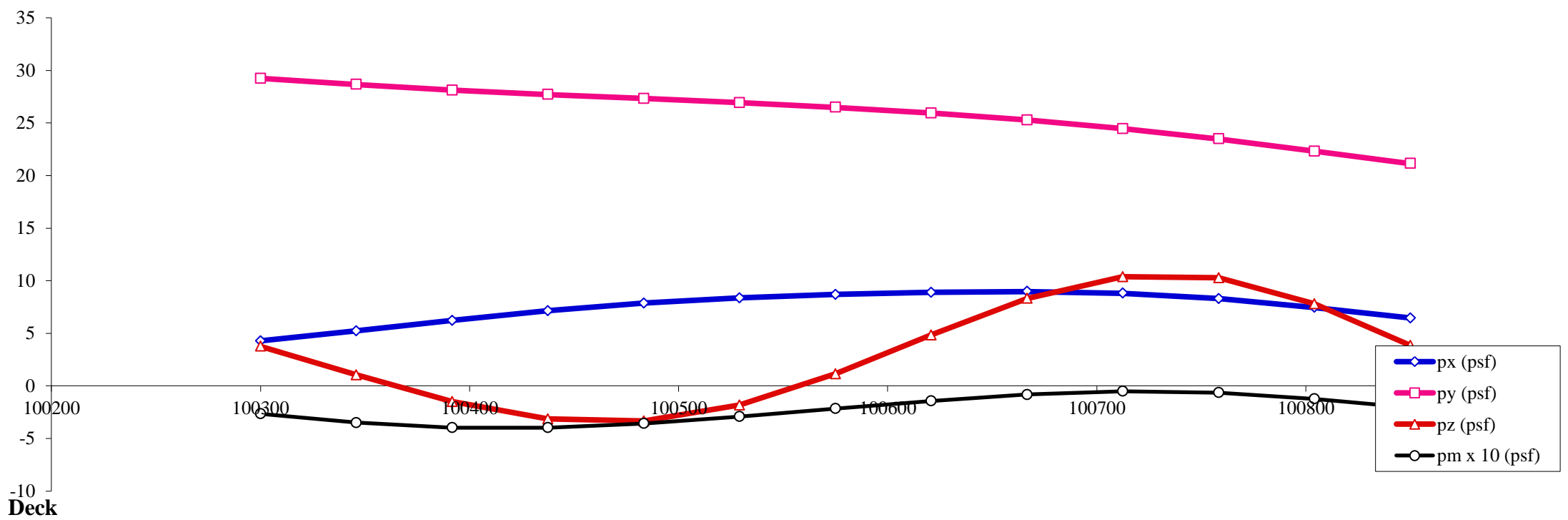
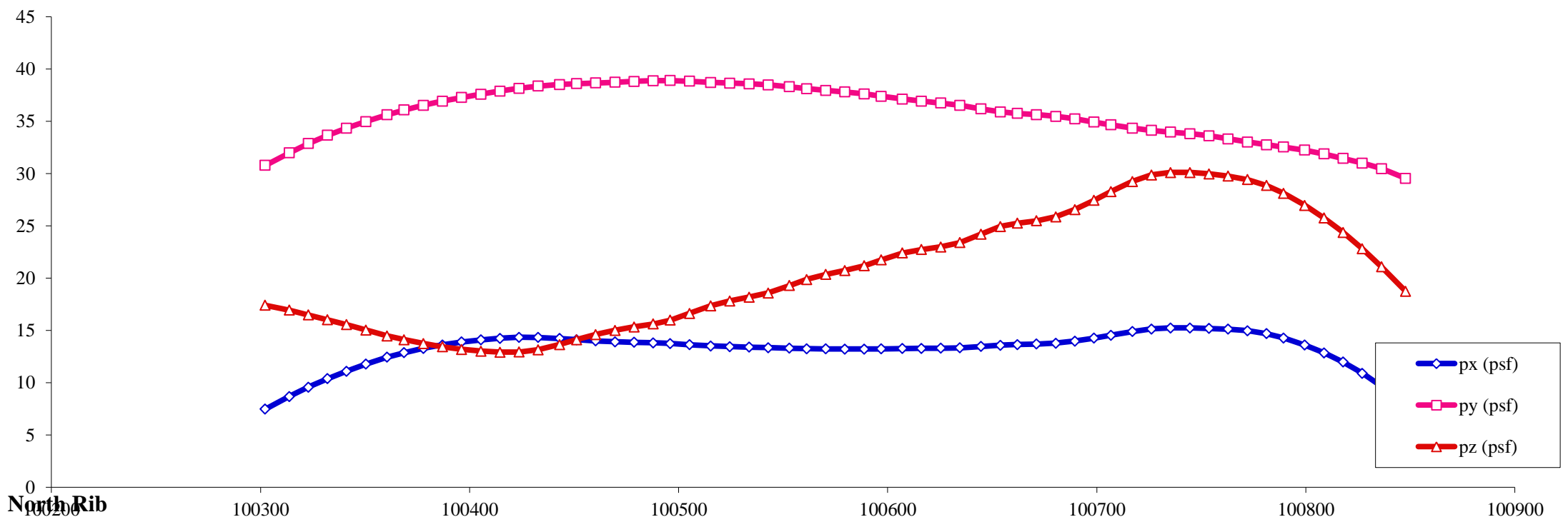
Load case : **13** Objective: Max uplift on deck, differential between 1/4 and 3/4 span



- Notes:
1. All pressures in (psf)
 2. All coordinates/elevations in (ft)
 3. Loads for hangers, arch bracings, columns, pier caps and footings are not presented here

Load Visualization Page

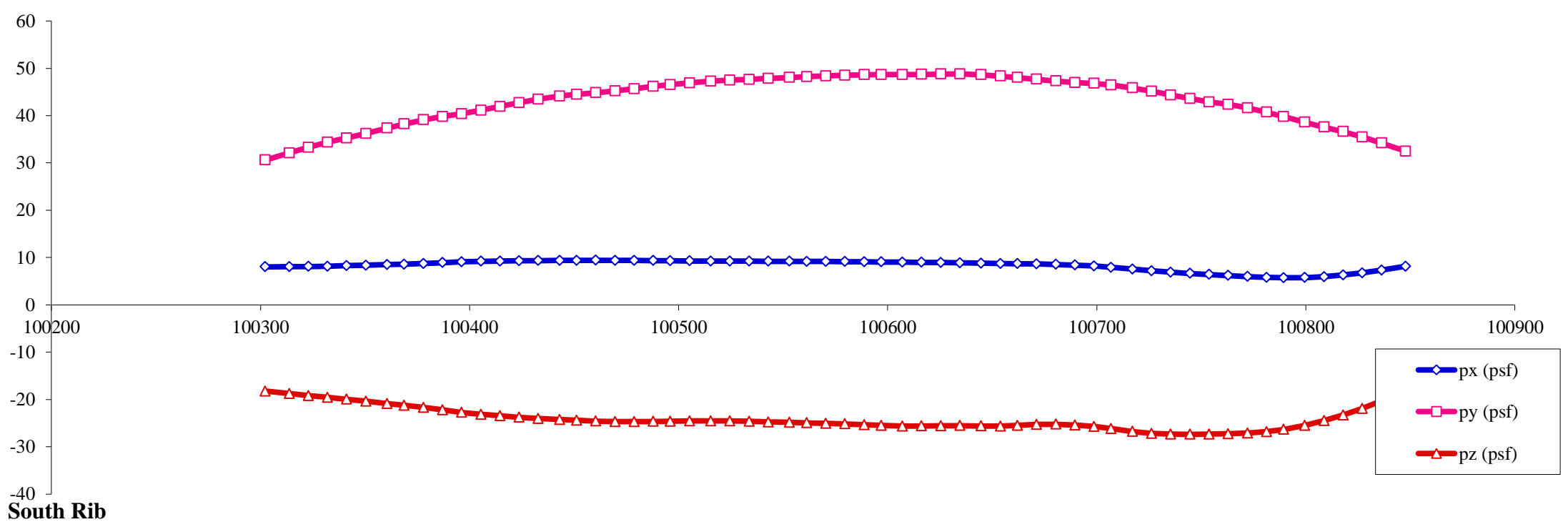
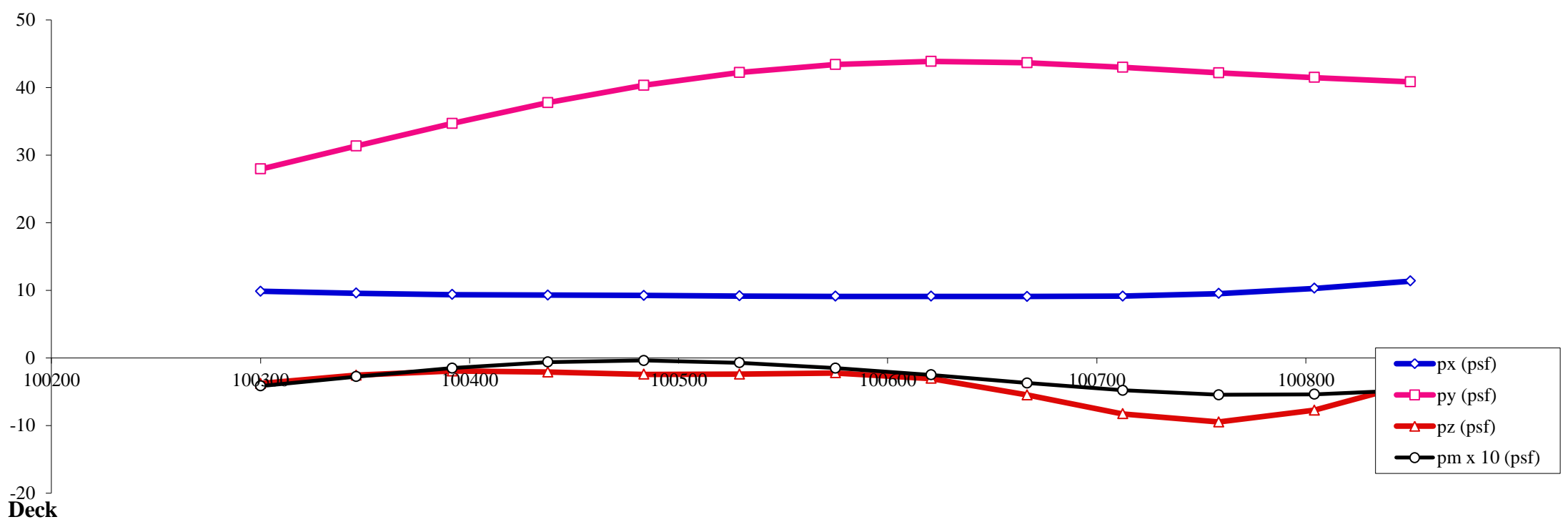
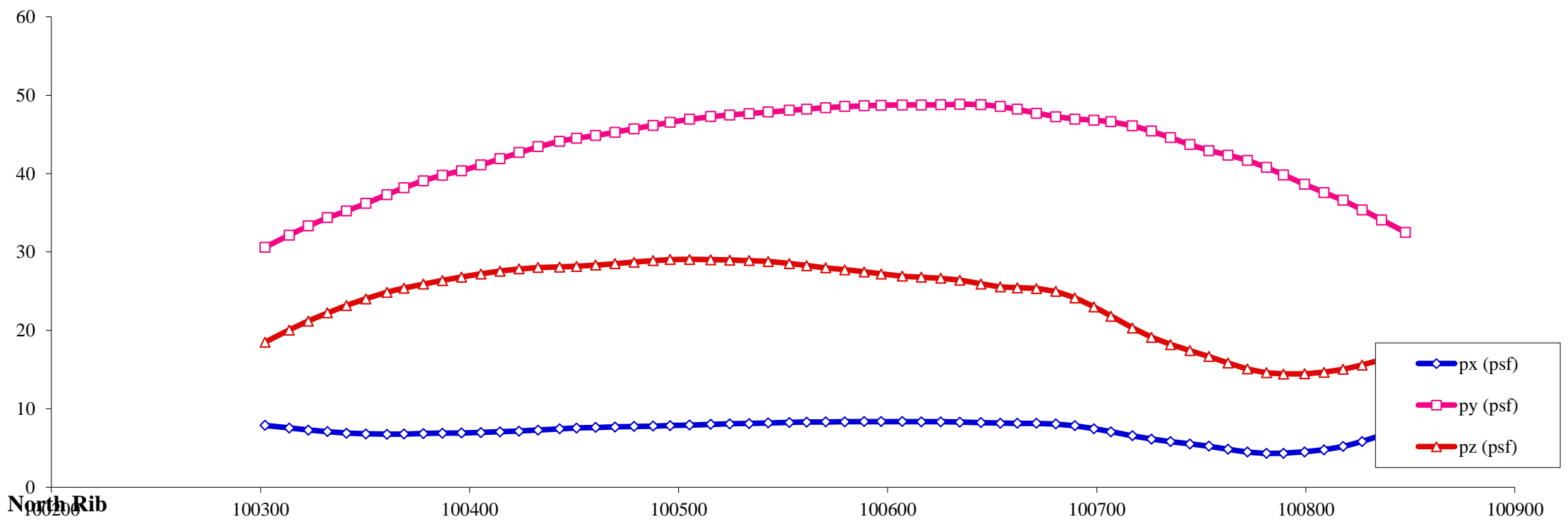
Load case : **14** Objective: Max uplift on deck, differential between 1/4 and 3/4 span



- Notes:
1. All pressures in (psf)
 2. All coordinates/elevations in (ft)
 3. Loads for hangers, arch bracings, columns, pier caps and footings are not presented here

Load Visualization Page

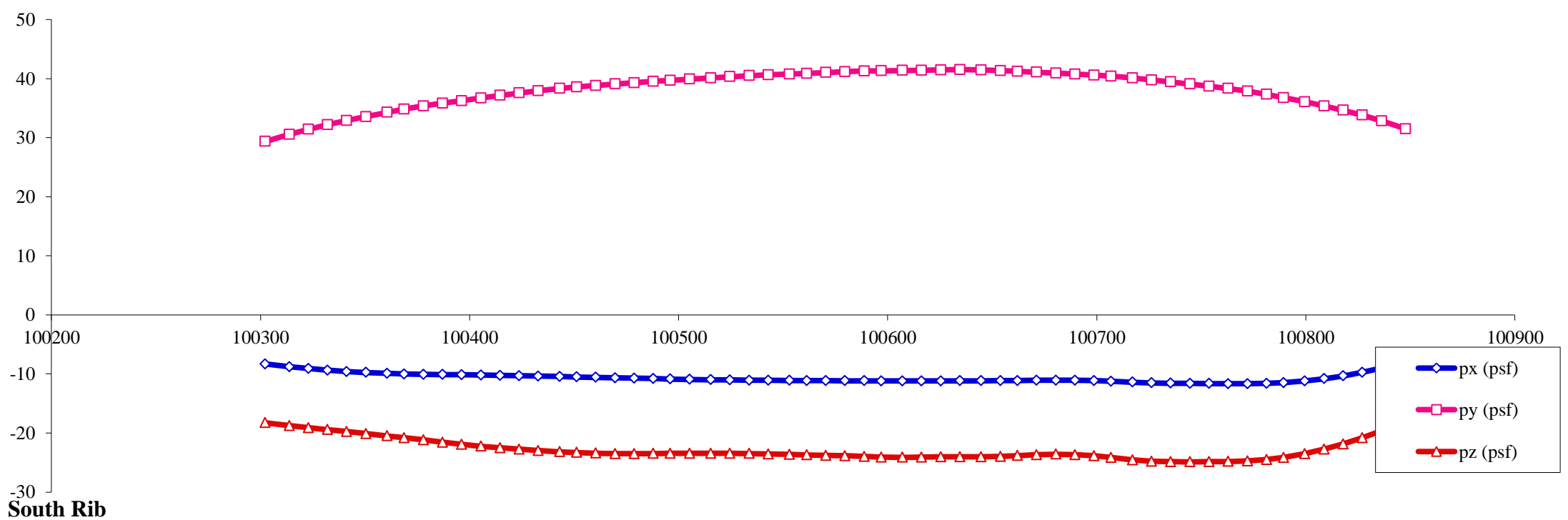
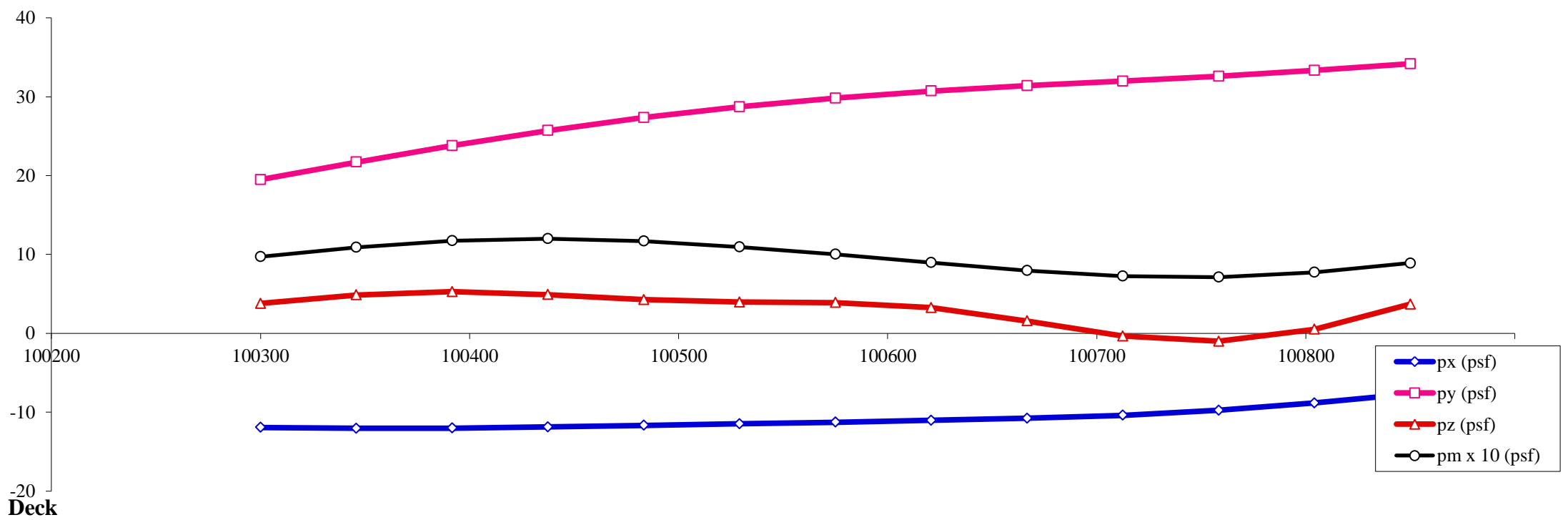
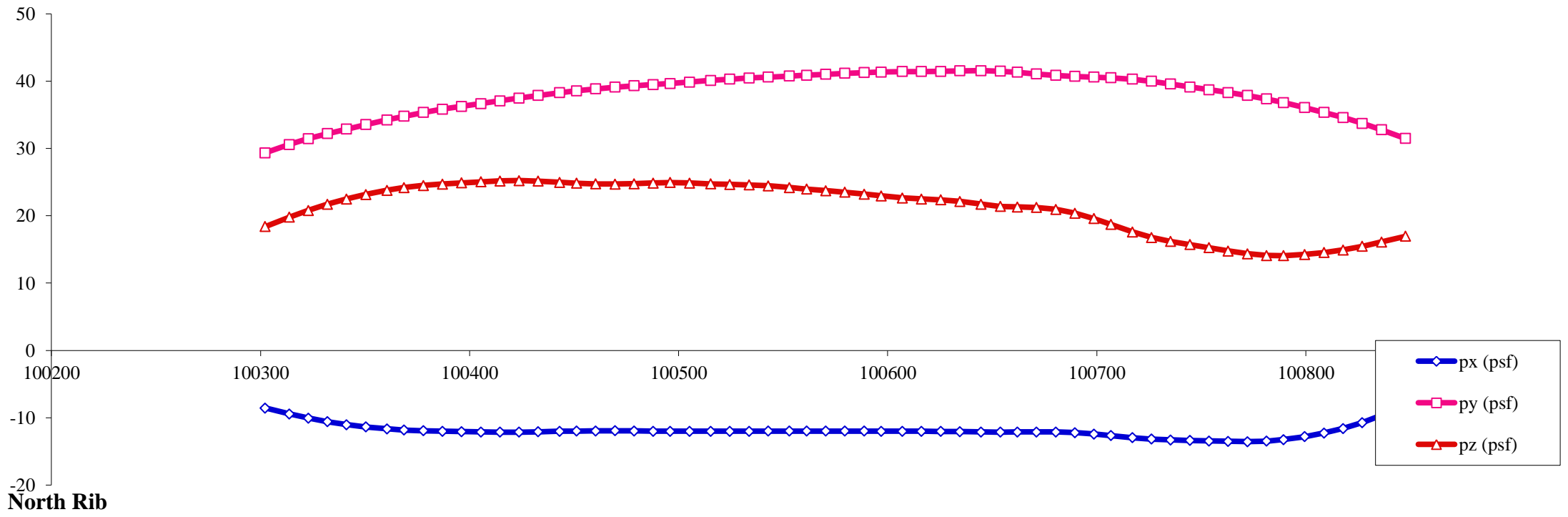
Load case : **15** Objective: Max moment on deck, differential between 1/4 and 3/4 span



- Notes:
1. All pressures in (psf)
 2. All coordinates/elevations in (ft)
 3. Loads for hangers, arch bracings, columns, pier caps and footings are not presented here

Load Visualization Page

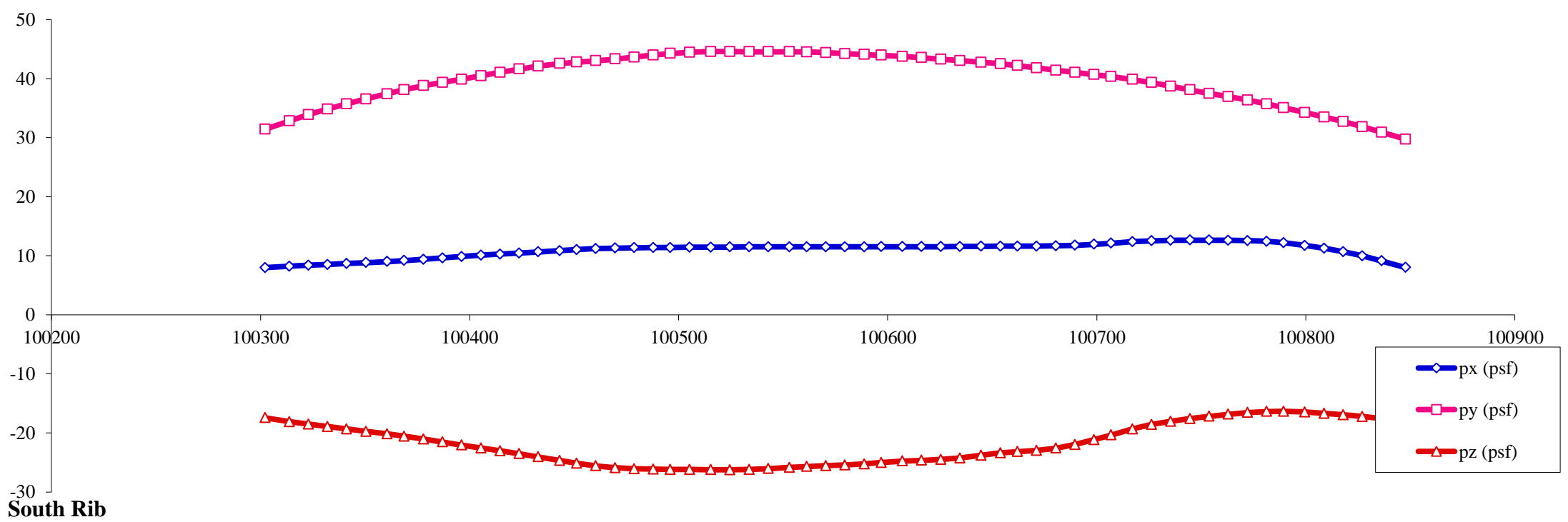
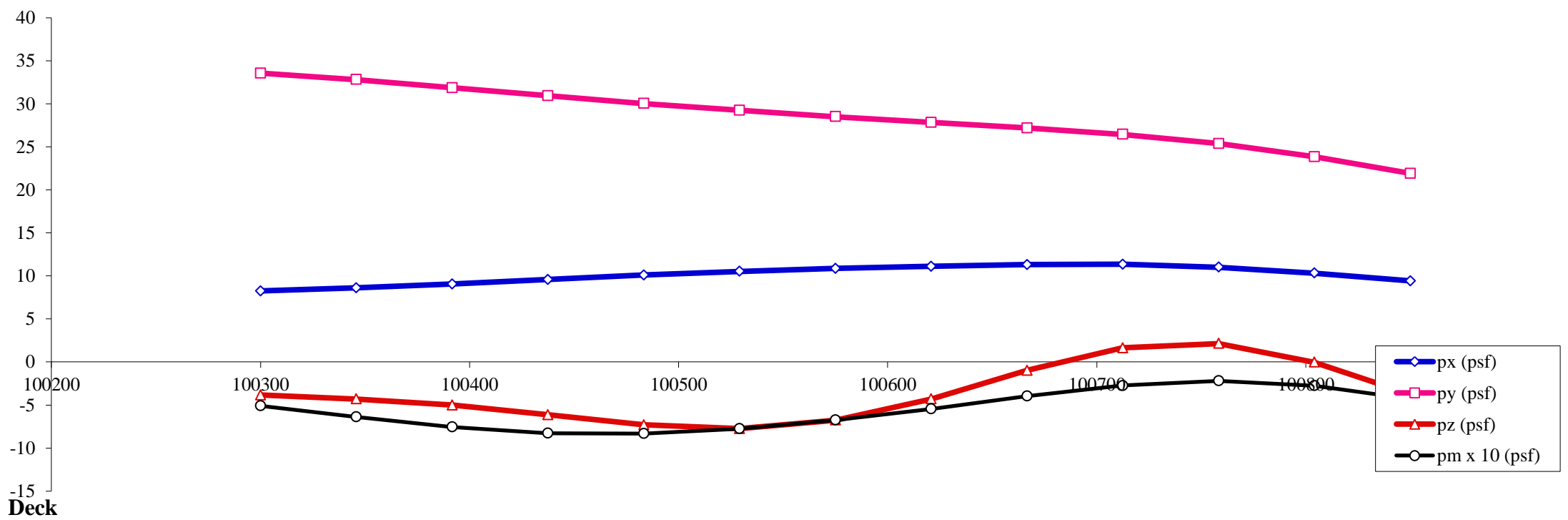
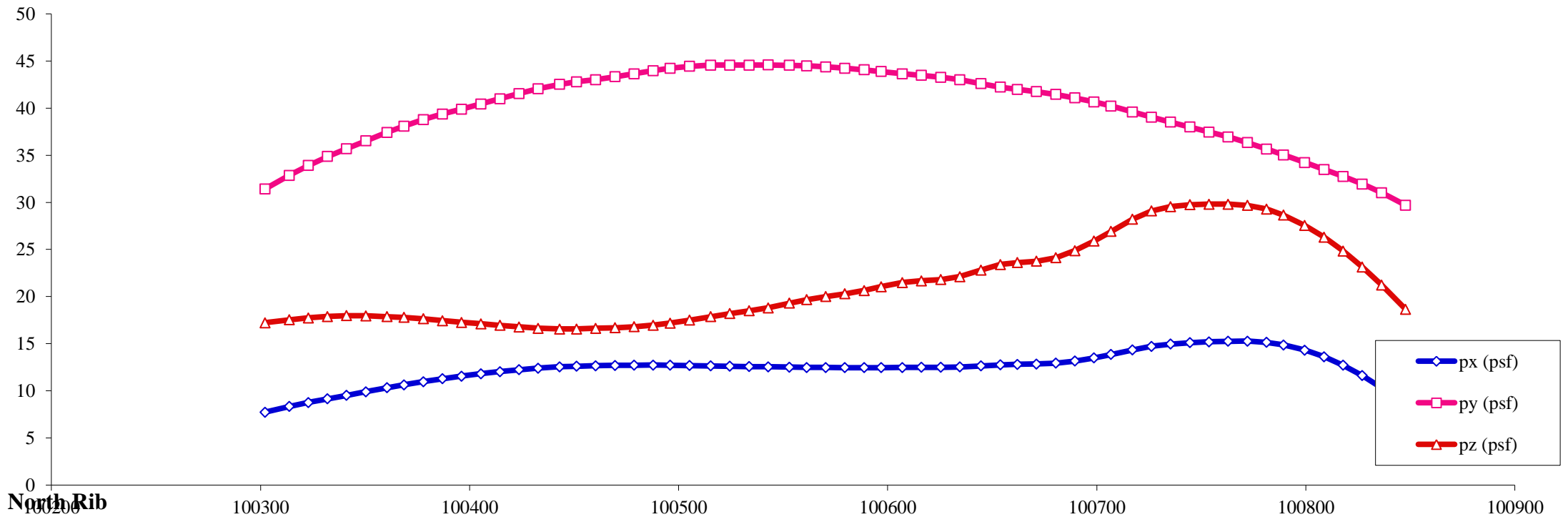
Load case : **16** Objective: Max moment on deck, differential between 1/4 and 3/4 span



- Notes:
1. All pressures in (psf)
 2. All coordinates/elevations in (ft)
 3. Loads for hangers, arch bracings, columns, pier caps and footings are not presented here

Load Visualization Page

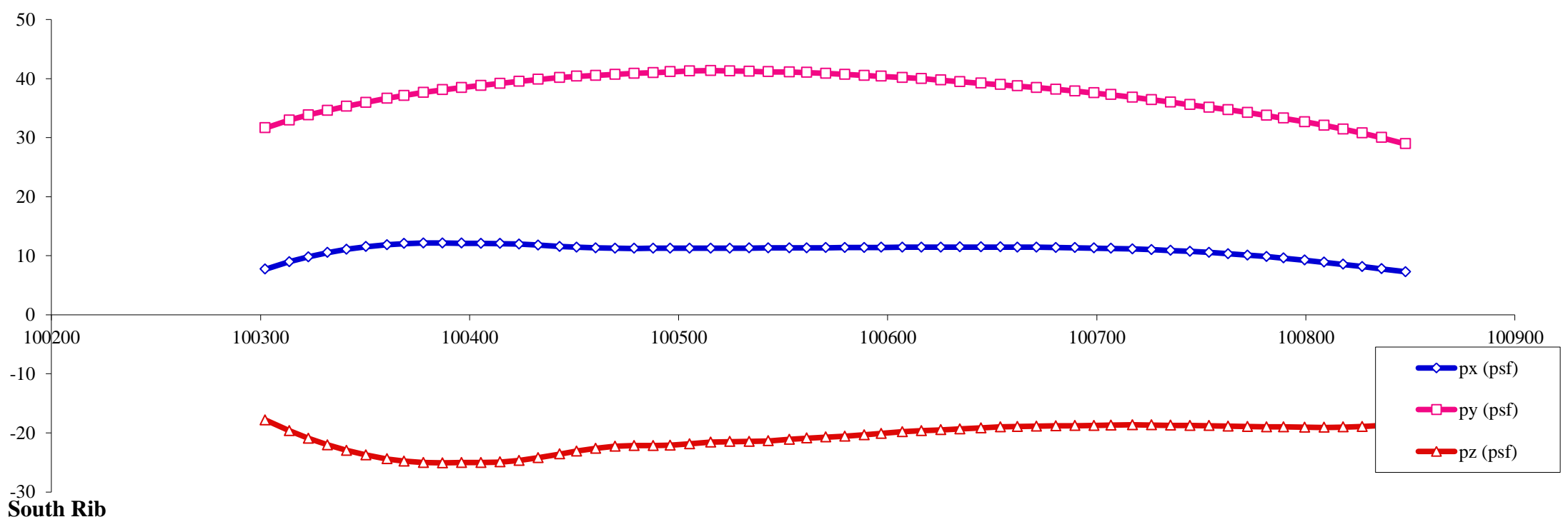
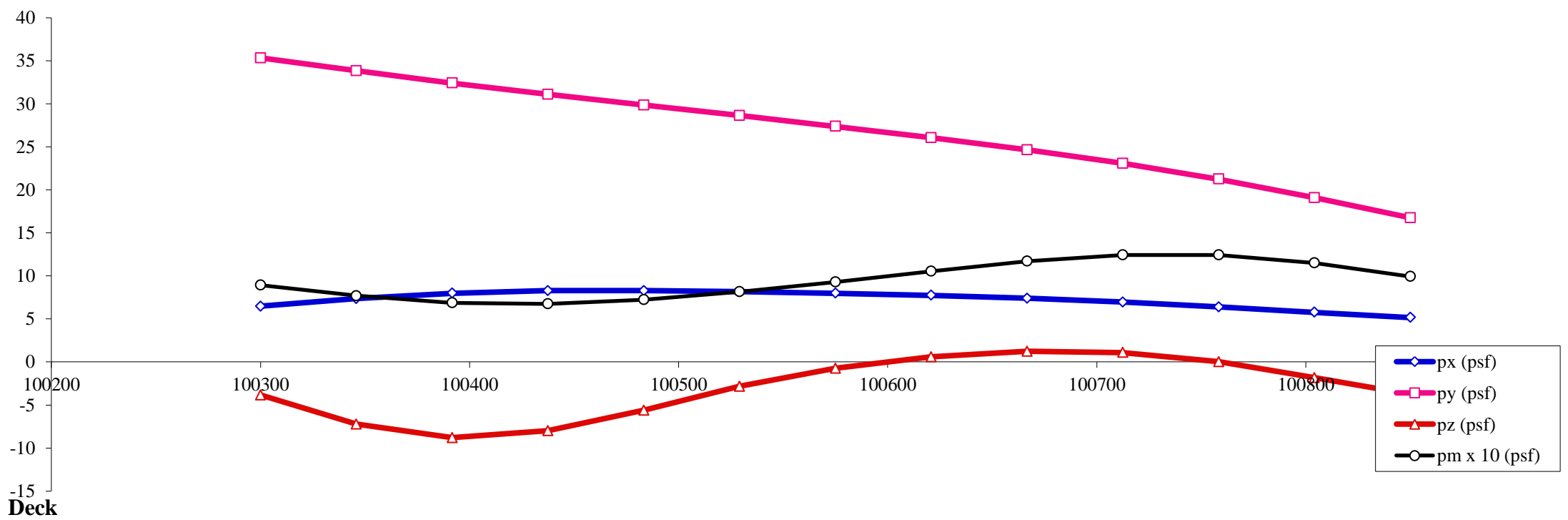
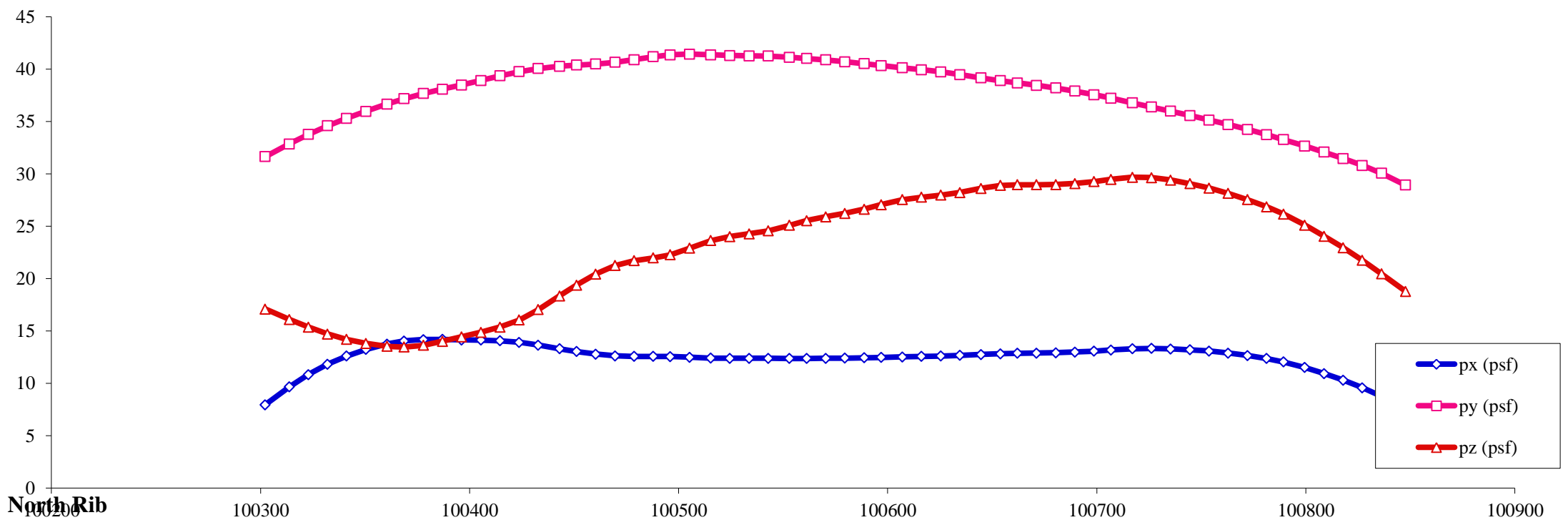
Load case : **17** Objective: Max moment on deck, differential between 1/4 and 3/4 span



- Notes:
1. All pressures in (psf)
 2. All coordinates/elevations in (ft)
 3. Loads for hangers, arch bracings, columns, pier caps and footings are not presented here

Load Visualization Page

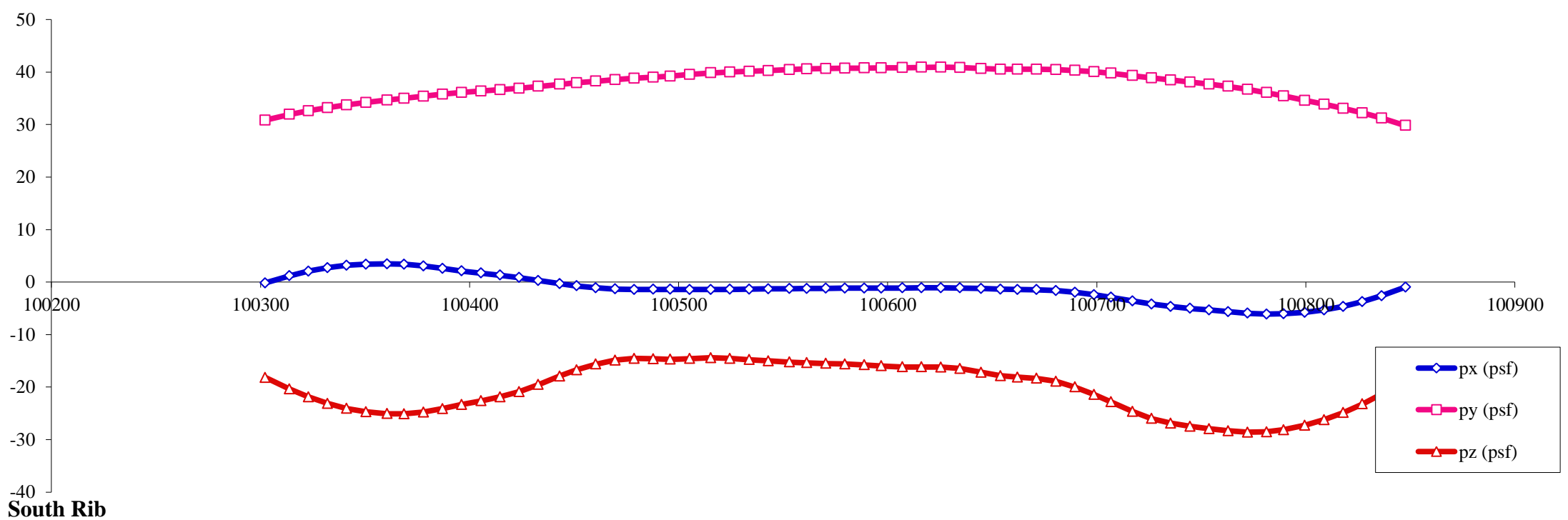
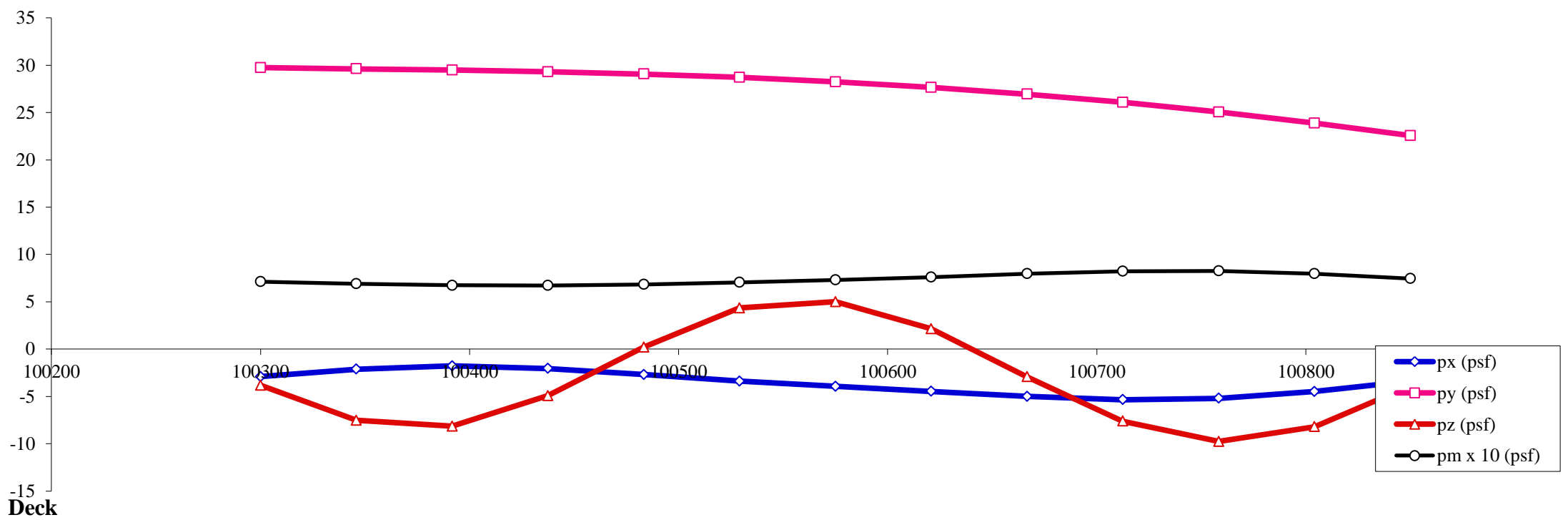
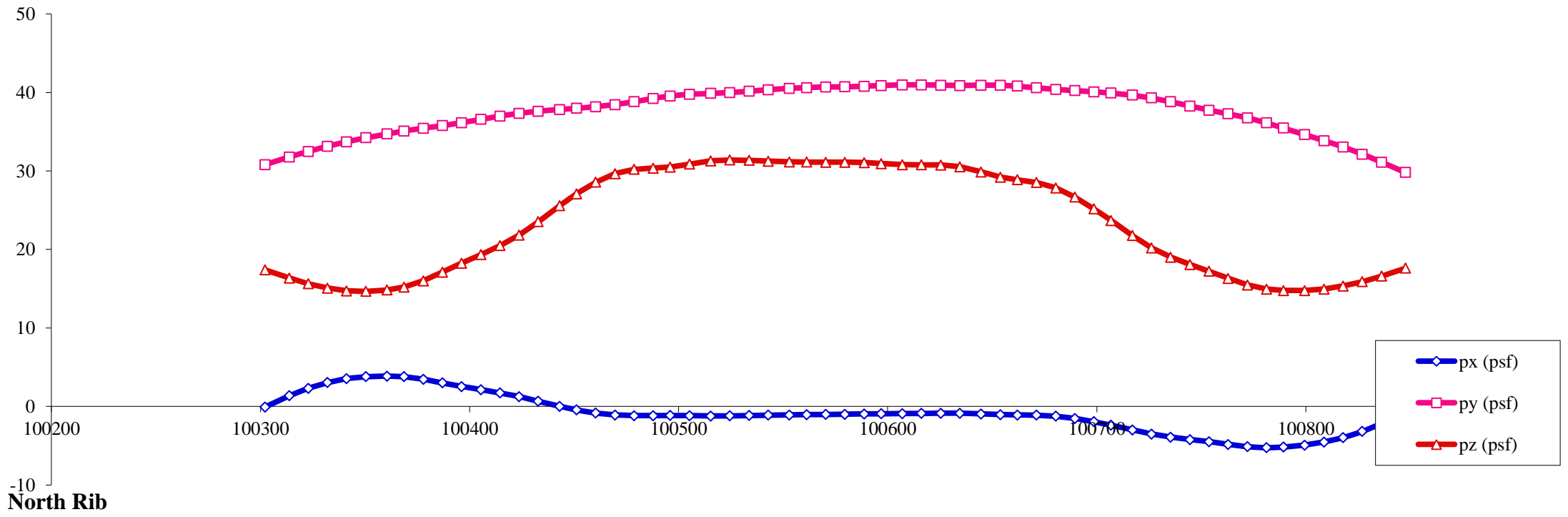
Load case : **18** Objective: Max moment on deck, differential between 1/4 and 3/4 span



- Notes:
1. All pressures in (psf)
 2. All coordinates/elevations in (ft)
 3. Loads for hangers, arch bracings, columns, pier caps and footings are not presented here

Load Visualization Page

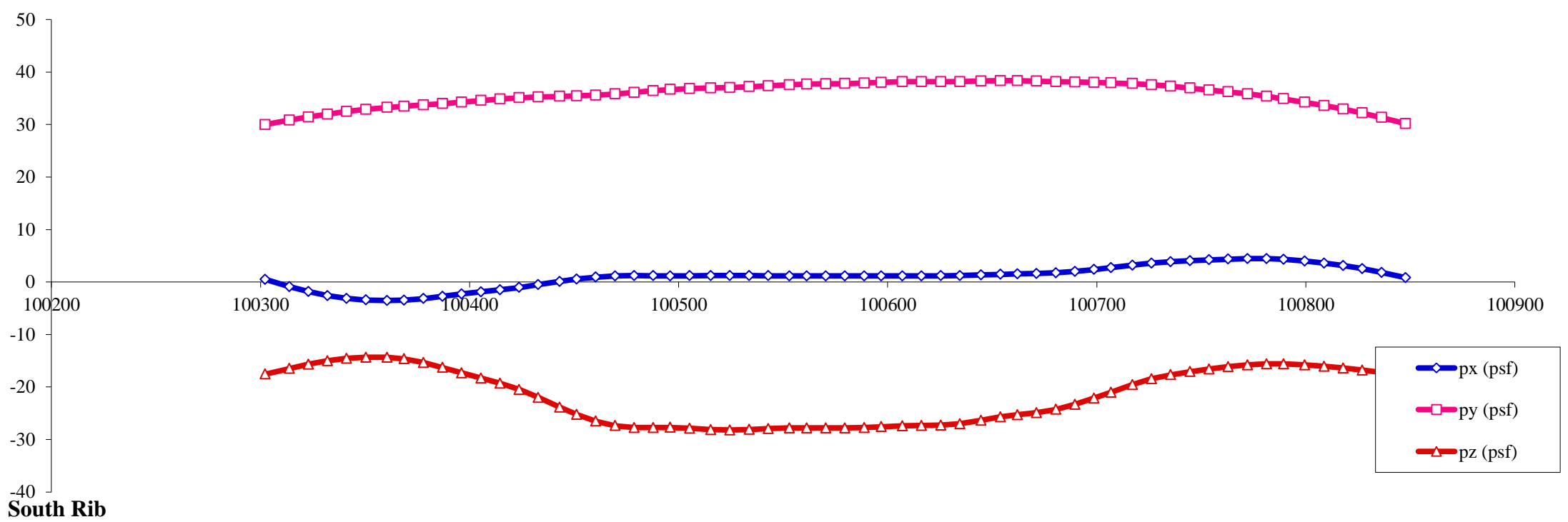
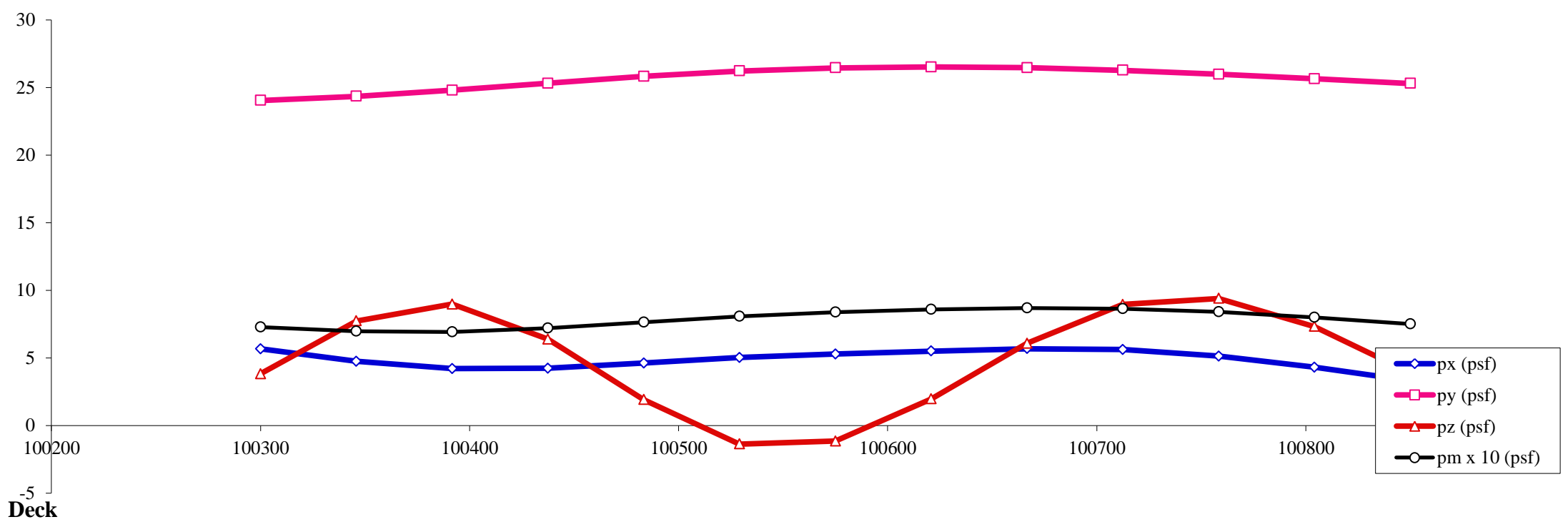
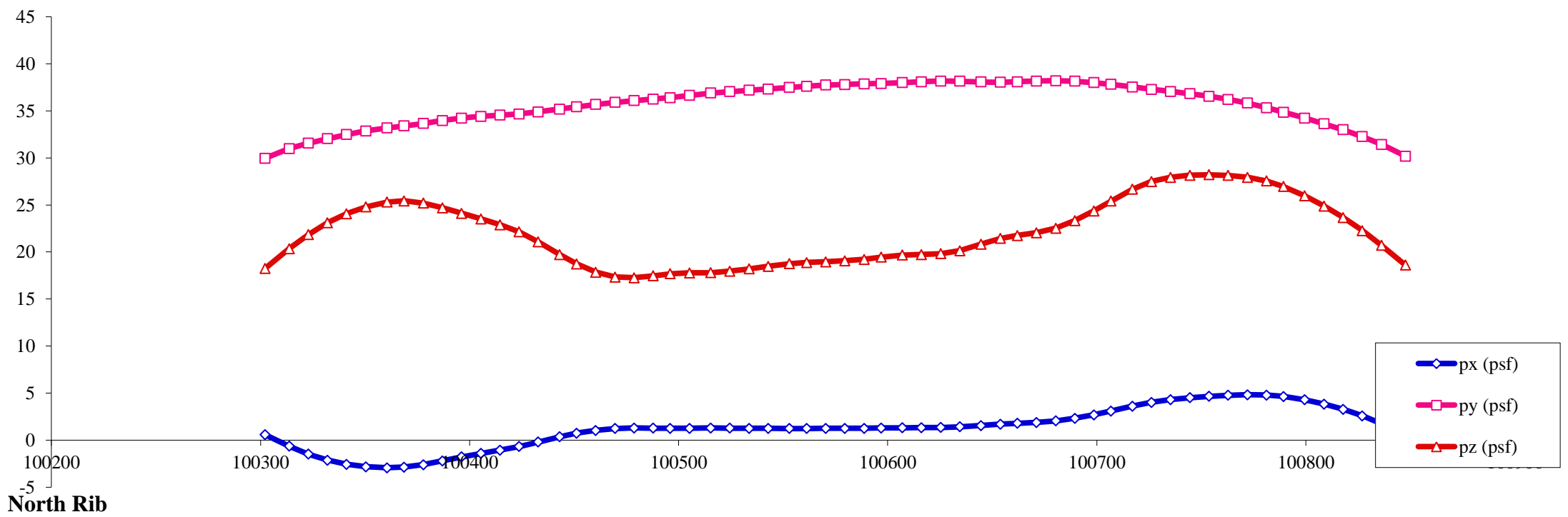
Load case : **19** Objective: Max uplift on deck, differential between middle and 1/4 & 3/4 span



- Notes:
1. All pressures in (psf)
 2. All coordinates/elevations in (ft)
 3. Loads for hangers, arch bracings, columns, pier caps and footings are not presented here

Load Visualization Page

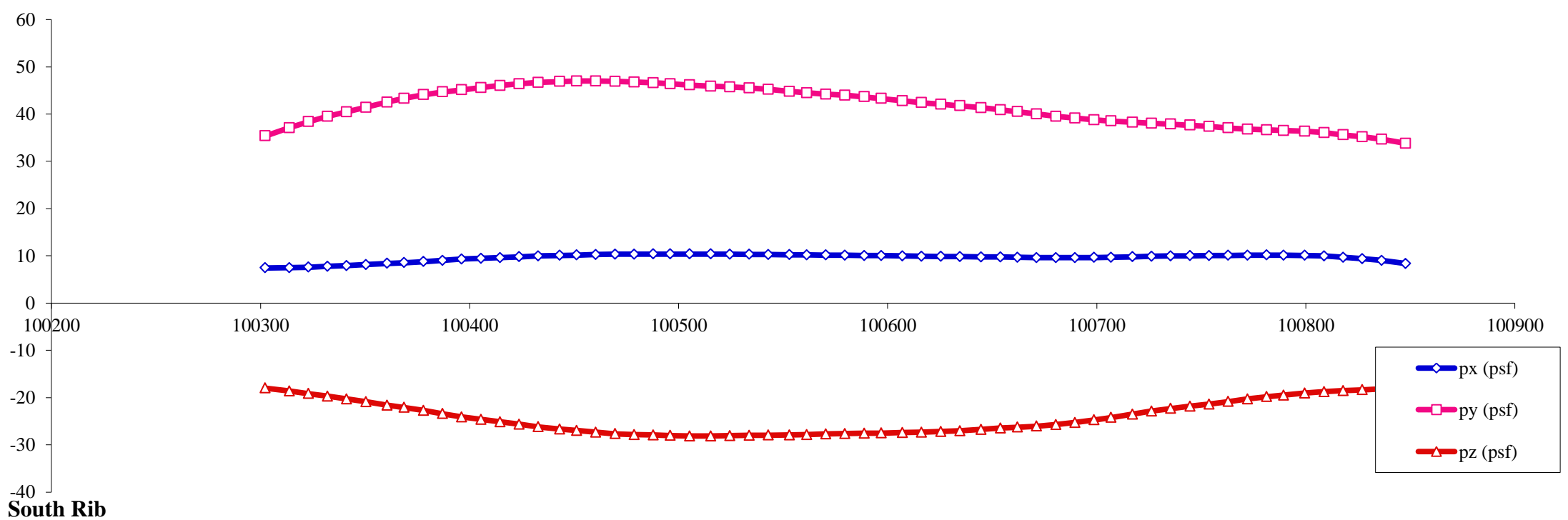
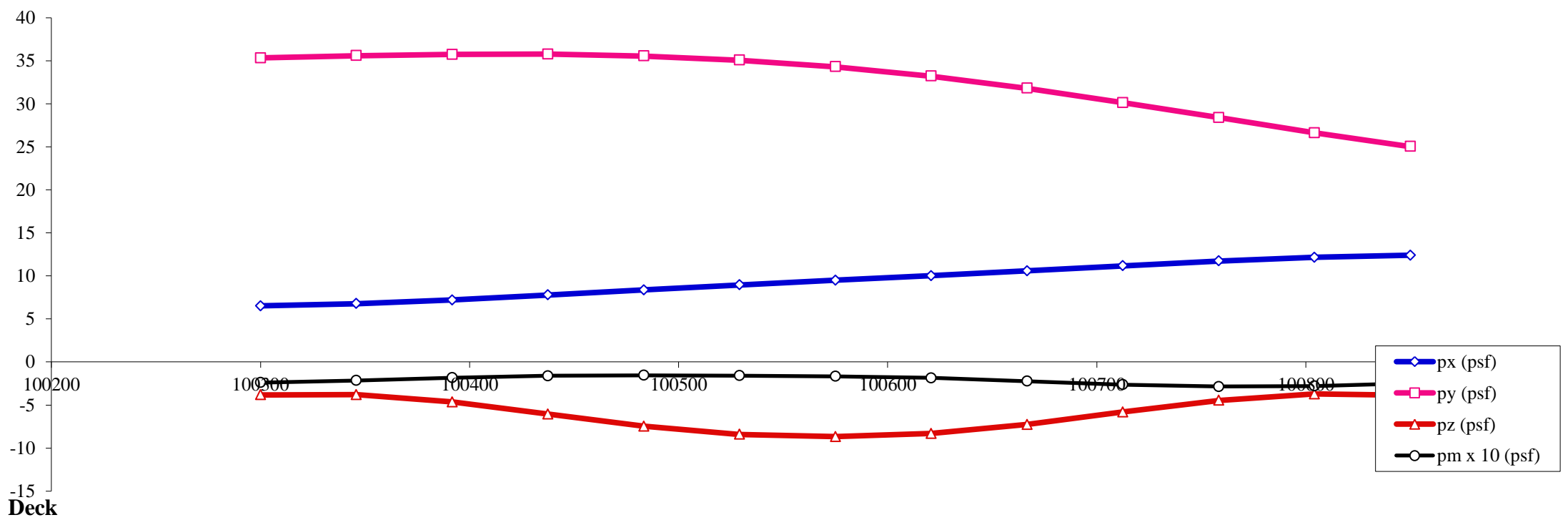
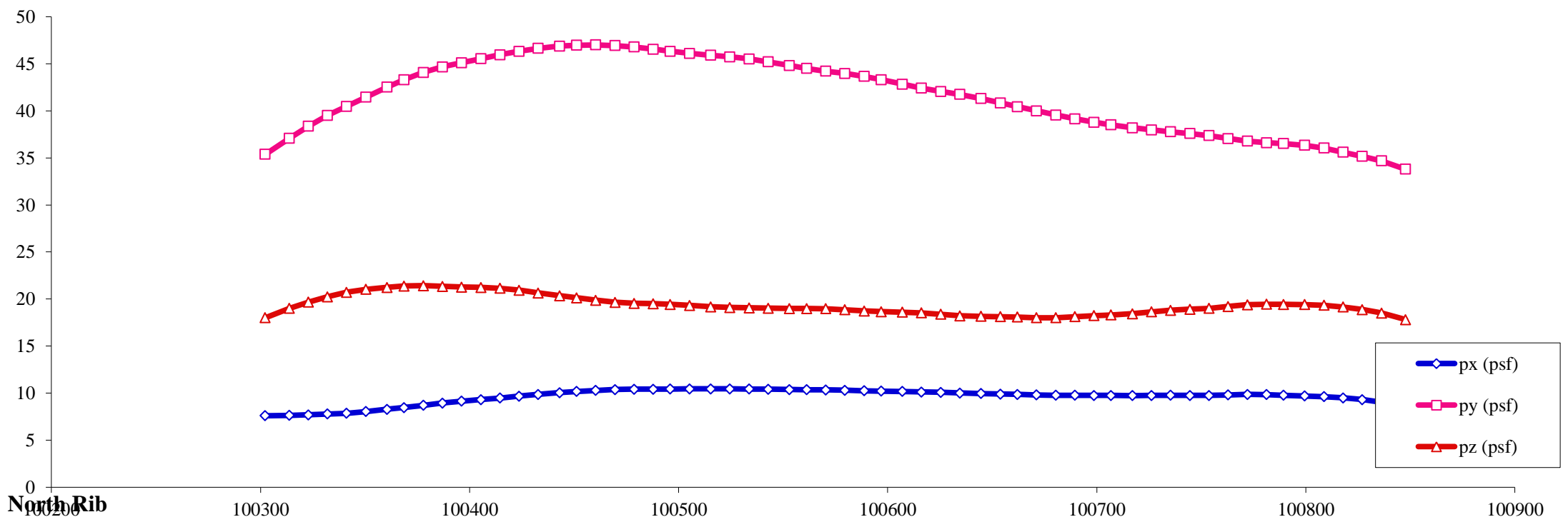
Load case : **20** Objective: Max uplift on deck, differential between middle and 1/4 & 3/4 span



- Notes:
1. All pressures in (psf)
 2. All coordinates/elevations in (ft)
 3. Loads for hangers, arch bracings, columns, pier caps and footings are not presented here

Load Visualization Page

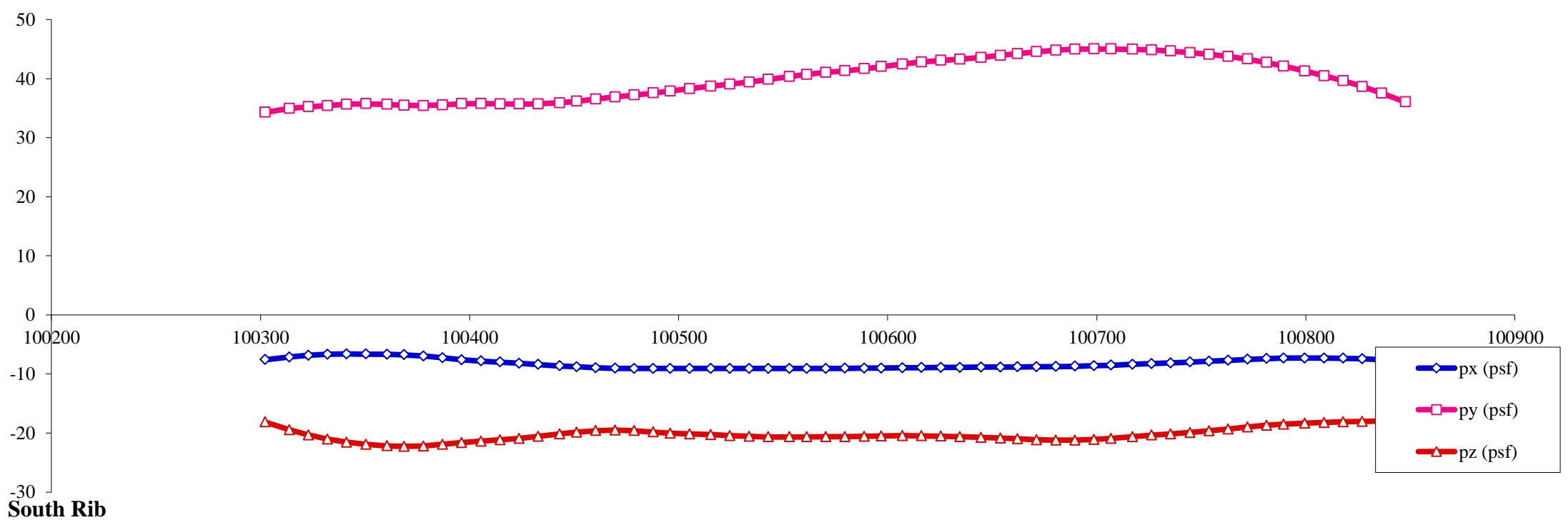
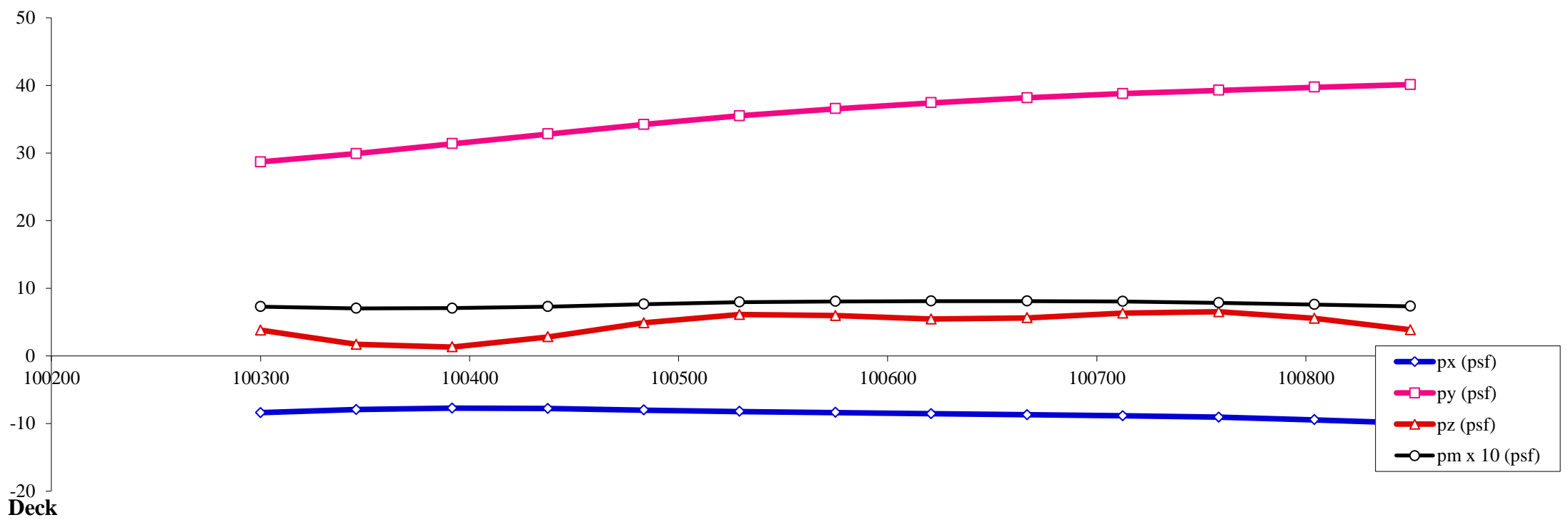
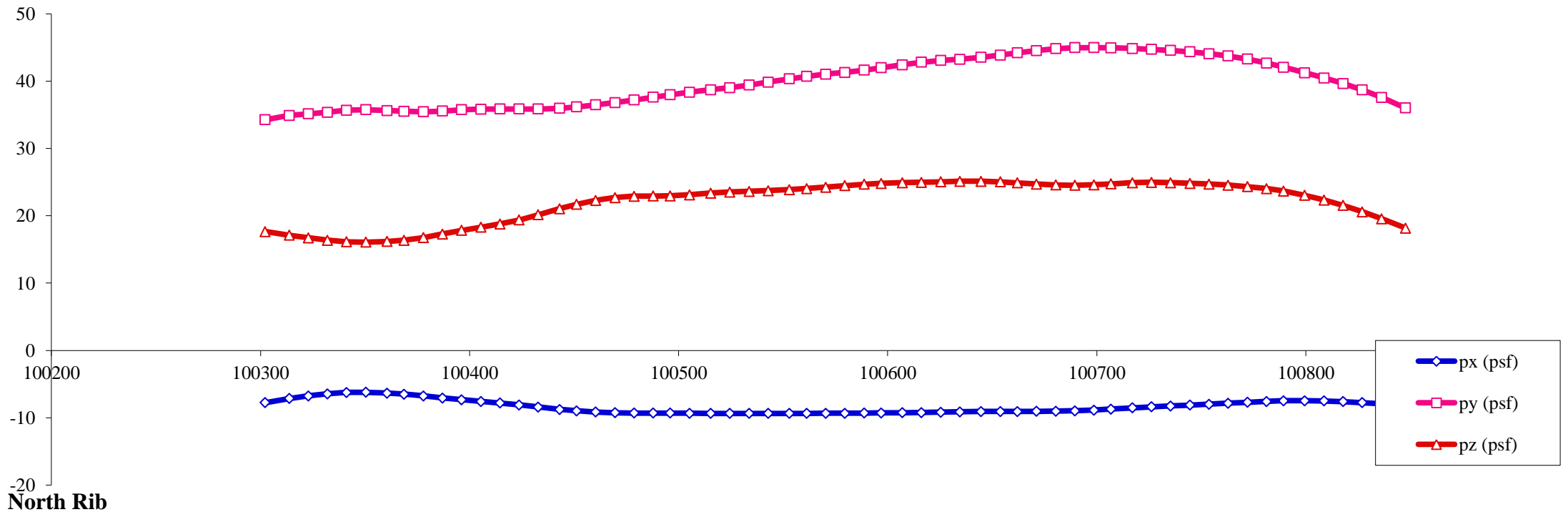
Load case : **21** Objective: Max lateral on arch ribs, differential between 1/4 and 3/4 span



- Notes:
1. All pressures in (psf)
 2. All coordinates/elevations in (ft)
 3. Loads for hangers, arch bracings, columns, pier caps and footings are not presented here

Load Visualization Page

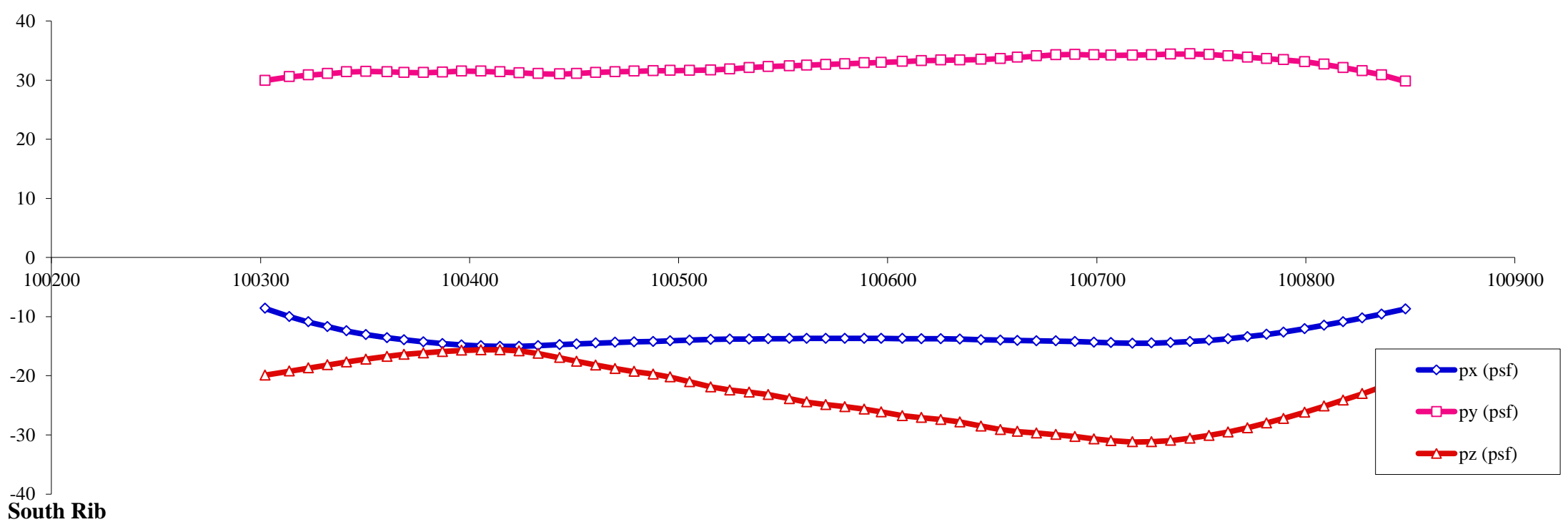
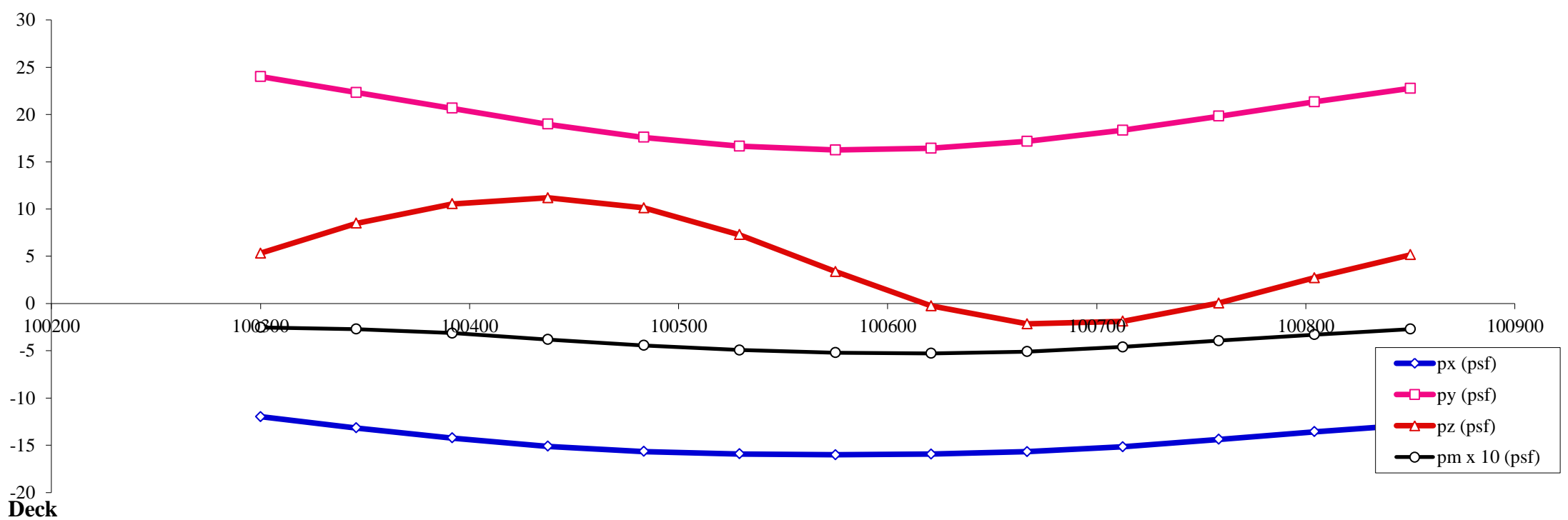
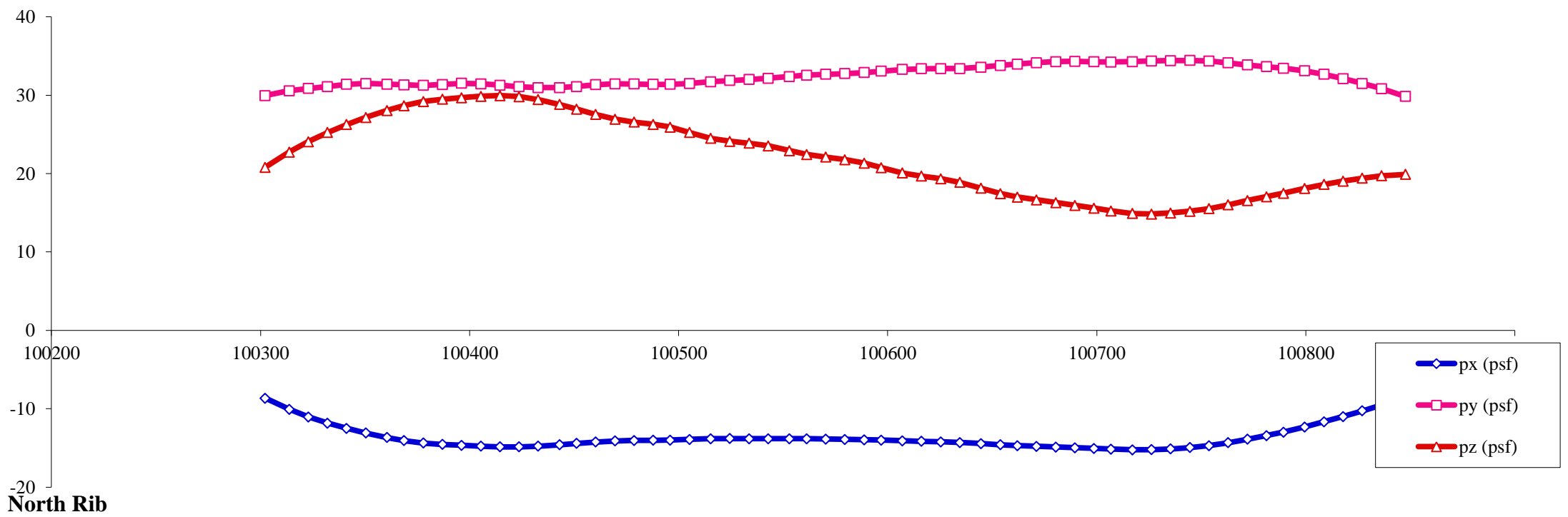
Load case : **22** Objective: Max lateral on arch ribs, differential between 1/4 and 3/4 span



- Notes:**
1. All pressures in (psf)
 2. All coordinates/elevations in (ft)
 3. Loads for hangers, arch bracings, columns, pier caps and footings are not presented here

Load Visualization Page

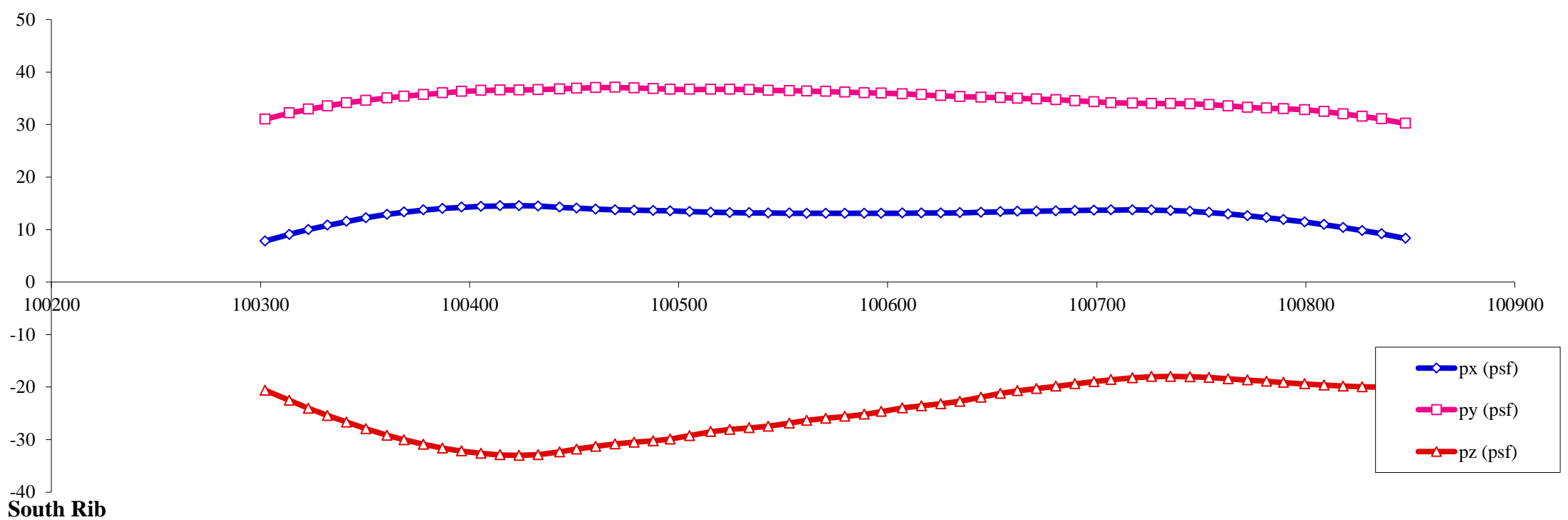
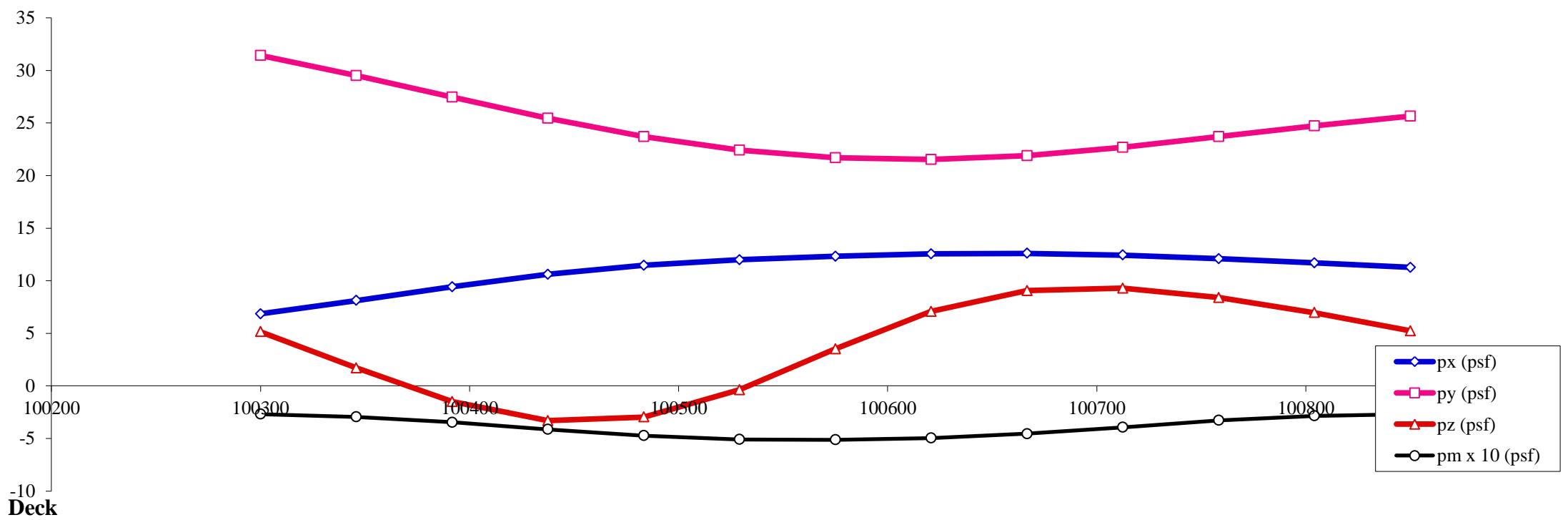
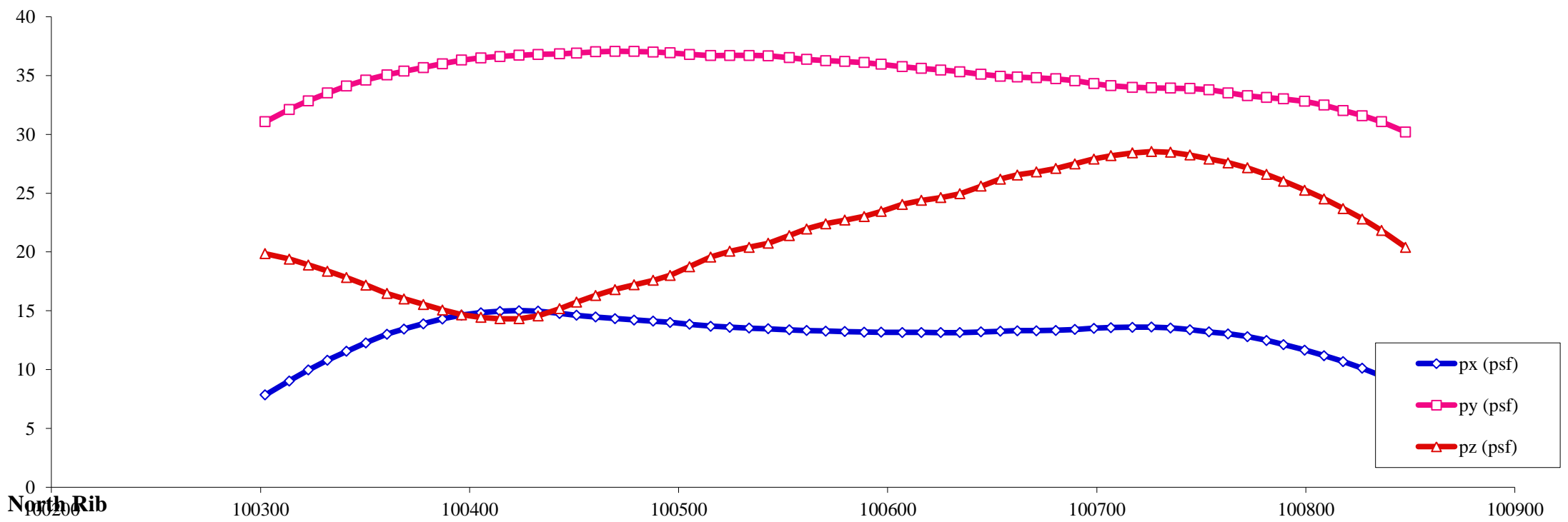
Load case : **23** Objective: Max uplift on arch ribs, differential between 1/4 and 3/4 span



- Notes:
1. All pressures in (psf)
 2. All coordinates/elevations in (ft)
 3. Loads for hangers, arch bracings, columns, pier caps and footings are not presented here

Load Visualization Page

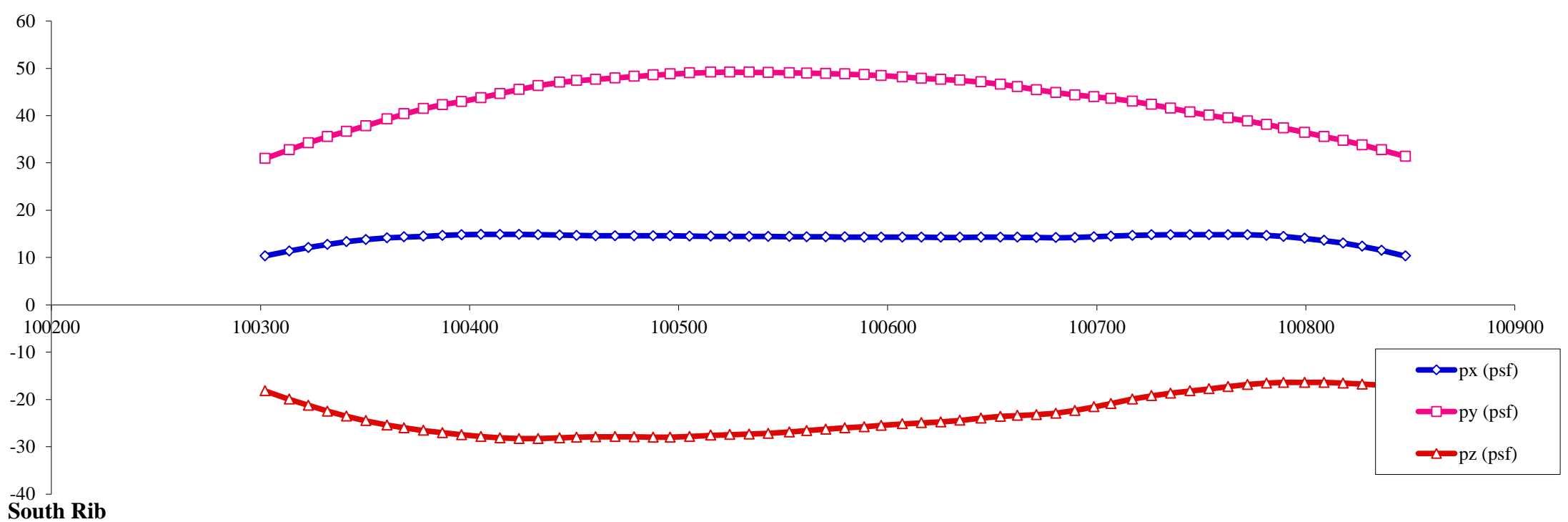
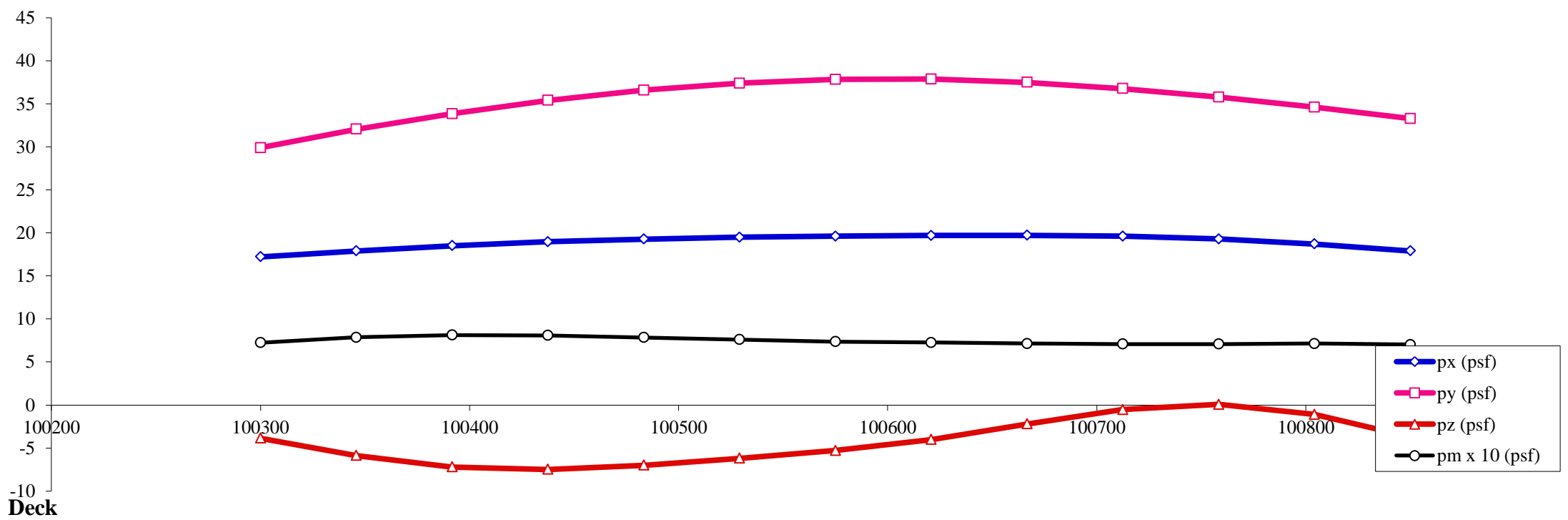
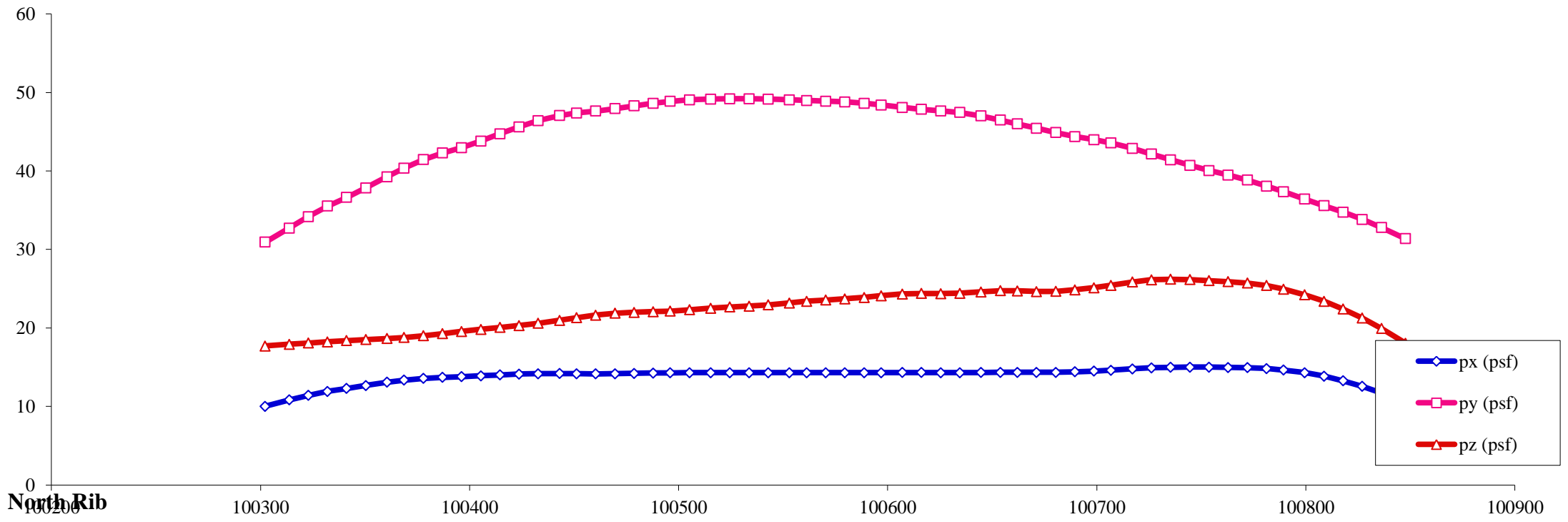
Load case : **24** Objective: Max uplift on arch ribs, differential between 1/4 and 3/4 span



- Notes:
1. All pressures in (psf)
 2. All coordinates/elevations in (ft)
 3. Loads for hangers, arch bracings, columns, pier caps and footings are not presented here

Load Visualization Page

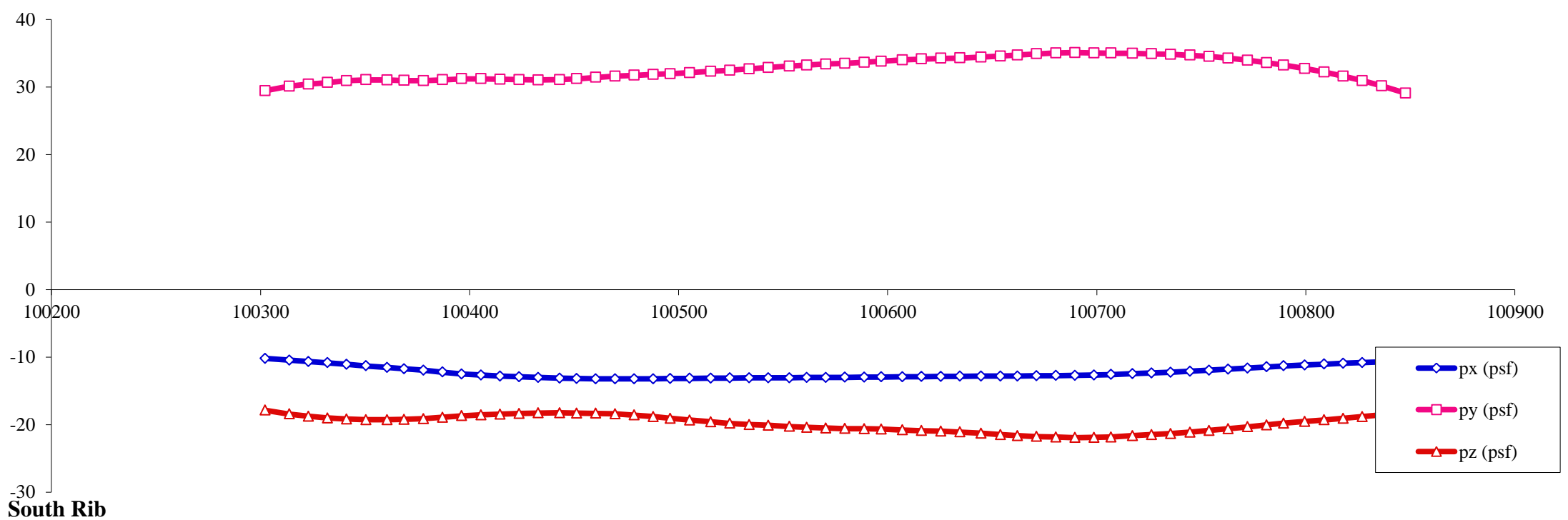
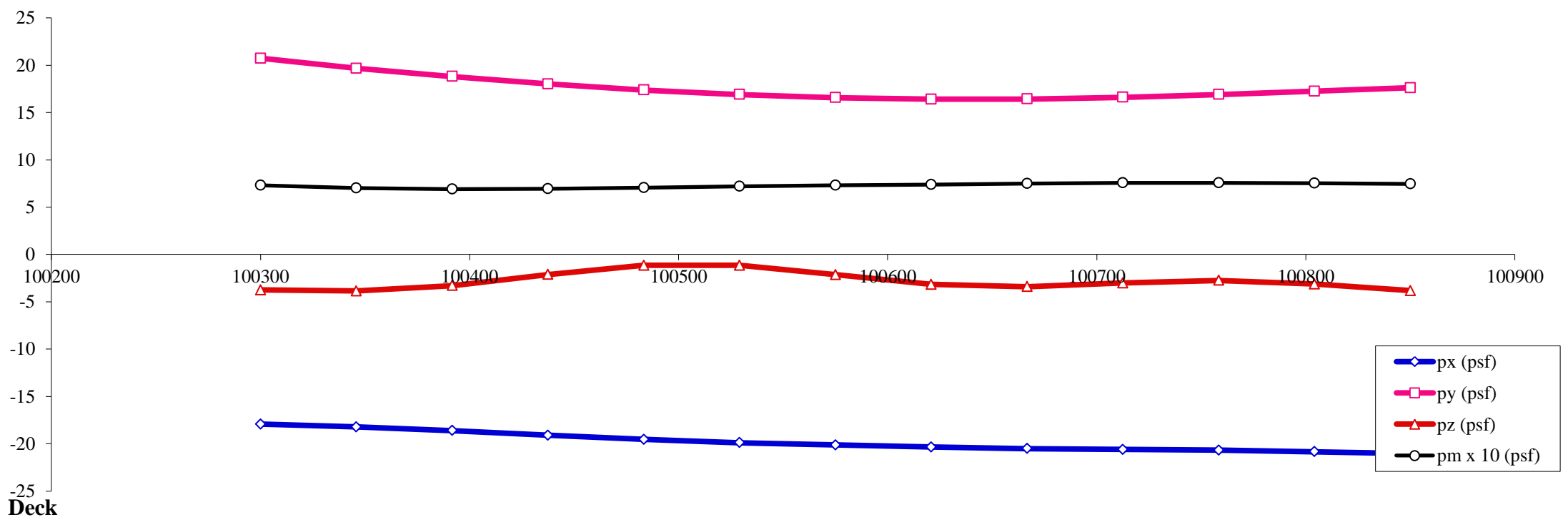
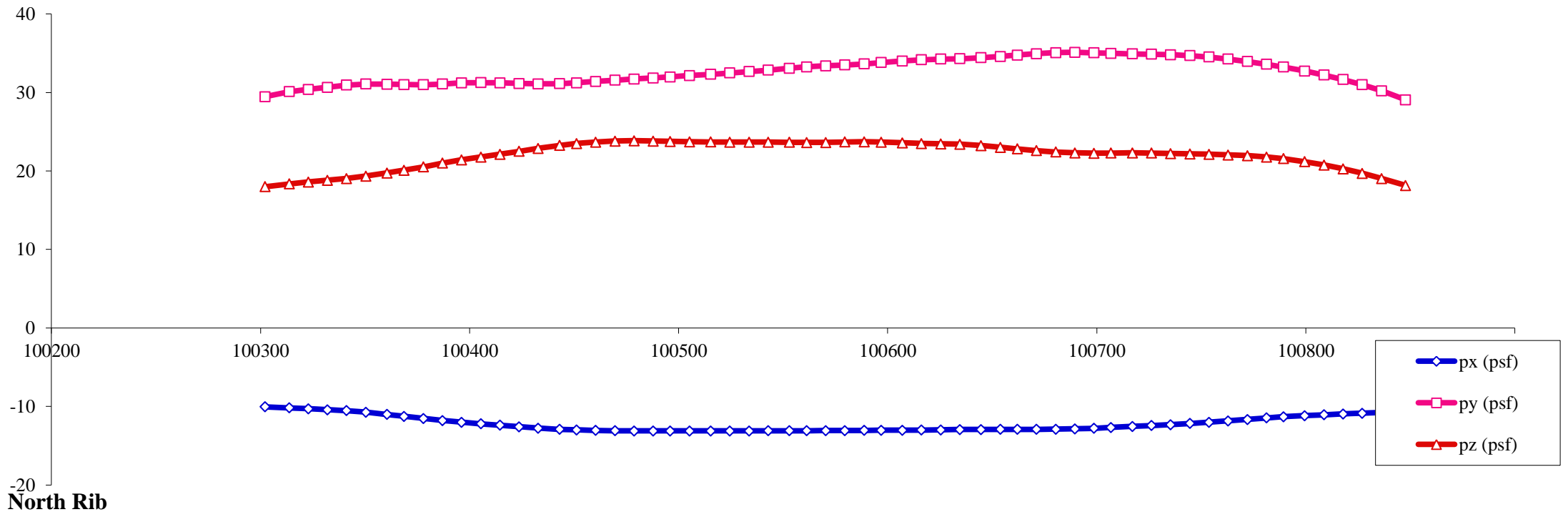
Load case : **25** Objective: Max positive longitudinal



- Notes:
1. All pressures in (psf)
 2. All coordinates/elevations in (ft)
 3. Loads for hangers, arch bracings, columns, pier caps and footings are not presented here

Load Visualization Page

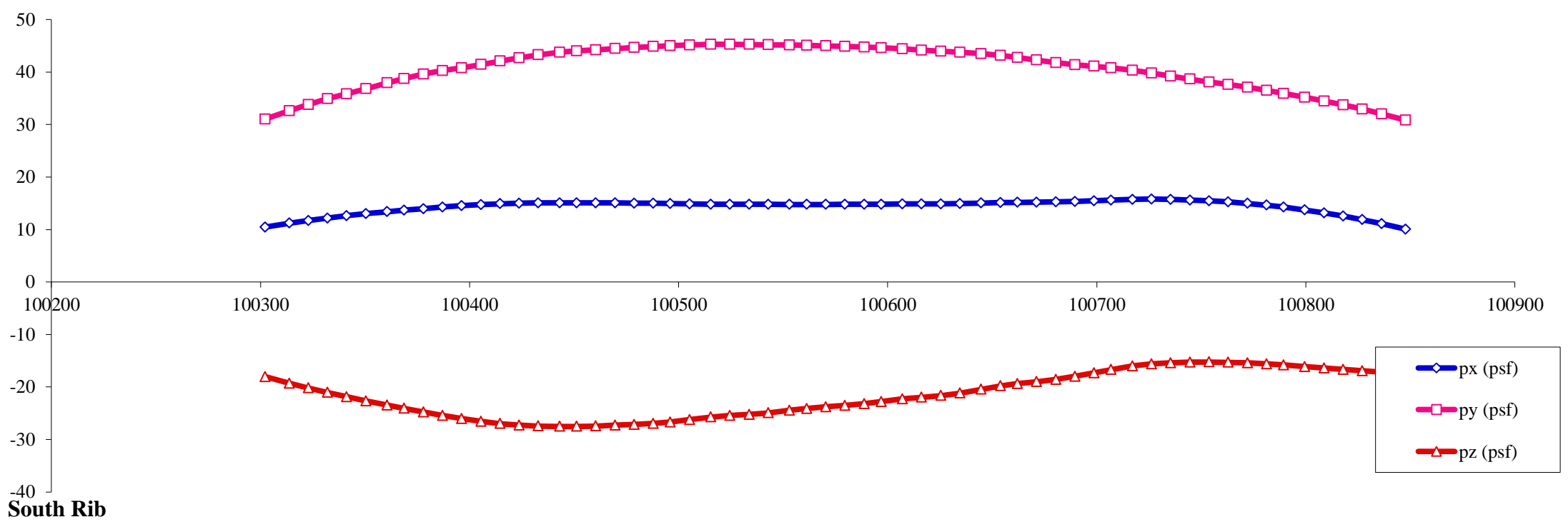
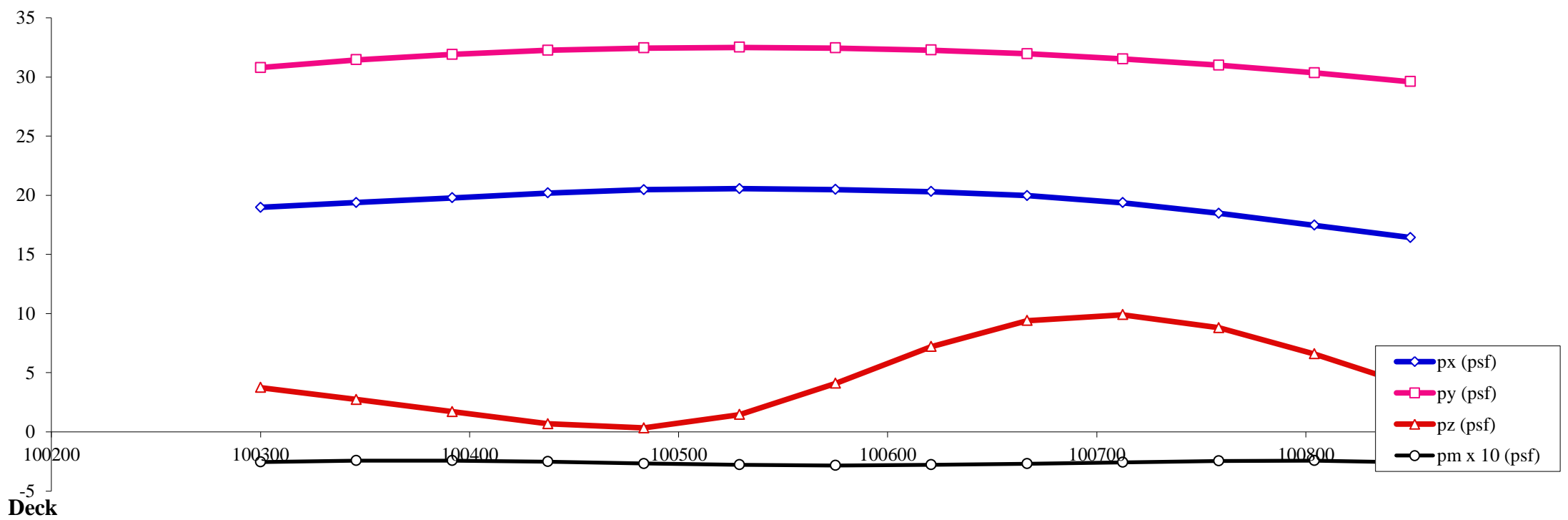
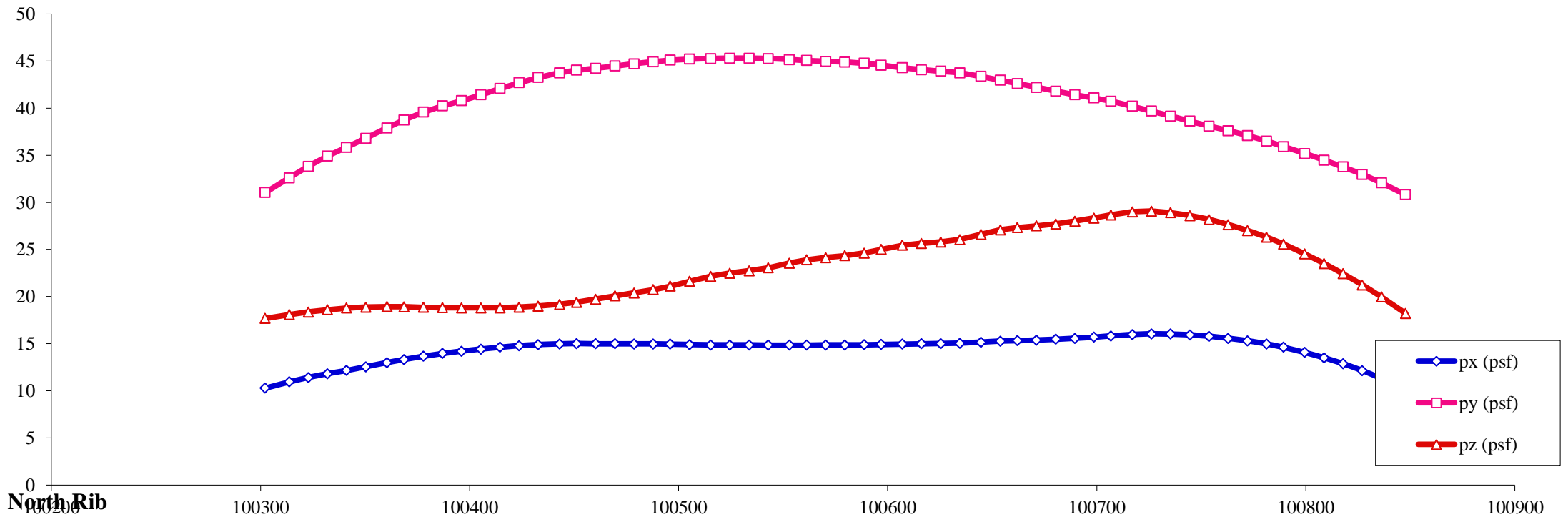
Load case : **26** Objective: Max negative longitudinal



- Notes:**
1. All pressures in (psf)
 2. All coordinates/elevations in (ft)
 3. Loads for hangers, arch bracings, columns, pier caps and footings are not presented here

Load Visualization Page

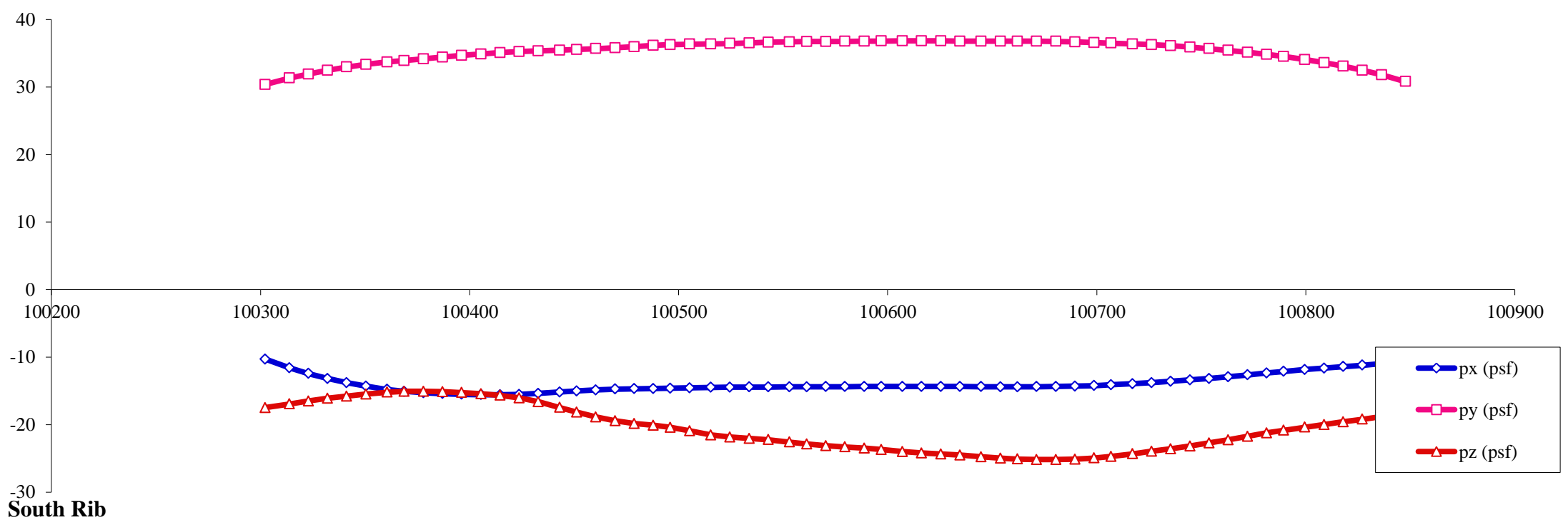
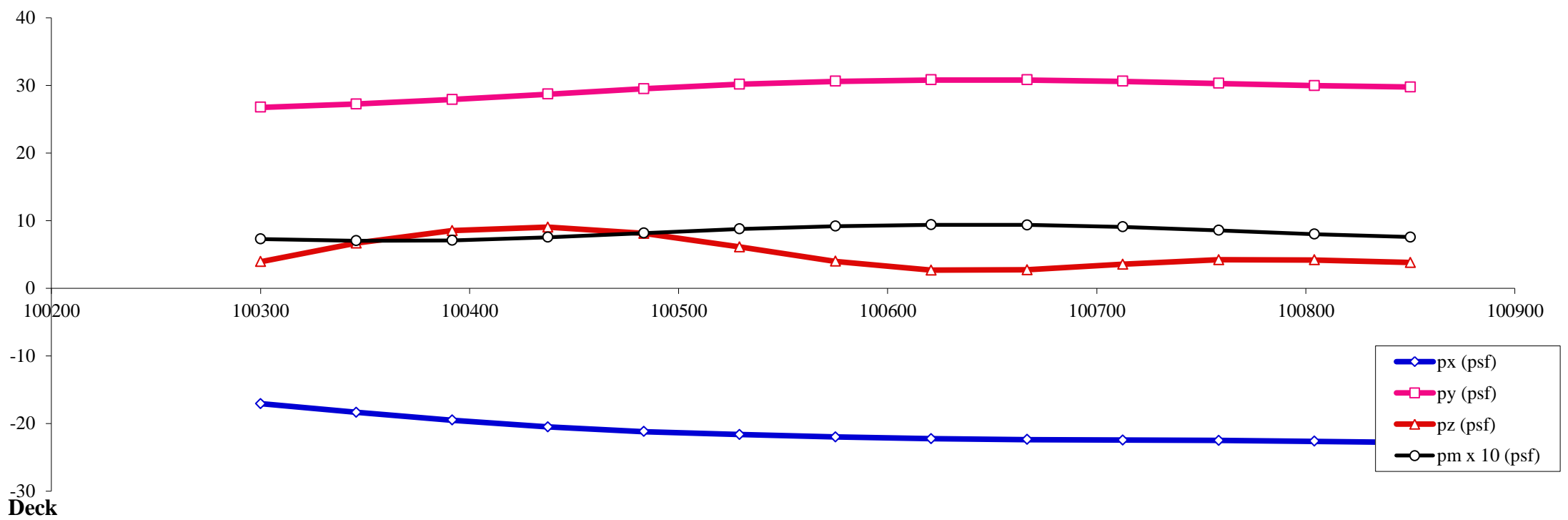
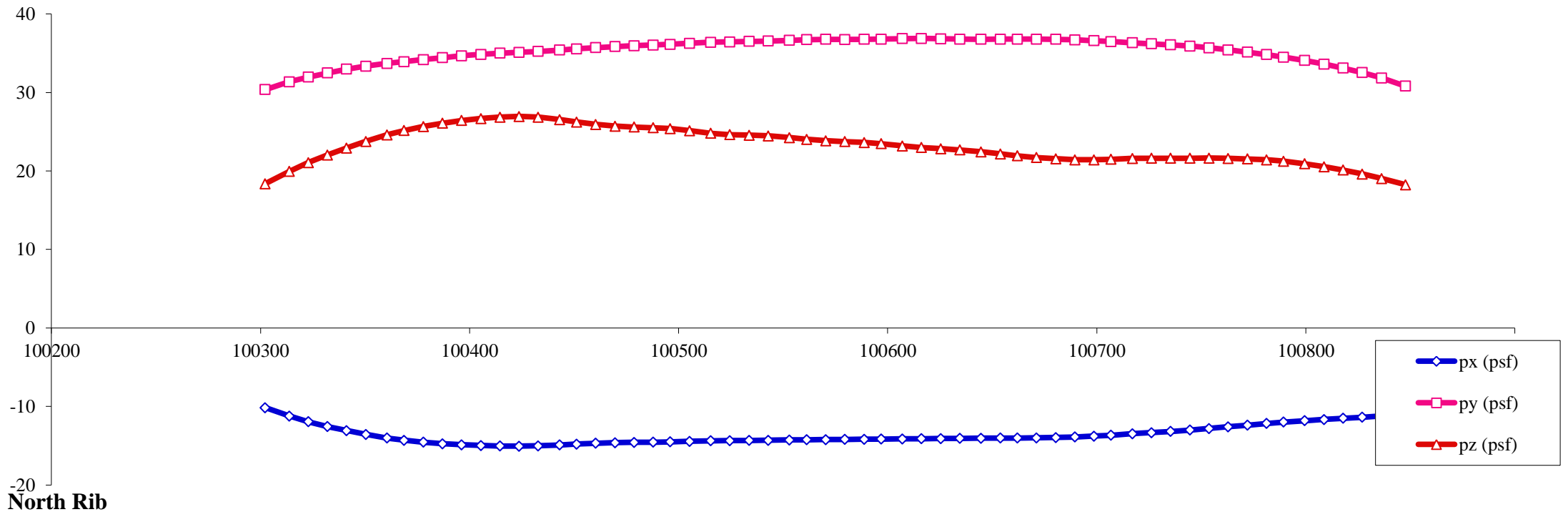
Load case : **27** Objective: Max positive longitudinal, differential between piers and deck



- Notes:
1. All pressures in (psf)
 2. All coordinates/elevations in (ft)
 3. Loads for hangers, arch bracings, columns, pier caps and footings are not presented here

Load Visualization Page

Load case : **28** Objective: Max positive longitudinal, differential between piers and deck



- Notes:
1. All pressures in (psf)
 2. All coordinates/elevations in (ft)
 3. Loads for hangers, arch bracings, columns, pier caps and footings are not presented here

APPENDIX D

Document RWDI BR02-2007

Reference Document
RWDI BR02-2007

WIND RESPONSE ANALYSIS

AND

DESIGN LOADS

by Stoyan Stoyanoff

March 30, 2007

1. Background

During the design of any bridge sensitive to wind, there are two fundamental requirements considering strong, turbulent winds:

- a) that the bridge should be stable and comfortable; and
- b) it must withstand to the wind storms without damages.

Therefore when examining bridge's response to wind, the first concern would be to ensure its stability against flutter, vortex shedding, and/or galloping. Once an aerodynamically stable bridge design is framed, design wind loads need to be applied for verification of its structural integrity. This design process requires experimental verifications and theoretical analyses for stability and response. The following document presents the fundamentals of the method currently utilized at RWDI for bridge studies or on other slender line-like structures such as towers. Its basic apparatus is a computer system called *3D Response Analysis* including an advanced stability (called *3D Flutter Analysis*) and buffeting response analyses (called *3D Buffeting Analysis*).

For derivation of the wind loads acting on a bridge, theoretical buffeting analysis is conducted. Background theory of buffeting response analysis has been under development and testing for many years at RWDI. Its methodology can be traced back to Davenport¹ (1961) and Irwin² (1977) available upon request on the more recent document RD01-1996. The required input parameters include static aerodynamic force coefficients, mass and polar moment of inertia, bridge dimensions, modal frequencies and shapes, structural damping, and wind turbulence properties. Typical forms of power spectra and co-spectra of turbulence, and representative aerodynamic admittance functions are also applied. Statistical predictions of peak responses are obtained from a solution of the dynamic equations of motion.

¹ Davenport, A.G., The response of Slender Line-Like Structures to a Gusty Wind, *Institute Civil Eng.* 23, 389-408, 1962.

² Irwin, P.A., Wind Tunnel and Analytical Investigations of the Response of Lions' Gate Bridge to a Turbulent Wind, National Research Council of Canada, *NAE Report LTR-LA-210*, June 1977.

An effective solution method is the direct integration of these basic equations in time domain.³ The time domain approach generally involves two steps during the analysis:

- a) numerical simulation of turbulence velocity histories and wind loads; and
- b) evaluation of the structural response due to these loads.

This method allows one to take into account a variety of complex events associated with the turbulent wind, the structure, and its response. Since the system stability problem is an inherent part of the selected solution technique, as a natural extension to the buffeting analysis method, *3D Flutter Analysis* was also incorporated. Its improved matrix formulation⁴ is based on the original “multi-mode-flutter” works of Xie,⁵ and Agar.⁶ Current extension of this analysis allows 3D stabilizing effects such as added mass and aerodynamic damping on the towers and main cables to be also included. The stability of complex coupled bridge modes can be verified which are difficult to examine solely via sectional model testing. As a result more reliable and less conservative flutter prediction could be attained.

This document offers detailed explanations of the theoretical methods employed at RWDI for

- a) flutter stability analysis;
- b) buffeting response analysis; and
- c) derivation of design wind loads.

To shorten current document, certain theoretical parts are only referenced to other sources or RWDI documents. Examples of application of the presented methodology are also given.

³ Stoyanoff, S. A unified approach for 3D stability and time domain response analysis with application of quasi-steady theory, *Journal of Wind Engineering and Industrial Aerodynamics*, v. 89, pp. 1591-1606, 2001.

⁴ Stoyanoff, S., *Wind Induced Vibrations of Cable-Stayed Bridges*, Ph.D. Thesis, Graduate School of Engineering, Kyoto University, Japan, 1993.

⁵ Xie, J. State Space Method for 3D Flutter Analysis of Bridge Structures, Asia-Pacific Symposium on Wind Engineering, Roorkee, India, pp. 269-276, 1985.

⁶ Agar, T. J. A. The Analysis of Aerodynamic Flutter of Suspension Bridges, *Computers & Structures*, vol. 30, pp. 593-600, 1988.

2. Numerical Simulations of Wind Loads

As Figure 1 shows, wind speeds are simulated at a finite number of locations. The bridge deck, towers, and cables are divided about these points into finite length segments called “strips” where their properties such as mass, exposed areas, and wind loads are lumped. For simulation of turbulent wind speeds, time series are created using autoregressive technique.^{7,8,9}

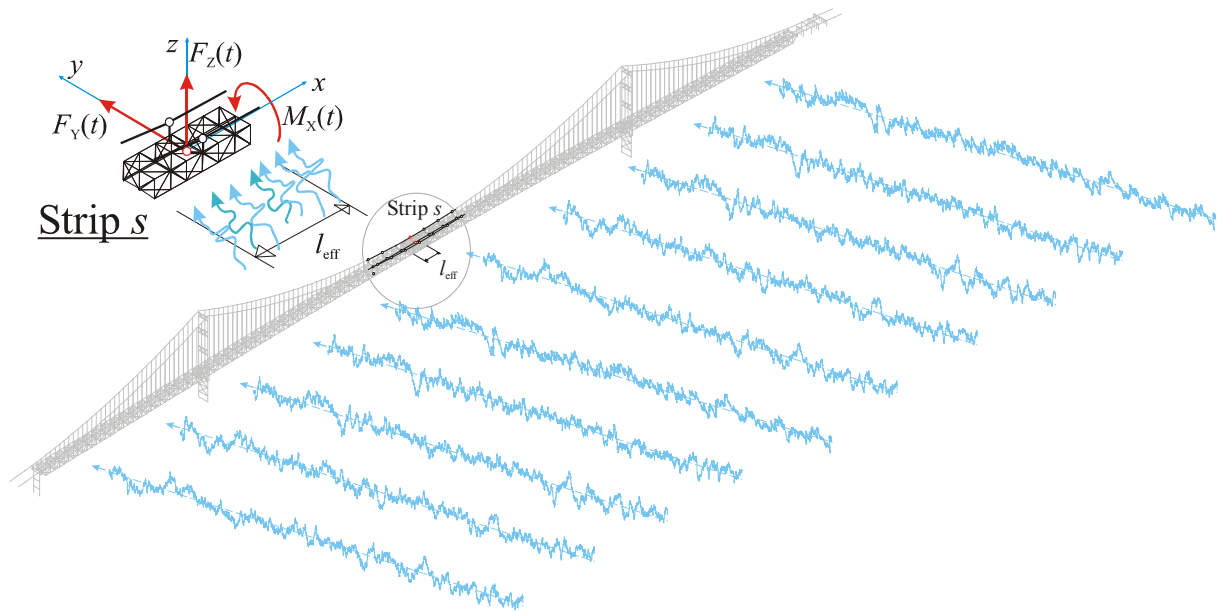


Figure 1: Simulation of wind speeds, forces and moments at discrete points over a bridge (the 3D FEA model is of the Existing Tacoma Bridge - courtesy of Parsons/HNTB/WSDOT).

The wind speeds are then converted into instantaneous drag and lift forces, and moments acting over these finite length parts of the deck, towers, and cables.³ Aerodynamic admittance is incorporated into these loads using Irwin’s equation.³ Based on the wind speed distribution, aeroelastic self-excited forces are estimated following either the quasi-static assumptions¹⁰ or using the unsteady aerodynamic theory.¹¹ Details of this numerical simulation technique are available in a separate technical document available upon request.⁹

⁷ Buchholdt, H.A., Moosavinejad, S., and Iannuzzi, A. Non-linear dynamic analysis of guyed masts subjected to wind and guy ruptures, Proc. Instn. Civ. Engrs., Part 2, Vol. 81, pp. 353-395, 1986.

⁸ Stoyanoff, S. and Irwin, P.A. Simulation of wind loads in time domain, RWDI Project 94-052, 1995.

⁹ BR01-2007, Numerical Simulation of Wind Turbulence, RWDI Reference Document, March 7, 2007.

¹⁰ Naudascher, N. and Rockwell, D. Flow-Induced Vibrations: An Engineering Guide, Balkema, Rotterdam, 1994.

¹¹ Scanlan, R. The action of flexible bridges under wind II: buffeting theory, Sounds Vibrations 60, 201-211, 1978.

3. Estimation of Bridge Response

Bridge stability and response in its various modes of vibration are calculated applying RWDI's advanced *3D Response Analysis* procedure. On several occasions in the past, buffeting response predictions of this method were compared satisfactory against the frequency domain method^{3,12,13} and results obtained from aeroelastic model tests.^{6,7} The flutter stability procedure was calibrated against various analytical wind tunnel experiments.^{4,14,15}

3.1 Equations of Motion

The equations of motion of a bridge exposed to the dynamic action of wind can be expressed by:

$$[M]\{\ddot{Z}\} + [C]\{\dot{Z}\} + [K]\{Z\} = \underbrace{\{F\}_{SE} + \{F\}_B}_{\{F\}_{Wind}} \quad (1)$$

where $\{F\}_{SE} = \{D_{SE}, L_{SE}, M_{SE}\}^T$, represents the self-excited, motion dependant load, $\{F\}_B$, the direct buffeting load, and $[M]$, $[C]$, $[K]$ and $\{Z\}$ have their usual meaning. The self-excited load is

$$\{F\}_{SE} = [A(k)]\{\dot{Z}\} + [B(k)]\{Z\}, \quad (2)$$

where $[A(k)]$ are the aerodynamic damping and $[B(k)]$ the aerodynamic stiffness matrixes, function of the reduced frequency $k = \omega b / U_{ref}$ (ω is the circular frequency of motion, b the reference width of given section and U_{ref} the reference mean speed). The stability and response solution method then employs a reduction into the modal space

$$\{Z(s, t)\} = [X(s)]\{\Phi(t)\}, \quad (3)$$

¹² Stoyanoff, S., Kelley, D., Irwin, P. Abrahams, M., and Bryson J. Aerodynamic Analysis and Wind Design for the Cooper River Bridges Replacement, in Proc. International Bridge Conference Pittsburgh, Pennsylvania, IBC 03-52, June 9-11, 2003.

¹³ Stoyanoff, S., Irwin, P., Xie, J., and Hunter, M. Wind Tunnel Testing of the Parallel Tacoma Bridges, in proc. International Symposium Steelbridge 2004, Millau, France, June 23-25, 2004.

¹⁴ Stoyanoff S., and Larose, G. Identification of Aerodynamic Derivatives: A Parametric Study, International Colloquium BBAA V, Ottawa, Canada, 2004.

¹⁵ Stoyanoff S. and Irwin, P. Flutter Analysis of Lions' Gate Bridge during Deck Replacement, 6th Asia-Pacific Conference on Wind Engineering (APCWE VI), Seoul, South Korea, 2005.

where $[X(s)]$ is a modal matrix composed of the first m spatial eigenvectors $\{X(s)\}_j$, and $\{\Phi(t)\}$ is the generalized coordinates vector. Leaving out the obvious spatial s , and temporal t variables, substituting Equations (2) and (3) in (1) and multiplying from left by $[X]^T$ results in

$$[M]^* \{\ddot{\Phi}\} + [\tilde{C}]^* \{\dot{\Phi}\} + [\tilde{K}]^* \{\Phi\} = \{\tilde{F}\}_B^* \quad (4)$$

where the generalized mass, damping, and stiffness matrices, and buffeting load vector are

$$\begin{aligned} [M]^* &= [X]^T [M] [X] = I, \quad (\text{the eigenvectors must be orthogonal}) \\ [\tilde{C}]^* &= [X]^T [C] [X] - [X]^T [A] [X] = \text{diag}[2\zeta_j \omega_j] - [A]^* \\ [\tilde{K}]^* &= [X]^T [K] [X] - [X]^T [B] [X] = \text{diag}[\omega_j^2] - [B]^* \\ \{F\}_B^* &= [X]^T \{F\}_B, \end{aligned} \quad (5)$$

with ζ_j and ω_j being the undamped circular frequency and structural damping ratio of the j^{th} mode. The generalized Equation (4) is then rewritten in its standard state-space form

$$\begin{bmatrix} -\tilde{C}^* & -\tilde{K}^* \\ I & 0 \end{bmatrix} \begin{Bmatrix} \dot{\Phi} \\ \Phi \end{Bmatrix} = \begin{Bmatrix} \ddot{\Phi} \\ \dot{\Phi} \end{Bmatrix} + \begin{Bmatrix} -F^* \\ 0 \end{Bmatrix}_B, \quad (6)$$

where Φ is the generalized deflection vector and its derivatives, or in short

$$[S]\{y\} = \{\dot{y}\} + \{Y\}. \quad (7)$$

The homogeneous solution of this differential equation of first order provides the stability of the system, which combined with its particular solution, describes fully the stability and buffeting response of the bridge³. In stability analysis, the effect of turbulence on flutter onset is not considered which typically was found as being conservative.¹⁶ This stabilizing effect of turbulence on flutter however could only be accounted for via aeroelastic model tests.

¹⁶ Wardlaw, R. L. Wind effects on bridges, International Colloquium BBAA I, 635-645, Kyoto, Japan, 1988.

3.2 Direct Buffeting Loads

Based on quasi-static assumption, the direct buffeting loads on the j^{th} strip of length l_j are calculated from the instantaneous wind speeds employing

$$\{f\}_{\text{BL},j} = [o]_j \{w\}_j, \quad (8)$$

where the force coefficient matrix in body coordinates takes the form

$$[o]_j = p_j l_j \begin{bmatrix} C_X & 2C_X & C'_X \\ C_Z & 2C_Z & C'_Z \\ bC_M & 2bC_M & bC'_M \end{bmatrix}_j, \text{ where } C'_{X(Z,M)} = \frac{dC_{X(Z,M)}}{d\alpha},$$

$$p = \frac{1}{2} \rho b U_j^2, \quad U_j = v_{\text{Scale},j} U_{\text{ref}} \left(\frac{z_j}{z_{\text{ref}}} \right)^{\alpha_p}, \text{ for } j = 1..n \text{ number of nodes.} \quad (9)$$

In Equation (9) U_{ref} is the reference speed, z_j the elevation and α_p the power law constant describing the wind profile at the site, and $v_{\text{Scale},j}$, a constant for local speed profile corrections. The wind velocity vector of the same strip is

$$\{w\}_j = \left\{ 1, \frac{u}{U_j}, \frac{w}{U_j} \right\}_j^T, \text{ for horizontal deck and the main cables or} \quad (10)$$

$$\{w\}_j = \left\{ 1, \frac{u}{U_j}, \frac{v}{U_j} \right\}_j^T, \text{ for vertical tower legs.}$$

In the above equations, C_X is the drag and C_Z lift force coefficient, and C_M the torsional moment coefficients. The slopes of these static coefficients $C'_{X(Z,M)}$ provide their rate of change against the angle of wind attack α . Body coordinates are used where all coefficients are normalized with the deck (or the tower) width b . Aerodynamic admittance is incorporated as spectral corrections into the zero-mean longitudinal velocity u , lateral v and vertical w components (for details refer to Reference Document BR01-2007).

3.3 Aerodynamic Damping and Stiffness

If a bridge section is allowed to move laterally, vertically, and to rotate, for winds close to normal to the bridge, motion dependent drag D_{SE} , lift L_{SE} , and moment M_{SE} per unit length can be modeled¹⁷ as

$$\begin{aligned} D_{SE} &= \frac{1}{2} \rho U^2 b \left[kP_1^* \frac{\dot{p}}{U} + kP_2^* b \frac{\dot{\alpha}}{U} + k^2 P_3^* \alpha + k^2 P_4^* \frac{p}{b} + kP_5^* \frac{\dot{h}}{U} + k^2 P_6^* \frac{h}{b} \right], \\ L_{SE} &= \frac{1}{2} \rho U^2 b \left[kH_1^* \frac{\dot{h}}{U} + kH_2^* b \frac{\dot{\alpha}}{U} + k^2 H_3^* \alpha + k^2 H_4^* \frac{h}{b} + kH_5^* \frac{\dot{p}}{U} + k^2 H_6^* \frac{p}{b} \right], \\ M_{SE} &= \frac{1}{2} \rho U^2 b^2 \left[kA_1^* \frac{\dot{h}}{U} + kA_2^* b \frac{\dot{\alpha}}{U} + k^2 A_3^* \alpha + k^2 A_4^* \frac{h}{b} + kA_5^* \frac{\dot{p}}{U} + k^2 A_6^* \frac{p}{b} \right], \end{aligned} \quad (11)$$

where the aerodynamic derivatives P_r^* , A_r^* , and H_r^* , $r=1..6$ are functions of the reduced frequency k , with ρ being the air density, and $U=U_j$. Here p is the lateral and h the vertical deflection, and α is the rotation components of vector $\{Z\}$ and its first derivative. Based of Equation (11) are produced the aerodynamic damping and stiffness matrices introduced in Equation (2). Equations (2) and (11) could be applied to the bridge's deck, towers and supporting cable system, providing aerodynamic derivatives of each section are available. Alternatively, quasi-static theory could be employed.¹⁸ At the j^{th} node the local matrixes can be evaluated as

	Aerodynamic derivatives	Quasi - static theory (body coordinates)
Aerodynamic damping	$[A]_j^{\text{AD}} = p_j \frac{l_j}{U_j} k_j \begin{bmatrix} P_1^* & P_5^* & bP_2^* \\ H_5^* & H_1^* & bH_2^* \\ bA_5^* & bA_1^* & b^2 A_2^* \end{bmatrix},$	$[A]_j^{\text{QS}} = p_j \frac{l_j}{U_j} \begin{bmatrix} -2C_X & -C'_X & 0 \\ -2C_Z & -C'_Z & 0 \\ -2bC_M & -bC'_M & 0 \end{bmatrix}_j,$
Aerodynamic stiffness	$[B]_j^{\text{AD}} = p_j l_j k_j^2 \begin{bmatrix} P_4^* \frac{1}{b} & P_6^* \frac{1}{b} & P_3^* \\ H_6^* \frac{1}{b} & H_4^* \frac{1}{b} & H_3^* \\ A_6^* & A_4^* & bA_3^* \end{bmatrix},$	$[B]_j^{\text{QS}} = p_j l_j \begin{bmatrix} 0 & 0 & C'_X \\ 0 & 0 & C'_Z \\ 0 & 0 & bC'_M \end{bmatrix}_j, \quad (12)$

Typically aerodynamic damping and stiffness on the deck could be calculated from the aerodynamic derivatives whereas over the cables and tower legs, the quasi-static formulae are used. On many

¹⁷ Singh, L., Jones, N., Scanlan, R., and Lorendeaux, O. Simultaneous identification of 3-dof aeroelastic parameters, In Proc. 9th International Conference on Wind Engineering, p. 972-981, New Delhi, India, 1995.

¹⁸ Scanlan R. Interpreting Aeroelastic Models of Cable-Stayed Bridges, Journal Engineering Mechanics Division, ASCE, vol. 113, No. 4, pp. 555-575, 1987.

bridges only 8 derivatives are evaluated corresponding to the 2DOF case of vertical and torsional motions. In general the lateral damping term $P_1^* = -(2/k)C_X$ is included in the analysis, whereas higher order terms $A_{5,6}^*$, $H_{5,6}^*$, and the remaining $P_{2..6}^*$ are set to zero. Recently however with the introduction of super long-span bridges such as Stonecutters and Messina, these lateral derivatives were recognised as being important and included into the analysis.

3.4 Assembling of the Overall Aerodynamic Matrixes

The nodal deflection and speed vectors for j^{th} node are written as $\{\dot{z}\}_j = \{\dot{p} \quad \dot{h} \quad \dot{\alpha}\}_j^T$, and $\{z\}_j = \{p \quad h \quad \alpha\}_j^T$, which are then rearranged to 6DOF per node as defined by the 3D finite element analysis model. The local matrixes are then expanded into 6DOF per node to form the overall aerodynamic matrixes as

$$\begin{aligned}
 [A(k)] &= \begin{bmatrix} [B]_1 & 0 & \dots & 0 \\ 0 & [B]_2 & \dots & 0 \\ \dots & \dots & \dots & \dots \\ 0 & 0 & \dots & [B]_n \end{bmatrix}_{6n \times 6n}, \\
 [B(k)] &= \begin{bmatrix} [B]_1 & 0 & \dots & 0 \\ 0 & [B]_2 & \dots & 0 \\ \dots & \dots & \dots & \dots \\ 0 & 0 & \dots & [B]_n \end{bmatrix}_{6n \times 6n}, \\
 [O] &= \begin{bmatrix} [O]_1 & 0 & \dots & 0 \\ 0 & [O]_2 & \dots & 0 \\ \dots & \dots & \dots & \dots \\ 0 & 0 & \dots & [O]_n \end{bmatrix}_{6n \times 6n},
 \end{aligned} \tag{13}$$

It should be noted that the strip model actually is reduced from the full 3D finite element model where typically depending on the bridge span from 50 to about 350 selected nodes would be sufficient for an adequate wind response analysis.

3.5 Stability Solution

The homogeneous solution of Equation (7) establishes the system stability. It comprises a set of conjugated complex eigenvalues λ_i and vectors $\{\Psi\}_i$, for the $i=1..2m$ modes retained for analysis

$$\{y(t)\} = \begin{Bmatrix} \{\dot{\Phi}(t)\} \\ \{\Phi(t)\} \end{Bmatrix} = \{\Psi\}e^{\lambda t}, \quad \{\Psi\} = \begin{Bmatrix} \lambda\{\phi\} \\ \{\phi\} \end{Bmatrix}, \quad (14)$$

where $\{\phi\}$ are the generalized eigenvectors of the transformed generalized system. The complex conjugated eigenvalue variable $\lambda_i = \mu_i \pm i \omega_i$, where $\tilde{\omega}_i = \sqrt{\mu_i^2 + \omega_i^2}$, is the pseudo-undamped circular frequency. The damping ratio and damped frequency are $\zeta_i = -\frac{\mu_i}{\omega_i}$, and $\omega_i = \tilde{\omega}_i \sqrt{1 - \zeta_i^2}$, where ζ_i is the total damping ratio comprising aerodynamic plus structural ($\delta_i = 2\pi\omega_i$ is the logarithmic decrement) and ω_i is the circular frequency of response.

The criterion for stability of any structure is the condition if

$\exists i : \zeta_i \leq 0$ divergent or non-decaying oscillations (i.e., flutter or galloping) or if

$\forall i : \zeta_i > 0$ decaying oscillations of a dynamically stable system.

That is, a system is regarded to be a dynamically stable if and only if the $\zeta_i > 0$ stability conditions are fulfilled for all modes.

The reduced frequency of mode i is calculated from the pseudo-undamped frequency as $k_i = \frac{\tilde{\omega}_i b}{U}$. The derivative model introduced by Equation (11) is based on a single reduced frequency k , i.e., it is assumed that only one “flutter” mode aeroelastically dominates the response at a given speed. Under flutter mode is understood any coupled or an uncoupled mode with a torsional component. Modes

where torsion is coupled with sway however are typically more stable since stabilizing damping is introduced through the sway motions. Therefore uncoupled torsional modes or modes with small coupled sway are the most probable flutter modes. The lower the natural frequency of such a “pure” torsional mode, the lower the critical flutter speed. Modes with large motions of the cables and towers are also more stable due to added mass and positive damping. On a suspension bridge is sometimes difficult *a priori* to estimate which mode would have the lowest flutter speed. Therefore the stability of many modes with torsional components has to be verified.

3.6 Buffeting Response Solution

The response to wind buffeting is found solving Equation (7) via the infamous Duhamel integral

$$\{y(t)\} = e^{t[S]}\{y(0)\} + \int_0^t e^{(t-\tau)[S]}\{Y(\tau)\}d\tau, \quad (15)$$

where $\{y(0)\}$ are the initial excitation conditions, $e^{t[S]}$ is the transition matrix with a state-space matrix $[S]_{2m \times 2m}$ where m is the number of modes retained for analysis. Based on the methodology proposed for calculation of this matrix,¹⁹ a very efficient time-marching solution scheme was developed.³ It is based on the fact that wind loads are numerically generated at discrete time $t=0\Delta t, 1\Delta t, 2\Delta t, \dots$ steps which allows calculation of the responses as time histories of modal deflections $\{Z\}_j$, velocities $\{\dot{Z}\}_j$ and accelerations $\{\ddot{Z}\}_j$ at any strip along the bridge. The integration is exact and allows using rather long time steps such as 0.1 sec. The overall response is found summing these time histories as

$$\{Z\} = \{Z\}_1 + \{Z\}_2 + \{Z\}_3 + \dots + \{Z\}_m, \quad \{\dot{Z}\} = \{\dot{Z}\}_1 + \{\dot{Z}\}_2 + \{\dot{Z}\}_3 + \dots, \quad \text{and} \quad \{\ddot{Z}\} = \{\ddot{Z}\}_1 + \{\ddot{Z}\}_2 + \{\ddot{Z}\}_3 + \dots \quad (16)$$

The mean, root-mean-square, and peak modal responses are then found from the statistic of these time series. It should be noted that this level of response information is very comprehensive and similar to what could be obtained via direct measurements from aeroelastic model tests.

¹⁹ Meirovitch, L. Elements of Vibration Analysis, 2nd edition, McGraw-Hill, New York, 1986.

4. Design Wind Loads

Combining wind with other loads such as dead and thermal, structural design could be carried out directly solving Equation (1) in the time domain. However the aerodynamic damping that might be several times higher than the structural inherent damping must be included and this causes problems. The aerodynamic damping and stiffness depend on the structural deflections and thus would greatly defer from one mode of vibration to another. Most of the FEA programs today would integrate Equation (1) directly where the challenge would be in converting the modal aerodynamic damping and stiffness into matrix proportional damping (Rayleigh damping).²⁰ Because this difficulty cannot completely be surmounted, design based on a direct integration is rarely used.

For derivation of design loads, Equation (1) could be rewritten as

$$[K]\{Z\} = \{F\}_{\text{Wind}} - \underbrace{[M]\{\ddot{Z}\}}_{\text{Inertia}} - \underbrace{[C]\{\dot{Z}\}}_{\text{Damping}}, \quad (17)$$

since any structure would resist to the external and internal loads with its stiffness alone. Equation (17) balances in time varying way where peak value of the damping term (including aerodynamic and structural) does not occur at the same instance with the external and inertial loading. Since the structural velocities are out of phase to the deflections and accelerations, the damping term could be neglected. The contribution of the aerodynamic stiffness in air is small and could also be discarded. The right-hand side of Equation (17) then simplifies to

$$\{F\}_{\text{WL}} = \{\{\bar{F}\} + \{\tilde{F}\}\}_{\text{B}} - [M]\{\{\ddot{Z}\}_1 + \{\ddot{Z}\}_2 + \dots + \{\ddot{Z}\}_m\} \quad (18)$$

where $\{\bar{F}\}$ is the mean and $\{\tilde{F}\}$ the dynamic part called *background wind load*, and the inertial part or *resonant loads*. Since these resonant and the background wind loads are statistically independent

$$\{\bar{F}\}_{\text{WL}} = \{\bar{F}\} \pm \sqrt{\{\tilde{F}\}^2 + \sum_i \left\{ \frac{[M]\{\ddot{Z}\}_i}{\{\tilde{F}\}_i} \right\}^2}. \quad (19)$$

²⁰ Clough, R. W. and Penzien, J. Dynamics of Structures, McGraw-Hill International Editions, Singapore, 1986.

provides their peak load envelope (square root of the sum of the squares SRSS). This formula however is not straightforward for design implementations. The loading envelope is never fully attained in any instance of time rather it represents the boundary of many possible load distributions. A reasonable technique is then to derive various expected loading cases that could cover the critical loading scenarios. The method of equivalent static load combinations is used

$$\{\hat{F}\}_{WL,k} = \bar{c}\{\bar{F}\} + [\tilde{c}]_{BG}\{\tilde{F}\} + c_{1,k}\{\hat{F}\}_1 + c_{2,k}\{\hat{F}\}_2 + \dots + c_{m,k}\{\hat{F}\}_m, \quad (20)$$

where the combination coefficients c need to be assigned to both background and resonant loads. The mean coefficient \bar{c} is normally set to 1.0 but it could be modified when sheltering modification effects are sought.

4.1 Combination Coefficients of Background Loads

Wind turbulence or gustiness causes fluctuations in wind loads about certain mean value. These loads are complex since the gusts are not well correlated along the span and even over the width of the deck. However, via integration of the instantaneous wind loads over the entire bridge structure in a time domain simulation, appropriate gust factors gf can be derived

$$gf_{Load} = \frac{\bar{F}_{Load} + pf_{Load}\sigma_{Load}}{\bar{F}_{Load}}, \quad (21)$$

where pf_{Load} is the peak factor and σ_{Load} is the standard deviation (or root-mean-square) of given load. It should be noted that for any *Load* being D - drag, V - lift or T - torsional moment, its peak factor would be different. An accurate technique for estimation of peak factors would be via integration over the bridge or part of it for given load at every time step and following statistical analysis of the resulting time series of overall loading

$$F_{Load}(t) = \int_0^L F_{Load}(t,s)ds, \quad (22)$$

and L could be either part or whole the deck length, tower height, or sometimes when overall gust loading effects are considered, even the whole bridge. The statistics of this partial or overall gust load is found as

$$\begin{aligned}\bar{F}_{\text{Load}} &= \frac{1}{T} \int_0^T F_{\text{Load}}(t) dt, \\ \sigma_{\text{Load}} &= \sqrt{\frac{1}{T} \int_0^T (\bar{F}_{\text{Load}} - F_{\text{Load}}(t))^2 dt}, \\ pf_{\text{Load}} &= E[99.9\%, (F_{\text{Load}} - \bar{F}_{\text{Load}})]\end{aligned}\tag{23}$$

The peak factor is found via integration of the probability distribution curve E with 99.9% confidence. These gust factors are then applied on the mean wind pressure to account for the direct gust loading on the bridge. The background forces and moments are derived multiplying the corresponding mean loads by

$$\begin{aligned}gf_{\text{Load,BG}} &= (gf_{\text{Load}} - 1), \text{ to obtain} \\ \tilde{F}_{\text{Load}} &= gf_{\text{Load,BG}} \bar{F}_{\text{Load}}.\end{aligned}\tag{24}$$

4.2 Load Combination Coefficients for Inertial Loading

Reference²¹ suggests $c_{j,k} = \pm 1.0$ for only one modal term, ± 0.8 , for two terms, ± 0.6 for four and more terms, with values being close to the expansion $\frac{\sqrt{m}}{m}$, where m is the number of modal terms retained in the combination. It should be noted that background load is also considered in the term count. Following simplified statistical considerations, the $\frac{\sqrt{m}-1}{m-1}$ formula could also be derived. Table 2 presents a rounded range of values provided by these formulae

²¹ Davenport, A.G. and King, J.P.C. Dynamic Wind Forces on Long Span Bridges Using Equivalent Static Loads, International Association for Bridge and Structural Engineering, 12th Congress, (IABSE) Session VI, Sept. 3-7, Vancouver, B.C., 1984.

Table 2: Load combination factors

m	$\frac{\sqrt{m}}{m}$	$\frac{\sqrt{m}-1}{m-1}$
1	1.0	--
2	0.70	0.45
3	0.60	0.40
4	0.50	0.35
5	0.45	0.30

that are typically found from the statistical analysis of dynamic responses measured from aeroelastic models.

4.3 Load Combinations

Various combinations than could be developed of load patterns on the bridge being distributed vertical, lateral, longitudinal, and torsional loads. Each of these loads would represent an individual worst case in terms of the vertical or lateral loading on the deck, lateral loading on the towers, or torsion, with various combinations of the bridge modes of vibration. The load patterns would include symmetric and asymmetric loads over various parts of the bridge. For design these loads are applied simultaneously as static in combination with other types of loads such as dead and temperature loads, and thereafter each main structural member is designed based on the corresponding loading combination that gives the worst loading effects (i.e., stress and strain). For symmetrical bridge designs, lateral loads and torsional moments could be mirrored about bridge's principal axis (typically it is along the deck centerline) thus reducing the number of load cases.

Based on our experience with aeroelastic model tests, any load pattern should include:

- the mean wind load; plus
- one principal dynamic mode of full value and 1 to 3 subordinating modes with combination coefficients in the range of values as shown in Table 2.

When composing load combinations other rules would also apply such as that:

- modes with similar shapes are only combined which allows a reduction in the possible modal combinations;
- the loading envelope according to Equation (19) should not be overly exceeded, therefore values lower than the highest values in Table 2 could also be applied;
- to reduce the number of load cases in some instances, higher values by about 10% could be applied to cover difficult “corners” the loading envelope; and
- a sufficient number of combination should be assembled to cover all branches of the loading envelope (not simultaneously).

Table 3 provides a simplified example for a development of load combinations. A simple one span bridge is considered.

Table 3: Example of load combinations

Load Case	Mean Load	\tilde{c} - Background			Combination factor c for various modes & shapes							
		D	V	T	1	2	3	4	5	6	7	8
					L1	V1	L2	V2	T1	L3	V3	T2
1	1.0	0.5	0.5	0.5	1.0	0.5	0.0	0.0	0.5	0.0	0.0	0.0
2	1.0	0.5	0.5	0.5	0.5	1.0	0.0	0.0	0.5	0.0	0.0	0.0
3	1.0	0.5	-0.5	0.5	0.5	-1.0	0.0	0.0	0.5	0.0	0.0	0.0
4	1.0	0.5	0.5	0.5	0.5	0.5	0.0	0.0	1.0	0.0	0.0	0.0
5	1.0	0.5	0.5	-0.5	0.5	0.5	0.0	0.0	-1.0	0.0	0.0	0.0
6	1.0	1.0	1.0	1.0	0.5	0.5	0.0	0.0	0.5	0.0	0.0	0.0
7	1.0	0.5	0.5	0.5	0.0	0.0	1.0	0.5	0.0	0.0	0.0	0.5
8	1.0	0.5	0.5	0.5	0.0	0.0	0.5	1.0	0.0	0.0	0.0	0.5
9	1.0	0.5	0.5	0.5	0.0	0.0	0.5	-1.0	0.0	0.0	0.0	0.5
10	1.0	0.5	0.5	0.5	0.0	0.0	0.5	0.5	0.0	0.0	0.0	1.0
11	1.0	0.5	0.5	0.5	0.0	0.0	0.5	0.5	0.0	0.0	0.0	-1.0
12	1.0	1.0	1.0	1.0	0.0	0.0	0.5	0.5	0.0	0.0	0.0	0.5
13	1.0	0.6	0.6	0.6	0.0	0.0	0.0	0.0	0.0	1.0	0.6	0.0
14	1.0	0.6	0.6	0.6	0.0	0.0	0.0	0.0	0.0	0.6	1.0	0.0
15	1.0	1.0	1.0	1.0	0.0	0.0	0.0	0.0	0.0	0.6	0.6	0.0

- Note:
1. L – denotes a lateral mode or a mode with a predominant lateral motion
 2. V – denotes a vertical mode or a mode with leading vertical motions
 3. T – denotes a torsional mode or a mode with principal motions in torsion
 4. The mode number shows its order of appearance in a branch of modes, not shape, for example V2 is the 2nd mode with predominant vertical motions.

Given in Table 3 combinations do not fully cover all the possible loading scenarios, depending on its complexity, on long-span bridges 15 to 30 load cases are typically recommended. It should be noted that on many bridges (especially during construction) the modes are highly coupled and separation in branches of lateral, vertical, and torsional modes is often difficult. Nevertheless the described above combination technique is fully applicable with a caution when reducing the number of combinations based on symmetry considerations.

It should be noted that normally given loads do not contain any additional safety or load factors and are to be applied to the structural system in the same manner as would wind loads calculated by code analytical methods.

5. Examples

5.1 Flutter Analysis of Ile d'Orléans Bridge

The Ile d'Orléans Bridge, located near Quebec city, Canada, was open to public in 1935. This steel suspension bridge has a main span of 323 m and side spans of 127 m. Its structure is quite alike the old Lions' Gate Bridge³ in Vancouver. Similarly the aged deck of the Ile d'Orléans Bridge has much deteriorated and is planned to be replaced by a modern, light orthotropic steel deck in an attempt to expand bridge's life and capacity. As part of recent wind engineering study, 3D Flutter Analysis was carried out. Figure 1 shows its strip model consisting of 213 segments (=59 deck + 2x61 main cables + 2x16 towers).

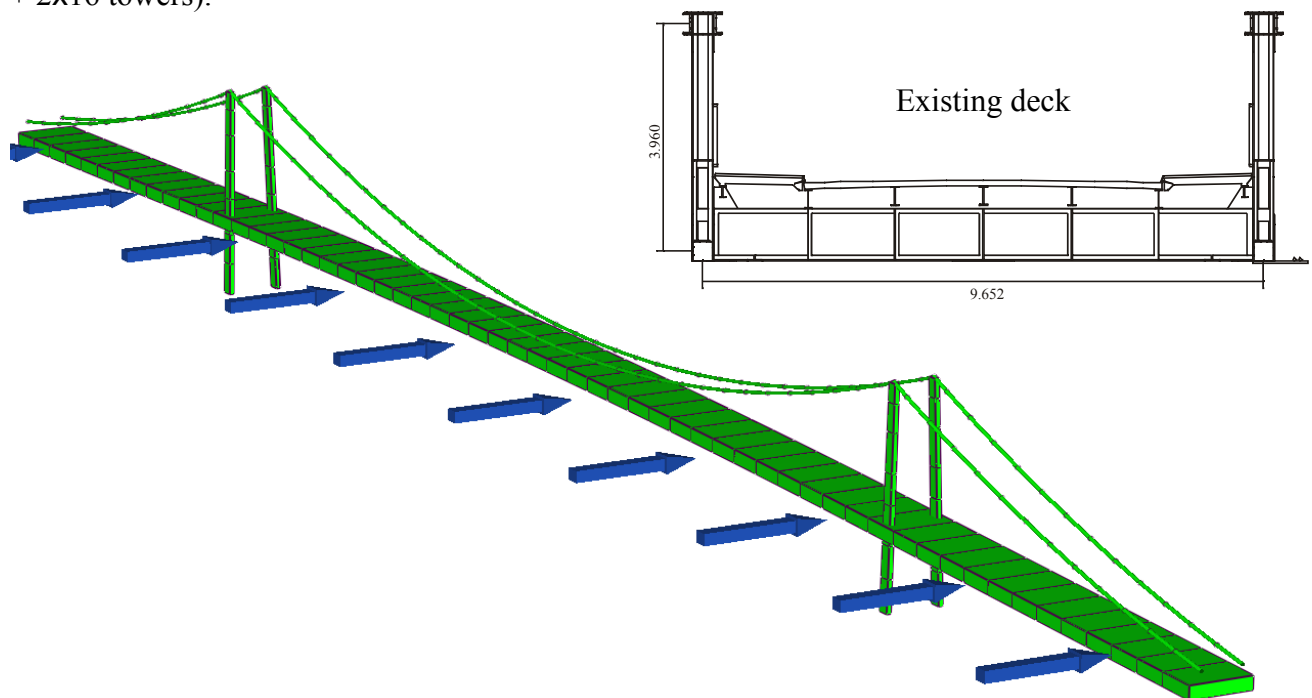


Figure 2: Bridge deck of the Ile d'Orléans Bridge and its 213-node strip model
(courtesy Ministère des Transports du Québec).

From the 2DOF sectional model test based on vertical and torsional motions, aerodynamic derivatives were extracted (Figure 3). Aerodynamic damping in lateral direction of the deck, the main cables and towers was included based on quasi-static theory. Drag coefficient $C_x=1.122$ was

measured of the deck, and $C_x = C'_z = 1.4$ estimated for the towers, and $C_x = C'_z = 1.0$ on the main cables (not of a smooth finish).

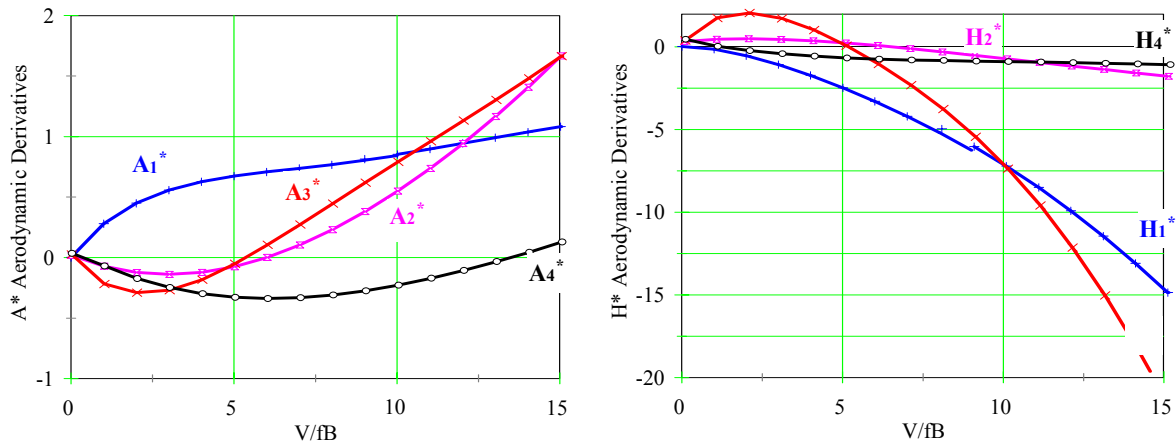


Figure 3: Aerodynamic derivatives of the existing bridge deck.

The sectional model test and direct 2DOF flutter analysis based on aerodynamic derivatives, showed the rather low wind speed of 35 m/sec (last row of Table 4). When the mass of the tower and cables was included, the higher critical speed of 38.1 m/sec was attained.

Table 4: Predicted flutter onset speeds for various conditions.

Modal comb.	Flutter speed		U_{red}	Aerodynamic damping			Mass participation			Type of analysis
	(kph)	(m/sec)		D-L	T	C	D	T	C	
1 to 34	141.2	39.2	10.2	+	+	+	+	+	+	3D Flutter Analysis
14, 19	141.4	39.3	10.2	+	+	+	+	+	+	3D Flutter Analysis
14, 19	138.7	38.5	10.0	+	-	-	+	+	+	3D Flutter Analysis
14, 19	137.1	38.1	9.8	-	-	-	+	+	+	3D Flutter Analysis
14, 19	127.6	35.8	9.3	-	-	-	+	+	-	3D Flutter Analysis
14, 19	125.0	35.0	8.9	-	-	-	+	-	-	Test/2DOF Analysis

Notes: 1. D – deck / D-L – deck lateral; T – tower; C – main cables;
 2. “+” – given component is included; “-” - component off;
 3. Structural damping ratio, vertical mode 1%, torsional mode 1.8% based on field tests.

The further inclusion of lateral aerodynamic damping of the deck and the main cables suggested a critical speed as high as 39.2 m/sec which is slightly higher than the wind speed of 37 m/sec observed at the bridge side over its 70 years of existence. There were never reported any significant vibrations in strong winds.

5.2 Buffeting Analysis of Tacoma Narrows Bridges

Half a century after rebuilding the Tacoma Narrows Bridge, the Washington State Department of Transportation initiated plans to construct a second bridge due to substantial increases in traffic. The new bridge is being built in a very close proximity at 61 m of the existing bridge (see Figure 4).

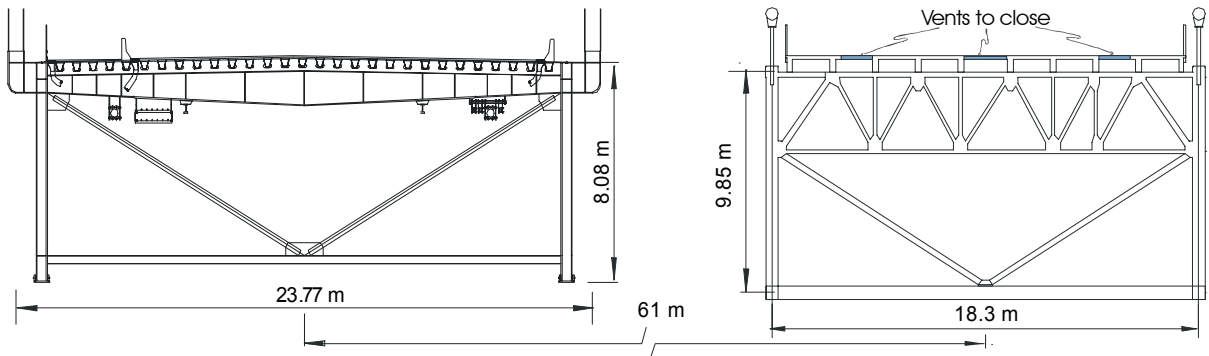


Figure 4: Truss decks of the Parallel Tacoma Bridges (courtesy of Parsons/HNTB/WSDOT).

Among the extensive studies undertaken, wind loads on both bridges were derived analytically based on sectional model tests and confirmed from the aeroelastic model tests (Figure 5).

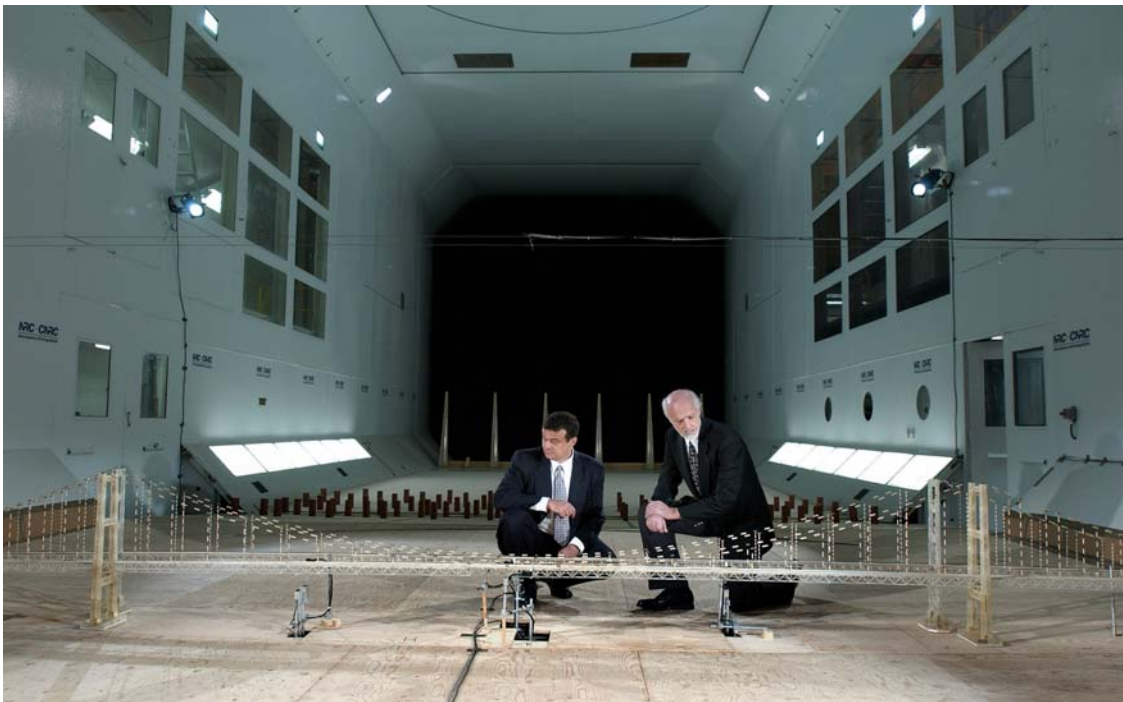


Figure 5: Parallel Tacoma Narrows Bridges – the full aeroelastic models in scale 1:211.

Force and moment coefficients were measured considering both bridges either upwind or downwind in their parallel arrangement (Figure 6). The following example shows only the Existing Bridge.

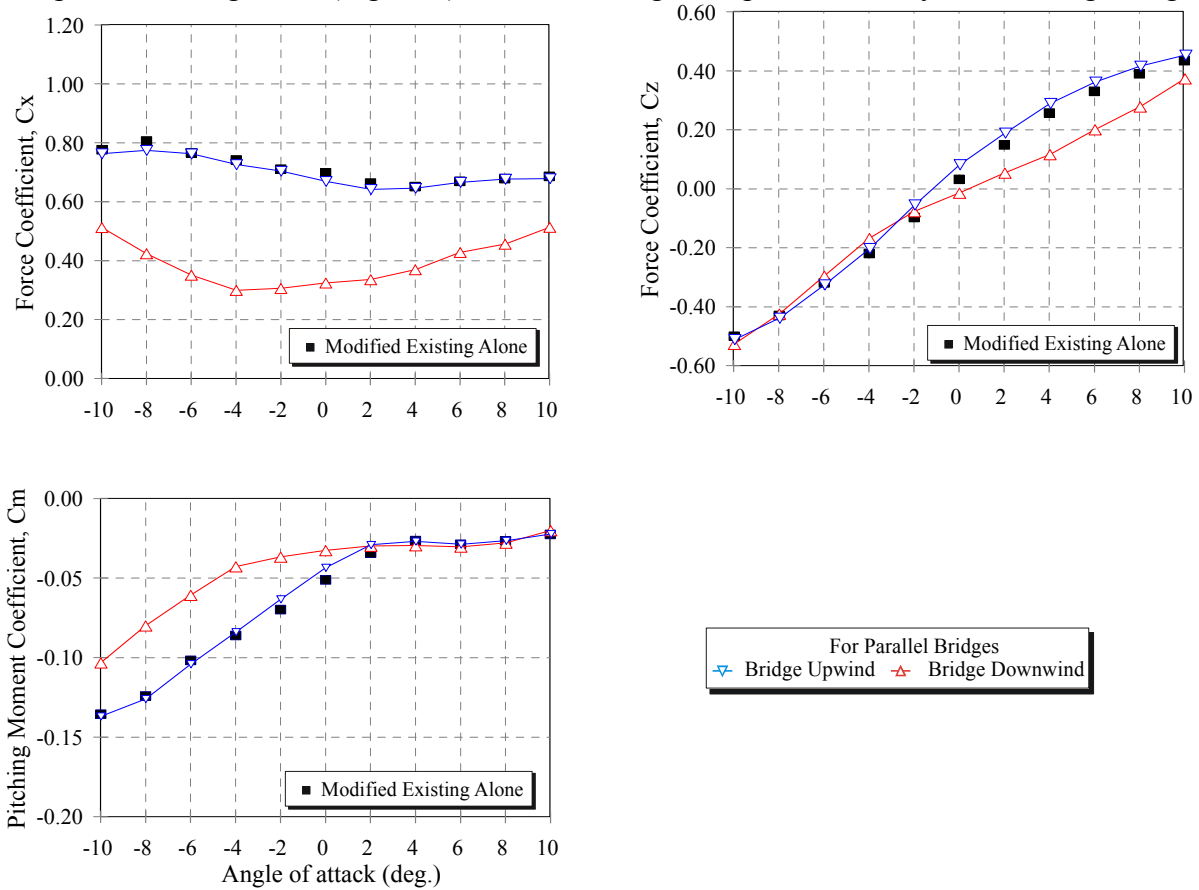


Figure 5: Static force and moment coefficients of the Existing Tacoma Bridge.

Response analysis based solely on the quasi-static buffeting theory (i.e., no aerodynamic derivatives were included) was carried out on a 163-segment model (=47 deck+2x36 main cables+2x22 towers). Turbulence with properties matching those simulated in the wind tunnel was simulated considering the following parameters: mean speed 27 m/sec at elevation 10 m, power law constant at the site 0.14, roughness $z_0 = 0.026$ m, time series of 55 min, integration time step $\Delta t=0.1$ sec. The simulated wind speed corresponds to 35.3 m/sec (127 kph) at deck level and is the design speed for this project. Figure 6 shows samples of longitudinal $U(t)$ and vertical velocities $w(t)$ at the middle of the main span and the corresponding power spectra. The aerodynamic admittance³ was incorporated into the wind speed histories. Buffeting response analysis was carried out considering both upwind and downwind bridge positions. In this analysis were used static coefficients measured from sectional models test, turbulence and dynamic properties of the bridges as predicted by the designers.

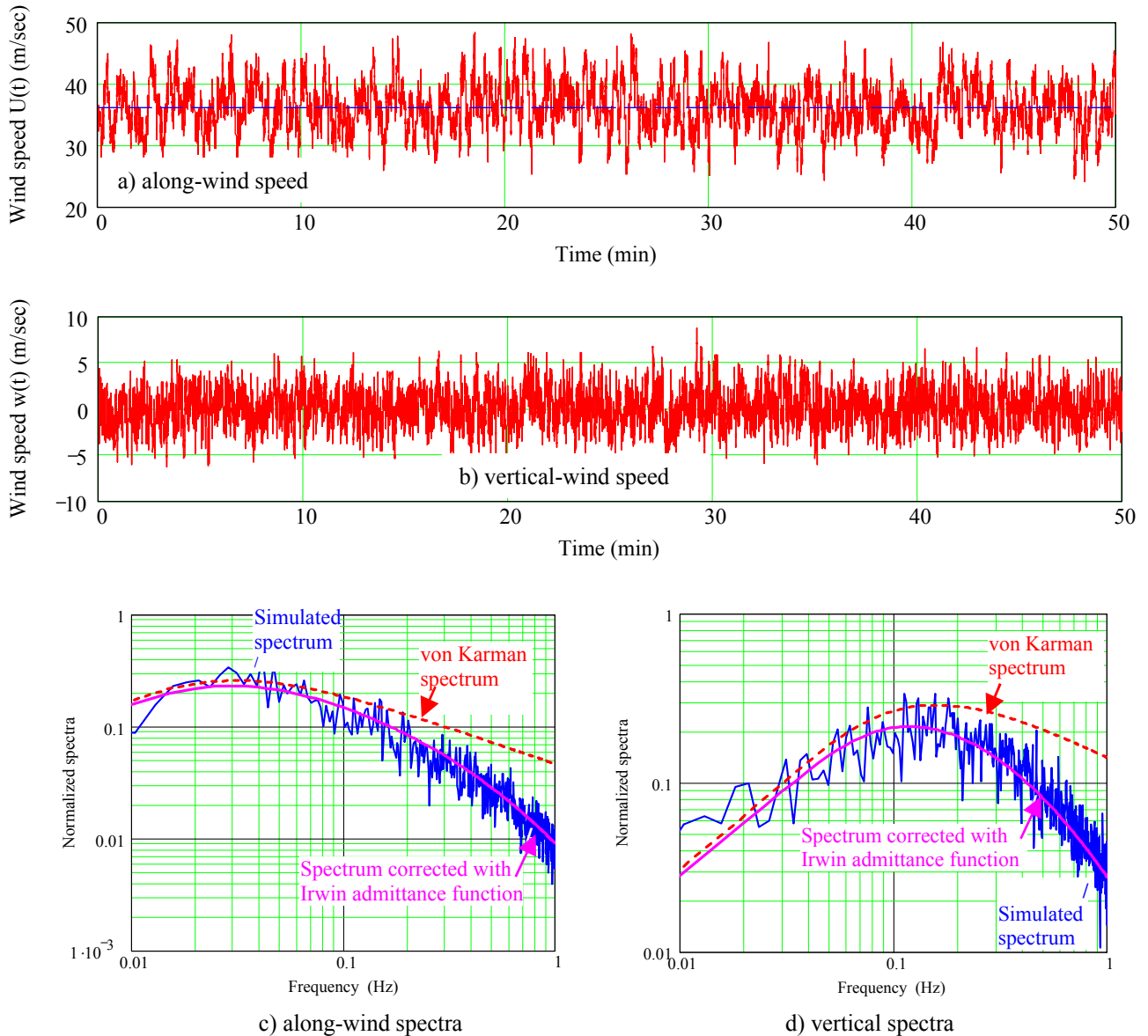
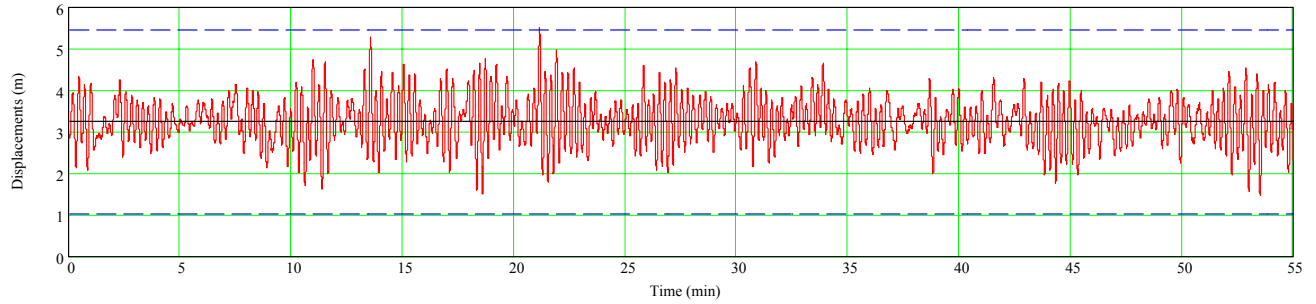
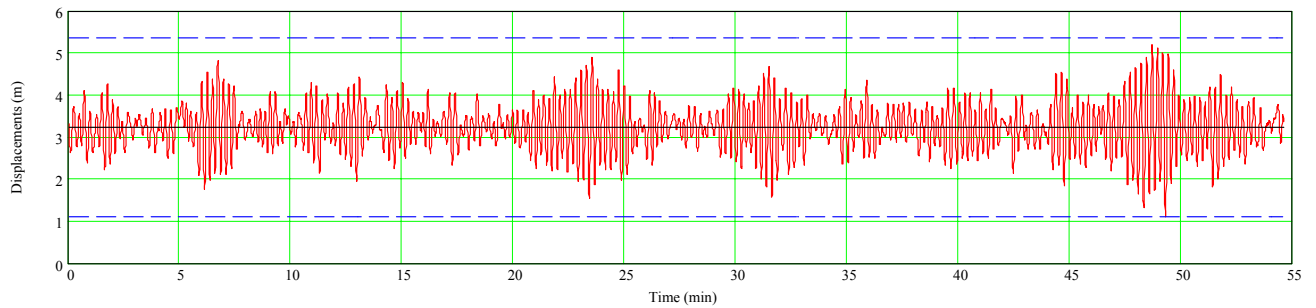


Figure 6: Turbulence properties at the middle of the main span of the Existing Tacoma Bridge (mean speed $\bar{U} = 35.3$ m/sec, longitudinal intensity $I_u = 14\%$, vertical intensity $I_w = 7.5\%$).

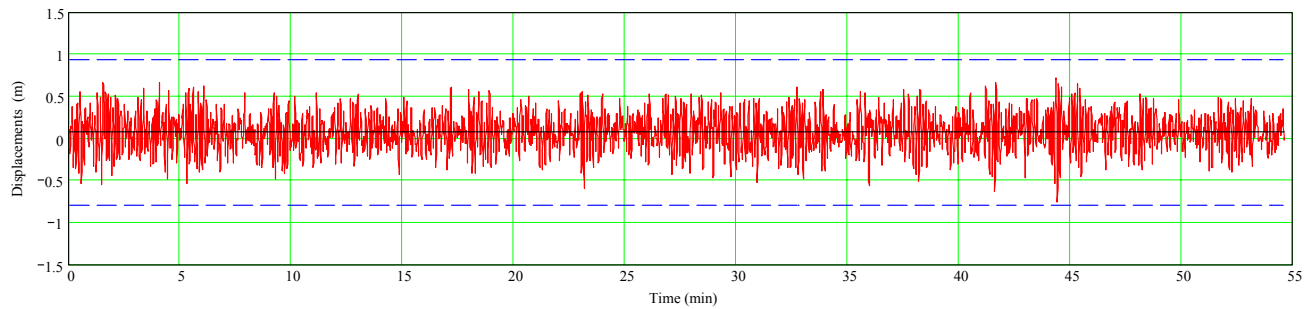
Figures 7 and 8 show lateral and vertical deflections and power spectra, both measured and numerically simulated for the middle of the main span of the existing bridge upwind. The responses measured on the aeroelastic models were converted to full scale using normal scaling methods. It can be seen that the numerically predicted mean and dynamic deflections were similar in magnitude and response pattern to those measured of the aeroelastic model. The spectral comparison is also satisfactory in terms both of modal responses and as well the overall shapes of the spectra.



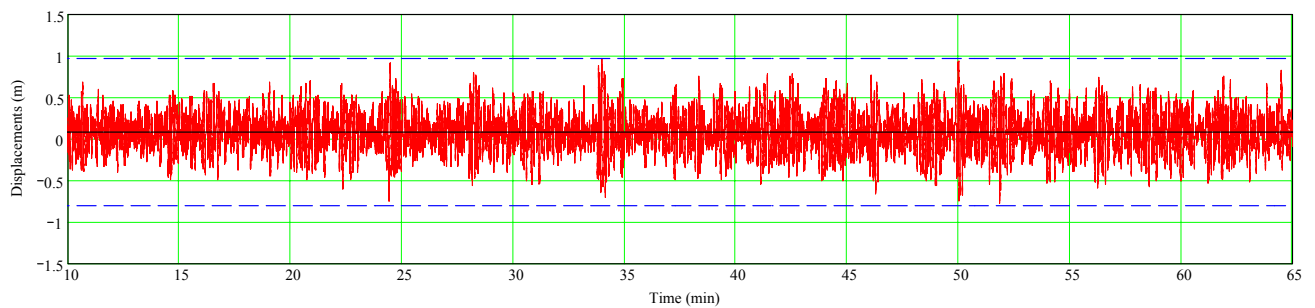
a) aeroelastic model - lateral deflections



b) numerical simulation - lateral deflections

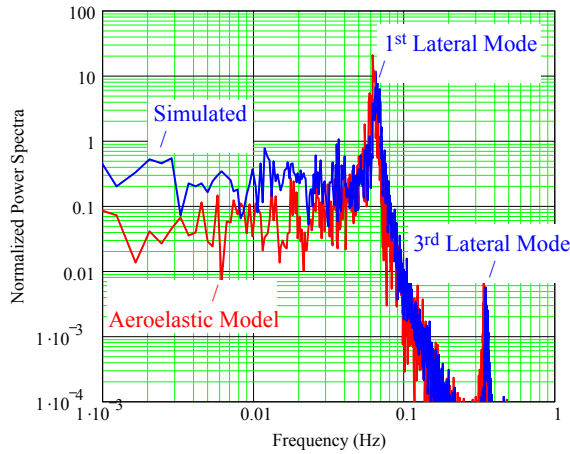


c) aeroelastic model - vertical deflections

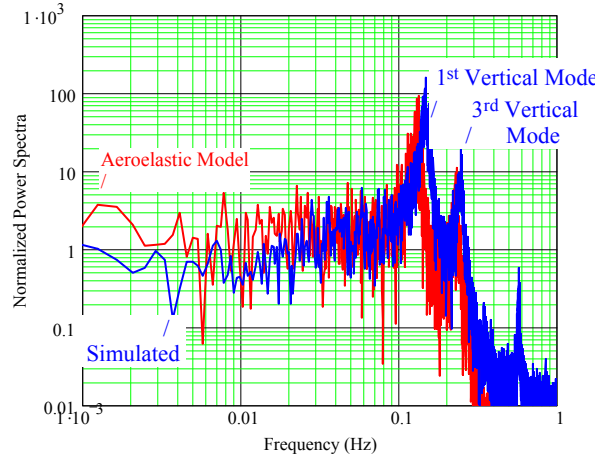


d) numerical simulation - vertical deflections

Figure 7: Existing Bridge upwind - time histories of responses at the middle of the main span (turbulent flow test/simulation, wind normal to the bridges, wind speed 27 m/sec, time 55 min).

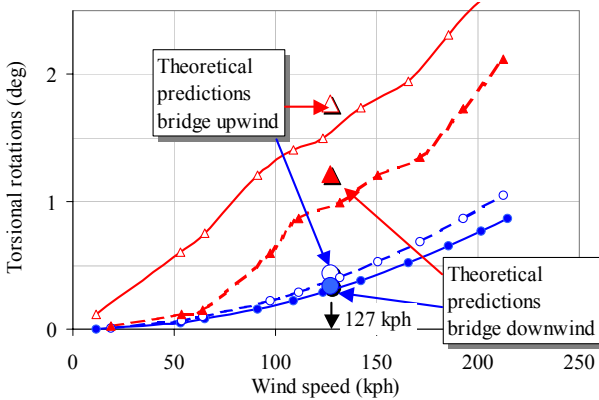
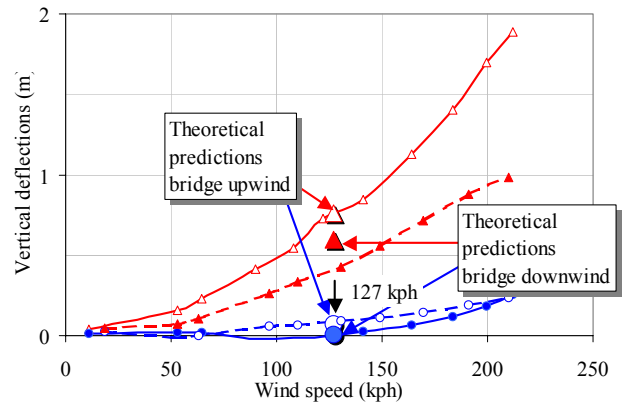
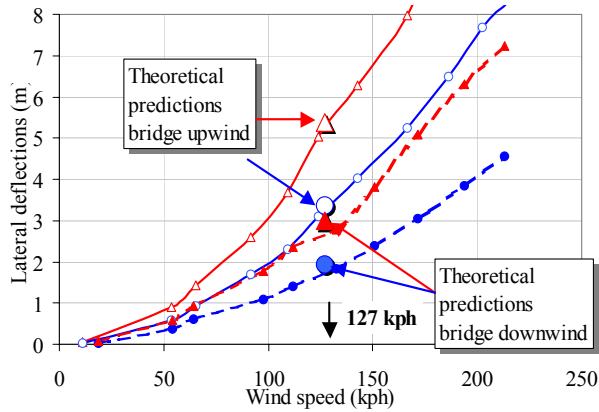


a) power spectra of lateral deflections



b) power spectra of vertical deflections

Figure 8: Existing Bridge upwind – power spectra of responses at the middle of the main span.



	Downwind	Upwind
Peak	▲	△
Mean	●	○

Figure 9: Existing Tacoma Narrows Bridge - measured from the aeroelastic model test and analytically predicted responses at the middle of the main span.

The deck mass of the Existing Tacoma Narrows Bridge is 10393 kg/m and its mass moment of inertia is 587308 kg.m²/m. Structural damping ratio of 0.5% was applied to all modes. Figure 9 shows mid-span responses for various wind speeds measured from the aeroelastic model of the in both upwind and downwind positions for wind normal to the bridge span. It can be seen that the predicted lateral responses were quite close for both upwind and downwind position. The vertical responses in the downwind position were higher than the measured. Higher torsional responses were predicted in both positions. This could be attributed to the fact that the quasi-static buffeting theory does not provide formulae for estimation of aerodynamic damping in torsion. In the response analysis this damping was set to zero which in case of stable bridge is conservative – hence higher torsional responses were predicted.

5.3 Wind Loads of the Existing Ile d'Orléans Bridge

This example involves Ile d'Orléans Bridge numerical model as described in Section 5.1. Simulation of wind turbulence was carried out based on the following parameters: mean speed 30 m/sec at elevation 10 m, power law constant at the site 0.13, roughness $z_o = 0.03$ m, time series of 55 min, integration time step $\Delta t=0.1$ sec. The simulated wind speed corresponds to the design speed of 36 m/sec at deck level. Static force and moment coefficients were derived from the sectional model test measurements of the existing section (Figure 2) and turbulence averaging considering intensity of vertical turbulence $I_w = 10\%$. For details of this estimation could be found in a reference document²² available upon request.

Table 5: Weighted average of force coefficients for Existing Bridge

C_X	C_Z	C_M	$dC_X/d\alpha$	$dC_Z/d\alpha$	$dC_M/d\alpha$
1.1216	-0.1231	0.1095	-0.2826	3.4426	0.1929

- Note:
1. Vertical turbulence intensity $I_w = 10\%$ was applied.
 2. Coefficients C_X and $dC_X/d\alpha$ were normalized with deck depth $D = 3.96$ m.
 3. All other coefficients were normalized with deck width $B = 9.656$ m.

Gust factors of background loads were calculated via integration of the time histories of loads over the deck length.

Table 6: Gust factors for background loads

Load	g_{Load}
Vertical	3.24
Along the deck	1.56
Lateral load	1.56
Moments	1.54

²² BR01-06, Background on Bridge Aerodynamics and Wind Tunnel Tests, RWDI Reference Document BR01-06, March 22, 2006.

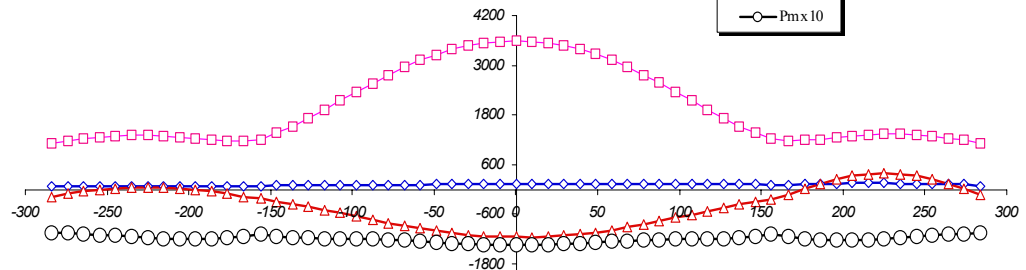
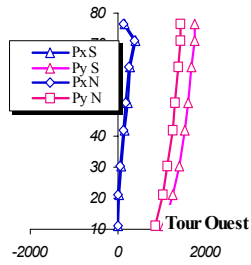
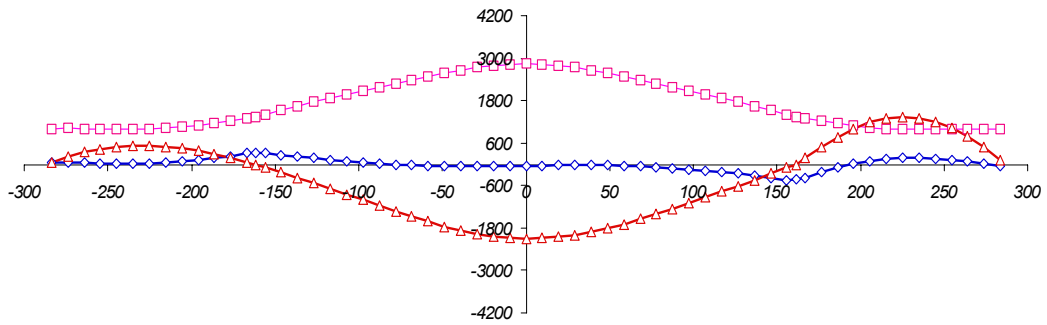
The peak modal responses were estimated for modes with frequencies up to 1 Hz (Table 7). The deck mass is 4699 kg/m and its mass moment of inertia is 72722 kg.m²/m. Structural damping ratio of 1% was applied for all modes except Mode 5 where damping ratio of 1.8% was retained based on field measurements.

Table 7: Peak modal deflection for the existing bridge, 100-year wind loads

Mode	f (Hz)	Mode Shape	Modal deflection (m)
1	0.2071	Along deck	0.1802
2	0.2243	1 st Lateral/Torsion	1.0153
3	0.2872	1 st Vertical	0.7478
4	0.3434	2 nd Vertical	0.5925
5	0.4069	2 nd Torsional	0.0701
6	0.4530	1 st Torsional/Lateral	0.2662
7	0.4533	1 st Torsional/Lateral MS/SS	0.1553
8	0.5430	3 rd Vertical	0.1663
9	0.6037	1 st Torsional SS	0.0461
10	0.6474	4 th Vertical	0.1183
11	0.6486	3 rd Torsional	0.0246
13	0.7380	Lateral/Torsional Cables	0.0362
15	0.7655	Torsional/Lateral Cables	0.0351
16	0.7903	Torsional/Lateral Cables	0.0167
17	0.7963	Torsional/Lateral Cables	0.0145
21	0.8292	Torsional/Lateral Cables	0.0168
22	0.9754	5 th Vertical MS	0.0276
23	1.0562	Torsional/Lateral Cables	0.0109

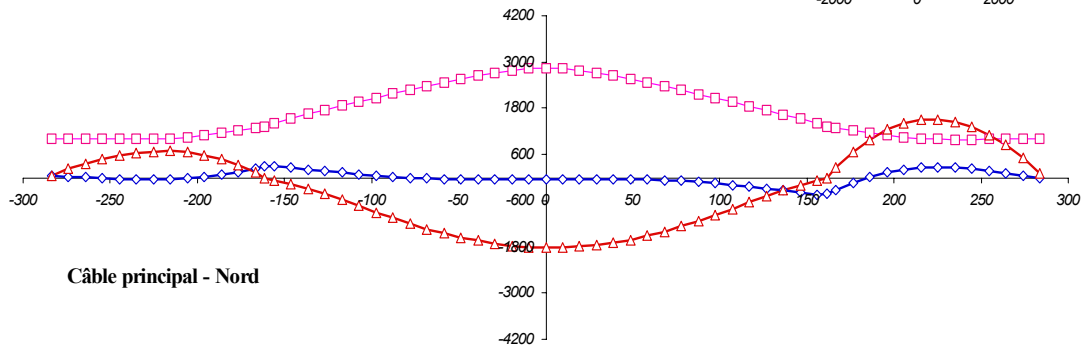
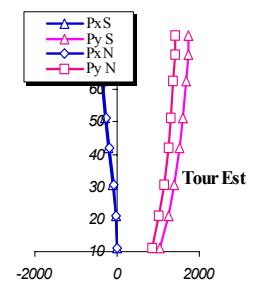
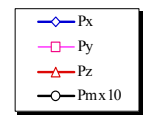
A total of 25 load combination were developed considering bridges symmetry about its along the deck axis x considering winds acting from one side of the bridge only. For design purposes however was recommended to mirror given load patterns about axis x to account for the reversed winds. Figures 10 and 11 present two load cases of symmetric loads with dominant 1st vertical and 1st lateral modes.

Câble principal - Sud



Tablier

Coordonnée x (m)



Câble principal - Nord

Coordonnée x (m)

Figure 10: Wind load patterns for a dominant Mode 2, all loads are in Pa.

Câble principal - Sud

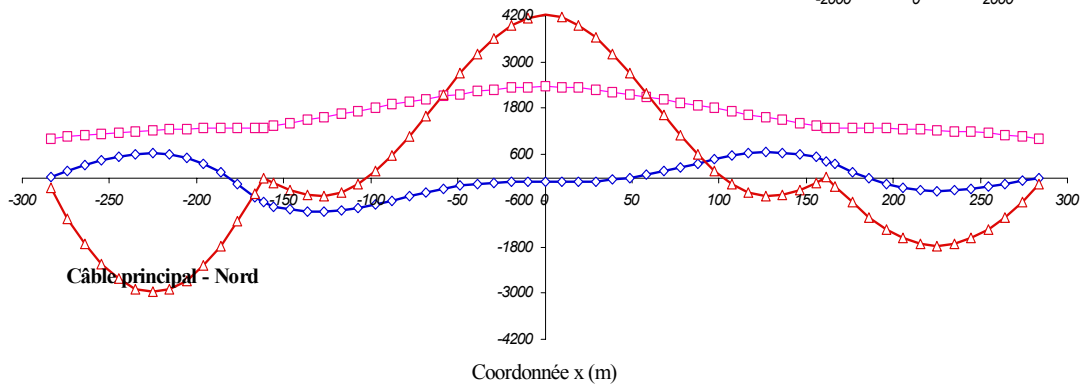
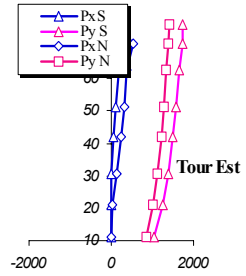
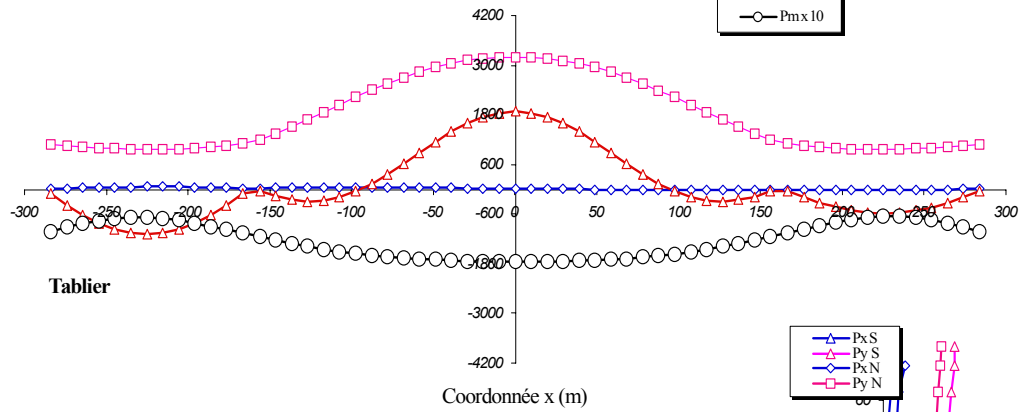
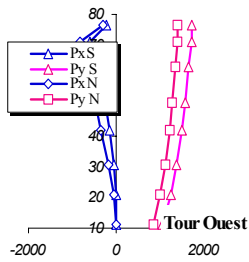
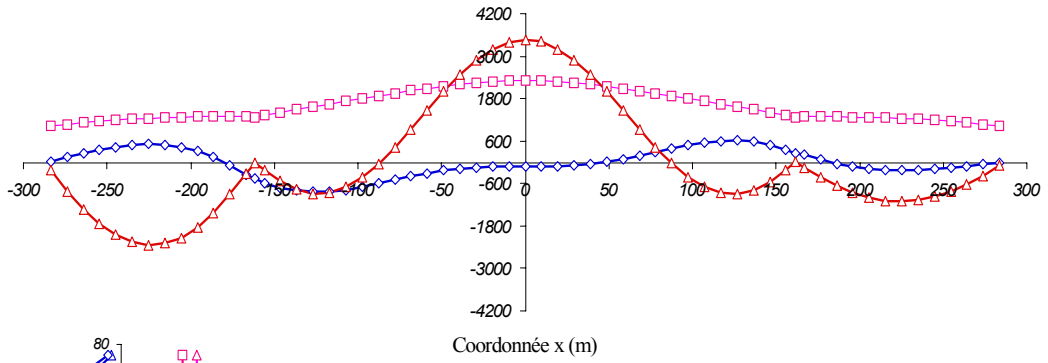


Figure 11: Wind load patterns for a dominant Mode 3, all loads are in Pa.

Using the above pressure distributions, loads per unit length of bridge deck are to be calculated as

Lateral loads,	$F_Y = p_Y d$
Longitudinal loads,	$F_X = p_X B$
Vertical loads,	$F_Z = p_Z B$
Torsional loads,	$M_x = p_m B^2$

where given wind loads should be applied at the centre of deck shear. Lateral and longitudinal (along the bridge) loads on the towers are calculated using the same formula with d being replaced with the leg lateral dimensions, and B with the leg longitudinal dimensions, which vary with the elevation. Given pressure notifications correspond to the FEA model of Ile d'Orléans Bridge coordinate system which differs from the coordinate system used in this document.

The loads per unit length of main cable:

Lateral loads,	$F_Y = p_Y d$
Longitudinal loads,	$F_X = p_X d$
Vertical loads,	$F_Z = p_Z d$

where main cable diameter $D = 0.254$ m. Lateral loads per unit length of hangers are also applied using a recommended pressure of 1600 Pa. On main cables, hangers and towers, given wind loads should be applied at their centres of mass.